The Role of Schwann Cells and Nerves in Pancreatic Cancer

Aysha Ferdoushi

B. Sc (Honours), M. Sc (Bangladesh)

Thesis submitted in fulfilment of the requirements for the degree of

Doctor of Philosophy in Medical Biochemistry

School of Biomedical Sciences and Pharmacy

The University of Newcastle, Australia

September 2020

This research was supported by an Australian Government Research Training Program (RTP) Scholarship

Declarations

STATEMENT OF ORIGINALITY

I hereby certify that the work embodied in the thesis is my own work, conducted under normal supervision. The thesis contains no material which has been accepted, or is being examined, for the award of any other degree or diploma in any university or other tertiary institution and, to the best of my knowledge and belief, contains no material previously published or written by another person, except where due reference has been made. I give consent to the final version of my thesis being made available worldwide when deposited in the University's Digital Repository, subject to the provisions of the Copyright Act 1968 and any approved embargo.

Aysha FERDOUSHI

THESIS BY PUBLICATION

I hereby certify that this thesis is in the form of a series of papers. I have included as part of the thesis a written declaration from each co-author, endorsed in writing by the Faculty Assistant Dean (Research Training), attesting to my contribution to any jointly authored papers.

Signature: …….. *Date: ...15.../...09.../...2020...*

Aysha FERDOUSHI *dd /mm/ yyyy*

Acknowledgements

In the name of Allah, the most gracious and the most merciful.

Alhamdulillah, all praises to Almighty ALLAH for the strengths and His blessing in completing this thesis. My humblest gratitude to the beloved Prophet Muhammad (peace be upon him) whose way of life has been a continuous guidance for me.

I have been blessed with the help and support of many individuals throughout my PhD research.

Firstly, I would like to express my deepest gratitude to my supervisor Professor Hubert Hondermarck for giving me the opportunity to complete my PhD under your expert supervision. Thank you for providing me with a positive environment and encouraging me to do my very best. Thanks very much for your mentoring and nurturing me to become the scientist I am today. I am really grateful for your constructive criticism, compliment, encouragement and thoughtful guidance over the last few years. I have learnt so much from you, thanks for always having faith in me. Thank you for respecting my religious beliefs. I can only express my debt of gratitude to you through becoming a better scientist, mentor, and a good human being.

I would like to thank my co-supervisors, Professor Dirk F. van Helden and Associate Professor Phillip Jobling, for their exceptional guidance, tremendous support and friendship during this time. Thank you for your constructive criticism, and enthusiasm for my project. I would like to convey my special thanks to Professor Dirk for introducing me with Professor Hubert and creating the opportunity to work under his expert supervision. You have played multiple roles during this journey, as a scientific mentor, a career mentor, and a friend.

I would also like to express my gratitude to my HDR Advisory Committee members, Associate Professor Mark Baker and Associate Professor Paul A Tooney. Thank you for your constructive critique, encouragement, and enthusiasm throughout my PhD journey. I am thankful to Professor Liz Milward for being very friendly, offering guidance and encouragement throughout the years.

Next, a big "THANK YOU" to all the amazing members of Hubert's Lab, past and present, Dr Sam Faulkner, Dr Chen Chen Jiang, Dr Hui Liu, Fangfang Gao, Nathan Griffin and Xiang Li for your optimism, solidarity, inspiration, support and help throughout this expedition. I truly appreciate your care and encouragement during one of the toughest times. I am also appreciative to Kristen McEwan and Mark Marsland for their support network over the years. Thanks to all for always making it such a welcoming, cheerful, and pleasant environment, thank you for all the memories!!

A special thank you goes to Sonia Tamanna who has been enormously supportive and has become my family away from home. I would also like to extend my sincere thanks to the following people: Dr. Muhammad Jamaluddin, Dr.Trisha Al Mazi, Aminah Ali Abid Al-Juboori, Farjana Afrin, Dr. Abdul Mannan and Dr. Arnab Ghosh for their kind assistance whenever it was needed.

Most importantly, my heartfelt deepest gratitude to my parents Md. Shah Alam Howlader and Farida Khanom, for their unconditional support, love, motivation and hope throughout this mission. Thanks to my big sister Dr. Fatema Tuz Zohora and my little brother H.M. Abdullah Omar Faruque for their understanding, constant encouragement and faith in me. Thanks to all for being very supportive at the beginning of my PhD journey when I decided to move from Japan to Australia, the very toughest period of this long voyage. Thanks for being such wonderful, understanding and supportive of my dream– I couldn't have done this without you!!

Finally, I thank all those who have helped me directly or indirectly in the successful completion of my thesis. Anyone missed in this acknowledgement are also thanked.

I dedicate this thesis to my beloved parents, my sister and my brother for their unconditional support, love and always keeping me in their prayers!!!

List of Publications Included as Part of this Thesis

Ferdoushi A, Li X, Jamaluddin MFB and Hondermarck H. **Proteomic Profile of Human Schwann Cells**. *Proteomics*. 2020 January; 20(1):1900294.

Ferdoushi A, Li X, Griffin N, Faulkner S, Jamaluddin MFB, Gao F, Jiang CC, Jobling P, Tanwar PS, Helden DFV, Hondermarck H. **Schwann Cell Stimulation of Pancreatic Cancer Cells: A Proteomic Analysis**. *Frontiers in Oncology*. 2020 August; 10:1601.

Ferdoushi A, Griffin N, Marsland M, Xu X, Faulkner S, Gao F, Liu H, King SJ, Denham JW, Helden DFv, Jobling P, Jiang CC, Hondermarck H. **Tumour innervation is associated with poor clinical outcome in pancreatic cancer** (Submitted to *Scientific Reports*).

List of Abbreviations

A	
ADRβ2	adrenergic receptor beta 2
ATCC	American Type Culture Collection
ACh	acetylcholine
ALF	acute liver failure
B	
BDNF	brain-derived neurotrophic factor
C	
CA19-9	carbohydrate antigen 19-9
CAFs	cancer-associated fibroblasts
CEA	carcinoembryonic antigen
CHRM1	type 1 muscarinic acetylcholine receptor
CNS	central nervous system
CCL2	C–C motif chemokine ligand 2
CM	conditioned media
CI	confidence interval
CDKN2A	cyclin-dependent kinase inhibitor 2A
CTLA-4	cytotoxic T-lymphocyte-associated antigen 4
CPECs	epithelial cells of choroid plexus
D	
DMEM	Dulbecco's Modified Eagle's Medium
DRG	dorsal root ganglion
DDA	data-dependent acquisition
DAVID	Database for Annotation, Visualization and Integrated Discovery
DTT	Dithiothreitol
E	
EGF	epidermal growth factor
EGFR	epidermal growth factor receptor
ERK	extracellular signal response kinase
EMT	epithelial-mesenchymal transition
ECM	extracellular matrix

F	
FBS	fetal bovine serum
FAP	fibroblast activation protein
5-FU	fluorouracil
G	
GDNF	glial-derived neurotrophic factor
GFAP	glial fibrillary acidic protein
GO	Gene Ontology
GAD	Genetic Association Database
Gal-1	galectin-1
Gal-3BP	galectin-3 binding protein
GCSF	granulocyte colony-stimulating factor
H	
HA	hyaluronic acid
HPDE	human pancreatic ductal epithelial
HR	hazard ratio
HER-2	human epidermal growth factor receptor-2
I	
IHC	immunohistochemistry
IL-6	interleukin-6
IL-1Ra	interleukin-1 receptor antagonist
IPA	Ingenuity Pathway Analysis
IAA	Iodoacetamide
IGFBP	insulin-like growth factor-binding proteins
K	
KEGG	Kyoto Encyclopedia of Genes and Genomes
KRAS	Kirsten RAt Sarcoma virus
L	
LC-MS/MS	liquid chromatography-tandem mass spectrometry
LIF	leukemia inhibitory factor
M	
MAPK	mitogen-activated protein kinase
MMPs	matrix metalloproteinases

MS	mass spectrometry
MW	molecular weight
mSCs	myelinating SCs
MAG	myelin-associated glycoprotein
MNA	mean nerve area
MUC1	mucin 1
MSCs	mesenchymal stem cells
N	
NGF	nerve growth factor
NGFR	nerve growth factor receptor
NK	natural killer
NT-3	neurotrophin-3
NT-4/5	neurotrophin-4/5
NTRs	neurotrophic receptors
NTRK	neurotrophic tyrosine receptor kinase
NA	noradrenaline
NK1R	neurokinin-1 receptor
NCCs	neural crest cells
nmSCs	non-myelinating Schwann cells
NRG1	neuregulin-1
NCAM1	neural cell adhesion molecule 1
NAT	normal adjacent tissue
O	
OS	overall survival
P	
$p75^{NTR}$	p75 neurotrophin receptor
PDAC	pancreatic ductal adenocarcinoma
PI3K	phosphatidylinositol 3-kinase
PNI	perineural invasion
PC	pancreatic cancer
PNS	peripheral nervous system
Pax3	paired box *gene* 3
PanINs	pancreatic intraepithelial neoplasms

PD	Proteome Discoverer
PD-1	programmed death-1
PSC	pancreatic stellate cells
PAI-1	plasminogen activator inhibitor-1
R	
RTKs	receptor tyrosine kinases
RFU	relative fluorescence unit
S	
SC	Schwann cell
SCP	Schwann cell precursor
SCM	Schwann cell medium
SF	serum free
SP	substance P
Shh	Sonic Hedgehog
SACC	salivary adenoid cystic carcinoma cell line
SD	standard deviation
SEM	standard error of mean
STAT3	signal transducer and activator of transcription 3
T	
TCGA	The Cancer Genome Atlas
TMA	tumour microarray
TME	tumour microenvironment
TNFα	tumour necrosis factor alpha
Trk	tyrosine kinase receptor
TP53	tumour protein p53
TRPA1	transient receptor potential ankyrin 1
U	
UCMSCs	umbilical cord mesenchymal stem cells
V	
VEGF	vascular endothelial growth factor
VEGFR	vascular endothelial growth factor
W	
WB	Western blot

Table of Contents

List of Figures

Abstract

With a 5-year survival rate of less than 9%, pancreatic cancer (PC) is the 7th leading cause of cancer-related deaths worldwide. The poor prognosis of this cancer is attributed to its highly invasive nature, early onset of metastasis and lack of effective treatments. While current chemotherapy and radiation therapy are largely ineffective in the treatment of this disease, surgical treatment offers the only hope for long term survival. Unfortunately, only ~15% of patients have resectable disease at the time of diagnosis.

The tumour microenvironment (TME) of PC is believed to hold a key for overcoming the challenges of treating PC. It has long been known that, in addition to being found in the vascular and lymphatic systems, cancer cells occur in neuronal spaces, which serve as an alternative route for dissemination. Emerging evidence indicates that nerve infiltration in the TME plays a stimulatory role in tumour progression. Some cancers have the ability to invade along nerves, an ominous event termed perineural invasion (PNI) that causes nerve dysfunction and makes the cancer more difficult to eradicate. PNI is one of the most common features of PC that causes severe abdominal and back pain. PNI has repeatedly been shown to be an adverse pathologic finding, heralding more aggressive local disease, higher recurrence rates, and worsened survival.

Schwann cells (SCs), the most prevalent glial cell type supporting peripheral nerves, wrap around nerves and facilitate their conduction. SCs are an essential component of peripheral nerves and are implicated in promoting nerve repair but can also be causative in various diseases involving neurodegeneration. Notably, recent studies have shown that these glial cells play an active role in promoting PC progression. SCs have also been reported to be involved in PNI, epithelial to mesenchymal transition, decreased cancer pain sensation and subsequent delayed diagnosis.

This dissertation focuses on developing a greater understanding on the role of nerves and supporting SCs in PC progression. We aimed to explore the role of SC-secreted mediators on PC progression and, at the same time, investigate the role of nerve infiltration on PC aggressiveness.

We described the proteome of human primary SCs analysed by mass spectrometry-based proteomics liquid chromatography-tandem mass spectrometry (LC-MS/MS). The normal human SC protein dataset that we have reported constitutes a reference for future molecular explorations of physiological and pathological processes where SC are involved. In addition, several novel nociceptors and synaptic proteins were identified. This proteomic dataset may also be of a more direct value in the areas of pain and oncology where the role of SCs has recently been uncovered. Overall, this dataset will serve as a resource for further functional and clinical investigations into the role of SCs in health and disease.

To investigate the paracrine function of SCs in the pancreatic TME, we have also profiled the secretome of human primary SCs using LC-MS/MS and explored the role of several identified proteins in PC progression. A total of 13,796 unique peptides corresponding to 1,470 individual secreted proteins were identified. Several proteins that can stimulate PC cell proliferation and invasion were validated by Western blot. The involvement of these secreted proteins was further validated by using blocking antibodies. PC cell proliferation and invasion induced by SC-conditioned media was decreased using blocking antibodies against the matrix metalloproteinase-2, cathepsin D, plasminogen activator inhibitor-1 and galectin-1. Blocking antibodies against the proteoglycan biglycan, galectin-3 binding protein, tissue inhibitor of metalloproteinases-2 decreased proliferation but not the invasion of PC cells. Together, this study delineates the secretome of human SCs and identifies proteins that can stimulate PC cell growth and invasion and could therefore constitute new therapeutic targets.

Following on with the study, we investigated the clinicopathological significance of nerves in PC. We have analysed the density and size of nerves in a cohort of 99 PC cases versus 71 normal pancreatic tissues. The presence of nerves was significantly correlated with worse overall survival. In addition, the size of nerves, measured by cross-sectional area, was found to be significantly higher in PC than in the normal adjacent tissue and larger nerves were directly associated with worse patient survival. From these findings, we suggested that the presence and size of nerves in the TME of PC are associated with tumour aggressiveness.

Collectively, this dissertation has presented the proteomic and secretomic profiles of human SCs that will also serve as an important resource for further functional and clinical investigations into the role of SCs in oncology. It also investigated the role of several identified SC-secreted proteins in the stimulation of PC growth and invasion, which may represent novel

potential targets for the development of future targeted treatments in PC. This work has also provided novel insight in understanding the molecular mechanism of PNI, suggesting that increased nerve infiltration might be a primary event leading to higher PNI levels observed in PC. Results from this work may ultimately develop into novel therapies for PC.

Chapter 1 | Thesis Introduction and Overview

1.1 Introduction

Recent studies have demonstrated a critical role for nerves in enabling tumour progression (Faulkner et al., 2019) and the field of cancer neuroscience is emerging (Monje et al., 2020). Peripheral nerves form complex TME, which are made of several cell types including supportive glial cells named SCs and recent studies have revealed that SCs enable cancer progression (Demir et al., 2014;Deborde et al., 2016). However, a detailed understanding of the molecular and cellular mechanisms involved in the regulation of cancer progression by nerves and supporting SCs is essential to design strategies to inhibit tumour progression.

1.2 Aims of the study

The overall purpose of my thesis was to establish a better understanding and insight of the role of peripheral nerves and their supporting glial cells in PC progression. More specifically, we aimed to investigate the paracrine effect of SCs (i.e. SC-secreted molecules) in enhancing PC. In addition to this, we aimed to determine the clinicopathological significance of nerve infiltration within the TME and investigate the potential value of the infiltrated nerves as a prognostic factor in PC.

1.3 Organization of the thesis

Chapter 1 is the **thesis introduction and overview** of the body of work.

Chapter 2 is a **literature review** about the role of peripheral nerves and SCs in cancer progression with a particular focus on PC. The role of different molecules, known to be secreted or expressed both by SCs or nerves in PC progression is discussed. Our literature review illustrates that the nervous system directly and indirectly influences tumorigenesis. Nerves and associated SCs are emerging as a largely unexplored element of the TME, providing a significant new player in the creation of tumour-favourable conditions through bi-directional

interaction with cancer cells. The hypothesis of a communication between nerves and the TME represents a fundamental yet unexploited concept that forms the core structure of this thesis.

The subsequent chapters, from **Chapter 3 to Chapter 5**, display the published or submitted articles of this thesis.

Chapter 3 is a published article entitled "**Proteomic Profile of Human Schwann Cells**" (published in Proteomics, 2020 January; 20(1):1900294) and constitute a profiling of SC proteome. We report the proteome of human SCs analysed by LC-MS/MS. This proteome dataset should serve as a resource for further functional and clinical investigations into the role of SCs in health and disease.

Chapter 4 is a published article entitled "**Schwann Cell Stimulation of Pancreatic Cancer Cells: A Proteomic Analysis**" (published in Frontiers in Oncology, 2020 August; 10:1601). Here we profiled the secretome of human SCs using LC-MS/MS and investigated the role of several identified proteins secreted by SCs that can stimulate PC cell proliferation and invasion. These proteins represent novel potential targets for the development of future treatments of PC.

Chapter 5 presents a manuscript entitled "**Tumour innervation is associated with poor clinical outcomes in pancreatic cancer**" that at the time of this thesis has been submitted to Scientific Reports. Here we investigated whether there is association between nerve infiltration in the pancreatic TME with cancer aggressiveness, analysing the density and size of nerves in a cohort of PC patients. The data show that the presence and size of nerves in the TME are associated with tumour aggressiveness in PC. In addition, these findings suggest that increased infiltration of larger sized nerves might be a primary event leading to higher PNI levels commonly observed in PC.

Chapter 6 presents a **General Discussion** in which the findings of the publications contained in this thesis are summarized. This chapter contains perspectives and potential future directions.

Chapter 2 | Literature Review

2.1 Pancreatic cancer (PC)

PC is an intractable malignancy and is the 7th leading cause of global cancer deaths in industrialized countries (Bray et al., 2018). Before focusing on this cancer in more details, the anatomy of normal pancreas is discussed briefly below.

2.1.1 The anatomy and functional components of the pancreas

The pancreas is a glandular organ with elongated, soft, flat, lobules located in the retroperitoneal space. It is roughly J-shaped and has a head near the midline of the body and a tail that extends to the left, where it touches the spleen (Talathi et al., 2020).

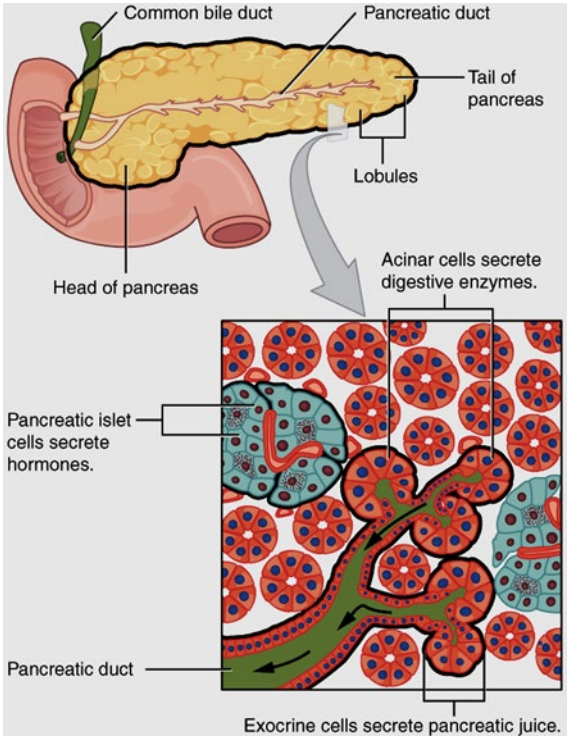

Figure 1. Anatomy and histology of the pancreas. *The pancreas has a head, a body and a tail. It delivers pancreatic juice to the duodenum through the pancreatic duct. From (Kelly A. Youn, Anatomy and Physiology, 2013).*

The pancreas is a complex organ composed of both endocrine and exocrine tissues **(Figure 1)**. The bulk of the pancreas (>90% of the organ) is composed of "exocrine" acinar cells that help producing digestive enzymes to digest food in the gut (Logsdon and Ji, 2013). The second functional component of the pancreas is the "endocrine" pancreas, which is composed of small islands of cells, called the islets of Langerhans. These endocrine cells release hormones, such as insulin and glucagon, into the blood stream, which help control blood glucose levels (Röder et al., 2016).

PC starts when cells in the pancreas become abnormal and grow out of control (Rawla et al., 2019). PC can occur in any part of the pancreas, but about 70% of cases develop in the head of the pancreas. PC may affect the functioning of the endocrine and/or exocrine function of the organ. Endocrine tumours which is also referred to as neuroendocrine tumours develop in islets of Langerhans (Asa, 2011). About 95% PCs are exocrine tumours that originate from epithelial cells in the exocrine pancreas (Feldmann et al., 2007). Of the different tumour types that arise in the pancreas, pancreatic ductal adenocarcinoma (PDAC) is the most common type of PC (Fesinmeyer et al., 2005) and also the most lethal one (Fesinmeyer et al., 2005;Wisnoski et al., 2008). This is the focus of my thesis. Herein, the terms PC and PDAC are used synonymously.

The pancreas is a highly innervated organ and both sympathetic, parasympathetic and sensory nerves innervate the pancreas to participate in its normal activities (Pour et al., 2003;Gasparini et al., 2019). Sympathetic innervation comes from the thoracic splanchnic nerves via the celiac and superior mesenteric plexuses. Parasympathetic nerve fibres to the pancreas are contained in the vagus nerve via its celiac branch. Parasympathetic nerves stimulate pancreatic secretion, whereas sympathetic nerves are largely inhibitory (Kiba, 2004). Afferent sensory nerve fibres in the pancreatic parenchyma can transmit pain of pancreatic origin (Gasparini et al., 2019). The head of the pancreas is innervated by the celiac plexus whereas the splenic plexus innervates the body and tail of the pancreas (Pour et al., 2003). Furthermore, the pancreas receives direct innervation from the enteric nervous system of the gut, mainly from the stomach and the duodenum (Kirchgessner and Gershon, 1990).

In the following section, more details on PC will be presented, specially focusing on epidemiology, survival, prognosis, and the TME.

2.1.2 Epidemiology, survival and risk factors of PC

PC is a fast-growing cancer accounting for 3% of newly diagnosed cancer patients in both sexes in the United States and United Kingdom (Siegel et al., 2016). In 2012, over 1,000 people in New South Wales, Australia were diagnosed with PC, and over 850 people died (Creighton et al., 2016). Mortality rates have closely followed incidence emphasizing the deadly nature of this disease (Lankadasari et al., 2019) .

PC is called a 'silent' killer as in its early stage the disease is usually asymptomatic and most patients have either locally advanced or metastatic disease at presentation (Jemal et al., 2010;Zhou et al., 2010) and consequently overall 5-year survival rates are less than 9% (Rawla et al., 2019). The median postoperative survival for early staged patients that undergo surgery is less than 2 years, and only one out of eight are actually cured (Schnelldorfer et al., 2008;Siegel et al., 2016). PC patients present with predominantly nonspecific symptoms including abdominal/back pain, indigestion, jaundice and weight loss (Jung et al., 2007;Sharma et al., 2011). The majority of patients present with advanced or metastatic disease upon diagnosis, while, only about 20% of patients are eligible for the surgical resection, the only curative therapy for PC (Wolfgang et al., 2013;Kleeff et al., 2016). The aggressiveness of the cancer, late stage diagnosis, lack of effective treatment options and the mortality rate make it a challenging disease. Consequently, PC is anticipated to become the 2nd leading cause of cancer-related death by 2030 (Rahib et al., 2014).

The risk factors might be related to heredity (5–10%), smoking (30%) and dietary habit (20%) (Klein, 2013), although the majority of cases are sporadic, with 40% of patients having no significant risk factors. Other related factors include age (increased frequency usually observed after 50 years), ethnicity and sex (highest occurrence has been reported in black men), occupational hazards such as exposure to pesticides, dyes, and chemicals used in metal refining, diet (diet rich in red meat may be associated with increased risk) (Nothlings et al., 2005;Olson et al., 2013;Siegel et al., 2016). The most prominent risk factors include pancreatitis (>2 years), smoking, body mass index (>35 kg/m2), and heavy alcohol consumption (Arslan et al., 2010;Bosetti et al., 2012;Duell et al., 2012;Lucenteforte et al., 2012). Although controversial, coffee consumption has also been reported to be associated with PC. Diabetes has been reported to be a risk factor for this malignancy (Batabyal et al., 2014).

The advancement of PC is a stepwise process that involves oncogene activation, tumour suppressor gene inactivation and cell cycle deregulation (Zhang et al., 2016). PC typically harbors multiple genetic alterations (Bailey et al., 2016). Those with a strong family history or an identifiable germline predisposition are at increased risk for PC. Common genetic mutations associated with PC are found in KRAS, TP53, CDKN2A, and SMAD4 genes, but drug-targeting these mutations has yet to show significant promise (Kleeff et al., 2016; Pelosi et al., 2017).

2.1.3 Treatment of PC

Surgery, radiation therapy and chemotherapy are treatment approaches that may prolong survival and/or relieve symptoms in many patients with PC, but they seldom produce a cure (Chandana and Mahadevan, 2009).

2.1.3.1 Surgery

Surgical removal of the pancreatic neoplasm remains the only potentially curative treatment mode (Bilimoria et al., 2007). For patients receiving a complete resection, 70% will survive more than one year (Cooper et al., 2013). Five-year survival among patients who have surgery is approximately 20-25% compared to less than 5% for patients with no resection of their primary tumour (Speer et al., 2012). Various surgical procedures are performed depending on the location of the tumour in the pancreas. For the tumour located in the head of the pancreas, a pancreatico-duodenectomy (commonly known as a "Whipple" procedure) is performed. Tumours in the tail of the pancreas require a distal pancreatectomy which is accompanied by thr removal of the spleen (Nathan et al., 2009). Distal pancreatectomy is now often performed laparoscopically resulting in a decrease in length of hospital stay as well as a decrease in surgical complications (Venkat et al., 2012). Locally advanced PC, in which the tumour has grown into nearby blood vessels and other tissues, but has not spread to the liver or distant organs or tissues, cannot be removed completely by surgery. The most advanced form of PC is the metastatic form, whereby their spread renders them impossible to be removed by surgery or treated by radiation therapy alone. Treatment for patients with advanced disease still remains largely palliative.

2.1.3.2 Radiation Therapy

Radiation therapy also has a recognised role in the treatment of patients with locally advanced PC but who are unsuitable for surgery either as neo-adjuvant treatment with the aim of shrinking the tumour to increase the potential for surgery, or as a definitive treatment for patients unsuitable for surgery (Gandy et al., 2016). Neoadjuvant chemoradiation therapy has been reported to be associated with improved survival with lower cost than a surgery first approach for patients with PC (Abbott et al., 2013). For patients with advanced disease or metastases, it has been shown that 60% of patients have pain control in response to palliative radiotherapy for pain management (Chow et al., 2012). The use of radiation is controversial in locally advanced PC, as no advantage has been shown for radiotherapy (Laquente et al., 2017). Some data suggest that adding radiation may have a negative overall effect when used in the adjuvant or neoadjuvant setting (Franke et al., 2015). Other researchers believe that the role of radiation therapy in PC is still evolving and by using the correct patient selection, in combination with the newer radiation technology, the role for radiation still exists (Landau and Kalnicki, 2018).

2.1.3.3 Chemotherapy

Chemotherapy is indicated in the treatment of PC in all cases, although the duration and type of chemotherapy depends on the therapeutic goals. Several different chemotherapeutic drugs, as a single compound or in combination, to treat PC include: Gemcitabine, 5-fluorouracil, Irinotecan, Oxaliplatin, Nab-paclitaxel, Capecitabine, Paclitaxel, Docetaxel (Walker and Ko, 2014). None of the current drugs however have been shown to be particularly successful. Gemcitabine monotherapy has long been used as the standard chemotherapy for PC, but most patients do not respond well and end up with Gemcitabine resistance and disease progression. Hence, few other options are available for patients that fail Gemcitabine based therapy (Arora et al., 2013;Karamitopoulou, 2013). Gemcitabine in combinations with several cytotoxic agents and targeted therapies have also been disappointing, except for the combination with Nab-Paclitaxel, paclitaxel bound to the protein albumin. Nab-paclitaxel has been shown to increase the survival of patients with metastatic PC when used in conjunction with Gemcitabine, compared to treatment with Gemcitabine alone (Von Hoff et al., 2013). There are attempts to find new drug combinations to further improve survival and quality of life for patients with advanced PC. FOLFIRINOX, the combination of chemotherapeutic agents

(fluorouracil [5-FU], leucovorin, irinotecan and oxaliplatin) is an effective (but not always well-tolerated) schedule for selected patients with metastatic or locally advanced PC (Moorcraft et al., 2014). The most important recent breakthrough of chemotherapy is in the adjuvant setting, where FOLFIRINOX has been shown to reduce the recurrence rate and improve the survival of patients operated for PC as compared with the Gemcitabine (Conroy et al., 2018).

2.1.3.4 Targeted Therapy

As researchers have learned more about the changes in PC cells that help them grow, they have developed newer drugs to specifically target these changes. These targeted drugs work differently from standard chemotherapeutic drugs. Sometimes they work when standard chemotherapeutic drugs don't, and they often have different side effects.

The tyrosine kinase inhibitor Erlotinib is the first and only molecularly targeted therapy approved by the FDA for first-line treatment of advanced PC (Ducreux et al., 2015). This drug can be given along with the chemo drug Gemcitabine. The combination of Erlotinib and Gemcitabine compared with placebo was associated with a median OS of 6.2 months versus 5.9 months ($p = 0.038$) (Moore et al., 2007). However, the data suggest that only a small fraction of patients benefited from the therapy.

A small number of PCs have changes in one of the neurotrophic tyrosine receptor kinase *(NTRK)* genes which can sometimes lead to abnormal cell growth and cancer. Larotrectinib (Drilon et al., 2018) and Entrectinib (Drilon et al., 2017) target the proteins made by the *NTRK* genes. These drugs can be used in people with advanced PC that have an *NTRK* gene change, typically when the cancer is still growing despite other treatments. Several monoclonal antibodies and oral tyrosine kinase (RTK) inhibitors have been studied in phase 3 trials, all of these have failed to demonstrate clinically meaningful activity, except for Sunitinib, which may have a role in maintenance therapy (Reni et al., 2013). Sunitinib as maintenance after 6 months of progression-free disease management, was able to prolong 2-year survival (23% vs 7%). Encouraging results were obtained in trials exploring RTK inhibitors (Lai et al., 2019). More about targeted therapy for PC has been described in section 2.1.4.

2.1.3.5 Immunotherapy

Immunotherapy has shown positive results in many cancer types including, lymphoma, melanoma, renal cell carcinoma and lung adenocarcinoma (Kruger et al., 2019). However, immune therapy for PC is still a challenging issue. Although inflammatory cells have been shown to infiltrate the TME in PC, these cells promote rather than inhibit PC growth (Gajewski et al., 2013;Khalafalla and Khan, 2017). Immune cells in the TME such as T cells, B cells, myeloid-derived suppressor cells and tumour-associated macrophages have emerged in patients with melanoma and lung cancer as excellent therapeutic targets, and have already shown some promising outcomes (Hogan et al., 2018;Kanwal et al., 2018). Immune therapy trials in PC include passive immunotherapeutic approach using monoclonal antibodies or effector cells generated in vitro and active immunotherapeutic approach using vaccination to stimulate antitumour response (Banerjee et al., 2018). Monoclonal antibodies employed in passive immunotherapeutic approaches block ligand-receptor signaling for growth leading to tumour cell death. They can target tumour associated antigens, such as mucin 1, Wilms tumour gene 1, human telomerase reverse transcriptase, mutated KRAS, Carcinoembryonic antigen (CEA), survivin, p53, human epidermal growth factor receptor 2 (HER-2/neu), vascular endothelial growth factor receptor (VEGFR) or epidermal growth factor receptor (EGFR) (Chang et al., 2016). Cellular therapies with genetically engineered T cells (CAR-T-cells or antigen-specific T cell receptors) or tumour infiltrating lymphocytes have also proven to be efficacious in certain hematopoietic malignancies and solid tumours (Winograd et al., 2015). Nevertheless, none of the PC immunotherapy trials have shown meaningful clinical benefit (Kunk et al., 2016). In genetically engineered mouse models, pancreatic ductal adenocarcinoma were fully refractory to an approach with only monoclonal antibodies that block programmed death 1 (PD-1) or cytotoxic T-lymphocyte-associated antigen 4 (CTLA-4), which is in line with what was seen in patients (Winograd et al., 2015).

2.1.4 Targeting the tumour microenvironment (TME) in PC treatment?

The process of tumour formation and progression is influenced by two factors, namely genetic/epigenetic changes in the tumour cells and the rearrangement of the components of the TME (Jahanban-Esfahlan et al., 2017). The TME is a dynamic environment and the privileged site where tumours are in close contact with the host. Within the last two decades, scientists have shifted their research interest also to the TME in addition to cancer cells themselves. By

addressing the biological significance of tumour stroma and its interactions with cancer cells, it has been possible to demonstrate the relevance of such interactions both biologically as well as clinically.

A histopathological hallmark of PC is the extremely dense desmoplastic environment, or abundance of ECM, that surrounds PC cells constituting up to 60–90% of the total tumour volume (Whatcott et al., 2015). The stroma is very heterogeneous and is comprised of cellular components, predominantly cancer-associated fibroblasts (CAFs), myofibroblasts, pancreatic stellate cells (PSC), immune cells, blood vessels, a rich ECM, cytokines and growth factors (Feig et al., 2012;Goel and Sun, 2015) (**Figure 2**). The role of the stroma to either promote or resist tumour formation and progression is influenced by the various signals.

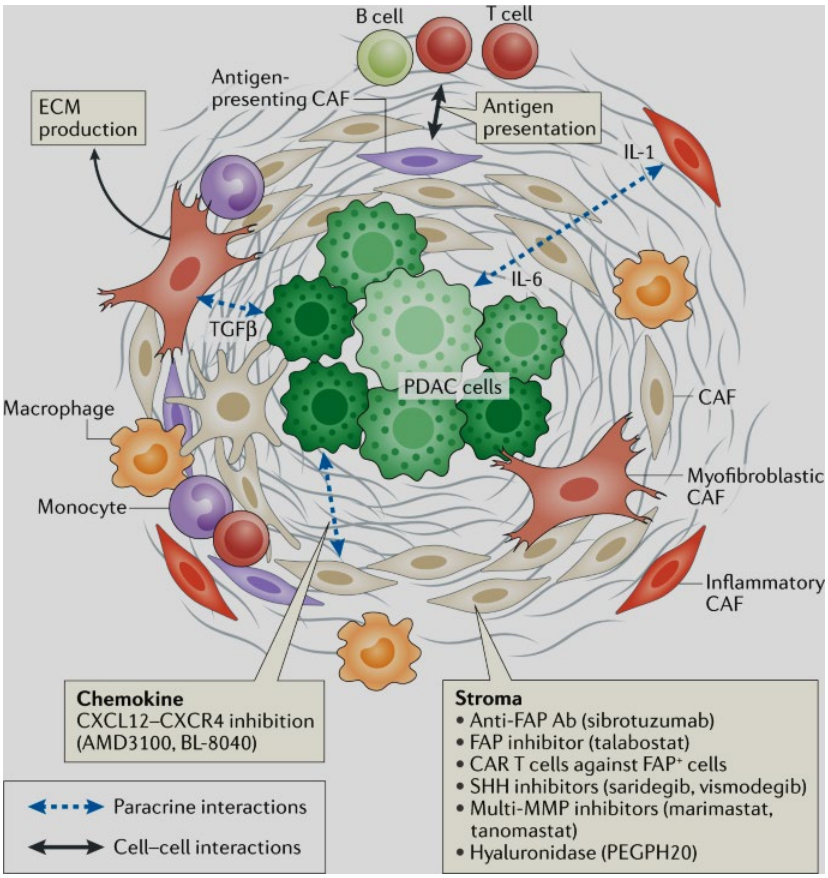

Figure 2: Targeting PC-associated stroma for treatment. *Approaches to deconstruct the stroma have included the use of matrix metalloproteinase (MMP) inhibitors, hyaluronidase, Sonic hedgehog (SHH) inhibitors, fibroblast activation protein (FAP) targeting agents and CXCR4 inhibitors. Ab, antibody; CAR, chimeric antigen receptor; ECM, extracellular matrix. From (Ho et al., 2020).*

Both cell–cell and paracrine interactions between CAFs and cancer cells are involved in programming the stroma. Not only does the desmoplastic stroma create a protective shield from therapeutics (Dauer et al., 2017), it also aids in the process of epithelial to mesenchymal transition and causes tumour cell dissemination into surrounding tissue. This process involves constant remodelling of the stroma, and activation of different signalling pathways in the TME (Lindsey and Langhans, 2014;Bynigeri et al., 2017). Therefore, the treatment of PC has become a huge challenge and the components of the TME offer potential therapeutic targets.

Compounds tested so far in clinical trials for PC as MMP inhibitors include Marimastat (multifamily MMP inhibitor) (Bramhall et al., 2002) and Tanomastat (which inhibits MMP-9 along with MMP-2, MMP-3 and MMP-13) (Moore et al., 2003) (**Figure 2**). Although these compounds possess different inhibitory potencies toward the various MMPs, none of them was found to be selective for a particular enzyme. Unfortunately, most of these clinical trials of MMPIs have yielded disappointing results so far. Hyaluronic acid (HA) provides support and structure to the stroma. It can also bind to surface receptors on tumour cells and promote proliferation, migration and invasion (Toole and Slomiany, 2008). Given the multifaceted role played by HA in pancreatic stroma, HA targeting has been of great interest and has shown to cause tumour depletion in several preclinical tumour models (Provenzano et al., 2012;Jacobetz et al., 2013). Pancreatic tumours treated with Halofuginone, an anti-fibrotic agent, targeted PSCs and led to reduced HA in the tumours and showed overall reduced ECM production (Elahi-Gedwillo et al., 2019). PEGylated recombinant hyaluronidase (PEGPH20) in combination with Gemcitabine provides therapeutic benefit (improvement in overall survival) to PC patients with high hyaluronic acid expression and is emerging as an attractive adjuvant therapy (Hingorani et al., 2016) (**Figure 2**).

2.1.5. Targeting nerves in the TME of PC?

One of the reasons for the dismal outcome of PC is cancer cells from tumours that escape and enter the bloodstream at the earliest stages of tumour progression, such that by the time the cancer is discovered it has usually already spread (Nguyen et al., 2019). In addition to being found in vascular and lymphatic systems, cancer cells invade neuronal spaces, which serve as an alternative route for dissemination. The normal pancreas is also rich in ganglia and myelinated and unmyelinated nerve cells, and invasive cancer cells are able to spread into the nerve sheath as an alternate route for dissemination (Bapat et al., 2011). Therefore, PC has one

of the highest incidences of PNI among all cancer types (Ceyhan et al., 2008). Undifferentiated tumours tend to have more PNI (Hirai et al., 2002). The exact mechanism by which PNI occurs is unclear, but it appears to be mediated by an interaction between molecules on the cancer cell and peripheral nerves. These include many signalling pathways involved in pain as well as TGF-α, EGFR, the NGF family and their receptors, the GDNF family and their receptors, chemokines and their receptors (CX3CR1, Sema3A, PlxnA1, NRP1 and MMPs) as well as other surface molecules and their receptors (Ceyhan et al., 2008). In particular, it was demonstrated that the neurotrophic factor artemin can influence PNI of PC cells (Ceyhan et al., 2006). Additionally, norepinephrine has been shown to promote PNI of PC by increasing levels of phosphorylated STAT3. Inhibition of STAT3 inhibited norepinephrine-induced expression of NGF, MMP2 and MMP9 to decrease invasion of PC cells (Guo et al., 2013). Therefore, in case of PC, the nervous system may directly or indirectly influence cancer progression, and although the neuronal component of the TME has received little attention so far, it could be the basis for further innovative therapeutic approaches. In the following sections, the relevant neural anatomy and histological structure of nerves in PC will be reviewed.

2.2 Nerve involvement in cancer progression

Peripheral nerves, which are composed of a variety of cells including neurons and glial cells, constitute an essential component of the TME. With the exception of cartilage and the lens of the eye, all human tissues are infiltrated by nerves of sensory, autonomic (sympathetic and parasympathetic) and/or motor origin. In this section, peripheral nerve architecture, the stimulatory role of nerves in cancer progression, more specifically in PC progression will be presented.

2.2.1 Peripheral nerve structure

Peripheral nerves are organized in three layers: the endoneurium, the perineurium and the epineurium **(Figure 3)**. The epineurium, the outermost layer, is comprised of dense tissue that encloses the entire peripheral nerve (Sunderland, 1965). It is heavily vascularised (Bove, 2008) and innervated by small axons deriving from the endoneurium (Stolinski, 1995).

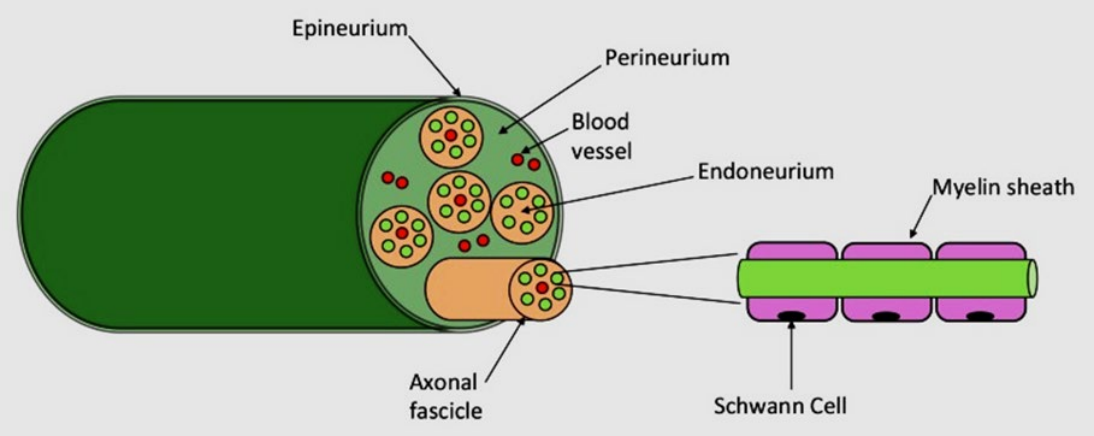

Figure 3. The structure of a peripheral nerve*. From (Gasparini et al., 2019).*

The perineurium is the middle layer that wraps around each nerve fascicle (Liu et al., 2018). The innermost layer of the endoneurium consists of nerve fibers composed of axons surrounded by different subtypes of SCs (myelinating and non–myelinating SCs) (Ubogu, 2013). The endoneurium also contains blood vessels, resident macrophages and fibroblasts (Jessen and Mirsky, 2016).

The normal function of the peripheral nervous system (PNS) is to connect the central nervous system (CNS) to the limbs and organs (Deborde and Wong, 2017). The nervous system is not an innocent bystander in cancer. Rather, the association of nerves with cancer cells has been established for a variety of malignant tumours including prostate cancer (Magnon et al., 2013) gastric cancer (Zhao et al., 2014;Hayakawa et al., 2017), PC (Bapat et al., 2011) which is often correlated with poor prognosis. The role of nerves in cancer progression is an emerging field and, until recently, nerves were not regarded as major contributors in tumorigenesis with their role in cancer growth under-studied (Faulkner et al., 2019). Until recently, our understanding of the role of nerves in cancer was essentially limited to PNI, a process in which cancer cells surround and eventually invade nerves (Liebig et al., 2009).

2.2.2 Innervation stimulates cancer progression

The existing literature proposes the concept of a tumour-neural microenvironment in which a reciprocally interacting loop between nerves and cancer cells mutually promotes cancer development (Heinemann et al., 2014;Murakami et al., 2019) (**Figure 4**).

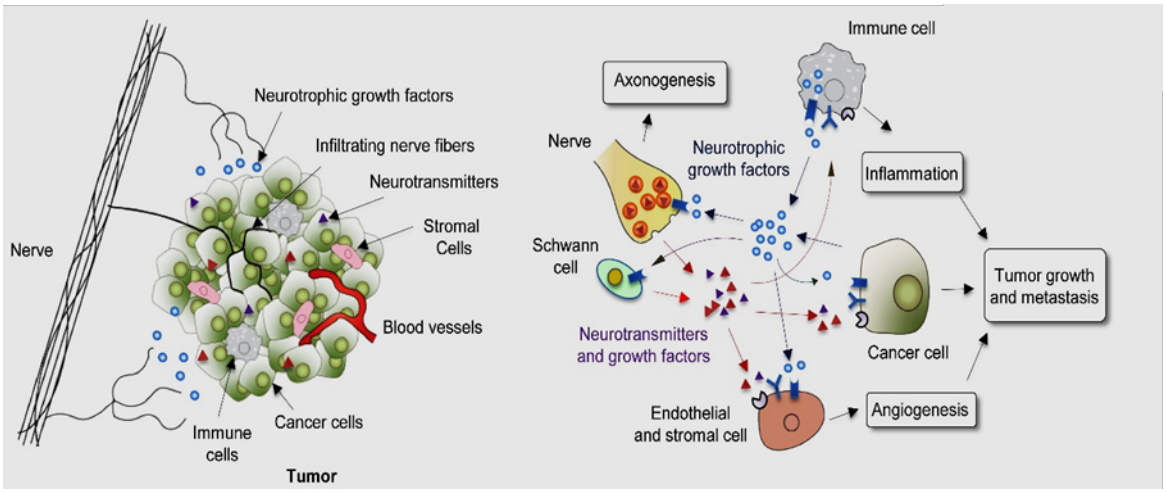

Figure 4. Nerve-cancer cross-talk in TME. *Neurotrophic growth factors (by cancer cells) and neurotransmitters (by nerve endings) released in the TME can also activate stromal, endothelial, and immune cells, and therefore have a stimulatory impact on tumour neo-angiogenesis and inflammation. The cross-talk between nerves, and cancer/stromal cells contributes to tumour growth and metastasis. From (Boilly et al., 2017).*

Cancer cells can be found inside or outside the nerves (Deborde and Wong, 2017). Notably, the nerve structure can be altered, damaged and destroyed upon invasion by cancer cells (Deborde and Wong, 2017). The nerve-cancer cell cross-talk and resultant enhancement of tumour progression involves the liberation of neurotransmitters (such as norepinephrine) and trophic factors by nerve endings (Boilly et al., 2017). This results in the activation of neuro-signalling in both stromal and cancer cells, while neurotrophic factors are released by cancer cells to attract nerve outgrowth in the TME (Boilly et al., 2017) (**Figure 4**).

Emerging data show that many solid tumours are innervated and that nerves actively participate in tumour initiation and progression (Boilly et al., 2017). In animal models of prostate (Magnon et al., 2013) and gastric (Zhao et al., 2014;Hayakawa et al., 2017) cancer, it has been shown that the infiltration of new nerves in the TME is necessary from early initiation to metastasis. In gastric tumorigenesis, the importance of cholinergic innervation has been reported (Zhao et al., 2014;Hayakawa et al., 2017). In prostate cancer, the importance of both adrenergic and cholinergic nerves has been demonstrated, and nerve density has been shown to be increased inside and around the prostate cancer compared to around benign prostate, and correlates with more aggressive tumours (Ayala et al., 2008;Magnon et al., 2013;Bründl et al., 2014). In breast

cancer, adrenergic innervation where nerves infiltrate the TME has been reported to be associated with lymph node invasion (Pundavela et al., 2015;Austin et al., 2017). Increased nerve densities have also been found in the TME of colorectal (Albo et al., 2011) and pancreatic (Ceyhan et al., 2010) carcinomas. In case of brain cancer, neurons stimulate cancer cell growth through the release of neuroligin-3 and pleiotropin promoting glioma cell invasion (Qin et al., 2017).

Sympathetic nerves drive tumour angiogenesis via the liberation of noradrenaline whereas sensory and parasympathetic nerves stimulate cancer stem cells. For example, in PC, sympathetic nerves release noradrenaline stimulating cancer cell proliferation through beta-adrenergic receptors (Renz et al., 2018a). In gastric cancer, the activation of muscarinic receptors in gastric cancer stem cells by acetylcholine liberated by cholinergic nerves stimulates stem cell expansion (Zhao et al., 2014;Hayakawa et al., 2017) and the release of noradrenaline by sympathetic nerves induces an angiogenic switch via the stimulation of beta-adrenergic receptors in endothelial cells (Zahalka et al., 2017). The activation of adrenergic signalling by the release of catecholamines from sympathetic nerves stimulates tumour growth, whereas cholinergic signalling activated by parasympathetic nerves stimulates tumour dissemination (Magnon et al., 2013). Interestingly, recent evidence indicates that parasympathetic nerves can eventually inhibit tumour progression, suggesting a yin–yang type of regulation of cancer by nerves (Faulkner et al., 2019) **(Figure 5)**. This will be discussed in more detail in the 'nerve dependence in PC' section. Furthermore, neuroendocrine cells have been shown as mediators of sensory nerve stimulation in early pancreatic tumorigenesis (Sinha et al., 2017).

2.2.3 Denervation can inhibit cancer progression

The initial demonstration that denervation can inhibit cancer progression was performed in experimental animal models of prostate cancer where the effects of hypogastric nerve denervation were reported (Magnon et al., 2013). Suppression of tumour growth and metastasis by denervation has also been demonstrated in animal models of pancreatic (Saloman et al., 2016a), gastric (Zhao et al., 2014) and skin cancer (Peterson et al., 2015). Additionally, a lower incidence of prostate cancer in patients with spinal cord injuries has been reported suggesting a nerve dependence in cancer progression (Rutledge et al., 2017). The profound impact of nerve ablation on cancer progression including delayed development of precancerous lesions, decreased tumour growth and metastasis has been reported (Saloman et al., 2016b).

2.2.4 Tumour axonogenesis in PC

The infiltration of tumours by growing nerves, or tumour axonogenesis, is emerging as a new hallmark of cancer. During embryonic development or tissue regeneration, axonogenesis is stimulated by the release of neurotrophic growth factors from tissues in order to attract nerve terminals (Boilly et al., 2017;Duraikannu et al., 2019). The mechanisms underlying axonogenesis involve neurotrophic growth factors such as those of the neurotrophin family, including NGF, brain-derived neurotrophic factor (BDNF), neurotrophin-3 (NT3), and neurotrophin-4/5 (NT4/5), which have been shown to drive axonogenesis through the stimulation of tyrosine kinase receptors expressed in nerve terminals (Park and Poo, 2013). A feed-forward loop has been reported wherein the upregulation of NGF and BDNF increases sympathetic innervation and local accumulation of noradrenaline to stimulate the growth of PC cells (Renz et al., 2018a). The production of the leukemia inhibitory factor (LIF), a member of the interleukin 6 family, by PC cells has also been shown to contribute to tumour innervation (Bressy et al., 2018).

2.2.5 Nerve dependence in PC

As mentioned earlier in section 2.1.5, the pancreatic tumour is known to undergo neural invasion in which the tumour accesses the neural network to spread further (Liebig et al., 2009). PNI in PC contributes to adverse pathologic finding including severe abdominal pain, tumour recurrence following curative surgical resection (Ceyhan et al., 2009a;Liebig et al., 2009) and poor prognosis (Liebl et al., 2014). Patients with PNI generally survive two years shorter than patients without PNI (Chatterjee et al., 2012). The finding that 100% of patients with PC exhibit PNI (Liu and Lu, 2002;Pour et al., 2003) has led to investigation of the interaction between cancer cells and nerves.

The normal pancreas is innervated by both sympathetic nerves and sensory nerves from the dorsal root ganglion (DRG) and vagus nerve respectively (Demir et al., 2015). In contrast to the normal pancreas, PC exhibits a higher neural density, marked neural hypertrophy and overexpression of norepinephrine (Ceyhan et al., 2009a;Demir et al., 2010). The neuronal architecture is distorted during PC development and several neuron-related genes are dysregulated to promote tumorigenesis (Ceyhan et al., 2006;Saloman et al., 2018).

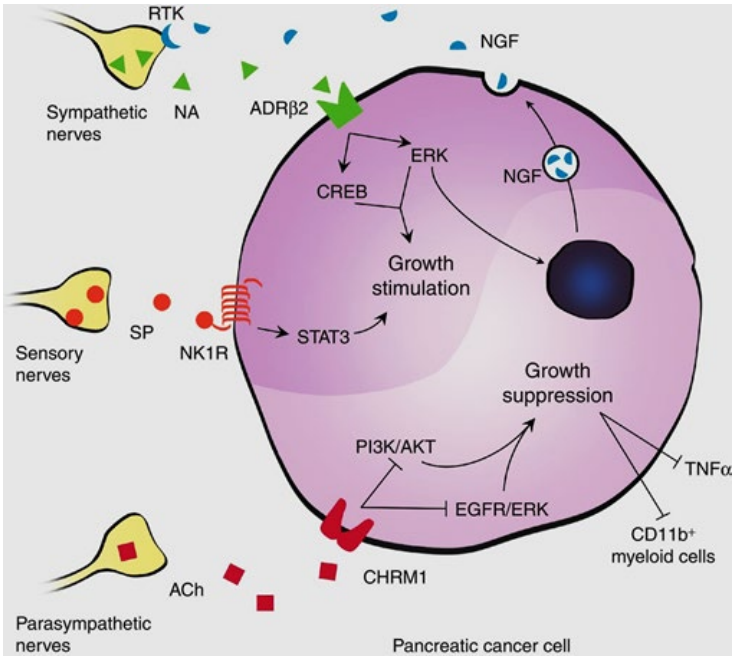

Figure 5. Yin–yang type of regulation by nerves in PC. *The growth of PC cells is regulated by sensory, sympathetic and parasympathetic nerves attracted in the TME by nerve growth factor (NGF) released from PC cells. Sensory and sympathetic nerve activate PC cells growth by releasing substance P (SP) and noradrenaline (NA) from nerve endings and the subsequent activation of the neurokinin-1 receptor (NK1R) in PC cells. On the other hand, parasympathetic nerves inhibit PC cells growth via the liberation of acetylcholine (Ach) and the activation of the cholinergic muscarinic receptor 1 (CHRM1). The opposing impact of sensory and sympathetic vs. parasympathetic nerves suggests the balanced neural innervation in the development of PC. PC, pancreatic cancer, ADRβ2, beta 2 adrenergic receptor; EGFR epidermal growth factor receptor; ERK, extracellular signal response kinase; PI3K/AKT, phosphatidylinositol 3-kinase/ AKT; STAT3, Signal transducer and activator of transcription 3; TNFα, tumour necrosis factor alpha. From (Faulkner et al., 2019).*

Adrenergic, cholinergic and sensory nerves are implicated in pancreatic tumour progression **(Figure 5)**. Sensory (Saloman et al., 2016a;Sinha et al., 2017;Renz et al., 2018a) and sympathetic (Renz et al., 2018a) nerves activate the growth of PC cells through the liberation of substance P (SP) and noradrenaline (NA), and the subsequent activation of the neurokinin-1 receptor (NK1R) as well as the beta 2 adrenergic receptor (ADRβ2), respectively. Sympathetic nerves also activate the release of NGF by cancer cells that activates the corresponding receptor tyrosine kinase TrkA in neurons, leading to more axonogenesis in the TME (Renz et al., 2018a). In contrast to sensory and sympathetic nerves, parasympathetic

nerves inhibit PC cell growth via the liberation of acetylcholine (ACh) and the activation of cholinergic muscarinic receptor 1 (CHRM1) in PC stem cells, leading to the inhibition of downstream PI3K/AKT and EGFR/ERK pathways in PC cells (Renz et al., 2018b). These findings indicate a yin–yang type of control by sympathetic and sensory versus parasympathetic nerves in the regulation of PC progression (**Figure 5**). However, a factor that has received little attention is the role of glial cells, which has been largely overlooked. This will be detailed below.

2.3 Schwann cells (SCs) in cancer progression

2.3.1 SCs: origin, development, function

SCs (named after German physiologist Theodor Schwann) are the most abundant glial cells of the PNS (Takahashi et al., 2013). Other glial cells in the PNS are satellite glial cells, enteric glial cells and olfactory ensheathing cells (Verkhratsky et al., 2019). SCs are vital components of the endoneurial microenvironment of peripheral nerves, serving both as ensheathing and secretory cells (Mizisin, 2014). Structurally, SCs are nucleated and elongated cells which are arranged longitudinally along nerve fibres (Garbay et al., 2000). Since the initial identification of SCs in the 19th century there have been many subsequent investigations into SC development, structure and function as will be discussed.

2.3.1.1 Neural crest cells

SCs originate from neural crest cells, a defining feature of vertebrates, as first described in 1868 by Wilhelm His (His, 1868). Neural crest cells differentiate into a variety of ectomesenchymal and non-ectomesenchymal cell types found throughout an organism (Donoghue et al., 2008). Neural crest cells can also give rise to multiple cell types, including peripheral neurons, melanocytes, chondrocytes, smooth muscle cells and SCs (Bronner and LeDouarin, 2012;Gandhi and Bronner, 2018) **(Figure 6)**.

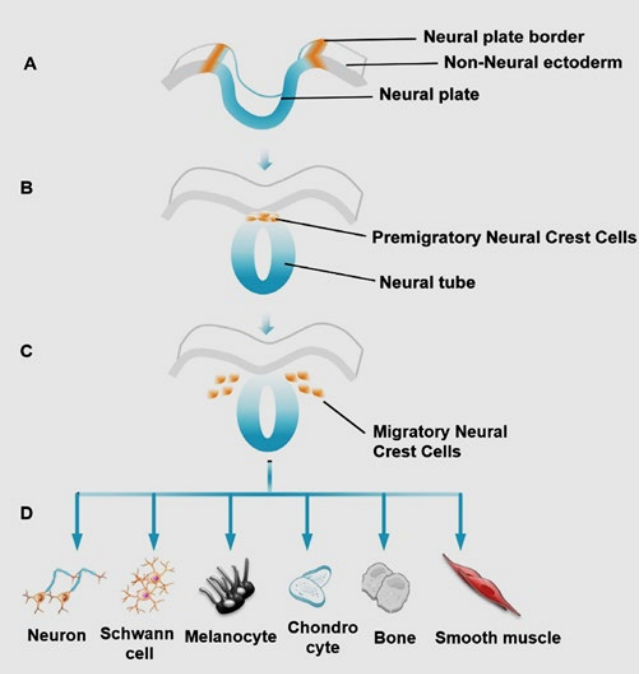

Figure 6: Adult cell types with neural crest ancestry. *A) The neural crest is first induced in the region of the neural plate border. B) After neural tube closure, pre-migratory neural crest cells are situated at the dorsal side. C) Neural crest cells then delaminate to become migratory NCCs. D) Neural crest cells differentiate into multiple cell types. From (Liu and Cheung, 2016).*

2.3.1.2 Developmental stages of SCs

The embryonic phase of SC development involves three transient cell populations such as migrating neural crest cells, SC precursors, immature SCs (Jessen and Mirsky, 2019) (**Figure 7)**. After differentiation from neural crest cells, SC precursors proliferate and migrate down peripheral axons and differentiate into immature SCs and eventually mature, myelinating SCs (mSCs), but they can also give rise to endoneurial fibroblasts, and populations of melanocytes and neurons, demonstrating their plasticity, which allows them to convert from one subtype to another one (Adameyko et al., 2009;Jessen and Mirsky, 2019).

Immature SCs surround axon bundles and perform radial sorting (**Figure 7)**. SCs that have selected a single axon are termed pro-myelinating SCs, which differentiate into mature SCs that generate myelin around an axon. Myelination occurs only in SCs that by chance envelop

large diameter axons, whereas, SCs that ensheath small diameter axons progress to become mature non-myelinating SCs (nmSCs) (Monk et al., 2015).

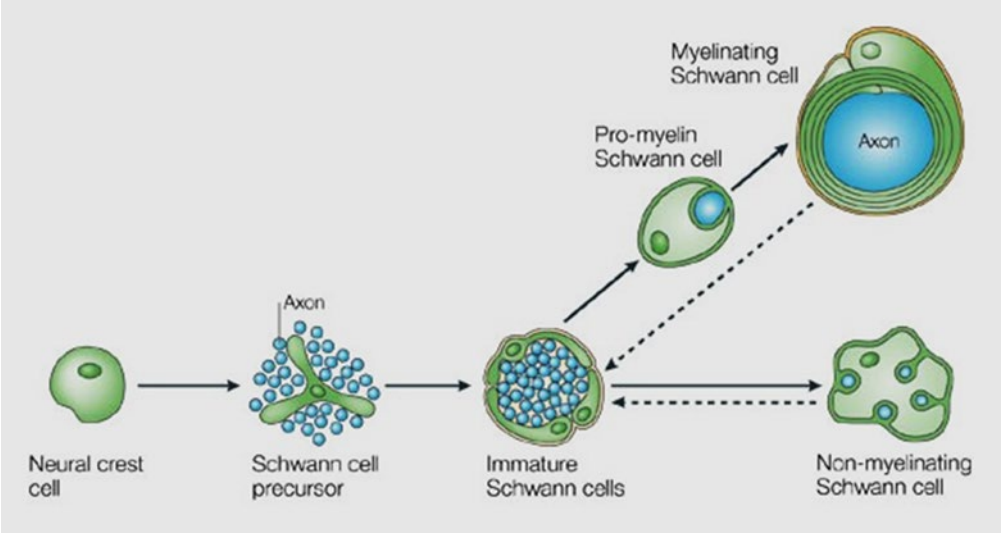

Figure 7: The main transitions in the SC lineage. *Schematic illustration of the main cell types and developmental transitions involved in SC development. Dashed arrows indicate the reversibility of the final, largely postnatal transition during which mature myelinating and non-myelinating cells are generated. From (Jessen and Mirsky, 2005).*

For the generation of SC precursors from neural crest cells **(Figure 7)**, transcription factor Sox10 is required, which is known as SC identity factor. Other molecules that are required in this differentiation process are neuregulin-1 (NRG1), a major regulator of SCs (Shah et al., 1994;Meyer and Birchmeier, 1995;Riethmacher et al., 1997), notch signalling (Morrison et al., 2000) and Pax3 (Jacob et al., 2013). The expression of neurotrophic factors by SCs such as NGF and their tyrosine-kinase receptors p75 neurotrophin receptor ($p75^{NTR}$) and Trk families is also essential for SC development, proliferation, migration, as well as myelination and neuronal regeneration (Woodhoo and Sommer, 2008;Jessen et al., 2015).

SC precursors and immature SCs differ largely in molecular expression, including up-regulation of S100 in immature SC (Jessen et al., 2015). SC precursors that maintain physical contact with nerves differentiate into SCs whereas SC precursors that are detached from nerves differentiate into melanocytes (Adameyko et al., 2009). Thus, the cell fate of SC precursors is

influenced by location (i.e. cellular contact), as well as external and internal signalling mechanisms.

2.3.1.3 SC types

SC precursors give rise to immature SCs, which give rise to mSCs and nmSCs (Gresset et al., 2015) (**Figure 7)**. In the peripheral nerve endoneurium, mSCs and nmSCs exist in a ratio of 2:1 (Salonen et al., 1988;Stierli et al., 2018). mSCs are the most abundant cells within the peripheral nerve trunk (Stierli et al., 2018). Both mSCs and nmSCs are also highly quiescent, forming architecturally stable structures. Once these cell have matured, they exist for the lifespan of the animal, not dividing at all (Stierli et al., 2019). In addition, in injuries or diseases that result in axonal loss or demyelination mSCs become a class of nmSCs that lack axons. Upon receiving appropriate neuronal signals, all of these nmSCs regain their myelinating potential (Taveggia et al., 2005;Griffin and Thompson, 2008). Other nmSCs constitute the satellite cells of the sensory and autonomic ganglia (Taveggia et al., 2005).

2.3.1.4 SC function

Wide variation of functional ability is the hallmark of SCs. SCs are largely responsible for the plasticity of the PNS owing to their ability to dedifferentiate, proliferate, migrate as well as for myelinating axons of motor and sensory neurons of peripheral nerves allowing fast electrical impulse propagation (Colomar and Robitaille, 2004). They also influence nerve repair, trophic support and regeneration of peripheral nerves (Jessen et al., 2015). SCs maintain neuronal homeostasis through the regulation of cell growth, survival and repair (Jessen, 2004;Kaplan et al., 2009). SCs have also been implicated in distal digit tip (mammals) and limb (amphibians) regeneration, extracellular matrix production, upregulation of neuritogenic and neurotrophic factors, initiation of an inflammatory response as well as antigen presentation (Wekerle et al., 1986;Colomar and Robitaille, 2004). SCs also play a vital role in neuroblastoma maturation (Ambros et al., 1996). SCs have been reported to promote synapse formation and function and stimulate the development and maintenance of the neuromuscular junction (Feng and Ko, 2008). At the developing neuromuscular junction SCs help in clearing of degenerating myelin and eliminate excess axons and synapses (Bishop et al., 2004;Allen, 2014;Schafer and Stevens, 2015). SCs play a critical role in many pathological processes including injury-induced nerve repair, neurodegenerative diseases, infections and neuropathic pain (Zhang et al., 2020). SCs

likely contribute significantly to the pathogenesis of diabetic neuropathy, as there is ample evidence demonstrating that hyperglycemic and oxidative stress damage SC mitochondria and lead to aberrant lipid metabolism, inflammation and neuropathy (Mizisin, 2014;Gonçalves et al., 2017). SCs have recently been highlighted for their involvement in cancer progression, which is the main focus of my study.

2.3.1.5 SC role following nerve injury

SCs play a unique role in orchestrating regeneration following peripheral nerve injury providing a growth supportive environment for axonal re- growth (Weiss et al., 2016).

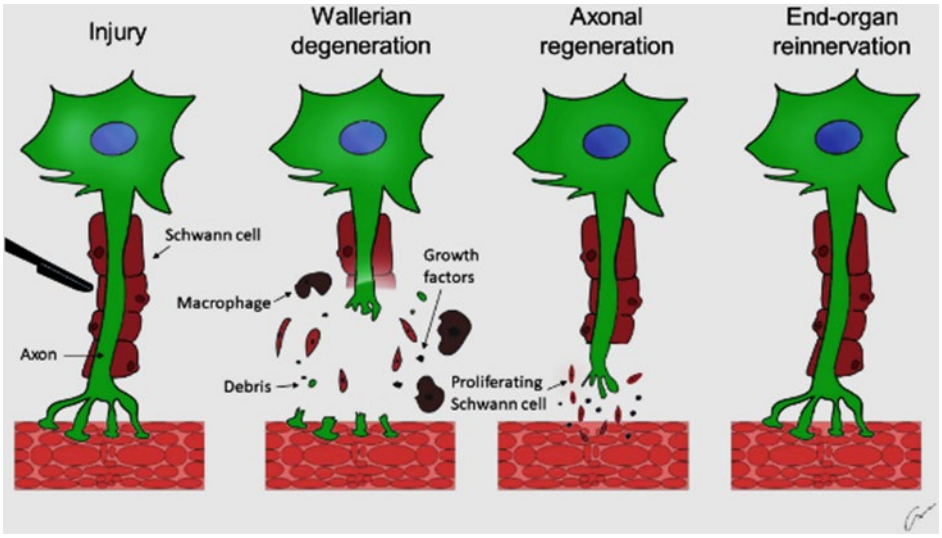

Figure 8: Nerve regeneration after injury in the PNS. *From (Schuh et al., 2020).*

The major goal of the regeneration process is for axons to regrow back to their targets (Stierli et al., 2019). Within hours of the nerve injury, SCs distal to the injury dedifferentiate, proliferate and upregulate a broad range of cytokines, chemokines and neurotrophic factors (Ydens et al., 2013;Tzekova et al., 2014;Jessen and Mirsky, 2016). Following peripheral nerve injury, a complex series of cellular events, called Wallerian degeneration, takes place distal to the site of the lesion in which axons downstream of the wound site degenerate (Stoll et al., 2002) (**Figure 8**). Part of the process involves SCs phagocytosing cell debris and recruiting macrophages to the site of the injury. SCs align to form bands of Büngner, creating a path for the axons to regenerate. Finally, the axons reinnervate the target organ. It is thought that

damaged neurons send injury signals sensed by SCs with the SCs then becoming activated to perform repair and guidance functions (Deborde and Wong, 2017).

Mature SCs have the ability to change between differentiation states in response to injury that allows the PNS to regenerate after damage **(Figure 8)**. Through an amazing reprogramming process, highly specialized quiescent adult mSCs de-differentiate to proliferating progenitor-like SCs (Mathon et al., 2001). After injury, mSCs lose their characteristic gene expression pattern, degrade their myelin and activate a set of repair-related phenotypes to become a class of nonmyelinating repair SCs which are capable of supporting axon regeneration and axon guidance (Jessen and Mirsky, 2016).

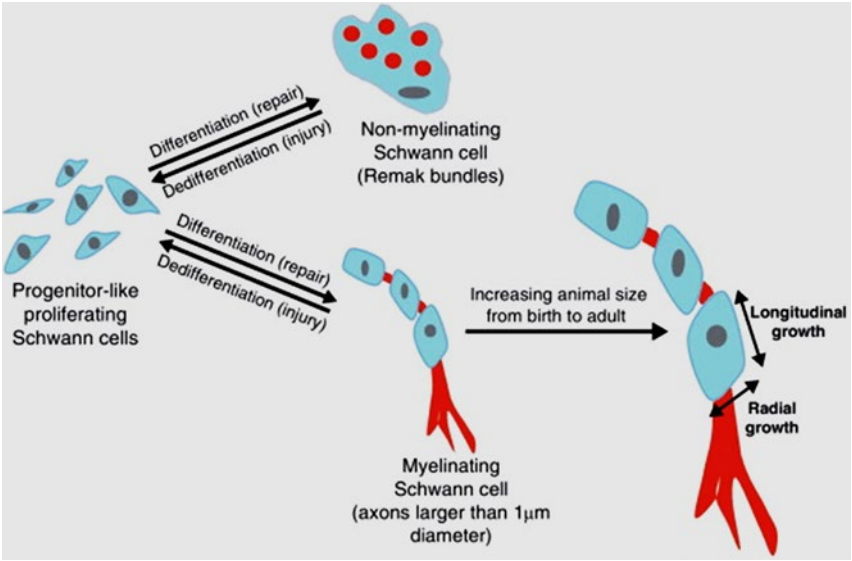

Figure 9. SCs de-differentiation to a progenitor-like state to aid axon regeneration upon injury. *From (Roberts and Lloyd, 2012).*

SCs from Remak bundles also convert into repair SCs. This process is called de-differentiation, activation or trans-differentiation of SCs (Jessen and Mirsky, 2016) **(Figure 9)**. To maintain SCs in their de-differentiated state, sustained expression of Sox-2 following nerve injury has been reported to be sufficient (Roberts et al., 2017). De-differentiated SCs express Olig1, Sonic Hedgehog (Shh) and glial-derived neurotrophic factor (GDNF) at higher levels than immature SCs (Arthur-Farraj et al., 2012).

From the above discussion, it is evident that SCs are abundant and extraordinarily plastic in most organs with a multitude of functions. Because of their regenerative capability, primary

human SCs have already been reported to have potential therapeutic potential for the treatment of spinal cord and peripheral nerve injuries in humans upon transplantation (Andersen et al., 2016;Anderson et al., 2017). Their role in creating a specific TME and supporting tumour progression will be discussed in the following section.

2.3.2 SCs in cancer

SCs have recently been implicated in the progression of several malignancies including pancreatic (Demir et al., 2014;Deborde et al., 2016;Fujii-Nishimura et al., 2018), prostate (Sroka et al., 2016), lung (Zhou et al., 2018), oral (Salvo et al., 2019) and cervical (Huang et al., 2020) cancers. In a normal nerve, the endoneurium consists mainly of axons and SCs. It also contains mast cells, resident macrophages, fibroblasts, and blood vessels. In cancer progression, due to the SC plasticity, SCs have been shown to adopt a de-differentiated phenotype similar to that in response to nerve injury (Stout et al., 2018) **(Figure 9)**.

It is likely that SCs may recruit immune cells to sites of PNI, given they are capable of recruiting macrophages during nerve repair (Jessen et al., 2015). An increase of the number of glial fibrillary acidic protein (GFAP)-positive SCs has been found when nerves are injured or invaded by cancer cells. For example, the SCs associated with cancer cells in human pancreatic (Demir et al., 2014;Deborde et al., 2016), colon (Demir et al., 2014), thyroid and salivary gland cancer are GFAP positive (Deborde et al., 2016). Three-dimensional (3D) co-culturing between cancer cells and SCs revealed that SCs are extremely dynamic and make repetitive contacts with individual cancer cells to promote migration (Deborde et al., 2016). SCs have been shown to be attracted by cancer cells and facilitate neural tracking (Gasparini et al., 2019).

Demir et al show that SCs migrate toward cancer cells by the help of NGF and its low affinity receptor $p75^{NTR}$ (Demir et al., 2014). SCs have also been reported to guide cancer cells while migrating to neurites in a similar way as SCs do in the axonal guidance process by inducing axon sprouting (Deborde et al., 2016). SCs are also able to degrade the matrix around cancer cells (Deborde et al., 2016). SCs help in cancer invasion by matrix remodelling and subsequent physical contact. Direct contact between SCs and cancer cells promotes cancer cell dissociation, migration, and invasion (Deborde et al., 2016). An SC paracrine function in PNI has also been proposed (Shan et al., 2016;Sroka et al., 2016).

2.3.3 SCs in PC

Long before the discovery of the role of SCs in cancer progression generally, PC cells were identified in the epineurium and perineurium in close association with SCs and axons of both intra and extra pancreatic nerves by electron microscopy **(Figure 10)** (Bockman et al., 1994). An increase in the level of SCs was detected in pancreatic intraepithelial neoplasms (PanINs) suggesting SC involvement at the early stage of cancer development (Demir et al., 2014). From this observation, it has been postulated that SCs are involved in the initiation of PC progression.

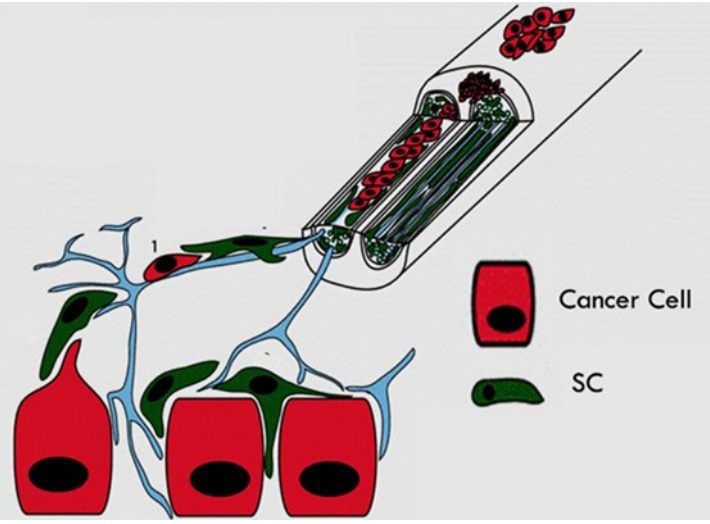

Figure 10. Schematic representation depicting the interaction of nerve, SCs and cancer cells. *Cancer cells can be present in the nerve sections or in the three different layers of the nerve. From (Deborde and Wong, 2017). SC, Schwann cell.*

2.3.3.1 SCs mediate perineural invasion (PNI)

SCs have also been reported to be involved in PNI in PC (Bockman et al., 1994;Deborde and Wong, 2017), the process by which cancer cells invade nerves with specific affinity toward pre–neoplastic and neoplastic PC cells (Demir et al., 2014). SCs have been shown to initiate epithelial-mesenchymal transition and support metastatic spread in PC (Fujii-Nishimura et al., 2018). Basically, SCs are attracted to cancer cells before cancer cells start migrating towards neurons due to a phenomena called SC carcinotropism (Fangmann et al., 2018). This carcinotropism of SCs has been revealed very recently in a 3D neural migration assay where SC-PC cells were co-cultured with DRG neurons and the migration of SCs tracked via digital time-lapse microscopy (Fangmann et al., 2018). This observation suggests that SCs serve as

the first metastatic access for cancer cells leading to tumour progression (Fangmann et al., 2018). Interaction of SCs and PC cells has been revealed by time-lapse video. microscopy (Deborde et al., 2016).

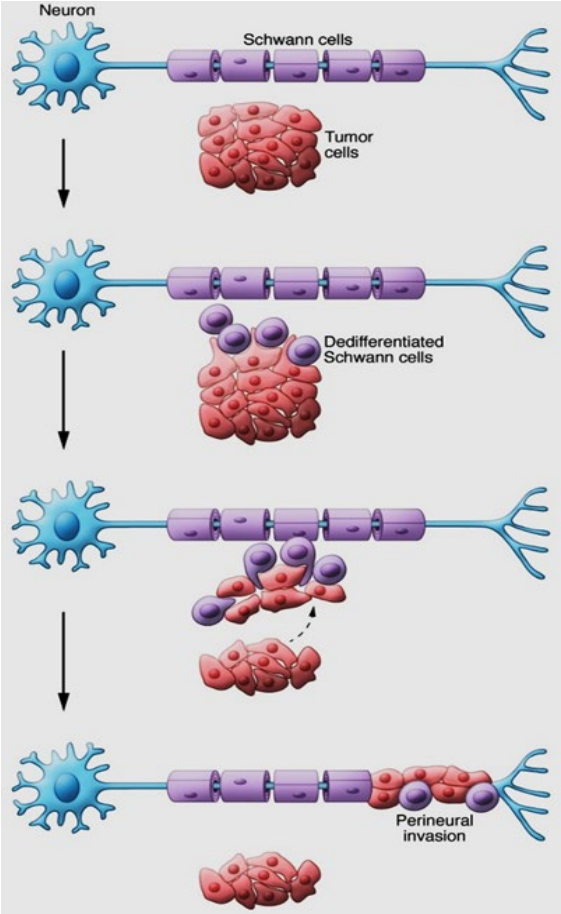

Figure 11. SCs mediate PNI. *From (Azam and Pecot, 2016).*

Physical contact between cancer cells and SCs has been reported to induce cancer cell protrusion formation, leading to cancer cell dispersion and migration which is obligatory for cancer cell invasion (Deborde et al., 2016) **(Figure 11)**. Dedifferentiated SCs come into direct contact with cancer cells. This direct contact results in the extension of protrusions from the cancer cells. SCs intercalate between cancer cells, thereby promoting cancer dispersal from the tumour and migration toward the neuron. This series of events ultimately lead to PNI **(Figure 11)**.

2.3.3.2 SCs mask cancer pain and delay diagnosis

It has been demonstrated that SCs express transient receptor potential ankyrin 1 (TRPA1) channels, known to contribute to nociceptor-mediated neuropathic pain (De Logu et al., 2017). In contrast to neuropathic pain, activated SCs have been reported to mask cancer-related pain, resulting in a prolonged asymptomatic phase both in case of humans and an animal model (Demir et al., 2016). It remains unclear how SC activation by cancers relates to pain sensation.

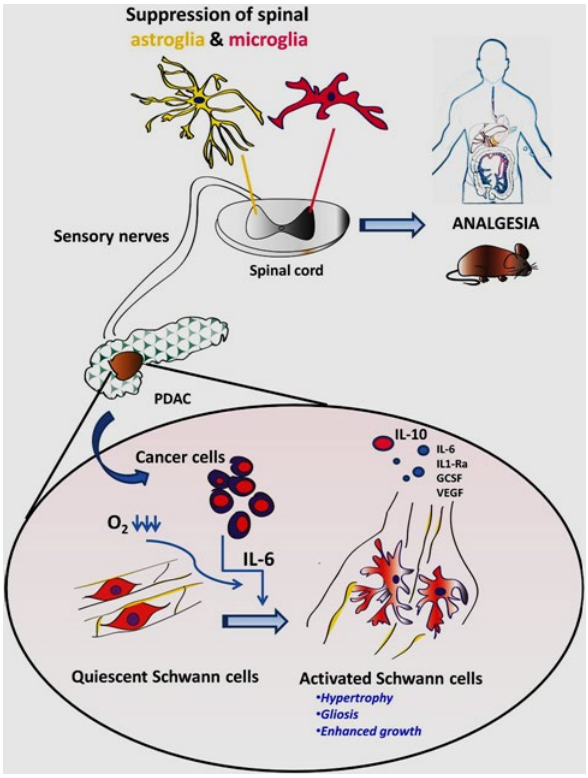

Figure 12. The impact of activated SCs on the course of PC. *SCs become activated in tissue hypoxic condition and by the influence of cancer cells secreted IL-6. These activated SCs suppress cancer pain by extinguishing spinal astroglial and microglial pain sensing activity. PC, pancreatic ductal adenocarcinoma; IL, interleukin; IL-1Ra, interleukin-1 receptor antagonist; GCSF granulocyte colony-stimulating factor; VEGF, vascular endothelial growth factor. From (Demir et al., 2016).*

Activated SCs are proposed to suppress spinal astroglial and microglial (the spinal cells involved in nociception) activity leading to a delay in diagnosis and treatment of PC (Demir et al., 2016) (**Figure 12**). The hypothesis is that SCs in PC become activated under the influence of tissue hypoxia and of interleukin (IL)-6 secreted from cancer cells. These activated SCs

exhibit the same features of 'reactive gliosis' as is the case for astrocytes of the CNS. Increased SC activity in PC results in suppression of spinal astroglial and microglial activity and causes reduced pain sensation, both in murine and human PC (Demir et al., 2016). Additionally, it has been shown that, pain is negatively correlated with SC density, as the expression of GFAP, a marker of SC, was lower in patients experiencing more pain (Demir et al., 2016). In addition to their direct effects on malignant cells, SCs can also indirectly influence cancer progression through their immunomodulatory functions within the TME (Bunimovich et al., 2016). Basically, SCs has been reported to release a multitude of chemokines and cytokines that can attract and modulate immune cells in nerve repair after damage and other pathological conditions.

Our study aims to elucidate the molecular mediators secreted by SCs and investigate their role in the pancreatic TME.

2.4 Secretome: Disease involvement, biomarkers and therapeutic targets

The cell secretome refers to the collection of proteins that contain a signal peptide and are processed via the endoplasmic reticulum and Golgi apparatus through the classical secretion pathway (Dowling and Clynes, 2011). The secretome also encompasses proteins shed from the cell surface and intracellular proteins released through non-classical secretion pathway or exosomes (Karagiannis et al., 2010). These secreted proteins include numerous enzymes, growth factors, cytokines and hormones or other soluble mediators (Dowling and Clynes, 2011). In addition, microRNA, lipids and messenger-RNA may be secreted by the cells via small membranous vesicles, the exosomes and macrovesicles (Théry et al., 2002;Muralidharan-Chari et al., 2010).

Secretome are involved in many cellular activities, such as cell interaction, signalling, proteolysis, adhesion, proliferation, migration, invasion, immune response and angiogenesis by regulating cell-to-cell and cell-to-extracellular matrix interactions (da Cunha et al., 2019). The secretome is very dynamic in nature and highly sensitive to changes of the overall cellular state, whether at physiological or pathological circumstances (Mustafa et al., 2017). Therefore, functional secretory pathways are necessary for the normal physiology of human body and any dysfunction or malfunction may lead to a various systemic problems including cancer (Wang and Kaufman, 2016).

Conditioned media (CM) contain secreted factors which are involved in intercellular communication and have significant biological effects (Weng et al., 2016). Therefore, they might also be a source for early detection and diagnosis of disease, and identification of released factors, including proteins, might help to discover novel biomarkers of potential clinical significance (Stastna and Van Eyk, 2012). Analysis of CM has proven to be a very successful strategy for the identification of candidate biomarkers for further validation in clinical samples and advances in mass spectrometry and bioinformatic approaches have had an influence on proteomics (Wong et al., 2009). These advances combined with the analysis of CM will facilitate the identification of candidate biomarkers. It is also very likely that candidate biomarkers for early detection or monitoring could be useful as therapeutic targets.

2.4.1 Secreted proteins in different diseases

CM from a variety of cells derived from the CNS has been shown to affect proliferation, survival and differentiation of neural stem/progenitor cells (Taupin et al., 2000;Chang et al., 2003;Kaneko et al., 2003;Faijerson et al., 2006). CM factors have been reported to provide signalling molecules for proliferation of neural progenitor cells required for neurogenesis in dopaminergic neurons (Aliaghaei et al., 2016). Adipocytes have been reported to release factors that contribute to increase heart failure risk (Lamounier-Zepter et al., 2006).

The therapeutic benefit of CM is attributed to the paracrine effects of cells in the cell-based therapy (Zagoura et al., 2012). CM taken from epithelial cells of choroid plexus (CPECs-CM) was capable of inducing neuronal and dopaminergic differentiation of umbilical cord mesenchymal stem cells (MSCs) (UCMSCs) (Aliaghaei et al., 2016). Systemic infusion of CM derived from MSCs has been shown to exhibit a therapeutic potential similar to that of MSC therapy for the treatment of acute liver failure (ALF) (Xagorari et al., 2013;Chen et al., 2015). MSC-CM, including their secreted factors, microvesicles and exosomes, exhibits an effect similar to that of MSCs for the treatment of ALF (Chen et al., 2015;Lotfinia et al., 2016;Chen et al., 2017;Phinney and Pittenger, 2017;Cha et al., 2018). Recent studies investigated that CM extracted from MSCs have neuromodulator effects even could prevent neurodegeneration (Mehrabadi et al., 2019). The administration of CM can overcome the genomic instability, immune reactivity, and tumorigenic potential of stem cell transplantation (Gazdic et al., 2017).

Adipose stem cell CM protects dopaminergic neurons in Parkinson's disease (Nakhaeifard et al., 2018). Consequently, the therapeutic potential of CM derived from different cells is attracting increased attention in the field of cell-based therapy (Fouraschen et al., 2012;Wang et al., 2015).

2.4.2 Secreted proteins in cancers

Factors secreted by cancer cells are involved in the cross-talk between cancer cells and other cells, and have an impact on cancer progression and metastasis (Bose and Masellis, 2005;Kaminski et al., 2006). Cancer cells modify their protein secretion due to the continuous growth and adaptation to the TME which is the hallmark of cancer (Zullo et al., 2015). Secreted proteins into the extracellular space interact between stroma and tumour cells and represent the main molecules involved in the intercellular communication, cell adhesion and invasion (Anderson et al., 2009). Peptides or low molecular weight proteins preferentially secreted by cancer cells may serve as tumour markers (Sato et al., 2001). Using the cancer cell secretome approach, more than 100 candidate biomarkers for different cancer types were discovered (Xue et al., 2008;Makridakis and Vlahou, 2010;Pavlou and Diamandis, 2010;Schaaij-Visser et al., 2013).

As secreted proteins are linked to the development of cancer, several studies have compared the secretome of cancer cells to the normal tissue and have seen a differential regulation of proteins (Makridakis and Vlahou, 2010). For instance, the glioma secretome includes proteins, nucleic acids, and metabolites that are often overexpressed in malignant tissue and contribute to virtually every aspect of cancer pathology (Hoelzinger et al., 2007;Skog et al., 2008;Katakowski et al., 2010;Li et al., 2013;Yeung et al., 2013;Haley and Kim, 2014), providing a strong rationale to target cancer cell-secretory mechanisms. The cancer secretome can also induce a resistance mechanism to chemotherapy (Madden et al., 2020). The proteins nodal and activin are necessary for cancer stem cells self-renewal in PC (Lonardo et al., 2012). It has been reported that nodal and activin in the CM of pancreatic stellate cells promoted the invasiveness of PC (Lonardo et al., 2012). IL-6 is a bioactive multifunctional cytokine which promotes the accumulation of myeloid derived suppressor cells (MDSC) and increased the migration of PC cells via STAT-3 pathway (Hamada et al., 2016;Wu et al., 2017). Therefore, detection and quantification of secretome composition could be instrumental for deciphering

the molecular architecture of PC and defining specific approaches toward patient management and therapy.

2.4.3 SC-secreted proteins in PC development

2.4.3.1 Adhesion proteins

Several molecules involved in the SC-PC cell cross-talk, which are either secreted or expressed by SC and/or PC cells, have recently been identified. One such molecule is the neural cell adhesion molecule 1 (NCAM1), which is expressed by neurons and developing SCs and has been found by many researchers to play a crucial role in neural growth, adhesion and regeneration (Gasparini et al., 2019). Notably, SCs guide cancer cells toward nerves via the production of NCAM1 that promotes PNI (Deborde et al., 2016). Moreover, decreased invasion of PC cells into the sciatic nerve in NCAM1 knockout mouse compared to wild type mice has been reported, indicating this adhesion molecule as a critical mediator in SC–induced PC cell invasion (Deborde et al., 2016).

2.4.3.2 Neurotrophic factors

In SC-PC cross-talk, the neurotrophin family of growth factors and their receptors play an active roles. NGF, brain-derived neurotrophic factor (BDNF) as well as neurotrophin-3 (NT-3) are expressed at higher levels in SCs of PC patients compared to healthy controls (Sakamoto et al., 2001). It was found that NT-3 is expressed in SCs from 73% PC patients whereas both NGF and BDNF are expressed in SCs from 27% of PC patients (Sakamoto et al., 2001). NGF has been shown to help migration of SCs toward PC cells prior to PNI (Demir et al., 2014). NGF mediates this migration through its low affinity $p75^{NTR}$ which is expressed on SC repair (Taniuchi et al., 1988;Jessen and Mirsky, 2016). Mice embryo lacking $p75^{NTR}$ show a defect in SC migration with an inhibition of axon growth (Bentley and Lee, 2000). A small molecule inhibitor of $p75^{NTR}$, RO.08.2750, caused reduced migration of SCs towards cancer cells preventing the binding of NGF to $p75^{NTR}$ (Demir et al., 2014). This suggested a role for NGF and $p75^{NTR}$ in promoting nerve infiltration via SC migration.

BDNF secreted by SCs in conditioned medium in culture have been reported to increase the epithelial-mesenchymal transition process in the case of salivary adenoid cystic carcinoma (Shan et al., 2016). The authors have also shown involvement of the BDNF receptor, TrkB, in this process (Shan et al., 2016). In another study, conditioned medium from SC lines was shown to increase the integrin-dependent invasion of prostate and PC cell lines (Sroka et al., 2016).

2.4.3.3 Cytokines and chemokines

Cytokine, IL-6, released by activated SCs, has been reported to augment PC cell migration and invasion (Su et al., 2020) and impede pain signalling in an animal model at the early stages of PC **(Figure 11)**. SC-secreted chemokine CCL2 induces cancer invasion leading to PNI (Bakst et al., 2017). In nerve repair, CCL2 contributes to macrophage recruitment facilitating nerve repair through myelin debris clearance (Jessen et al., 2015). In the case of lung cancer, the promotion of epithelial–mesenchymal transition and metastatic spread were mediated by SC-derived chemokine CXCL5 (Zhou et al., 2018).

2.4.3.4 Glycoproteins

SC-expressed myelin-associated glycoprotein (MAG) binds to the transmembrane protein mucin 1 (MUC1) which is overexpressed in PC. Adhesive interactions between MUC1 and MAG have also been shown to be responsible for PNI, metastasis and poor prognosis of PC (Nakamori et al., 1994).

Together, the above studies have shown the emerging importance of SCs in PC progression. Although few neurotrophic factors, secreted cytokines (Roger et al., 2019) and adhesion molecules (Na'ara et al., 2019) have been described in SC-PC cross-talk, the secretome of SCs and its impact in PC remain largely unknown. In our project, we have profiled the secretome of human SCs using LC-MS/MS and investigated the role of several identified proteins in the stimulation of PC growth and invasion. Therefore, a more detailed understanding of the cellular and molecular mechanisms involved in the regulation of cancer progression by SCs is warranted and has been explored throughout this PhD project. A better understanding of the SC-secretome and their role may help in the development of therapeutics to target neuronal involvement in cancer.

Chapter 3 | Proteomic Profile of Human Schwann Cells

3.1 Preface

Chapter 3 contains an original research article entitled "**Proteomic Profile of Human Schwann Cells**" published in the journal *Proteomics*. To define the protein expression profile of primary human SCs, we performed a proteomic analysis by LC-MS/MS. Using various bioinformatics software, we have detailed the most enriched pathways and biological functions in SCs. These findings fit with the supportive role of SCs in peripheral nerves. In addition, several pain receptors and synaptic proteins have been identified which may contribute to the recently discovered role of SCs in pain sensation in cancer. This proteome analysis will serve as a reference for future investigations of biological processes where SCs are involved.

3.2 Publications

Published article "**Ferdoushi A**, Li X, Jamaluddin MFB and Hondermarck H: **Proteomic Profile of Human Schwann Cells.** Proteomics. 2020 January; 20(1): 1900294" displays from page 37 to 41.

Supplementary Files

Supplementary file displays on page 42 to 46.

Proteomics
Proteomics and Systems Biology
www.proteomics-journal.com

Proteomic Profile of Human Schwann Cells

*Aysha Ferdoushi, Xiang Li, Muhammad Fairuz Bin Jamaluddin, and Hubert Hondermarck**

Schwann cells (SC) are essential for the growth, maintenance, and regeneration of peripheral nerves, but the proteome of normal human SC is poorly defined. Here, a proteomic analysis by LC–MS/MS is performed to define the protein expression profile of primary human SC. A total of 19 557 unique peptides corresponding to 1553 individual proteins are identified. Ingenuity Pathway Analysis (IPA), Gene Ontology (GO), and Database for Annotation, Visualization, and Integrated Discovery (DAVID) are used to assign protein localization and function, and to define enriched pathways. EIF2, mTOR, and integrin signaling are among the most enriched pathways and the most enriched biological function is cell–cell adhesion, which is in agreement with the supportive role of SC in peripheral nerves. In addition, several nociceptors and synaptic proteins are identified and may contribute to the recently discovered role of SC in pain sensation and cancer progression. This proteome analysis of normal human SC constitutes a reference for future molecular explorations of physiological and pathological processes where SC are involved.

Schwann cells (SC) are the glial cells of the peripheral nervous system. Aside from their well-established role in producing the myelin sheaths around axons, SC also influence impulse conduction along axons and provide trophic support for repair and regeneration of peripheral nerves.[1] Undifferentiated SC are increasingly described to participate in human health and disease, and are involved in pathologies, such as schwannomatosis, by acting through growth factors secretion, the regulation of inflammation, and macrophages activation.[2] Recent studies have also revealed SC involvement in tumorigenesis[3] where they contribute to the stimulatory role of nerves in cancer progression, by facilitating the crosstalk between cancer cells and nerves.[4] Despite the important biological and pathological implications of SC, there are limited data on the proteome of normal human SC,[5] which remains poorly defined.

A. Ferdoushi, X. Li, Dr. M. F. B. Jamaluddin, Prof. H. Hondermarck
School of Biomedical Sciences and Pharmacy, Faculty of Health and Medicine
University of Newcastle
Callaghan, NSW 2308, Australia
E-mail: hubert.hondermarck@newcastle.edu.au
A. Ferdoushi, X. Li, Dr. M. F. B. Jamaluddin, Prof. H. Hondermarck
Hunter Medical Research Institute
University of Newcastle
New Lambton NSW 2305, Australia

The ORCID identification number(s) for the author(s) of this article can be found under https://doi.org/10.1002/pmic.201900294

DOI: 10.1002/pmic.201900294

In the present study, we performed a proteomic analysis by LC–MS/MS to identify the protein profile of normal human SC in primary culture. An outline of our experimental protocol is shown in **Figure 1**. Primary human SC, obtained from spinal nerve cells of healthy donors, were purchased from ScienCell Research Laboratories (Catalog #1700, Carlsbad, CA, USA) and maintained according to manufacturer instructions. T-75 flask poly-L-lysine-coated culture vessels (2 µg cm^{-2}) were prepared by adding 15 µL of poly-L-lysine stock solution (10 mg mL^{-1}, Catalog #0413, Carlsbad, CA, USA) in 10 mL sterile water and incubated overnight at 37 °C. Cells were seeded at 5000 cells cm^{-2} density on the poly-L-lysine coated flask after washing the vessel with sterile milli-Q water. Cells were grown to 80% confluency in SC medium (SCM, Catalog #1701, Carlsbad, CA) supplemented with 5% fetal bovine serum (FBS, Catalog #0025, Carlsbad, CA, USA), 1% of SC growth supplement (SCGS, Catalog #1752, Carlsbad, CA, USA), and 1% of penicillin/streptomycin solution (P/S, Catalog #0503, Carlsbad, CA, USA) in a humidified incubator at 37 °C with 5% CO_2. Harvested cells (1×10^7 cells) were centrifuged at 800 × *g* for 5 min and cell pellets was collected after washing three times with cold phosphate buffered saline (PBS). Cell pellet was solubilized in 400 µL ice-cold 0.1 M Na_2CO_3 (pH 11) with protease and phosphatase inhibitor cocktail (Roche, Indianapolis, IN, USA) and subjected to probe tip sonication (Hielscher Ultrasound Technology, Germany) for 3 × 10 s intervals at 4 °C. Protein concentration was measured by bicinchoninic acid (BCA) assay (Pierce, Thermo Fisher Scientific, IL, USA) and 200 µg proteins were mixed with urea/thiourea denaturation buffer to a final concentration of 6 M urea/2 M thiourea followed by cysteine reduction using 10 mM dithiothreitol for 30 min at room temperature. The samples were subsequently alkylated in the presence of 20 mM iodoacetamide for 30 min at room temperature in the dark. Proteins were then digested with Lys-C/trypsin (Promega, Madison, WI) at 1:40 (enzyme/protein, w/w) for 3 h at room temperature in the dark. Following Lys-C/trypsin digestion, the solution was diluted below 1 M urea, 0.33 M thiourea by adding 20 mM triethylammonium bicarbonate (pH 7.8) and incubated overnight at room temperature to activate trypsin digestion. After digestion, (2% v/v) formic acid was added to the peptide solutions following centrifugation at 14 000 × *g* for 10 min at 4 °C to precipitate lipids.

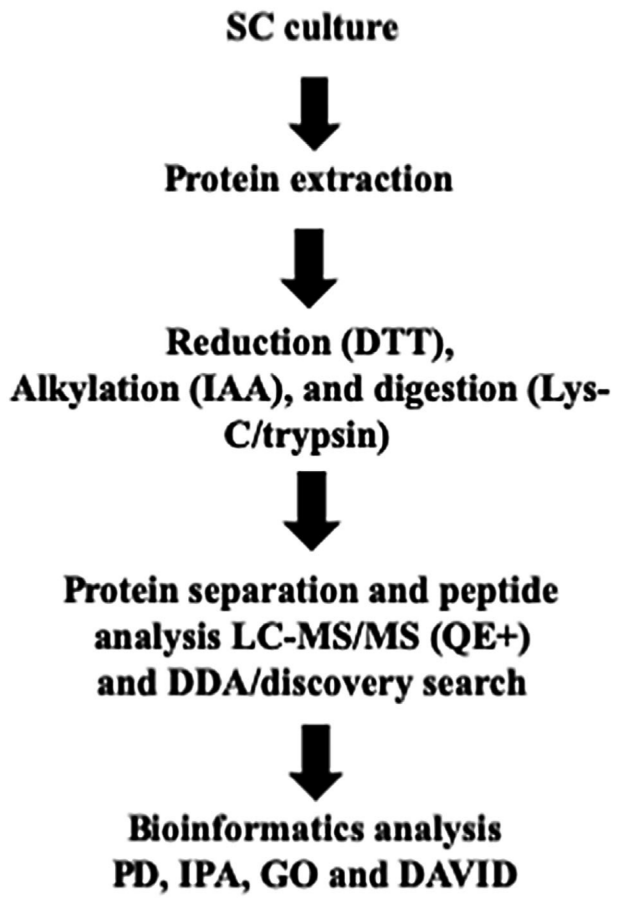

Figure 1. Proteomics workflow. Proteins isolated from primary human SC cultures were extracted and subjected to reduction (DTT), alkylation (IAA) and Lys-C/trypsin digestion before analysis in LC–MS/MS. DDA discovery search was performed to identify the total number of peptides and proteins. IPA, GO, and DAVID bioinformatics tools were used to assign protein localization, function, and to define the canonical pathways. DDA, data-dependent acquisition; DAVID, Database for Annotation, Visualization and Integrated Discovery; DTT, dithiothreitol; GO, Gene Ontology; IAA, iodoacetamide; IPA, ingenuity pathway analysis; PD, Proteome Discoverer; SC, Schwann cells.

The supernatant of peptide samples was desalted using Visiprep vacuum manifold (12-port, Sigma–Aldrich) coupled with Empore C18 Solid phase extraction (SPE) cartridge (4 mm mL^{-1}) according to manufacturer instructions. Digested peptides were acidified (pH 2–3) using 10% trifluoroacetic acid (TFA) before loading on SPE cartridge. The SPE cartridge was activated with 100% acetonitrile followed by washing with 0.1% TFA, and the acidic samples were loaded and washed with 0.1% TFA. Subsequently, peptides were eluted sequentially with 60% acetonitrile, 0.1% TFA then 80% acetonitrile, 0.1% TFA, and 100% acetonitrile. The peptide eluents were quantified using Invitrogen Qubit Protein Assay (Life Technologies Australia Pty Ltd), followed by lyophilization and resuspension with MS loading buffer (2% acetonitrile, 0.1% TFA). All resuspended samples were stored at −80 °C. A total of 500 ng peptides were injected and separated prior to MS using a Dionex ultimate Nano/Cap 3500-RS LC system (Thermo Fisher Scientific) at a constant flow rate of 300 nL min^{-1} using an EASY-Spray PepMap C18 LC column (75 µm × 15 cm, C_{18}, 2 µm, 100 Å, Thermo Fisher Scientific), with a 150 min gradient. Solvent A was water, 0.1% formic acid, and solvent B was acetonitrile, 0.1% formic acid; peptides were first injected with 2% solvent B for 6 min and eluted by a gradient from 2% to 35% solvent B from 6 to 126 min, then 35% to 90% solvent B over a further 0.1 min, the remaining peptides were washed away using 90% solvent B for 1.9 min followed by a 22 min equilibration step (2% solvent B) before LC returning to the starting conditions. Q-Exactive Plus High Resolution Quadrupole-Orbitrap (Thermo Fisher Scientific) MS/MS was used for discovery MS assay. Precursor ions were measured with a full mass scan (400–2000 m/z, with a resolution of 70 000), an AGC target value at 1e6, and maximum injection fill time 50 ms. The product ions were fragmented with a normalized collision energy of 27.0 and measured at resolution of 35 000 on the Orbitrap. AGC target value was set at 2e5 and maximum injection fill time is 120 ms to control the correct ion population within the Orbitrap. Dynamic exclusion was employed for 30 s. The MS raw files were processed using Proteome Discoverer (PD) software (version 2.1, Thermo Fisher Scientific, San Jose, CA) and searched against the Uniprot human protein database (downloaded March 05, 2018, with a total of 71 773 entries).[6] The tolerance of precursor masses and fragment masses were set at 10 ppm and 0.02 Da, respectively. Trypsin was set as the digestion enzyme with two missed cleavage permitted. Protein confidence indicators were set at 1% false discovery rate (FDR). The precursor ion (MS) spectra were also manually validated using Xcalibur Software (version 4.0.27.13, Thermo Fisher Scientific) to avoid false positive detection.

The results show that a total of 19 557 unique peptides corresponding to 1553 individual proteins were identified in two replicates, with a confidence corresponding to a false discovery rate < 1% (Figure S1 and Tables S1 and S2, Supporting Information). Only high confidence identification, represented by at least two unique peptides, was included in the analysis. The dataset has been deposited in the Mass Spectrometry Interactive Virtual Environment (MassIVE) database with the dataset identifier: MSV000084303 and are publicly accessible by using the following link: https://massive.ucsd.edu/ProteoSAFe/dataset.jsp?task=3c44b37f1b1949d8a446c2fd7f942e68 (username: aysha; password: Reviewer). Out of the 1553 proteins identified, a total of 1329 proteins were found in the two replicates (85.6% of total protein number; Figure S1, Supporting Information). Detailed information on identified peptides and proteins is provided in Tables S1 and S2, Supporting Information. The list of common proteins was extracted to perform Ingenuity Pathway Analysis (IPA; QIAGEN Redwood City). Proteins were classified according to subcellular localization (**Figure 2**a; Table S3, Supporting Information), functions (Figure 2b; Table S3, Supporting Information), as well as the most predominant and significant canonical pathways (**Figure 3**; Table S4, Supporting Information). Most proteins were cytoplasmic (65%), others were nucleic (21%), or in the plasma membrane (9%), as well as the extracellular space (4%; Figure 2; Table S3, Supporting Information). In addition, the functions of these proteins were classified as related to catalytic activity (42%), transportation (8%), regulation of transcription (6%), translation (4%), ion channel (1%), and others (39%) including cytokine and growth

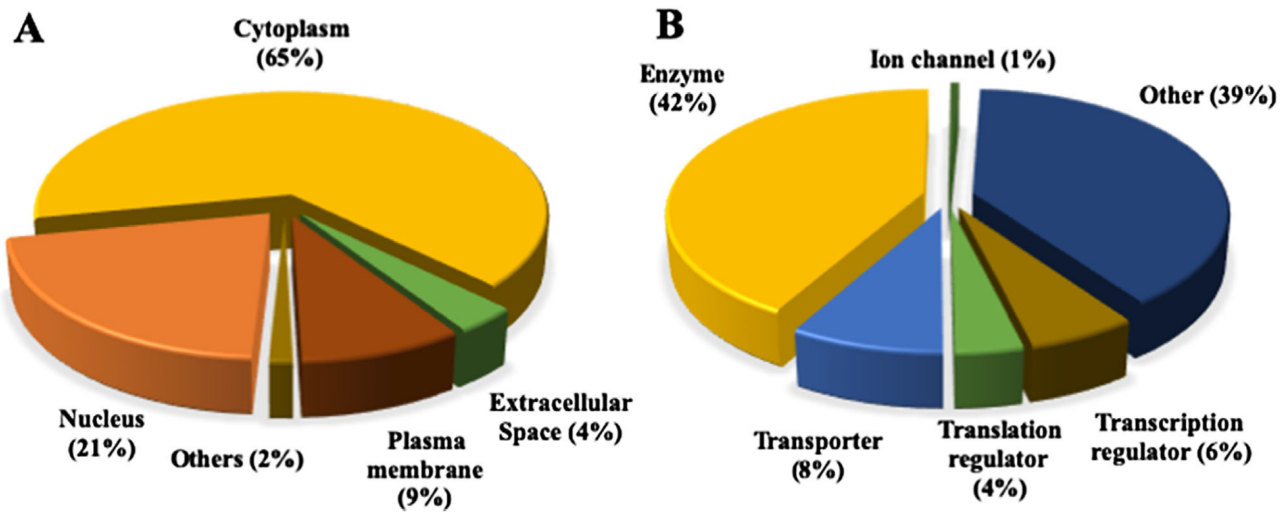

Figure 2. Categorization of human SC proteins by subcellular localization (a) and general function (b). Presented as percentages of the total number of identified proteins.

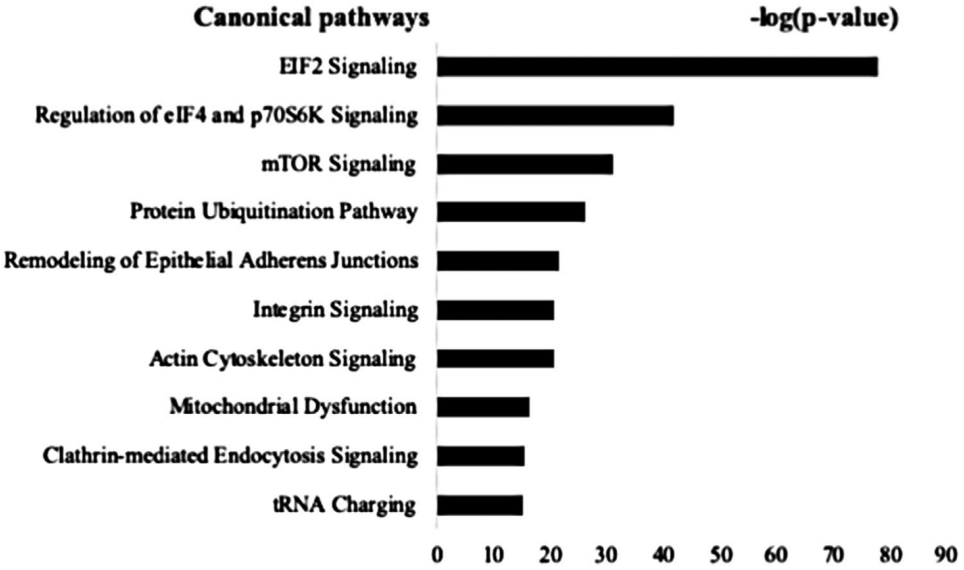

Figure 3. Canonical pathways analysis of human SC proteome using IPA. The top ten most significant pathways are presented.

factors activities (Figure 2b; Table S3, Supporting Information). Canonical pathway analysis was performed with the standard IPA library. The results (Figure 3; Table S4, Supporting Information) revealed a number of pathways including EIF2 signaling (–logP value = 77.7), mTOR signaling (–logP value = 30.9), integrin signaling (–logP value = 20.5), epithelial adherens junction signaling (–logP value = 14), and PI3K/AKT signaling (–logP value = 10.3). The significant enrichment of the EIF2 signaling suggested that there is an elevated rate of protein synthesis and Ephrin receptor signaling presumably associated with the reported regenerative abilities of SC.[1] In addition, mTOR signaling has also been previously reported to control axon growth and myelination after axonal sorting[7] and integrin signaling promotes proliferation, maturation, and differentiation of SC.[8] While, Rho Family GTPases signaling indirectly regulate SC migration,[9] the PI3K/AKT pathway has been described the control of myelination.[10] Functional-enrichment analysis for Gene Ontology (GO) term was performed using Database for Annotation, Visualization, and Integrated Discovery (DAVID, v6.8, https://david.ncifcrf.gov/) searching against the entire *Homo sapiens* genome and the biological processes and molecular functions were analyzed by GO annotation and are presented in Figure S2 and Tables S5 and S6, Supporting Information. Cell–cell adhesion was found to be the most enriched function. Cell–cell adhesion are required in many developmental stages of myelinating SC, such as cell attachment, process extension, axon ensheathment, as well as nodes of Ranvier construction.[11] Other significant biological processes include translational initiation, oxidation–reduction process, viral transcription, and protein binding (Figure S2, Supporting Information). To

investigate the potential associations of the identified proteins with diseases, the dataset was subjected to DAVID Genetic Association Database (GAD) analysis, an annotated resource that links human genes and polymorphisms to diseases. The top identified diseases were infectious diseases (21%), cancer (20%), and neurological disorders (19%; Figure S3 and Table S7, Supporting Information). We also examined the top 20 diseases related to SC proteome and presented in Figure S4 and Table S8, Supporting Information. Neurodegenerative disorders were found among the top identified diseases.

In terms of physiological relevance, it is difficult to extrapolate biological functions from a descriptive proteomic analysis. However, the SC protein dataset that we report here constitutes a reference list of proteins expressed in normal SC that will be useful as a control for studies investigating pathological situations where SC are involved. This is the case for instance in schwannomatosis, where an aberrant proliferation of SC leads to the development of a benign tumor that, although not cancerous, can be particularly invalidating for patients.[12] Pathological SC lines or primary cultures are used for in vitro and in vivo investigations in schwannomatosis, and although protein expression profile would be different from cultured SC to SC–neuron interactions, the present dataset provides a proteome reference for SC in basal conditions that can be accessed and downloaded by the community. In addition, the present dataset may also be of a more direct value in the areas of pain and oncology, where SC have recently been shown to be involved.

A recent landmark paper has reported the discovery that SC can initiate pain sensation.[13] Until now, it was considered that pain sensation in the skin was initiated by direct activation of pain receptors (nociceptors) in nociceptive sensory nerve endings. However, Abdo et al.[13] have shown that SC convey painful thermal and mechanical sensitivity to nerve endings, and therefore SC now appear to be inherently sensitive and transmit pain information to nerves. Whereas this paradigm shift is specific to the skin or does apply to other organs and tissues remains to be investigated, but it is noteworthy to point that in the SC proteome reported here, there are several nociceptors. For instance, the thermosensitive ion channel TRPV2 (transient receptor potential v2) and the cold receptor TRPM8 (transient receptor potential cation channel subfamily member 8)-associated proteins were identified with high confidence (Table S1, Supporting Information). As far as we are aware, this is the first time that these nociceptors, which are normally found in sensory nerves, are described in SC and this data suggest that TRPV2 and TRMP8 may be involved in the initiation of pain sensation occurring in SC.[13] Additionally, the transmission of pain signal from SC to neurons involves synapse-like structures and we have also identified several proteins specific of synaptic complexes in SC proteome. This is for instance the case of the synaptic vesicle membrane protein VAT-1, that participates in the release of neurotransmitter containing vesicles, or synaptotagmin-1 (SYT1) that functions as a Calcium sensor for the release of neurotransmitters (Table S1, Supporting Information). Synaptogenesis signaling pathway was also among the top canonical pathways identified by Ingenuity Pathway Analysis (Table S4, Supporting Information). Further functional investigations are warranted to determine the molecular mechanism by which SC initiate pain, and our SC protein database provides a valuable listing of potential protein candidates that should be further investigated for their role in pain signaling. These proteins may ultimately constitute novel molecular targets for future innovative pain treatment.

Aside from pain, cancer progression is another health issue where the involvement of SC has recently been demonstrated. SC have been shown to directly stimulate tumor growth[14] and facilitate the process of perineural invasion by which cancer cells use nerve tracks to disseminate.[3] The crosstalk between cancer cells and neuronal cells is emerging as a new driver of tumorigenesis and SC are an essential component of this interaction.[4] At this stage cancer cells have been shown to produce neurotrophic growth factors, such as nerve growth factor, to stimulate neuronal outgrowth[15,16] and conversely neuronal cells, liberate neurotransmitters such as noradrenalin to stimulate cancer growth[16,17] but this is still early stage and the full extent of molecular mediators involved in the nerve cancer cell crosstalk are yet to be fully defined and in particular the molecular contributors produced by SC. Here again, our SC proteome dataset may provide clues in identifying candidate molecular mediators produced by SC and that may be involved in cancer progression. For instance, the mesencephalic astrocyte-derived neurotrophic factor (MANF) has been identified with high confidence (Table S1, Supporting Information) and should be explored for its potential involvement as an SC mediator in cancer progression. Similarly, other growth factors such as myeloid derived growth factor (MYDGF) and the hepatoma-derived growth factor (HDGF) have also been identified (Table S1, Supporting Information) and further investigations are warranted to determine if they participate in the stimulation of cancer cell growth. Interestingly, proteins normally produced by neuronal cells, including SC, are increasingly regarded as potential new biomarkers and therapeutic targets in cancer[18] and the SC dataset reported here may serve as a reservoir of potential candidates to be further explored in functional in vivo studies.

In summary, this study is an extensive shotgun proteomic analysis of human SC that will serve as an important resource for further functional and clinical investigations of the role of SC in health and diseases.

Supporting Information

Supporting Information is available from the Wiley Online Library or from the author.

Acknowledgements

The authors thank the University of Newcastle and the Maitland Cancer Appeal Committee to support the research.

Conflict of Interest

The authors declare no conflict of interest.

Author Contributions

A.F. and H.H. designed experiment. X.L. and A.F. performed the research. A.F. and M.F.B.J. analyzed the data. A.F., X.L., M.F.B.J., and H.H. wrote

the paper. H.H. supervised the study, editing, and final approval of the manuscript. All authors reviewed, approved, and commented on the manuscript.

Keywords

human Schwann cells, LC–MS/MS, proteomic profiling

Received: September 10, 2019
Revised: October 22, 2019
Published online: December 23, 2019

[1] K. R. Jessen, R. Mirsky, A. C. Lloyd, *Cold Spring Harbor Perspect. Biol.* **2015**, *7*, a020487.
[2] J. B. Aquino, R. Sierra, *Glia* **2018**, *66*, 465.
[3] S. Deborde, T. Omelchenko, A. Lyubchik, Y. Zhou, S. He, W. F. McNamara, N. Chernichenko, S. Y. Lee, F. Barajas, C. H. Chen, R. L. Bakst, E. Vakiani, S. He, A. Hall, R. J. Wong, *J. Clin. Invest.* **2016**, *126*, 1538.
[4] S. Faulkner, P. Jobling, B. March, C. C. Jiang, H. Hondermarck, *Cancer Discov*. **2019**, *9*, 702.
[5] T. Weiss, S. Taschner-Mandl, A. Bileck, A. Slany, F. Kromp, F. Rifatbegovic, C. Frech, R. Windhager, H. Kitzinger, C. H. Tzou, P. F. Ambros, C. Gerner, I. M. Ambros, *Glia* **2016**, *64*, 2133.
[6] R. J. Chalkley, P. R. Baker, K. F. Medzihradszky, A. J. Lynn, A. L. Burlingame, *Mol. Cell. Proteomics* **2008**, *7*, 2386.
[7] J. K. Ness, K. M. Snyder, N. Tapinos, *Nat. Commun.* **2013**, *4*, 1912.
[8] D. L. Sherman, M. Krols, L. M. Wu, M. Grove, K. A. Nave, Y. G. Gangloff, P. J. Brophy, *J. Neurosci.* **2012**, *32*, 1817.
[9] J. Yamauchi, J. R. Chan, E. M. Shooter, *Proc. Natl. Acad. Sci. USA* **2004**, *101*, 8774.
[10] T. Ogata, S. Iijima, S. Hoshikawa, T. Miura, S. Yamamoto, H. Oda, K. Nakamura, S. Tanaka, *J. Neurosci.* **2004**, *24*, 6724.
[11] I. Spiegel, K. Adamsky, M. Eisenbach, Y. Eshed, A. Spiegel, R. Mirsky, S. S. Scherer, E. Peles, *Neuron Glia Biol* **2006**, *2*, 27.
[12] S. R. Plotkin, A. Wick, *Semin. Neurol.* **2018**, *38*, 73.
[13] H. Abdo, L. Calvo-Enrique, J. M. Lopez, J. Song, M. D. Zhang, D. Usoskin, A. El Manira, I. Adameyko, J. Hjerling-Leffler, P. Ernfors, *Science* **2019**, *365*, 695.
[14] G. V. Shurin, O. Kruglov, F. Ding, Y. Lin, X. Hao, A. A. Keskinov, Z. You, A. E. Lokshin, W. A. LaFramboise, L. D. Falo, M. R. Shurin, Y. L. Bunimovich, *Cancer Res.* **2019**, *79*, 2736.
[15] J. Pundavela, S. Roselli, S. Faulkner, J. Attia, R. J. Scott, R. F. Thorne, J. F. Forbes, R. A. Bradshaw, M. M. Walker, P. Jobling, H. Hondermarck, *Mol. Oncol.* **2015**, *9*, 1626.
[16] Y. Hayakawa, K. Sakitani, M. Konishi, S. Asfaha, R. Niikura, H. Tomita, B. W. Renz, Y. Tailor, M. Macchini, M. Middelhoff, Z. Jiang, T. Tanaka, Z. A. Dubeykovskaya, W. Kim, X. Chen, A. M. Urbanska, K. Nagar, C. B. Westphalen, M. Quante, C. S. Lin, M. D. Gershon, A. Hara, C. M. Zhao, D. Chen, D. L. Worthley, K. Koike, T. C. Wang, *Cancer Cell* **2017**, *31*, 21.
[17] B. W. Renz, R. Takahashi, T. Tanaka, M. Macchini, Y. Hayakawa, Z. Dantes, H. C. Maurer, X. Chen, Z. Jiang, C. B. Westphalen, M. Ilmer, G. Valenti, S. K. Mohanta, A. J. R. Habenicht, M. Middelhoff, T. Chu, K. Nagar, Y. Tailor, R. Casadei, M. Di Marco, A. Kleespies, R. A. Friedman, H. Remotti, M. Reichert, D. L. Worthley, J. Neumann, J. Werner, A. C. Iuga, K. P. Olive, T. C. Wang, *Cancer Cell* **2018**, *33*, 75.
[18] X. Li, M. D. Dun, S. Faulkner, H. Hondermarck, *Proteomics* **2018**, *18*, 1800049.

Supplementary Figure S1. Venn diagram summarizing the overlap in protein identification between two independent proteomic analysis which identified 1478(I) and 1404(II) proteins respectively. Additional details are listed in Supplementary Table S2.

Supplementary Figure S2. GO enrichment analysis. GO analysis was performed to comprehend the (A) biological process (BP) and (B) molecular function (MP) of identified proteins using DAVID. Percentage (%) descriptor of DAVID was used to graphically represent the enrichment analysis output. DAVID: Database for Annotation, Visualization and Integrated Discovery. GO: Gene Ontology. Only top 10 BP and MP have been shown here for vertical sizing. See Supplementary Table S5 and S6 for additional details.

Supplementary Figure S3. Distribution of the identified proteins based on disease classes using DAVID. See Supplementary Table S7 for additional details.

Supplementary Figure S4. Disease involvement of the identified proteins (top 20 diseases have been shown here) analysed by DAVID based on GAD. GAD: Genetic Association Database. See Supplementary Table S8 for additional details.

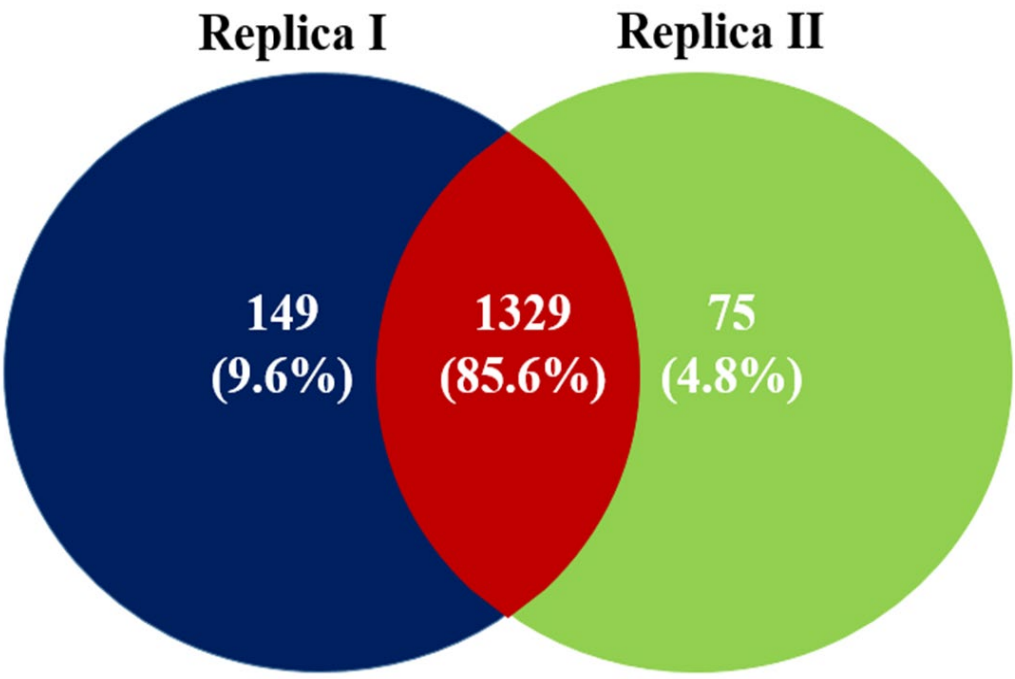

Supplementary Figure S1

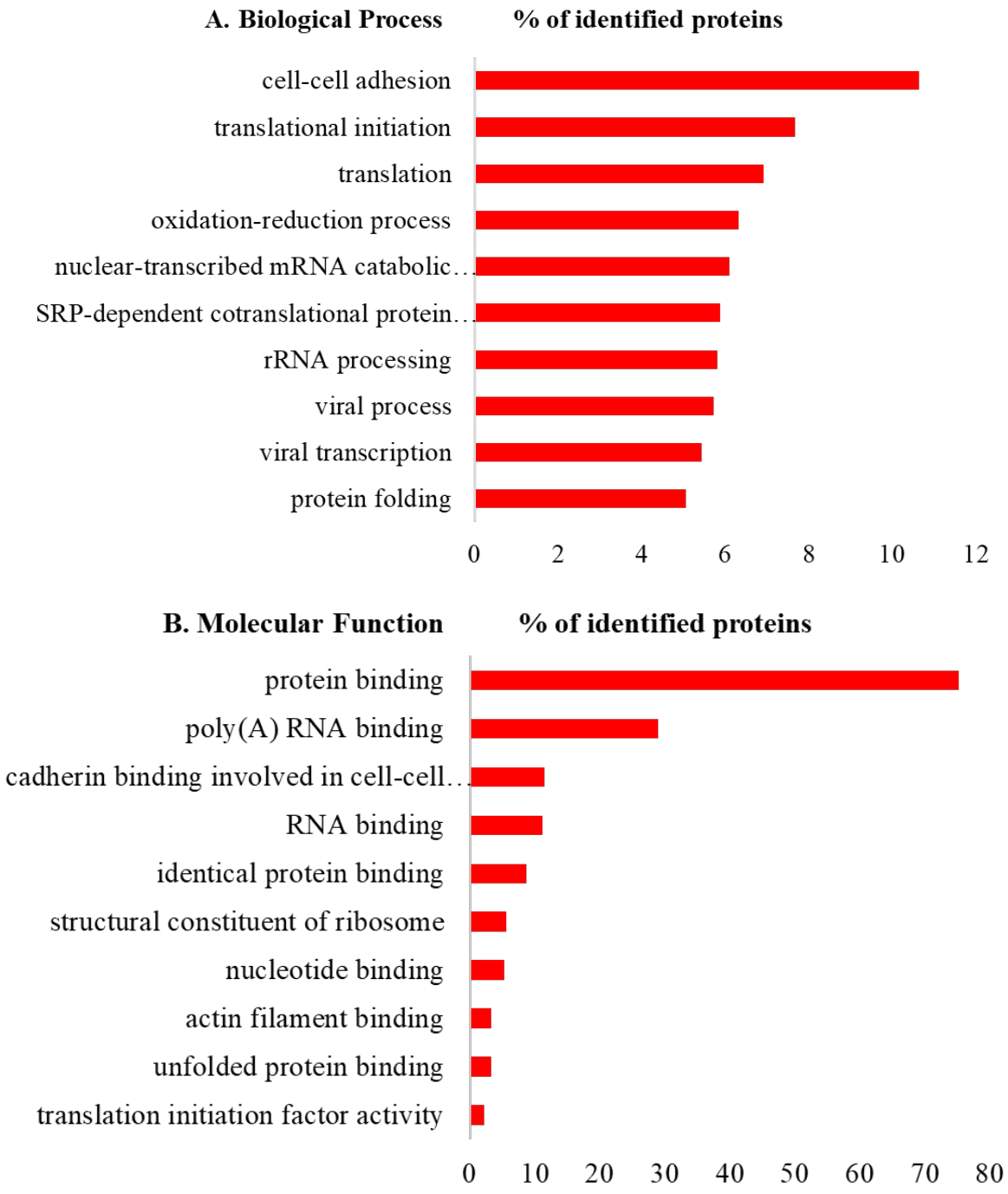

Supplementary Figure S2

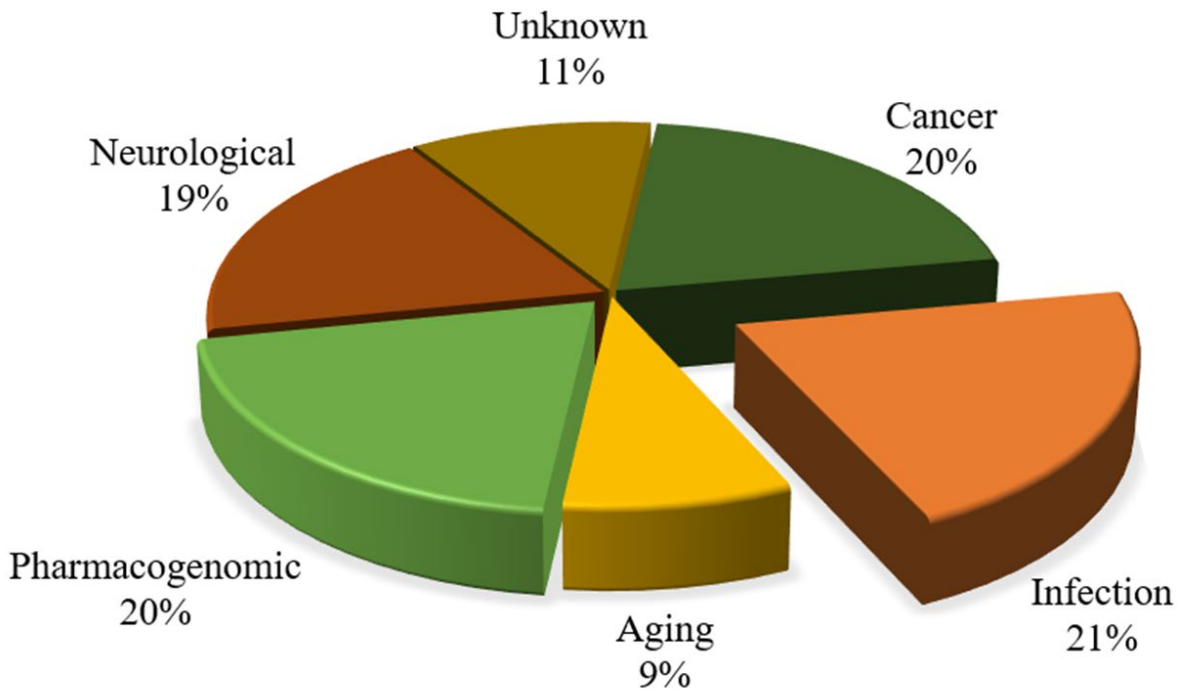

Supplementary Figure S3

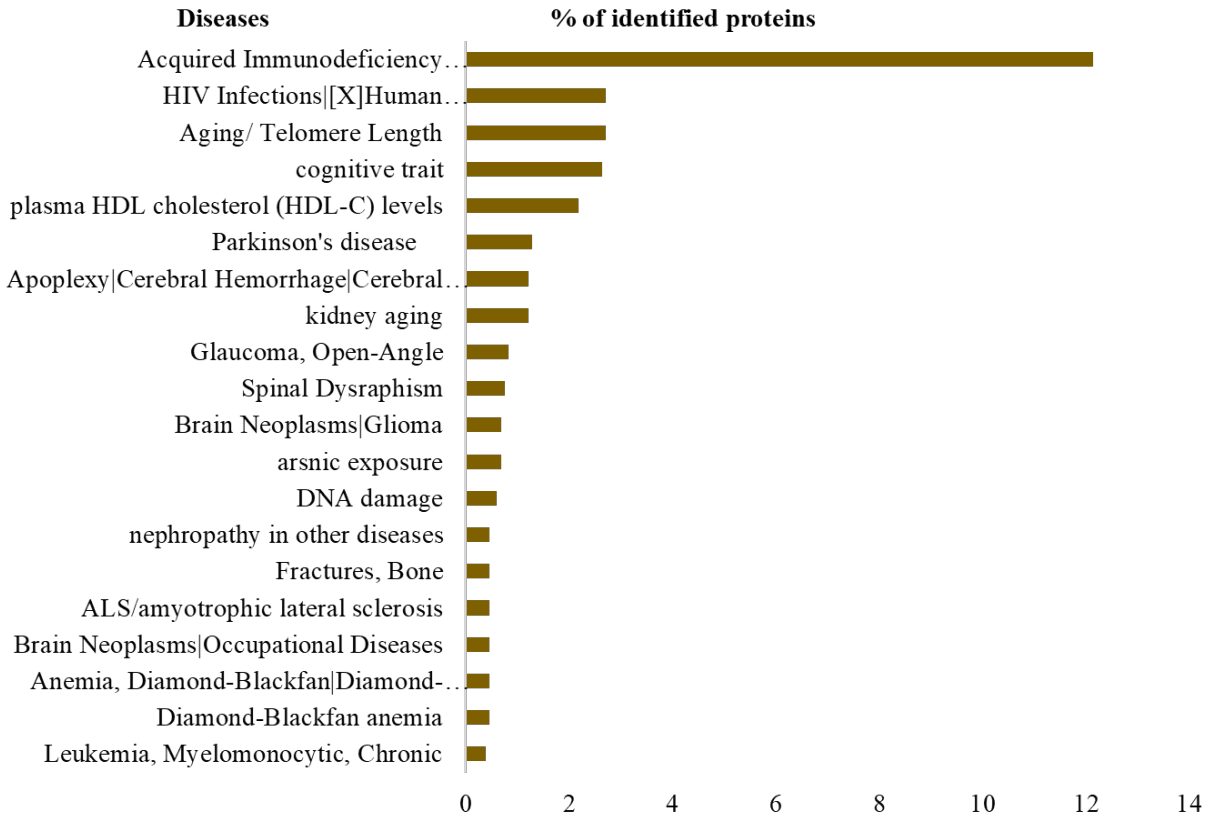

Supplementary Figure S4

Chapter 4 | Schwann Cell Stimulation of Pancreatic Cancer Cells: A Proteomic Analysis

4.1 Preface

Chapter 4 contains an original research article entitled "**Schwann Cell Stimulation of Pancreatic Cancer Cells: A Proteomic Analysis**" which has been published in *Frontiers in Oncology*. We profiled the secretome of human SCs by LC-MS/MS and using various bioinformatics software we have detailed the most enriched pathways and biological functions of SC secreted proteins. We further validated several secreted proteins by WB and investigated their role in PC cell proliferation and invasion using blocking antibodies. These candidate proteins represent potential novel therapeutic targets for the development of future targeted treatments in PC. Furthermore, this proteomic dataset will also serve as a resource for further functional and clinical investigations into the role of SCs in cancer.

4.2 Publications

Published article "**Ferdoushi A**, Li X, Griffin N, Faulkner S, Jamaluddin MFB, Gao F, Jiang CC, Jobling P, Tanwar PS, Helden DFV, Hondermarck H: **Schwann Cell Stimulation of Pancreatic Cancer Cells: A Proteomic Analysis**. *Frontiers in Oncology*. 2020 August; 10:1601." displays from page 48 to 61.

4.3 Supplementary Files

Supplementary file displays on page 62 to 74.

frontiers in Oncology

ORIGINAL RESEARCH
published: 25 August 2020
doi: 10.3389/fonc.2020.01601

Schwann Cell Stimulation of Pancreatic Cancer Cells: A Proteomic Analysis

*Aysha Ferdoushi[1,2,3], Xiang Li[1,2], Nathan Griffin[1,2], Sam Faulkner[1,2], M. Fairuz B. Jamaluddin[1,2], Fangfang Gao[1,2], Chen Chen Jiang[2,4], Dirk F. van Helden[1,2], Pradeep S. Tanwar[1,2], Phillip Jobling[1,2] and Hubert Hondermarck[1,2]**

[1] School of Biomedical Sciences and Pharmacy, Faculty of Health and Medicine, University of Newcastle, Callaghan, NSW, Australia, [2] Hunter Medical Research Institute, University of Newcastle, New Lambton, NSW, Australia, [3] Department of Biotechnology and Genetic Engineering, Mawlana Bhashani Science and Technology University, Tangail, Bangladesh, [4] School of Medicine and Public Health, The University of Newcastle, Callaghan, NSW, Australia

OPEN ACCESS

Edited by:
Suman S. Thakur,
Centre for Cellular & Molecular Biology (CCMB), India

Reviewed by:
Helmut Friess,
Technical University of Munich, Germany
Dileep Kumar,
The University of Utah, United States
Marco Artico,
Sapienza University of Rome, Italy

***Correspondence:**
Hubert Hondermarck
hubert.hondermarck@newcastle.edu.au

Specialty section:
This article was submitted to Molecular and Cellular Oncology, a section of the journal Frontiers in Oncology

Received: 19 April 2020
Accepted: 23 July 2020
Published: 25 August 2020

Citation:
Ferdoushi A, Li X, Griffin N, Faulkner S, Jamaluddin MFB, Gao F, Jiang CC, van Helden DF, Tanwar PS, Jobling P and Hondermarck H (2020) Schwann Cell Stimulation of Pancreatic Cancer Cells: A Proteomic Analysis. Front. Oncol. 10:1601. doi: 10.3389/fonc.2020.01601

Schwann cells (SCs), the glial component of peripheral nerves, have been identified as promoters of pancreatic cancer (PC) progression, but the molecular mechanisms are unclear. In the present study, we aimed to identify proteins released by SCs that could stimulate PC growth and invasion. Proteomic analysis of human primary SC secretome was performed using liquid chromatography–tandem mass spectrometry, and a total of 13,796 unique peptides corresponding to 1,470 individual proteins were identified. Gene Ontology and Kyoto Encyclopedia of Genes and Genomes pathway enrichment were conducted using the Database for Annotation, Visualization, and Integrated Discovery. Metabolic and cell–cell adhesion pathways showed the highest levels of enrichment, a finding in line with the supportive role of SCs in peripheral nerves. We identified seven SC-secreted proteins that were validated by western blot. The involvement of these SC-secreted proteins was further demonstrated by using blocking antibodies. PC cell proliferation and invasion induced by SC-conditioned media were decreased using blocking antibodies against the matrix metalloproteinase-2, cathepsin D, plasminogen activator inhibitor-1, and galectin-1. Blocking antibodies against the proteoglycan biglycan, galectin-3 binding protein, and tissue inhibitor of metalloproteinases-2 decreased only the proliferation but not the invasion of PC cells. Together, this study delineates the secretome of human SCs and identifies proteins that can stimulate PC cell growth and invasion and therefore constitute potential therapeutic targets.

Keywords: pancreatic cancer, Schwann cells, secretome, cancer cell proliferation and invasion, LC-MS/MS, therapeutic targets

Abbreviations: cat. no., catalog number; CM, conditioned media; DAVID, Database for Annotation, Visualization, and Integrated Discovery; ECM, extracellular matrix; GAD, Genetic Association Database; Gal-1, galectin-1; Gal-3BP, galectin-3 binding protein; GO, Gene Ontology; IGFBP, insulin-like growth factor-binding proteins; IHC, Immunohistochemistry; KEGG, Kyoto Encyclopedia of Genes and Genomes; LC-MS/MS, liquid chromatography–tandem mass spectrometry; MMP-2, matrix metalloproteinase-2; PAI-1, plasminogen activator inhibitor-1; PC, pancreatic cancer; RFU, relative fluorescence unit; SC, Schwann cell; SCM, Schwann cell medium; SD, standard deviation; SF, serum-free; TCGA, The Cancer Genome Atlas; TIMP-2, tissue inhibitor of metalloproteinases-2; TMA, tissue micro array; WB, western blot.

INTRODUCTION

Pancreatic cancer (PC) is one of the most lethal malignancies (1) and is predicted to become the second leading cause of cancer-related death by 2030 (2). Eighty-five percent of PC cases are ductal adenocarcinomas with a 5-year survival rate less than 7% (3). The poor patient survival is attributed to late-stage diagnosis, high incidence of local recurrence, development of distant metastases, and therapeutic resistance (4, 5). In addition, there is currently no targeted therapy for PC, and therefore the identification of potential therapeutic targets is essential.

Schwann cells (SCs) are the major glial component in the peripheral nervous system (6). SCs maintain neuronal homeostasis through the regulation of cell growth, survival, and repair (7, 8). The primordial role of SCs is myelination (9), however SCs have recently been implicated in several malignancies including pancreatic (10–12), prostate (13), lung (14), oral (15), and cervical (16) cancers. In PC, SCs are involved in the initiation of disease, and their presence is associated with increased perineural invasion, the process by which cancer cells invade nerves (10). SCs guide cancer cells toward nerves via the production of neural cell adhesion molecule 1 (NCAM 1) that promotes perineural invasion (11). SCs have also been shown to initiate epithelial–mesenchymal transition and support metastatic spread (12), and SCs have been reported to mask cancer-related pain, resulting in a prolonged asymptomatic phase and delayed cancer diagnosis (17). Additionally, SC-derived interleukin 6 has been reported to augment PC cell migration and invasion (18). Although few SC-secreted cytokines (19) and adhesion molecules (20) have been described, the secretome of SC and its impact in PC remain largely unknown.

In the present study, we have profiled the secretome of human SCs using liquid chromatography–tandem mass spectrometry (LC-MS/MS) and investigated the role of several identified proteins in the stimulation of PC growth and invasion. These secreted proteins may constitute new therapeutic targets for PC.

MATERIALS AND METHODS

Human SC Culture

Primary human SCs, obtained from the spinal nerve cells of a healthy donor, were purchased from ScienCell (cat. no. 1700, CA, United States) and maintained (maximum of 10 passages) according to manufacturer instructions described previously (21). Briefly, T-75 culture flasks were coated with 10 mg/mL poly-L-lysine (cat. no., 0413, ScienCell) and incubated overnight at 37 C. Cells were seeded at 5,000 cells/cm^2 on the poly-L-lysine–coated flask after washing the vessel twice with sterile milli-Q water. Cells were grown in complete SC medium (SCM, cat. no., 1701, ScienCell), supplemented with 5% fetal bovine serum (FBS, cat. no., 0025, ScienCell), 1% SC growth supplement cocktail (SCGS, cat. no., 1752, ScienCell), and 1% penicillin/streptomycin (P/S, cat. no., 0503, ScienCell) in a humidified incubator at 37 C with 5% CO_2. SCs were characterized by immunoblotting using antibodies against human SC marker proteins, SOX10, and p75 (**Supplementary Figure S1**).

Pancreatic ductal adenocarcinoma cells, PANC-1 and MIA PaCa-2, were obtained from the American Type Culture Collection (ATCC, Manassas, VA, United States) and maintained in Dulbecco modified eagle medium (cat. no., ATC302002, ATCC) supplemented with 10% (vol/vol) FBS (JRH Biosciences, St. Louis, MO, United States) and 2 mM L-glutamine in a humidified incubator at 37 C with 5% (vol/vol) CO_2.

SC Conditioned Media Preparation

SCs were grown to 70–80% confluency in SCM and washed three times with sterile phosphate-buffered saline (PBS) (Invitrogen, CA, United States) and once with serum-free (SF) media. SCs were then incubated in SF media for 20 h, after which SC-conditioned media (SC-CM) was collected, centrifuged (1,000 *g* at 4 C for 10 min), and the supernatant was filtered through a 0.22- m nylon filter (Merck Millipore, MA, United States) to remove any cell debris or floating cells. SC-CM was further centrifuged (4,000 *g* at 4 C for 30 min) to concentrate using a 3-kDa cutoff Amicon Ultra-15 filter unit (Merck Millipore) until the media was concentrated 400-fold. The recovered SC-CM concentrate was stored at 80 C. An outline of SC-CM collection and concentration workflow are shown in **Figure 1A**.

Mass Spectrometry–Based Proteomic Analysis of SC Secretome

Discovery proteomic analysis was performed by LC-MS/MS to describe the secretome profile of primary human SCs. Experimental protocol outlined in **Figure 1B** has been previously described (21) with additional sample preparation steps added for the secretome analysis. The secretome of SCs have been analyzed in an unstimulated state, i.e., without previous exposure to PC cells.

Sample Preparation for LC-MS/MS

Two hundred micrograms of secreted proteins was measured by bicinchoninic acid (BCA) assay (Pierce, Thermo Fisher Scientific, IL, United States) and dissolved in urea (6 M urea 2 M thiourea) buffer followed by reduction step using 10 mM dithiothreitol (30 min at room temperature). The samples were subsequently alkylated using 20 mM iodoacetamide (30 min at room temperature in the dark). Proteins were digested using 1:40 ratio Lys-C/trypsin (cat. no., VA1170, Promega, Madison, WI, United States) to protein concentration (3 h, room temperature, in the dark). The concentration of the urea was brought down to less than 1 M by adding 20 mM triethylammonium bicarbonate (pH 7.8) and incubated overnight at room temperature. Peptides were desalted and cleaned up using a Visiprep^{TM} vacuum manifold (12-port, cat. no. 57030-U, Sigma-Aldrich, St. Louis, MO, United States) coupled with Empore C18 solid-phase extraction cartridge (4 mm/1 mL) according to manufacturer instructions.

LC-MS/MS

A Dionex UltiMate 3000 nanoLC system (Thermo Fisher Scientific) with a 15-cm EASY-Spray Column was used to

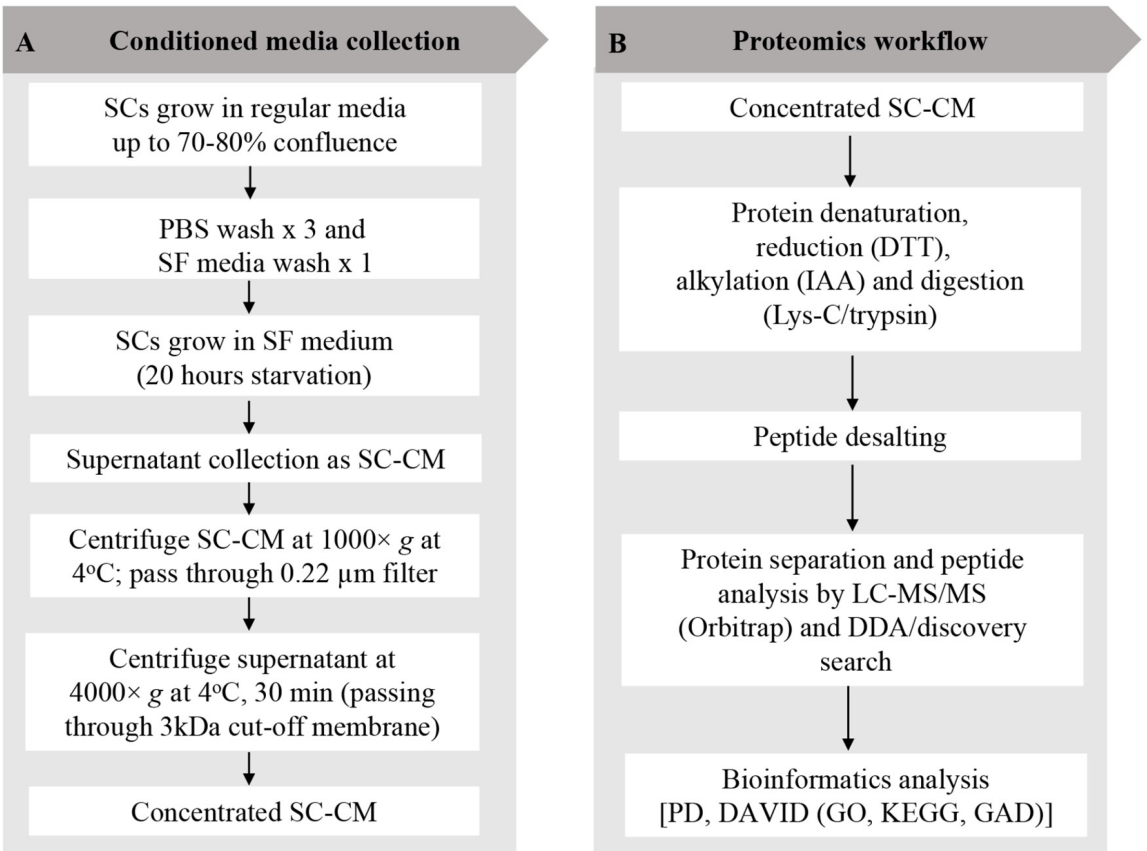

FIGURE 1 | Schwann cell–conditioned media (SC-CM) collection and proteomic workflow. **(A)** For SC-CM collection, SCs were grown to 70–80% confluence. Cells were washed three times with sterile PBS and once with SF media before incubation in SF media for additional 20 h. SC-CM were then collected and centrifuged (1,000 × *g*, 4°C, 10 min), and the supernatant was filtered through a 0.22-µm nylon filter to remove any cell debris or floating cells. Collected supernatant was concentrated using 3-kDa cutoff Amicon Ultra-15 filter unit (4,000 × *g*, 4°C, 30 min). **(B)** Proteomic analysis of the secretome was performed using LC-MS/MS. Concentrated SC-CM was subjected to reduction (DTT), alkylation (IAA), and Lys-C/trypsin digestion before analysis in LC-MS/MS. DDA discovery search was performed to identify the total number of peptides and proteins. To profile the SC-secretome, functional clustering of the secreted proteins was performed using DAVID bioinformatics software and displayed in GO and KEGG. Identified proteins were classified based on disease classes using DAVID-GAD analysis. SC, Schwann cell; PBS, phosphate-buffered saline; SF, serum-free; SC-CM, Schwann cell–conditioned media; DTT, dithiothreitol; IAA, iodoacetamide; LC-MS/MS, liquid chromatography–tandem mass spectrometry; DDA, data-dependent acquisition; PD, Proteome Discoverer; DAVID, Database for Annotation, Visualization, and Integrated Discovery; GO, Gene Ontology; KEGG, Kyoto Encyclopedia of Genes and Genomes; GAD, Genetic Association Database.

separate 500 ng of peptides using a 150-min gradient at a flow rate of 300 nL/min. Peptides were analyzed on Q-Exactive Plus Orbitrap (Thermo Fisher Scientific) mass spectrometer. Precursor scan of intact peptides was measured in the Orbitrap by scanning from m/z 400–2,000, with a resolution of 70 K with maximum ion injection time of 50 ms and automated gain control (AGC) target of 1E6. The 15 most intense multiply charged precursors were selected for HCD fragmentation with a normalized collision energy of 27.0 and then measured in the Orbitrap at a resolution of 35 K with maximum ion injection time of 120 ms, and AGC target was set at 2E5. Dynamic exclusion was set for 30 s.

MS Data Analysis

LC-MS/MS data were analyzed using Proteome Discoverer software v.2.1 (Thermo Fisher Scientific) and searched against the Uniprot human protein database (downloaded March 5, 2018, with a total of 71,773 entries). Precursor mass tolerance was set to 10 ppm, and fragment ion tolerance was 0.02 Da. Trypsin was designated as the digestion enzyme with two missed cleavages permitted. Carbamidomethylation on cysteine (+57.021 Da) was set as static modifications, and oxidation on methionine (+15.995 Da) was set as variable modification. Only high confidence identification, represented by at least two unique peptides, was included in the analysis. Protein confidence indicators were set at 1% false discovery rate criteria using a percolator. The precursor ion (MS) spectra were also manually validated using Xcalibur Software version 4.0.27.13 (Thermo Fisher Scientific) to avoid false-positive detection.

Proliferation Assay

Pancreatic cancer cells (PANC-1 and MIA PaCa-2) were starved for 24 h and seeded (∼5,000 cells/well) in a 96-well culture plate.

Cells were cultured in 200 L SF media, serum-supplemented media (noted as FBS), and SC-CM, with or without specific blocking antibodies (6 g/mL) (detailed information of the antibodies is listed in **Table 1**). Antibodies were used to block specific proteins in SC-CM. Of note, the commercial producers have reported blocking activity for the antibodies that we have used, but we have not independently confirmed it. Cells were cultured for 72 h and subsequently incubated with CellTiter-Blue® (Promega Corporation, cat. no., G8081) at 37 C for 4 h before recording fluorescence at 560/590 using a FLUOstar OPTIMA fluorescence plate reader (BMG Labtech, Durham, NC, Untied States). All the experiments were repeated three times.

Invasion Assay

Cell invasion assays were performed on serum-starved PC cells (PANC-1 and MIA PaCa-2) using the QCM ECM Cell Invasion Assay kit (cat. no., ECM554; Merck Millipore). The supplied 24-well assay plate contains upper invasion chamber inserts with 8-mm pore size membranes. The extracellular matrix (ECM) layer was rehydrated with 300 L of prewarmed SF media for 30 min at room temperature. Serum-starved cells (60,000) were loaded into the Transwell chamber insert in 250 L of SF media or SC-CM with or without specific antibody (6 g/mL). Five hundred microliters of SF medium, serum-supplemented media (noted as FBS), and SC-CM, with or without specific antibody (6 g/mL), was added to the lower chamber. After 24 h, invading cells were dislodged, and the fluorescence was recorded at 480/520 nm using a FLUOstar OPTIMA fluorescence plate reader (BMG Labtech) as described previously (22). All the experiments were repeated three times.

TABLE 1 | Antibodies used for WB.

No.	Antibody name	Source (working dilution)	Company (cat. no.)
Antibodies used to detect protein in SC-CM			
1	Gal-3BP	Goat polyclonal (1:700)	R&D System (AF2226)
2	MMP-2	Goat polyclonal (1:500)	R&D System (AF902)
3	Cathepsin D	Goat polyclonal (1:100)	R&D System (AF1014)
4	PAI-1	Goat polyclonal (1:100)	R&D System (AF1786)
5	Biglycan	Goat polyclonal (1:1,000)	R&D System (AF2667)
6	TIMP-2	Goat polyclonal (1:500)	R&D System (AF971)
7	Gal-1	Goat polyclonal (1:1,000)	R&D System (AF1152)
Antibodies used to detect protein in cell lysate			
8	Sox10	Mouse monoclonal (1:400)	Abcam (ab212843)
9	p75	Rabbit polyclonal (1:200)	Santa Cruz, (H-137): sc-8317
Antibodies used to detect loading control			
10	-actin	Mouse monoclonal (1:2,000)	Abcam (ab8226)
11	-actin	Rabbit polyclonal (1:2,000)	Abcam (ab8227)

Antibodies used to detect proteins both in SC-CM and cell lysate are presented here with source, dilution, company name, and cat. no. SC-CM, Schwann cell–conditioned media; Gal-3BP, galectin-3 binding protein; MMP-2, matrix metalloproteinase-2; PAI-1, plasminogen activator inhibitor-1; TIMP-2, tissue inhibitor of metalloproteinases-2; Gal-1, galectin-1; cat. no., catalog number.

Western Blotting

Concentrated SC-CM and cellular lysates underwent western blot (WB) analysis to detect specific proteins of interest from LC-MS/MS in the SC secretome and SCs, respectively. After collecting the SC-CM for secretome profiling and functional analysis, the remaining cells were washed three times with PBS, trypsinized, and collected by gently scrapping into PBS media. Cells were subsequently pelleted by centrifugation at 800 *g* for 5 min. Total proteins were extracted from cell pellets using RIPA buffer [25 mM Tris–HCl (pH 7.6)], 150 mM NaCl, 1% NP-40, 1% sodium deoxycholate, 0.1% sodium dodecyl sulfate (SDS)] (Thermo Fisher Scientific) and commercial protease inhibitor and phosphatase inhibitor cocktail tablets (Roche, Mannheim, Germany), aliquoted, and stored at 20 C. The total protein concentration of cell extracts and concentrated SC-CM was determined using a BCA assay (Pierce), according to the manufacturer's instructions.

Thirty micrograms of protein from each sample was resuspended in an equal volume of Laemmli buffer (Bio-Rad, Hercules, CA, United States). The cell extract or concentrated SC-CM was subjected to SDS–polyacrylamide gel electrophoresis under reducing conditions, and the separated proteins were transferred to 0.4-mm pore nitrocellulose membranes (Amersham, GE Healthcare Life Sciences, Pittsburgh, PA, United States). Blots were blocked with blocking buffer (LI-COR Biosciences, Lincoln, NE, United States) for 1 h at room temperature and then probed with antibodies against specific proteins (**Table 1**). Identical antibodies were used for both WB and functional analysis. -Actin protein expression was used as loading control. All antibodies were diluted in blocking buffer (LI-COR Biosciences). After washing with PBS containing 0.1% Tween-20, membranes were probed with goat anti–mouse or goat anti–rabbit IR-Dye 670 or 800 cw labeled secondary antisera, and then washes were repeated after labeling. WB was imaged using the LI-COR Odyssey infrared imaging system (LI-COR Biosciences).

Pancreatic Tissue Samples and Immunohistochemistry

High-density tumor micro arrays (TMAs) were obtained from US Biomax Inc. (Maryland, MD, United States). The TMAs used (HPan-Ade170Sur-01) included a total of 99 pancreatic adenocarcinomas and 71 normal adjacent pancreatic tissues. For each specimen collected, informed consent was obtained from both the hospital and the individual. Discrete legal consent was obtained, and the rights to hold research uses for any purpose or further commercialized uses were waived. The study was approved by the University of Newcastle's Human Research Ethics Committee.

Immunohistochemistry (IHC) was performed as described previously (23). Following deparaffinization and rehydration of the TMA slides using standard procedures, heat-induced epitope retrieval was carried out in a low-pH, citrate-based antigen unmasking solution (catalog number H-3300, Vector Laboratories, California, CA, United States) by a decloaking chamber (Biocare, West Midlands, United Kingdom) at 95 C for

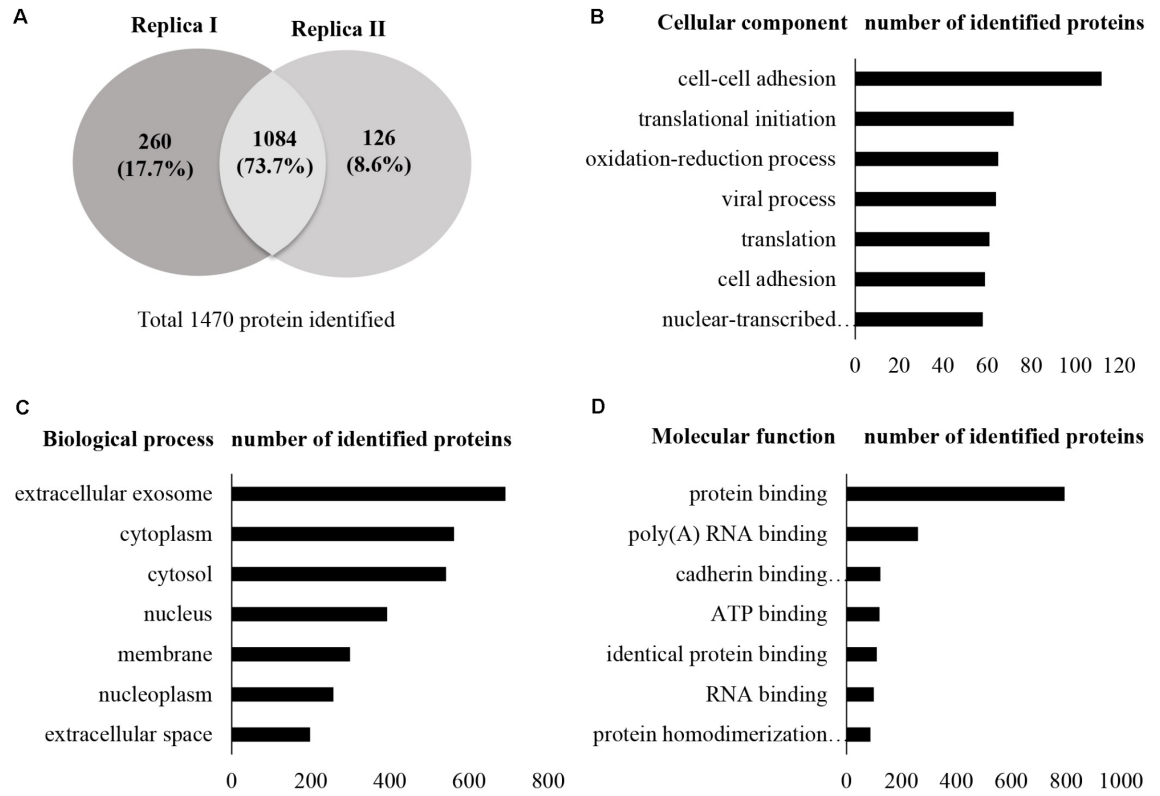

FIGURE 2 | Secretome profile and functional clustering of human SCs. **(A)** Venn diagram summarizing the overlap in protein identification between two independent proteomic analyzes of SC-CM, which identified 1,344 (replica I) and 1,210 (replica II) proteins, respectively. Additional details are listed in **Supplementary Tables S2–S4**. **(B–D)** DAVID bioinformatics resource was used to analyze the secretome of SCs in order to identify enriched biological terms in the common secreted proteins extracted from the MS analysis. **(B)** GO enrichment analysis of cellular components. Proteins localized in extracellular exosomes were highly enriched. **(C)** GO enrichment analysis of biological processes. Highly enriched SC secreted proteins are involved in cell–cell adhesion. **(D)** GO enrichment analysis of molecular function. Highly enriched SC secreted proteins are involved in protein binding. Only the top seven cellular components, biological processes, and molecular functions have been shown here for vertical sizing. Additional details are listed in **Supplementary Tables S5–S7**. SC-CM, Schwann cell–conditioned media; GO, Gene Ontology; DAVID, Database for Annotation, Visualization, and Integrated Discovery.

30 min and 90°C for 10 s. IHC was then performed using an ImmPRESS^{TM} horseradish peroxidase (HRP) immunoglobulin G (peroxidase) Polymer Detection Kit (Vector Laboratories), as per the manufacturer's recommendations. After inactivation of endogenous peroxidases with 0.3% H_2O_2 and blocking with 2.5% horse serum, primary antibody followed by secondary antibodies was applied to the sections and revealed with DAB peroxidase (HRP) Substrate Kit (catalog number SK-4100, Vector Laboratories). Primary antibodies used are listed in **Supplementary Table S1**. Finally, TMA slides were counterstained with hematoxylin (Gill's formulation, Vector Laboratories), dehydrated, and cleared in xylene before mounting in Ultramount #4 mounting media (Thermo Fisher Scientific, Victoria, Australia). Following IHC staining, slides were scanned with a Leica Aperio AT2 Scanner (Leica Biosystems, Vista, CA, United States) (23).

Bioinformatics Analysis

UniProt was used to identify protein cellular localization. Functional clustering of the identified secreted proteins was performed using the Database for Annotation, Visualization, and Integrated Discovery (DAVID, v6.8[1]) searching against the entire Homo sapiens genome (access date, March 25, 2020). DAVID classified the characteristic protein sets according to Gene Ontology (GO) terms for cellular compartments, biological processes, and molecular functions. DAVID was also used to recognize functional Kyoto Encyclopedia of Genes and Genomes (KEGG) pathway categories. All the DAVID categories were ranked according to the number of proteins in each group and not with *p*-value. To investigate the potential associations between the identified proteins and diseases, the dataset was subjected to DAVID Genetic Association Database (GAD) analysis.

The cBio Cancer Genomics Portal[2] was used to determine the association of selected proteins with prognosis of PC using The Cancer Genome Atlas (TCGA) on pancreatic adenocarcinoma (access date, February 25, 2020). Our search was set to a total of 184 pancreatic adenocarcinoma samples (TCGA, PanCancer

[1]https://david.ncifcrf.gov/
[2]http://cbioportal.org

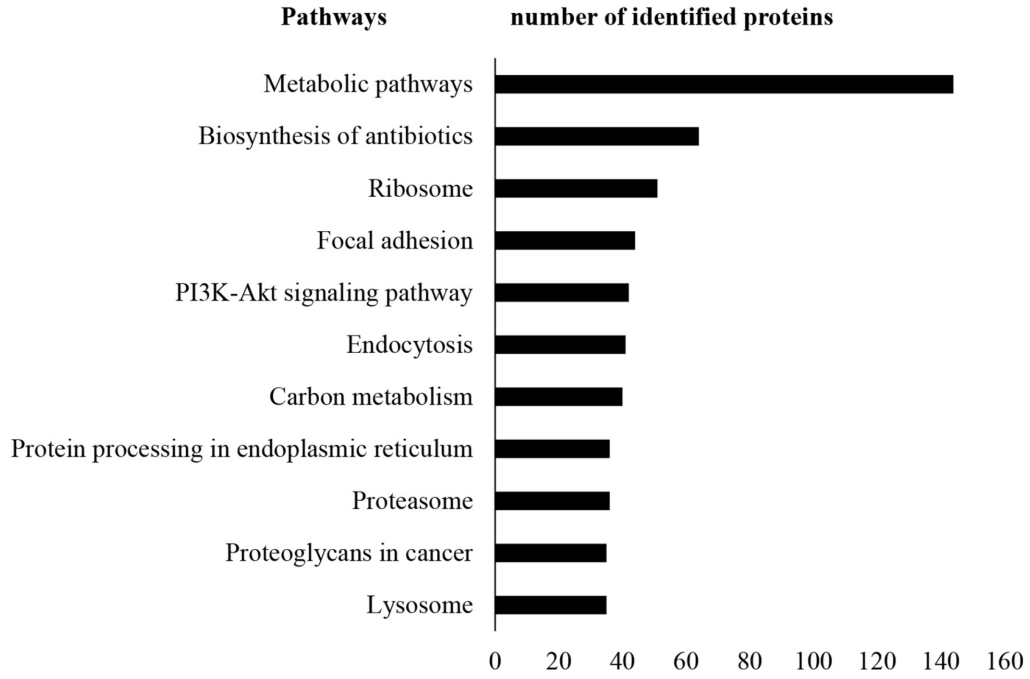

FIGURE 3 | KEGG pathway analysis. KEGG pathway enrichment analysis was performed using DAVID. Metabolic pathways were found as most enriched. Only the top 10 enriched pathways are shown here for vertical sizing. Additional details are listed in **Supplementary Table S8**. KEGG, Kyoto Encyclopedia of Genes and Genomes; DAVID, Database for Annotation, Visualization, and Integrated Discovery.

Atlas) and mRNA expression with a *z*-score threshold ±2.0. The role of selected candidates in cancer development was explored via the Cancer Hallmarks Analytics Tool, which allows organization and classification of cancer-related literature based on a text-mining analysis of 26 million PubMed abstracts (24).

Statistical Analysis

Statistical analysis was conducted using the GraphPad Prism software version 8.0 (GraphPad Software Inc., La Jolla, CA, United States). Statistical significance was determined by one-way analysis of variance (ANOVA). $p < 0.05$ was set the level of statistical significance. Data are presented as mean, with error bars representing the standard deviation. *p*-value is displayed as $^{*}p < 0.05$, $^{**}p < 0.01$, $^{***}p < 0.001$.

RESULTS

Protein Map of SC Secretome and Pathway Analysis

A total of 13,796 unique peptides corresponding to 1,470 individual proteins were identified in two replicates, with a confidence corresponding to a false discovery rate <1% (**Figure 2A** and **Supplementary Table S2–S4**). Of the 1,470 proteins identified, 74% (1,084 proteins) were common across the two replicates. According to DAVID GO enrichment analysis of the cellular components, proteins localized in extracellular exosomes were highly enriched (692 proteins). Others were in cytoplasm (562 proteins), cytosol (542 proteins), nucleus (393 proteins), membrane (299 proteins), and nucleoplasm (257 proteins), as well as the extracellular space (198 proteins) (**Figure 2B** and **Supplementary Table S5**). To gain further insights into the enriched biological processes, common secreted proteins were subjected to GO enrichment analysis. The results showed that cell–cell adhesion was the most enriched (112 proteins) biological function. Other significant biological processes include translational initiation (72 proteins), oxidation–reduction process (65 proteins), and translation (61 proteins) (**Figure 2C** and **Supplementary Table S6**). GO enrichment analysis was also used to depict the molecular function of the identified proteins. Protein binding was the most enriched (794 proteins) molecular function. Other enriched molecular functions were mainly related to poly (A) RNA binding (260 proteins), cadherin binding (123 proteins), and ATP binding (120 proteins) (**Figure 2D** and **Supplementary Table S7**). KEGG pathway analysis was performed to map the important and representative pathways in human SCs using the DAVID resource, and the top 10 pathways based on enrichment were defined (**Figure 3** and **Supplementary Table S8**). Metabolic pathways were among the most enriched (144 proteins). Proteins from our list were also found to be potentially involved in focal adhesion (44 proteins), PI3K-Akt signaling pathway (42 proteins), endocytosis (41 proteins), protein processing in endoplasmic reticulum (36 proteins), and proteoglycans in cancer (35 proteins). Exploration of potential associations of the identified proteins with diseases using GAD resources revealed that approximately 21% (226 proteins) of the SC-secreted proteins were associated with cancer followed

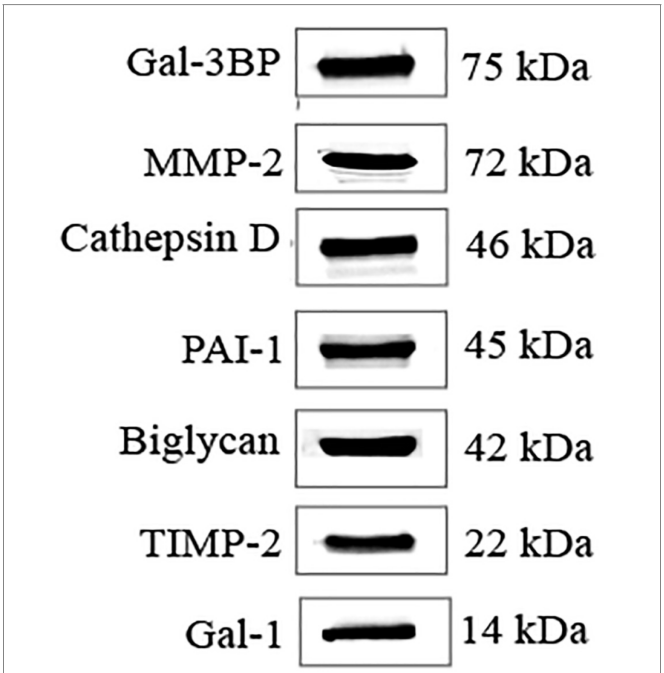

FIGURE 4 | WB validation of candidate molecules. WB analysis confirmed the presence of secreted candidate molecules in SC-CM. WB, western blot; SC-CM, Schwann cell–conditioned media; Gal-3BP, galectin-3 binding protein; MMP-2, matrix metalloproteinase-2; PAI-1, plasminogen activator inhibitor-1; TIMP-2, tissue inhibitor of metalloproteinases-2; Gal-1, galectin-1.

by neurological disorders (204 proteins) and infectious diseases (177 proteins). The remaining portion of our identified proteins was also associated with renal disease (113 proteins), aging (93 proteins), reproduction (73 proteins), and vision (58 proteins) (**Supplementary Figure S2** and **Supplementary Table S9**).

Protein Validation by WB

From the list of secretory proteins identified by LC-MS/MS, galectin-3–binding protein (Gal-3BP), matrix metalloproteinase-2 (MMP-2), cathepsin D, plasminogen activator inhibitor-1 (PAI-1), biglycan, tissue inhibitor of metalloproteinases-2 (TIMP-2), and galectin-1 (Gal-1) were validated by WB (**Figure 4**). We initially picked those proteins because they were known to be involved in tumor progression. These proteins are reported in **Table 2** with their identified peptide count, coverage, and observed function in PC progression. WB analyses of SC lysates for the identified proteins have also been provided in **Supplementary Figure S3**. Validated proteins with their Cancer Hallmarks Analytics Tool analysis results are presented in **Supplementary Figure S4**.

Impact of Targeting SC Secreted Proteins on PC Cell Growth

Significant increase of PC cells (PANC-1 and MIA PaCa-2) proliferation was observed in the presence of SC-CM compared with negative control (SF media, noted as SF) ($p < 0.05$), and the increment was similar to that in the positive control (serum-supplemented media, noted as FBS) (**Figure 5**), demonstrating that SC-CM stimulates PC cell proliferation. To determine if the proliferative effect of SC-CM was due to specific SC-secreted proteins, proliferation assay was performed in the presence of blocking antibodies against the WB-validated proteins. Blocking antibodies against Gal-3BP, MMP-2, cathepsin D, PAI-1, biglycan, TIMP-2, or Gal-1 caused a significantly decreased ($p < 0.05$) proliferation in PC cells compared to control (SC-CM only, without blocking antibody) (**Figures 5A,B**). No significant inhibitory effect on PC cell proliferation was observed when control media (SF and serum-supplemented media) was treated with blocking antibodies ($p > 0.05$) (**Supplementary Figure S5**).

Impact of Targeting SC Secreted Proteins on PC Cell Invasiveness

A significant increase in PC cell (both PANC-1 and MIA PaCa-2) invasion was observed in the presence of SC-CM compared with negative control (SF media, noted as SF) ($p < 0.05$), and the increment was similar to the positive control (serum-supplemented media, noted as FBS) (**Figure 6**). To specifically determine the SC-secreted proteins that induce increased invasion of PC cells, Transwell invasion assays were performed with blocking antibodies against the identified proteins. Among the blocking antibodies tested, neutralization of MMP-2, cathepsin D, PAI-1, and Gal-1 significantly ($p < 0.05$) decreased the invasion of PC cell lines compared to control

TABLE 2 | SCs secreted proteins whose targeting with antibodies resulted in a decreased PC cell proliferation and invasion.

No.	Accession no.	Protein name	Gene name	Unique peptides	MW (kDa)	Coverage (%)	Role in PC progression
1	Q08380	Gal-3BP	*LGALS3BP*	23	65.3	42.90	Proliferation
2	P08253	MMP-2	*MMP2*	40	73.8	61.81	Proliferation and invasion
3	P07339	Cathepsin D	*CTSD*	21	44.5	56.55	Proliferation and invasion
4	P05121	PAI-1	*SERPINE1*	41	45	62.68	Proliferation and invasion
5	P21810	Biglycan	*BGN*	18	41.6	53.53	Proliferation
6	P16035	TIMP-2	*TIMP2*	14	24.4	49.54	Proliferation
7	P09382	Gal-1	*LGALS1*	14	14.7	74.81	Proliferation and invasion

Commonly secreted proteins (between two replicates) identified using LC-MS/MS and validated by WB are presented here. Unique peptides: number of different peptides found by MS analyses; molecular weight: found by MS analyses; coverage: percentage of related protein found by MS analyses. LC-MS/MS, liquid chromatography–tandem mass spectrometry; Gal-3BP, galectin-3 binding protein; MMP-2, matrix metalloproteinase-2; PAI-1, plasminogen activator inhibitor-1; TIMP-2, tissue inhibitor of metalloproteinases-2; Gal-1, galectin-1.

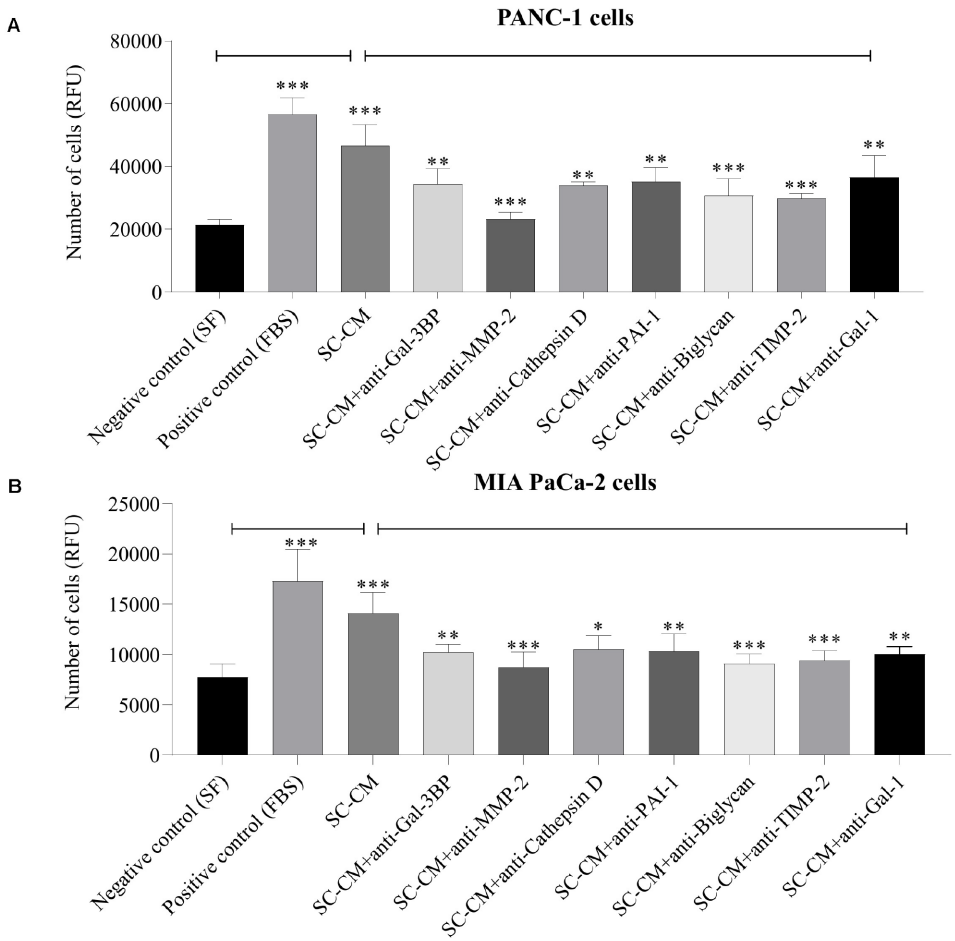

FIGURE 5 | *In vitro* blockage of SC-secreted proteins results in decrease of PC cell proliferation. The effects of SC-CM on PC cells (PANC-1 and MIA PaCa-2) proliferation were studied *in vitro* using resazurin-based proliferation assay. For both treatment and control, ~5,000 cells were initially plated onto 96-well plate dishes and allowed to proliferate for 72 h in the presence of SC-CM or control media. Serum-free media was used as negative control, and serum-supplemented media was used as positive control. Cell number was quantified as described in section "Materials and Methods." A significantly greater number of PC cells were observed in presence of SC-CM compared to negative control ($p < 0.05$). To find out if the effect of increased proliferation of PC cells in presence of SC-CM was due to secreted proteins from SCs, proliferation assays were performed using blocking antibodies against the proteins of interest. Blocking antibodies were used at 6 μg/mL concentration. Significant decrease in cancer cell (both PANC-1 and MIA PaCa-2) proliferation was observed in presence of blocking antibodies against Gal-3BP, MMP-2, cathepsin D, PAI-1, biglycan, TIMP-2, and Gal-1 compared to SC-CM alone ($p < 0.05$). Representative data are shown from three independent experiments, performed in at least six replicates each. Statistical significance was confirmed by one-way ANOVA. The error bars represent the SD of the mean. *p*-values are displayed as $*p < 0.05$, $**p < 0.01$, and $***p < 0.001$. SC-CM, Schwann cell–conditioned media; PC, pancreatic cancer; Gal-3BP, galectin-3 binding protein; MMP-2, matrix metalloproteinase-2; PAI-1, plasminogen activator inhibitor-1; TIMP-2, tissue inhibitor of metalloproteinases-2; Gal-1, galectin-1; RFU, relative fluorescence unit.

(SC-CM only, without blocking antibody) (**Figures 6A,B**). In contrast, blocking Gal-3BP, biglycan, and TIMP-2 in SC-CM had no significant ($p > 0.05$) inhibitory effect on PC invasion. No significant decrease in PC cell invasiveness was observed when control media (both SF and serum-supplemented media) was treated with blocking antibodies ($p > 0.05$) (**Supplementary Figure S6**).

Immunohistochemical Detection of Identified Proteins in PC

The seven SC-secreted proteins having an effect on PC cell growth and invasion were investigated by IHC. The results revealed moderate to high levels of expression of these proteins in PC (**Supplementary Figures S7A–G**). Briefly, strong cytoplasmic immunoreactivity was observed in case of Gal-3 BP (**Supplementary Figure S7A**). In case of MMP-2, most malignant cells and surrounding stroma showed weak to moderate immunoreactivity (**Supplementary Figure S7B**). Cathepsin D was more strongly found in the PC cells and in SCs (**Supplementary Figure S7C**). In case of PAI-1, all cancer tissues were negative, and few tumor stroma were weakly positive (**Supplementary Figure S7D**). In case of biglycan, strong tumor and stromal immunoreactivity was observed (**Supplementary Figure S7E**). In case of TIMP-2, most cancer tissues were negative, whereas few malignant

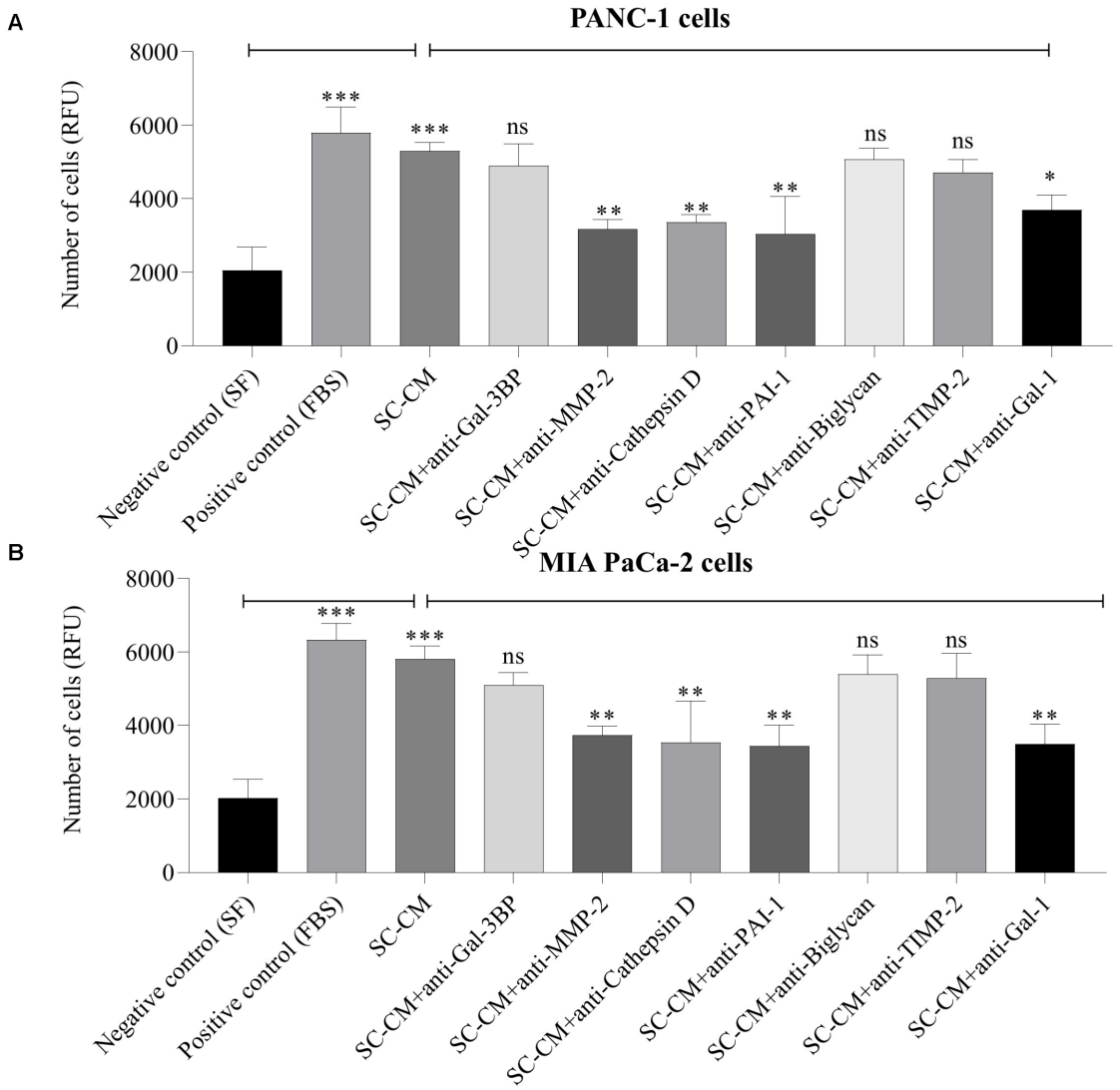

FIGURE 6 | *In vitro* blockage of SC-secreted proteins results in decreased invasion of PC cells. The effects of SC-CM on PC cells (PANC-1 and MIA PaCa-2) invasiveness were studied *in vitro* using Transwell invasion assay. For both treatment and control, cells (~60,000) were plated to the insert of a Transwell plate coated with collagen and allowed to invade for 24 h through a collagen-coated matrix toward SC-CM or control media as applicable. Serum-free media was used as negative control and serum-supplemented media was used as positive control. The non-invaded cells were removed from the top of the insert, and invaded cells were quantified using the QCM ECMatrix Cell Invasion Assay Kit described in section "Materials and Methods." A significantly greater number of invaded PC cells in presence of SC-CM was observed compared to negative control ($p < 0.05$). To determine if the proteins of interest were involved in the stimulation of PC cells by SCs, the invasion assay was performed with blocking antibodies. Among the tested blocking antibodies, neutralization of MMP-2, cathepsin D, PAI-1, and Gal-1 decreased the invasiveness of both types of PC cell line compared to SC-CM alone ($p < 0.05$). Blocking antibodies were used at 6 μg/mL concentration. Blocking Gal-3BP, biglycan, and TIMP-2 in SC-CM had no significant inhibitory effect on PC invasiveness ($p > 0.05$). Representative data are shown from three independent experiments, performed in at least three replicates each. Statistical significance was obtained by one-way ANOVA. The error bars represent the SD of the mean. *p*-values are displayed as $*p < 0.05$, $**p < 0.01$, and $***p < 0.001$. SC-CM, Schwann cell–conditioned media; PC, pancreatic cancer; Gal-3BP, galectin-3 binding protein; MMP-2, matrix metalloproteinase-2; PAI-1, plasminogen activator inhibitor-1; TIMP-2, tissue inhibitor of metalloproteinases-2; Gal-1, galectin-1; RFU, relative fluorescence unit; ns, non-significant.

cells displayed moderate cytoplasmic immunoreactivity (**Supplementary Figure S7F**). Gal-1 expression levels were mostly restricted to stroma of PC cells and in SCs (**Supplementary Figure S7G**). Positive labeling in IHC validates the presence of the identified proteins in the tumor microenvironment of PC. However, SCs are difficult to localize in the tumor microenvironment, and IHC cannot provide a clear demonstration that those proteins are released by SCs.

Prognostic Value of Protein Candidates

To explore the prognostic value of candidate proteins for which targeting with antibodies inhibited proliferation and invasion of PC cells, a meta-analysis at the mRNA was carried out

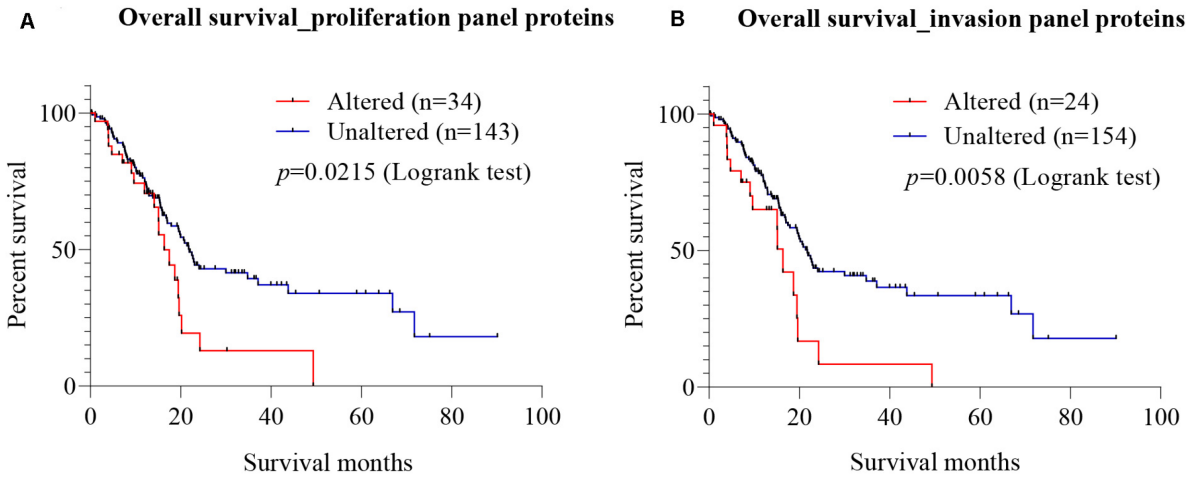

FIGURE 7 | Prognostic value of mRNA expression corresponding to the identified candidate proteins. Using cBioportal, Kaplan–Meier estimates of survival for PC patients with alterations in different gene combination were performed using The Cancer Genome Atlas (TCGA) on pancreatic adenocarcinoma. **(A)** Survival analysis showed that patients with alterations in the seven-gene proliferation panel (Gal-3BP, MMP-2, cathepsin D, PAI-1, biglycan, TIMP-2, and Gal-1) had worse overall survival than those without alterations (log-rank test $p = 0.0215$). **(B)** In the cases of invasion panel proteins (MMP-2, cathepsin D, PAI-1, and Gal-1), worse prognosis was also observed for patients with alterations in the four genes than those without alterations (log-rank test $p = 0.0058$). PC, pancreatic cancer; Gal-3BP, galectin-3 binding protein; MMP-2, matrix metalloproteinase-2; PAI-1, plasminogen activator inhibitor-1; TIMP-2, tissue inhibitor of metalloproteinases-2; Gal-1, galectin-1.

using TCGA on pancreatic adenocarcinoma, using the cBio Cancer Genomics Portal. Using Kaplan–Meier analysis of overall survival, based on the median mRNA expression levels, the prognostic values of the combined seven proteins involved in proliferation (Gal-3BP, MMP-2, cathepsin D, PAI-1, biglycan, TIMP-2, and Gal-1) (called proliferation protein panel) and four proteins involved in invasion (MMP-2, cathepsin D, PAI-1, and Gal-1) (called invasion protein panel) were investigated. The proliferation protein panel showed a significant association with poor prognosis (log-rank test *p*-value 0.0215), where 34 patients from a total of 177 showed alterations in this gene signature (**Figure 7A**). The invasion protein panel showed significant association with poor prognosis (log-rank test $p = 0.0058$), where 24 patients from a total of 178 showed alterations in this gene signature (**Figure 7B**). Overall, both protein panels may constitute a molecular signature for poor prognosis in PC. The data are useful in showing a prognostic relevance of the combination, but there is no demonstration that SCs are the major source for these proteins that may equally be produced by PC cells.

DISCUSSION

The present study has used proteomic analysis to define the secretome of SCs and has identified several proteins that can be targeted *in vitro* to inhibit growth and invasion of PC cells. These findings are summarized in **Figure 8**. In addition, several of the identified proteins were shown to contribute to PC cell growth and invasion and may constitute future therapeutic targets.

The LC-MS/MS–based proteomic analysis that has been implemented in this study has enabled the identification of 1,084 SC-secreted proteins. Bioinformatics analysis was performed. In GO analysis, the "extracellular exosome" was found to be the most represented localization, and that is in accordance with the fact that the exosome compartment is a key part of the secretome. Cell–cell adhesion was the most enriched biological function, and this is in line with the supportive role of SC in nerves (25) and their role in promoting the nerve-cancer cell interaction (11). Strikingly, GO analysis also revealed that 73% of the identified proteins possessed molecular functions related to protein binding. Gal-3 BP or insulin-like growth factor BP (IGFBP), for instance, is well described for its binding activities that contribute to the regulation of cell growth (26, 27). The SC secretome was also enriched in proteins involved in molecular functions related to "catalytic activity," which may play important roles in cancer progression. For instance, cathepsin D is a catalytic protein that stimulates cancer cell proliferation and tumor angiogenesis and can also provide protection against tumor apoptosis (28). Similarly, other significantly enriched molecular functions including receptor binding, fibroblast growth factor binding, and platelet-derived growth factor binding are all pertinent to tumorigenesis and metastasis. Collectively, these findings indicate that the protein signatures identified in the SC secretome match molecular networks and biological processes associated with tumor progression. In future studies, it would be of interest to investigate the proteome of SCs when stimulated by PC cells to further delineate the crosstalk between PC cells and SC in the tumor microenvironment.

Some of the identified proteins were validated by WB, and blocking antibodies were used to test the effect of their inhibition on PC cell proliferation and invasion *in vitro*. We observed that blocking antibodies against Gal-3BP, MMP-2, cathepsin D, PAI-1, biglycan, TIMP-2, and Gal-1 inhibited the proliferation of PC cells induced by SC-CM. Additionally, blocking MMP-2, cathepsin D, PAI-1, and Gal-1also reduced cancer cell invasion.

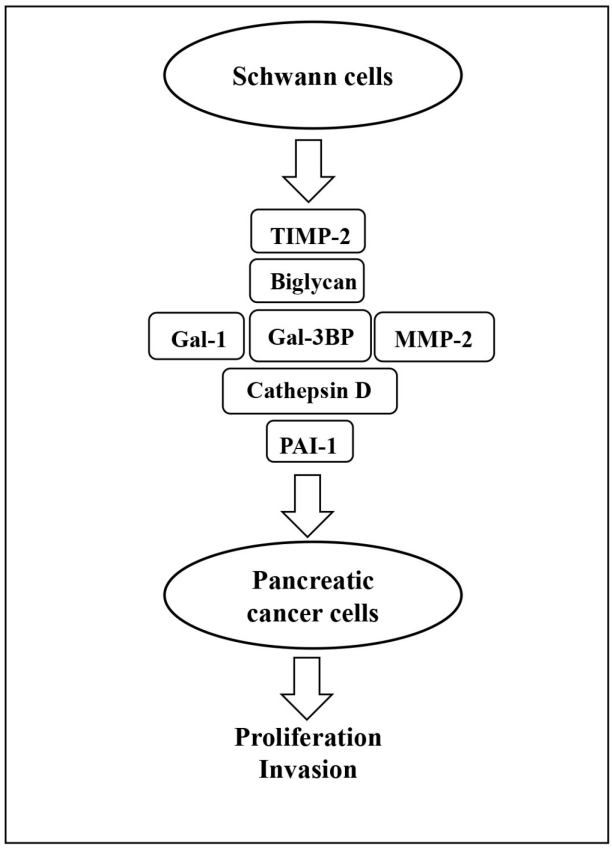

FIGURE 8 | Schematic representation of SC-stimulation of PC cells. Gal-3BP, MMP-2, cathepsin D, PAI-1, biglycan, TIMP-2, and Gal-1 are the SC-secreted proteins that have been identified as potential promoters of PC cell proliferation and invasion in this study. SC, Schwann cell; PC, pancreatic cancer; Gal-3BP, galectin-3 binding protein; MMP-2, matrix metalloproteinase-2; PAI-1, plasminogen activator inhibitor-1; TIMP-2, tissue inhibitor of metalloproteinases-2; Gal-1, galectin-1.

The potential role of each of these proteins in PC cancer is discussed below.

Galectin-3 BP, also known as tumor-associated antigen 90K, is a large oligomeric heavily glycosylated and secreted protein (26). It is a binding partner of Gal-1 and Gal-3, which promote integrin-mediated cell adhesion, and significantly elevated expression of Gal-3 BP in the serum or tumor tissues is associated with poor prognosis in a variety of malignancies including breast cancer (29), lung cancer (30), and PC (31). Additionally, Gal-3 BP is involved in the promotion of integrin-mediated tumor cell adhesion to the ECM proteins in colon cancer (32), breast cancer (33), and the formation of metastasis in lung cancer (34). Our study reveals that targeting Gal-3 BP may prevent the stimulatory effect of SCs in PC cancer cells. In addition, Gal-1, a binding target of Gal-3 BP, has also been identified in our study.

Galectin-1 is a dimeric carbohydrate BP that facilitates the malignant cellular activities by cross-linking glycoproteins (35). It has been reported to play a role in cell invasion of several tumor types, including pancreatic (36), lung (37), and epithelial ovarian tumors (38). Knockdown of this protein can decrease the invasiveness of cancer cells in cervical cancer (39) and oral squamous cell carcinomas (40). Gal-1 has been reported to promote cancer cell invasion by enhancing the expression and enzymatic activities of MMP-2 and MMP-9 (40). It also appears to promote epithelial–mesenchymal transition in lung cancer cell lines (41), and our study points to the role of this protein in the SC-induced stimulation of PC cell growth and invasion.

Matrix metalloproteinase-2, a zinc-dependent endopeptidase, has been implicated in the malignant potential of tumor cells, because of its ability to degrade ECM proteins (42). MMP-2 is associated with the development of desmoplastic reaction in PC (43), and downregulation of MMP-2 reduces PC cell migration (44) and invasion (45). Our study reveals that MMP-2 is a potential mediator of the stimulatory role of SCs in PC cell proliferation and invasion. Interestingly, TIMP-2, tissue inhibitor of metalloproteinases (TIMPs) family, has also been identified in our study. TIMP-2 was described to decrease cell proliferation and migration *in vitro* via the inhibition of MMPs (46). However, it is associated with poor patient outcomes in cancers including gastric (47), renal (48), and oral squamous cell cancers (49). In lung cancer, TIMP-2 has been reported to inhibit tumor growth by promoting an antitumoral transcriptional profile both *in vitro* and *in vivo* (50). High expression of TIMP-2 has been shown to correlate with adverse prognosis in breast cancer (51). Our study indicates that MMP-2 and TIMP-2 are both released by SC and that they can contribute to the stimulation of PC cell growth and invasion. Similarly, PAI-1, another protease inhibitor also known as serpin (52), has also been identified in our study. It has been reported to inhibit proliferation of hepatocellular (53) and prostate cancer cell growth (54). In ovarian cancer, PAI-1 facilitates cell growth and inhibits apoptosis (55). Overexpression of PAI-1 inhibited cell migration and invasion in PC (56). Our study shows that PAI-1 is secreted by SC and can stimulate PC cell proliferation and invasion.

Cathepsin D is a secreted aspartic protease, which when highly expressed is associated with unfavorable clinical outcomes in patients with PC (57). It has been shown that cathepsin D expression can accelerate the metastatic spread of PC by upregulation of S100P (58). Combination of cathepsin D with CA-19-9 and MMP-7 has been reported to be an important panel of markers for screening PC (59). High cathepsin D expression in PC has been shown to decrease the effectiveness of adjuvant gemcitabine (60). The present study reveals the potential role of cathepsin D as a promoter of PC cell proliferation and invasion induced by SC.

Biglycan is a leucine-rich proteoglycan whose overexpression is related to enhanced angiogenesis and tumor invasion (61). Correlations of biglycan expression with aggressive clinicopathological features and poor survival in human cancers such as pancreatic adenocarcinoma (62), colorectal cancer (61), and gastric cancer (63) have been reported. High biglycan expression has been shown to promote invasiveness of melanoma cells (64). It has been reported to promote tumor invasion, migration, and metastasis of gastric cancer cells both *in vitro* and *in vivo* through activating the FAK signaling pathway (63). Our

results suggest that biglycan is secreted by SC and can stimulate PC cell proliferation.

Our proteomic analysis also identified several other proteins of interest that, although they were not tested in functional analysis, may still be important in the stimulation PC cells by SCs. This is, for instance, the case of IGFBPs (IGFBP-2, IGFBP-4, IGFBP-5, IGFBP-6, IGFBP-7) and transforming growth factors (TGF- 1, TGF- 2, TGF-BI). Further studies are warranted to determine the possible involvement of these proteins in cancer PC progression and their potential value as therapeutic targets.

CONCLUSION

In summary, this proteomic and functional analysis identified a number of SC-secreted proteins that seem to be involved in the proliferation and invasiveness of PC cancer cells induced by SC. Further preclinical studies *in vivo* are warranted to determine whether these proteins may become new targets for therapeutic intervention in PC.

DATA AVAILABILITY STATEMENT

The original contributions presented in the study are publicly available. This data can be found here: the Mass Spectrometry Interactive Virtual Environment (MassIVE) database with the dataset identifier MSV000084303 (https://massive.ucsd.edu/ProteoSAFe).

AUTHOR CONTRIBUTIONS

HH and AF designed the study and wrote the manuscript. AF and XL carried out the experiments. AF analyzed the data. XL, NG, SF, MJ, FG, CJ, DH, PT, and PJ edited the manuscript. All authors contributed to manuscript revision, read, and approved the submitted version.

FUNDING

This research was supported by the Maitland Cancer Appeal Committee (NSW Australia), the Hunter Medical Research Institute (HMRI), and the Hunter Cancer Research Alliance (HCRA).

ACKNOWLEDGMENTS

The authors thank the University of Newcastle, and the funding bodies for supporting this research and Kristen McEwan as well as Mark Marshland for providing excellent research assistance.

SUPPLEMENTARY MATERIAL

The Supplementary Material for this article can be found online at: https://www.frontiersin.org/articles/10.3389/fonc.2020.01601/full#supplementary-material

REFERENCES

1. Are C, Chowdhury S, Ahmad H, Ravipati A, Song T, Shrikandhe S, et al. Predictive global trends in the incidence and mortality of pancreatic cancer based on geographic location, socio-economic status, and demographic shift. *J Surg Oncol*. (2016) 114:736–42. doi: 10.1002/jso.24410
2. Rahib L, Smith BD, Aizenberg R, Rosenzweig AB, Fleshman JM, Matrisian LM. Projecting cancer incidence and deaths to 2030: the unexpected burden of thyroid, liver, and pancreas cancers in the United States. *Cancer Res*. (2014) 74:2913–21. doi: 10.1158/0008-5472.Can-14-0155
3. Siegel RL, Miller KD, Jemal A. Cancer statistics, 2018. *CA Cancer J Clin*. (2018) 68:7–30. doi: 10.3322/caac.21442
4. Siegel RL, Miller KD, Jemal A. Cancer statistics, 2017. *CA Cancer J Clin*. (2017) 67:7–30. doi: 10.3322/caac.21387
5. Ryan DP, Hong TS, Bardeesy N. Pancreatic adenocarcinoma. *N Engl J Med*. (2014) 371:1039–49. doi: 10.1056/NEJMra1404198
6. Takahashi Y, Sipp D, Enomoto H. Tissue interactions in neural crest cell development and disease. *Science*. (2013) 341:860–3. doi: 10.1126/science.1230717
7. Jessen KR. Glial cells. *Int J Biochem Cell Biol*. (2004) 36:1861–7. doi: 10.1016/j.biocel.2004.02.023
8. Kaplan S, Odaci E, Unal B, Sahin B, Fornaro M. Chapter 2: development of the peripheral nerve. *Int Rev Neurobiol*. (2009) 87:9–26. doi: 10.1016/s0074-7742(09)87002-5
9. Lehmann HC, Hoke A. Use of engineered Schwann cells in peripheral neuropathy: hopes and hazards. *Brain Res*. (2016) 1638(Pt A):97–104. doi: 10.1016/j.brainres.2015.10.040
10. Demir IE, Boldis A, Pfitzinger PL, Teller S, Brunner E, Klose N, et al. Investigation of Schwann cells at neoplastic cell sites before the onset of cancer invasion. *J Natl Cancer Inst*. (2014) 106:dju184. doi: 10.1093/jnci/dju184
11. Deborde S, Omelchenko T, Lyubchik A, Zhou Y, He S, McNamara WF, et al. Schwann cells induce cancer cell dispersion and invasion. *J Clin Investig*. (2016) 126:1538–54. doi: 10.1172/jci82658
12. Fujii-Nishimura Y, Yamazaki K, Masugi Y, Douguchi J, Kurebayashi Y, Kubota N, et al. Mesenchymal-epithelial transition of pancreatic cancer cells at perineural invasion sites is induced by Schwann cells. *Pathol Int*. (2018) 68:214–23. doi: 10.1111/pin.12641
13. Sroka IC, Chopra H, Das L, Gard JMC, Nagle RB, Cress AE. Schwann cells increase prostate and pancreatic tumor cell invasion using laminin binding A6 integrin. *J Cell Biochem*. (2016) 117:491–9. doi: 10.1002/jcb.25300
14. Zhou Y, Shurin GV, Zhong H, Bunimovich YL, Han B, Shurin MR. Schwann cells augment cell spreading and metastasis of lung cancer. *Cancer Res*. (2018) 78:5927–39. doi: 10.1158/0008-5472.CAN-18-1702
15. Salvo E, Saraithong P, Curtin JG, Janal MN, Ye Y. Reciprocal interactions between cancer and Schwann cells contribute to oral cancer progression and pain. *Heliyon*. (2019) 5:e01223. doi: 10.1016/j.heliyon.2019.e01223
16. Huang T, Fan Q, Wang Y, Cui Y, Wang Z, Yang L, et al. Schwann cell-derived CCL2 promotes the perineural invasion of cervical cancer. *Front Oncol*. (2020) 10:19. doi: 10.3389/fonc.2020.00019
17. Demir IE, Tieftrunk E, Schorn S, Saricaoglu OC, Pfitzinger PL, Teller S, et al. Activated Schwann cells in pancreatic cancer are linked to analgesia via suppression of spinal astroglia and microglia. *Gut*. (2016) 65:1001–14. doi: 10.1136/gutjnl-2015-309784
18. Su D, Guo X, Huang L, Ye H, Li Z, Lin L, et al. Tumor-neuroglia interaction promotes pancreatic cancer metastasis. *Theranostics*. (2020) 10:5029–47. doi: 10.7150/thno.42440
19. Roger E, Martel S, Bertrand-Chapel A, Depollier A, Chuvin N, Pommier RM, et al. Schwann cells support oncogenic potential of pancreatic cancer cells through TGF signaling. *Cell Death Dis*. (2019) 10:886. doi: 10.1038/s41419-019-2116-x

20. Na'ara S, Amit M, Gil Z. L1CAM induces perineural invasion of pancreas cancer cells by upregulation of metalloproteinase expression. *Oncogene*. (2019) 38:596–608. doi: 10.1038/s41388-018-0458-y
21. Ferdoushi A, Li X, Jamaluddin MFB, Hondermarck H. Proteomic profile of human Schwann cells. *Proteomics*. (2020) 20:1900294. doi: 10.1002/pmic.201900294
22. Faulkner S, Jobling P, Rowe CW, Rodrigues Oliveira SM, Roselli S, Thorne RF, et al. Neurotrophin receptors TrkA, p75(NTR), and sortilin are increased and targetable in thyroid cancer. *Am J Pathol*. (2018) 188:229–41. doi: 10.1016/j.ajpath.2017.09.008
23. Gao F, Griffin N, Faulkner S, Rowe CW, Williams L, Roselli S, et al. The neurotrophic tyrosine kinase receptor TrkA and its ligand NGF are increased in squamous cell carcinomas of the lung. *Sci Rep*. (2018) 8:8135. doi: 10.1038/s41598-018-26408-2
24. Baker S, Ali I, Silins I, Pyysalo S, Guo Y, Hogberg J, et al. Cancer hallmarks analytics tool (CHAT): a text mining approach to organize and evaluate scientific literature on cancer. *Bioinformatics*. (2017) 33:3973–81. doi: 10.1093/bioinformatics/btx454
25. Corfas G, Velardez MO, Ko C-P, Ratner N, Peles E. Mechanisms and roles of axon-schwann cell interactions. *J Neurosci*. (2004) 24:9250. doi: 10.1523/JNEUROSCI.3649-04.2004
26. Koths K, Taylor E, Halenbeck R, Casipit C, Wang A. Cloning and characterization of a human Mac-2-binding protein, a new member of the superfamily defined by the macrophage scavenger receptor cysteine-rich domain. *J Biol Chem*. (1993) 268:14245–9.
27. Forbes BE, McCarthy P, Norton RS. Insulin-like growth factor binding proteins: a structural perspective. *Front Endocrinol*. (2012) 3:38. doi: 10.3389/fendo.2012.00038
28. Berchem G, Glondu M, Gleizes M, Brouillet JP, Vignon F, Garcia M, et al. Cathepsin-D affects multiple tumor progression steps in vivo: proliferation, angiogenesis and apoptosis. *Oncogene*. (2002) 21:5951–5. doi: 10.1038/sj.onc.1205745
29. Tinari N, Lattanzio R, Querzoli P, Natoli C, Grassadonia A, Alberti S, et al. High expression of 90K (Mac-2 BP) is associated with poor survival in node-negative breast cancer patients not receiving adjuvant systemic therapies. *Int J Cancer*. (2009) 124:333–8. doi: 10.1002/ijc.23970
30. Marchetti A, Tinari N, Buttitta F, Chella A, Angeletti CA, Sacco R, et al. Expression of 90K (Mac-2 BP) correlates with distant metastasis and predicts survival in stage I non-small cell lung cancer patients. *Cancer Res*. (2002) 62:2535–9.
31. Kunzli BM, Berberat PO, Zhu ZW, Martignoni M, Kleeff J, Tempia-Caliera AA, et al. Influences of the lysosomal associated membrane proteins (Lamp-1, Lamp-2) and Mac-2 binding protein (Mac-2-BP) on the prognosis of pancreatic carcinoma. *Cancer*. (2002) 94:228–39. doi: 10.1002/cncr.10162
32. Ulmer TA, Keeler V, Loh L, Chibbar R, Torlakovic E, Andre S, et al. Tumor-associated antigen 90K/Mac-2-binding protein: possible role in colon cancer. *J Cell Biochem*. (2006) 98:1351–66. doi: 10.1002/jcb.20784
33. Noma N, Simizu S, Kambayashi Y, Kabe Y, Suematsu M, Umezawa K. Involvement of NF-kappaB-mediated expression of galectin-3-binding protein in TNF-alpha-induced breast cancer cell adhesion. *Oncol Rep*. (2012) 27:2080–4. doi: 10.3892/or.2012.1733
34. Ozaki Y, Kontani K, Teramoto K, Fujita T, Tezuka N, Sawai S, et al. Involvement of 90K/Mac-2 binding protein in cancer metastases by increased cellular adhesiveness in lung cancer. *Oncol Rep*. (2004) 12:1071–7.
35. Cousin JM, Cloninger MJ. The role of galectin-1 in cancer progression, and synthetic multivalent systems for the study of galectin-1. *Int J Mol Sci*. (2016) 17:1566. doi: 10.3390/ijms17091566
36. Xue X, Lu Z, Tang D, Yao J, An Y, Wu J, et al. Galectin-1 secreted by activated stellate cells in pancreatic ductal adenocarcinoma stroma promotes proliferation and invasion of pancreatic cancer cells: an in vitro study on the microenvironment of pancreatic ductal adenocarcinoma. *Pancreas*. (2011) 40:832–9. doi: 10.1097/MPA.0b013e318217945e
37. Chung L-Y, Tang S-J, Sun G-H, Chou T-Y, Yeh T-S, Yu S-L, et al. Galectin-1 promotes lung cancer progression and chemoresistance by upregulating p38 MAPK, ERK, and cyclooxygenase-2. *Clin Cancer Res*. (2012) 18:4037–47. doi: 10.1158/1078-0432.ccr-11-3348
38. Kim HJ, Jeon HK, Cho YJ, Park YA, Choi JJ, Do IG, et al. High galectin-1 expression correlates with poor prognosis and is involved in epithelial ovarian cancer proliferation and invasion. *Eur J Cancer*. (2012) 48:1914–21. doi: 10.1016/j.ejca.2012.02.005
39. Kim HJ, Do IG, Jeon HK, Cho YJ, Park YA, Choi JJ, et al. Galectin 1 expression is associated with tumor invasion and metastasis in stage IB to IIA cervical cancer. *Hum Pathol*. (2013) 44:62–8. doi: 10.1016/j.humpath.2012.04.010
40. Wu M-H, Hong T-M, Cheng H-W, Pan S-H, Liang Y-R, Hong H-C, et al. Galectin-1-mediated tumor invasion and metastasis, up-regulated matrix metalloproteinase expression, and reorganized actin cytoskeletons. *Mol Cancer Res*. (2009) 7:311. doi: 10.1158/1541-7786.MCR-08-0297
41. Hsu Y-L, Wu C-Y, Hung J-Y, Lin Y-S, Huang M-S, Kuo P-L. Galectin-1 promotes lung cancer tumor metastasis by potentiating integrin 6 4 and Notch1/Jagged2 signaling pathway. *Carcinogenesis*. (2013) 34:1370–81. doi: 10.1093/carcin/bgt040
42. Nelson AR, Fingleton B, Rothenberg ML, Matrisian LM. Matrix metalloproteinases: biologic activity and clinical implications. *J Clin Oncol*. (2000) 18:1135–49. doi: 10.1200/jco.2000.18.5.1135
43. Ellenrieder V, Alber B, Lacher U, Hendler SF, Menke A, Boeck W, et al. Role of MT-MMPs and MMP-2 in pancreatic cancer progression. *Int J Cancer*. (2000) 85:14–20. doi: 10.1002/(sici)1097-0215(20000101)85:13.0.co;2-o
44. Zou Y, Li J, Chen Z, Li X, Zheng S, Yi D, et al. miR-29c suppresses pancreatic cancer liver metastasis in an orthotopic implantation model in nude mice and affects survival in pancreatic cancer patients. *Carcinogenesis*. (2015) 36:676–84. doi: 10.1093/carcin/bgv027
45. Layton T, Stalens C, Gunderson F, Goodison S, Silletti S. Syk tyrosine kinase acts as a pancreatic adenocarcinoma tumor suppressor by regulating cellular growth and invasion. *Am J Pathol*. (2009) 175:2625–36. doi: 10.2353/ajpath.2009.090543
46. Wang W, Li D, Xiang L, Lv M, Tao L, Ni T, et al. TIMP-2 inhibits metastasis and predicts prognosis of colorectal cancer via regulating MMP-9. *Cell Adh Migr*. (2019) 13:273–84. doi: 10.1080/19336918.2019.1639303
47. Hsu KW, Fang WL, Huang KH, Huang TT, Lee HC, Hsieh RH, et al. Notch1 pathway-mediated microRNA-151-5p promotes gastric cancer progression. *Oncotarget*. (2016) 7:38036–51. doi: 10.18632/oncotarget.9342
48. Kawata N, Nagane Y, Hirakata H, Ichinose T, Okada Y, Yamaguchi K, et al. Significant relationship of matrix metalloproteinase 9 with nuclear grade and prognostic impact of tissue inhibitor of metalloproteinase 2 for incidental clear cell renal cell carcinoma. *Urology*. (2007) 69:1049–53. doi: 10.1016/j.urology.2007.02.044
49. Katayama A, Bandoh N, Kishibe K, Takahara M, Ogino T, Nonaka S, et al. Expressions of matrix metalloproteinases in early-stage oral squamous cell carcinoma as predictive indicators for tumor metastases and prognosis. *Clin Cancer Res*. (2004) 10:634–40. doi: 10.1158/1078-0432.ccr-0864-02
50. Bourboulia D, Han H, Jensen-Taubman S, Gavil N, Isaac B, Wei B, et al. TIMP-2 modulates cancer cell transcriptional profile and enhances E-cadherin/beta-catenin complex expression in A549 lung cancer cells. *Oncotarget*. (2013) 4:166–76. doi: 10.18632/oncotarget.801
51. Remacle A, McCarthy K, Noel A, Maguire T, McDermott E, O'Higgins N, et al. High levels of TIMP-2 correlate with adverse prognosis in breast cancer. *Int J Cancer*. (2000) 89:118–21. doi: 10.1002/(sici)1097-0215(20000320)89:23.0.co;2-8
52. Fang H, Placencio VR, DeClerck YA. Protumorigenic activity of plasminogen activator inhibitor-1 through an antiapoptotic function. *J Natl Cancer Inst*. (2012) 104:1470–84. doi: 10.1093/jnci/djs377
53. Morita Y, Hayashi Y, Kanamaru T, Itoh T, Suzuki S, Yamamoto M, et al. Inhibitory role of plasminogen activator inhibitor-1 in invasion and proliferation of HLE hepatocellular carcinoma cells. *Jpn J Cancer Res*. (1999) 90:747–52. doi: 10.1111/j.1349-7006.1999.tb00810.x
54. Chen SC, Henry DO, Reczek PR, Wong MK. Plasminogen activator inhibitor-1 inhibits prostate tumor growth through endothelial apoptosis. *Mol Cancer Ther*. (2008) 7:1227–36. doi: 10.1158/1535-7163.Mct-08-0051
55. Mashiko S, Kitatani K, Toyoshima M, Ichimura A, Dan T, Usui T, et al. Inhibition of plasminogen activator inhibitor-1 is a potential therapeutic strategy in ovarian cancer. *Cancer Biol Ther*. (2015) 16:253–60. doi: 10.1080/15384047.2014.1001271
56. Inoue M, Sawada T, Uchima Y, Kimura K, Nishihara T, Tanaka H, et al. Plasminogen activator inhibitor-1 (PAI-1) gene transfection inhibits the liver metastasis of pancreatic cancer by preventing angiogenesis. *Oncol Rep*. (2005) 14:1445–51.

57. Niedergethmann M, Hildenbrand R, Wolf G, Verbeke CS, Richter A, Post S. Angiogenesis and cathepsin expression are prognostic factors in pancreatic adenocarcinoma after curative resection. *Int J Pancreatol*. (2000) 28:31–9. doi: 10.1385/ijgc:28:1:31
58. Whiteman HJ, Weeks ME, Dowen SE, Barry S, Timms JF, Lemoine NR, et al. The role of S100P in the invasion of pancreatic cancer cells is mediated through cytoskeletal changes and regulation of cathepsin D. *Cancer Res*. (2007) 67:8633–42. doi: 10.1158/0008-5472.Can-07-0545
59. Park HD, Kang ES, Kim JW, Lee KT, Lee KH, Park YS, et al. Serum CA19-9, cathepsin D, and matrix metalloproteinase-7 as a diagnostic panel for pancreatic ductal adenocarcinoma. *Proteomics*. (2012) 12:3590–7. doi: 10.1002/pmic.201200101
60. Mahajan UM, Goni E, Langhoff E, Li Q, Costello E, Greenhalf W, et al. Cathepsin D expression and gemcitabine resistance in pancreatic cancer. *JNCI Cancer Spectr*. (2019) 4:kz060. doi: 10.1093/jncics/pkz060
61. Gu X, Ma Y, Xiao J, Zheng H, Song C, Gong Y, et al. Up-regulated biglycan expression correlates with the malignancy in human colorectal cancers. *Clin Exp Med*. (2012) 12:195–9. doi: 10.1007/s10238-011-0155-4
62. Aprile G, Avellini C, Reni M, Mazzer M, Foltran L, Rossi D, et al. Biglycan expression and clinical outcome in patients with pancreatic adenocarcinoma. *Tumor Biol*. (2013) 34:131–7. doi: 10.1007/s13277-012-0520-2
63. Hu L, Duan Y-T, Li J-F, Su L-P, Yan M, Zhu Z-G, et al. Biglycan enhances gastric cancer invasion by activating FAK signaling pathway. *Oncotarget*. (2014) 5:1885–96. doi: 10.18632/oncotarget.1871
64. Andrlova H, Mastroianni J, Madl J, Kern JS, Melchinger W, Dierbach H, et al. Biglycan expression in the melanoma microenvironment promotes invasiveness via increased tissue stiffness inducing integrin-beta1 expression. *Oncotarget*. (2017) 8:42901–16. doi: 10.18632/oncotarget.17160

Conflict of Interest: The authors declare that the research was conducted in the absence of any commercial or financial relationships that could be construed as a potential conflict of interest.

4.3 Supplementary Files

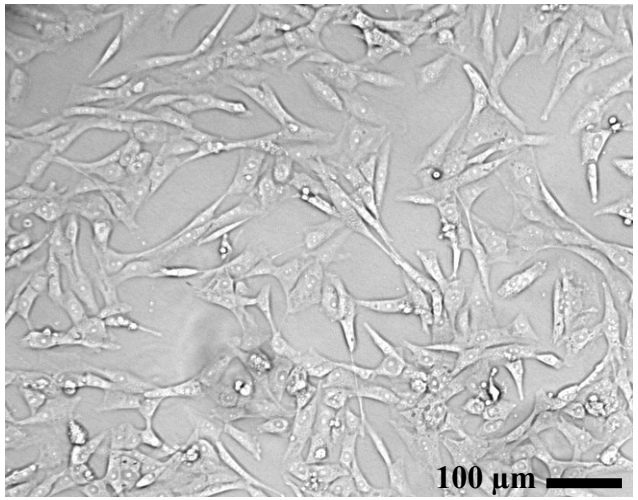

SUPPLEMENTARY FIGURE S1 | Representative image of human SCs. Cells show distinctive SC phenotype such as spindle-shaped morphology. Growing SCs were characterized by immunoblotting using antibodies against SC marker proteins p75 and SOX10 . Scale bar = 100µm. Abbreviation: SC, Schwann cell.

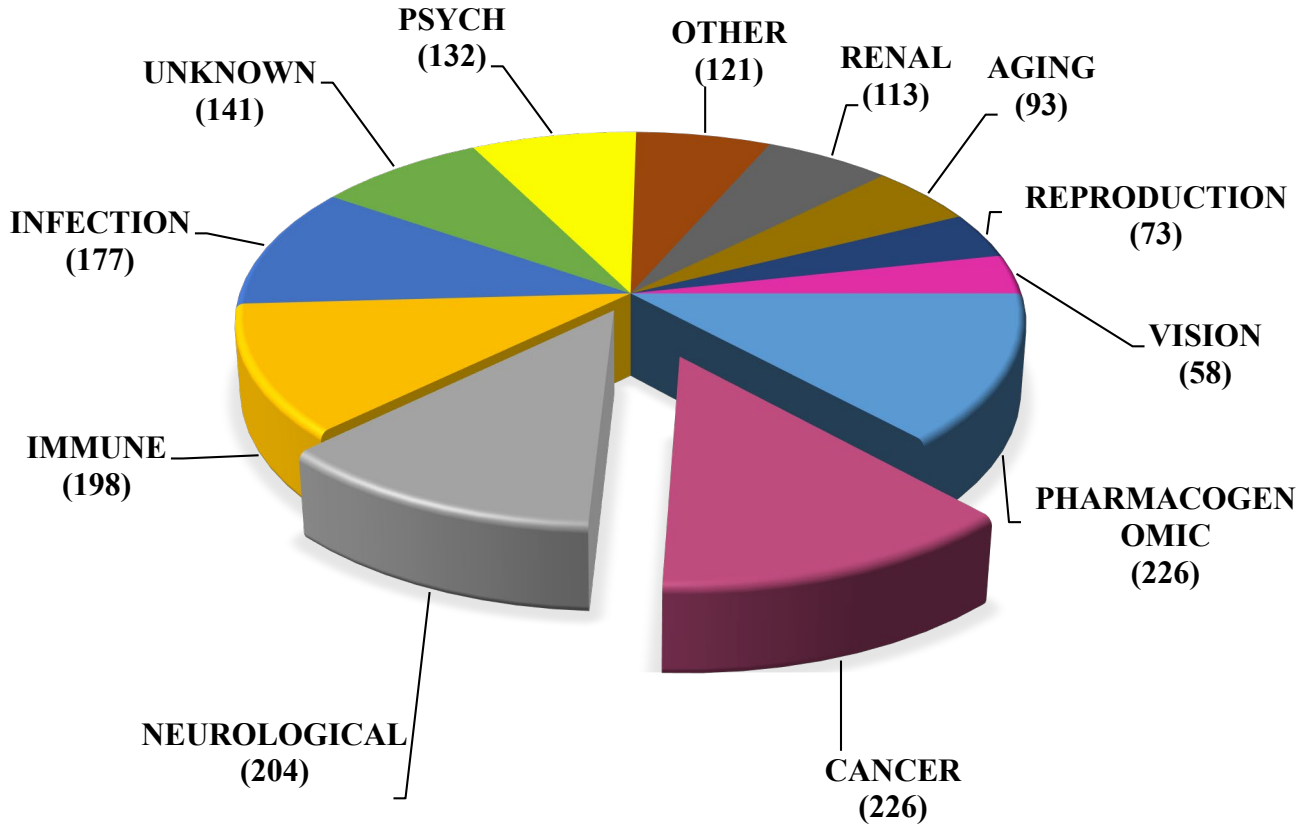

SUPPLEMENTARY FIGURE S2 | Distribution of the identified proteins based on disease classes. GAD analysis was performed using DAVID to investigate the potential association of the identified proteins with diseases. Number of proteins involved in different disease classes are displayed within brackets (multiple protein entries possible). Additional details are listed in Supplementary Table S9. Abbreviations: GAD, Genetic Association Database; DAVID, Database for Annotation, Visualization and Integrated Discovery.

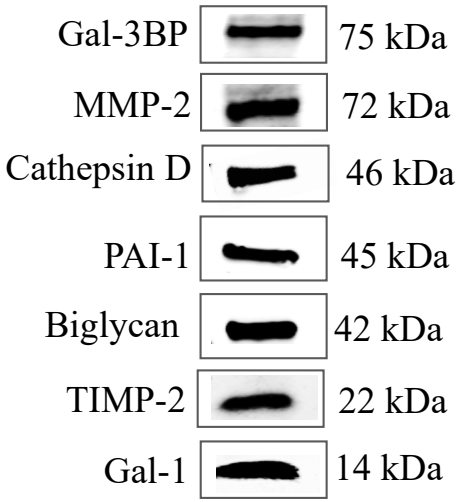

SUPPLEMENTARY FIGURE S3 | WB confirmation of candidate molecules in SC-lysate. WB analysis confirmed the presence of candidate molecules in SC-lysate. Abbreviations: WB, western blot; SC, Schwann cell; Gal-3BP, galectin-3 binding protein; MMP-2, matrix metalloproteinase-2; PAI-1, plasminogen activator inhibitor-1; TIMP-2, tissue inhibitor of metalloproteinases-2; Gal-1, galectin-1.

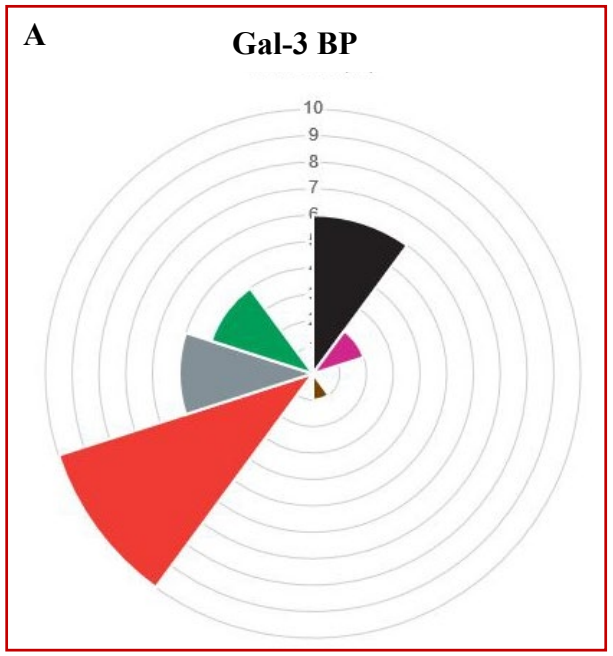
A
Gal-3 BP
10
9
8
7

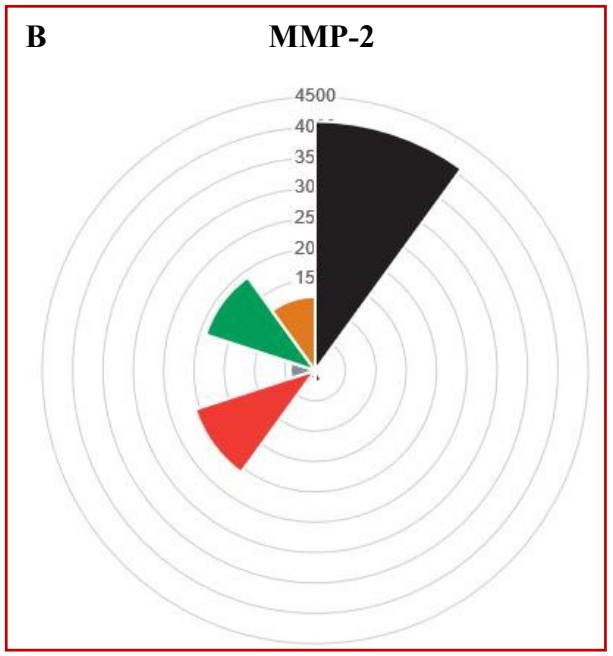
B
MMP-2
4500
40
35
30
25
20
15

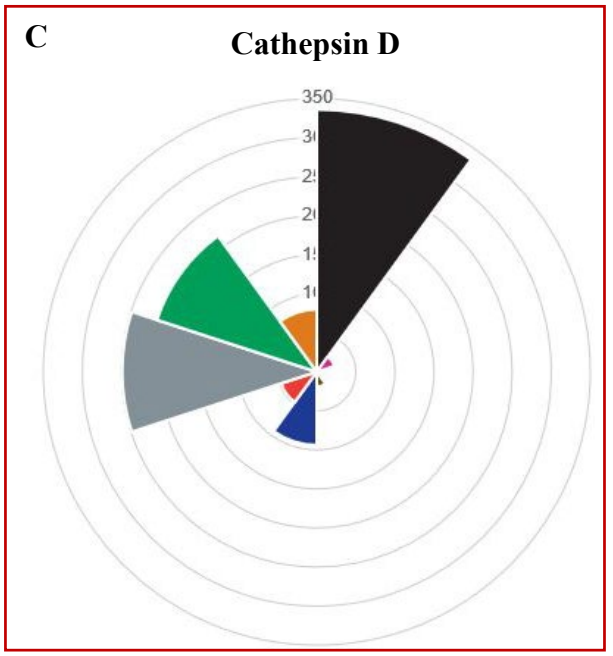
C
Cathepsin D
350

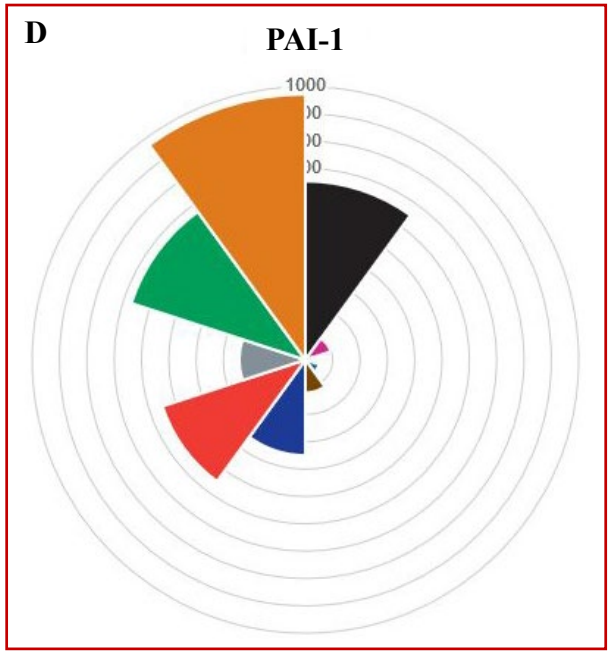
D
PAI-1
1000

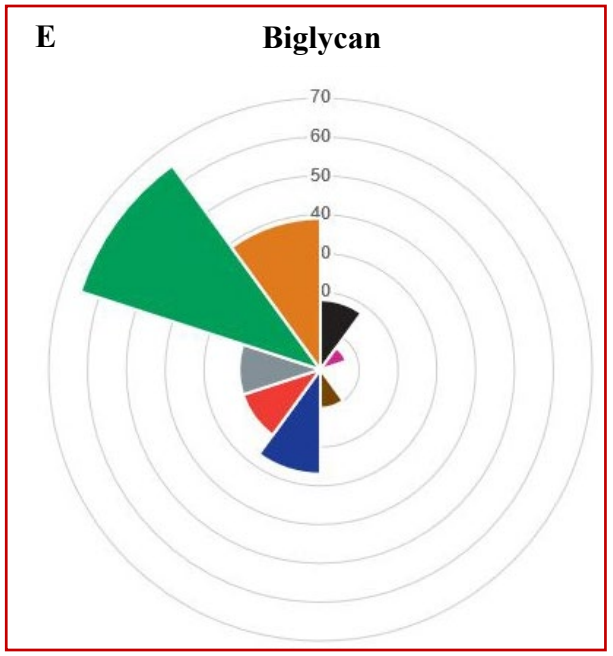
E
Biglycan
70
60
50
40

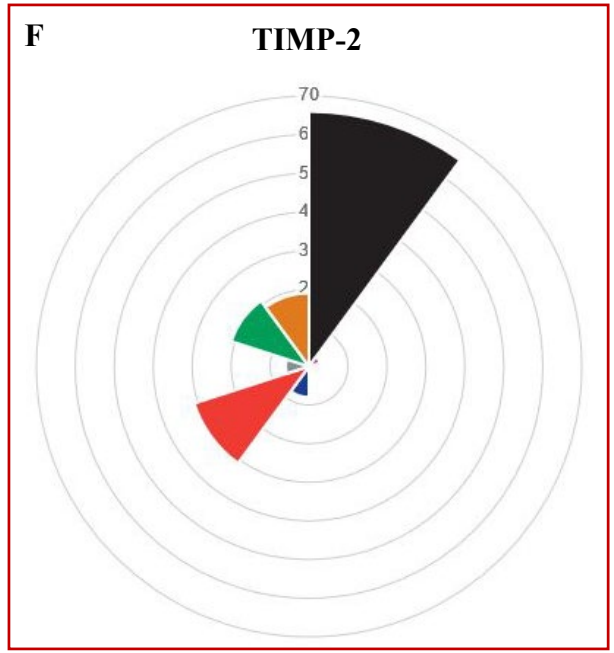
F
TIMP-2
70

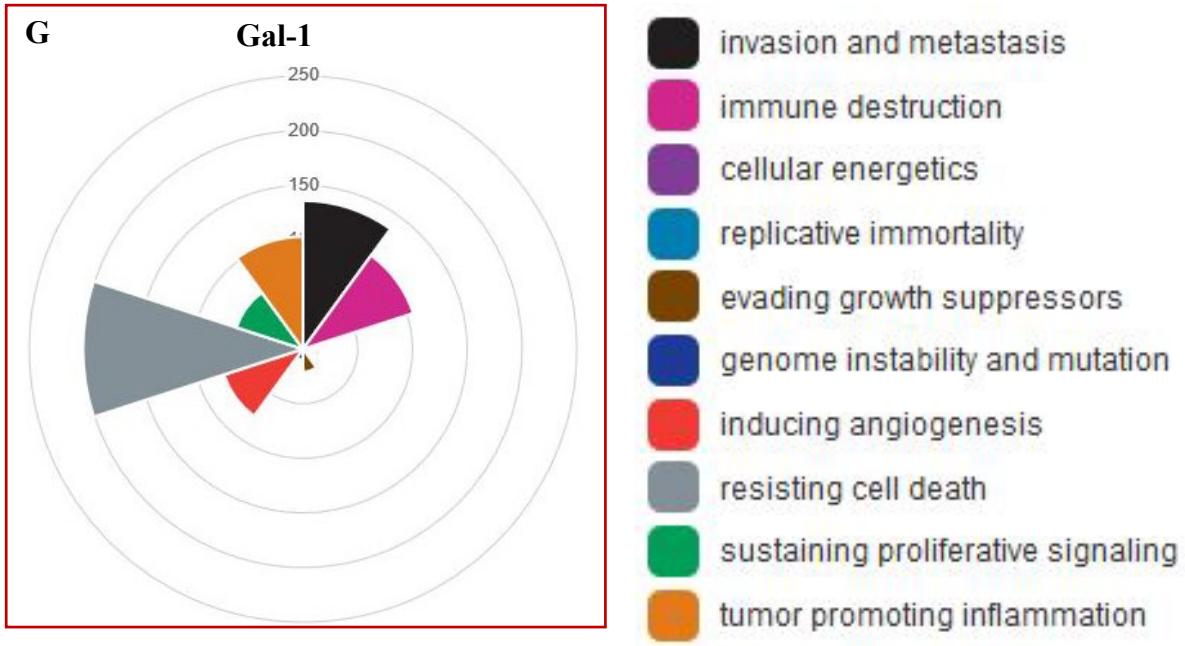

SUPPLEMENTARY FIGURE S4 | Role of candidate molecules in cancer progression. Investigations of the candidate molecules in cancer research using the Cancer Hallmarks Analytics Tool (CHAT) mainly focus on their crucial role in invasion and metastasis, sustaining proliferative signalling, inducing angiogenesis, tumour promoting inflammation and immune destruction in cancer development. CHAT can be accessed at: http://chat.lionproject.net. Abbreviations: Gal-3BP, galectin-3 binding protein; MMP-2, matrix metalloproteinase-2; PAI-1, plasminogen activator inhibitor-1; TIMP-2, tissue inhibitor of metalloproteinases-2; Gal-1, galectin-1.

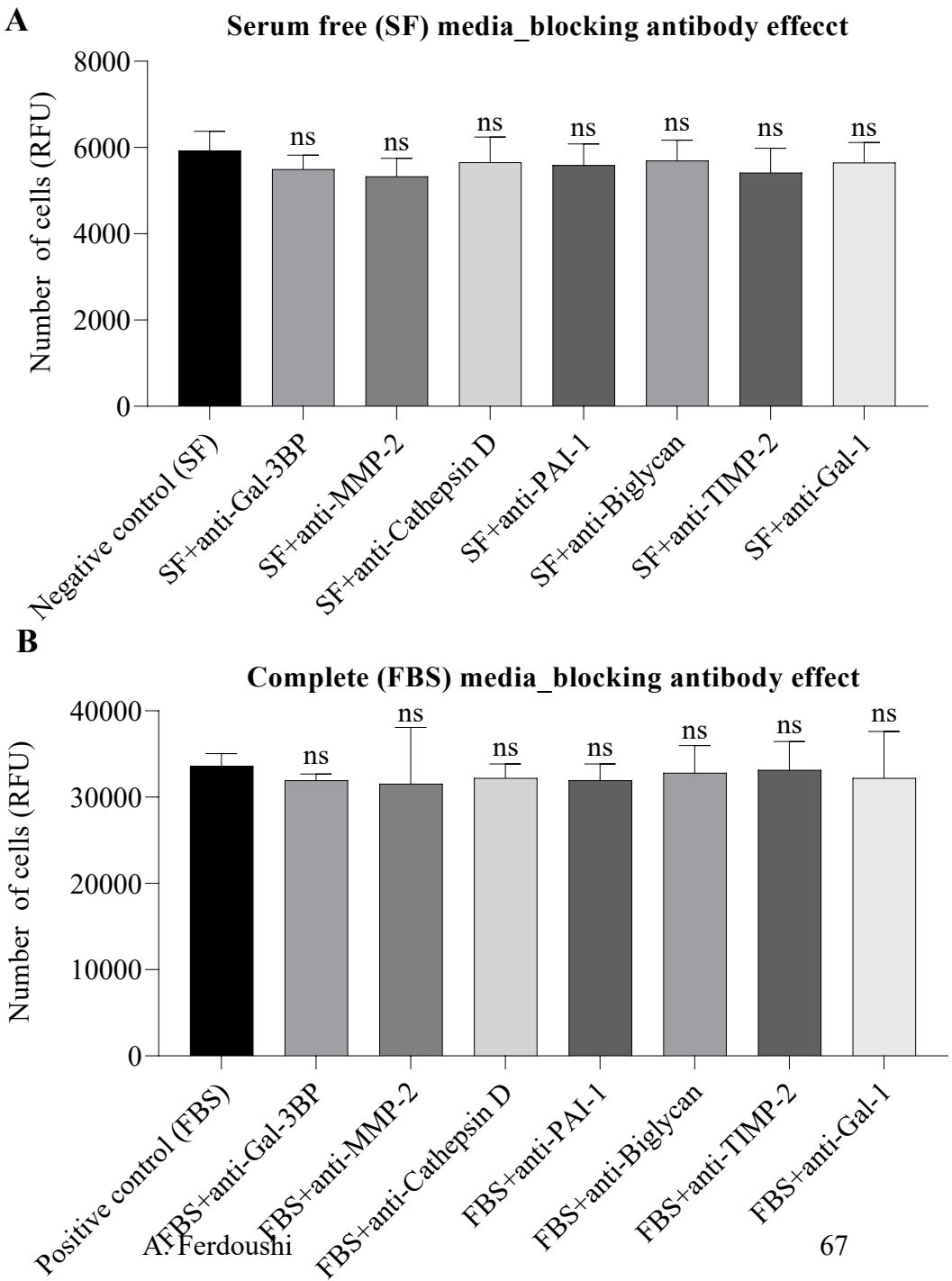

SUPPLEMENTARY FIGURE S5 | Blocking antibodies did not change the proliferative effect induced by SF or complete media on PC cells. To find out if the effect of increased proliferation of PC cells in presence of SC-CM was due to secreted proteins from SCs, or blocking antibodies themselves have any effect in absence of SC-CM, proliferation assays were performed using blocking antibodies against the proteins of interest. No significant decrease in PC cell (MIA PaCa-2) proliferation was observed in presence of blocking antibodies compared to either negative control (SF media only, **Figure A**) or positive control (serum supplemented media only, denoted FBS, **Figure B)** ($p>0.05$). Blocking antibodies were used at 6 μg/ml concentration. Statistical significance was confirmed by one-way ANOVA. The error bars represent the SD of the mean. Abbreviations: SF, serum free; FBS, fetal bovine serum; SC-CM, Schwann cell-conditioned media; PC, pancreatic cancer; Gal-3BP, galectin-3 binding protein; MMP-2, matrix metalloproteinase-2; PAI-1, plasminogen activator inhibitor-1; TIMP-2, tissue inhibitor of metalloproteinases-2; Gal-1, galectin-1; *RFU, relative fluorescence* unit; ns, non-significant.

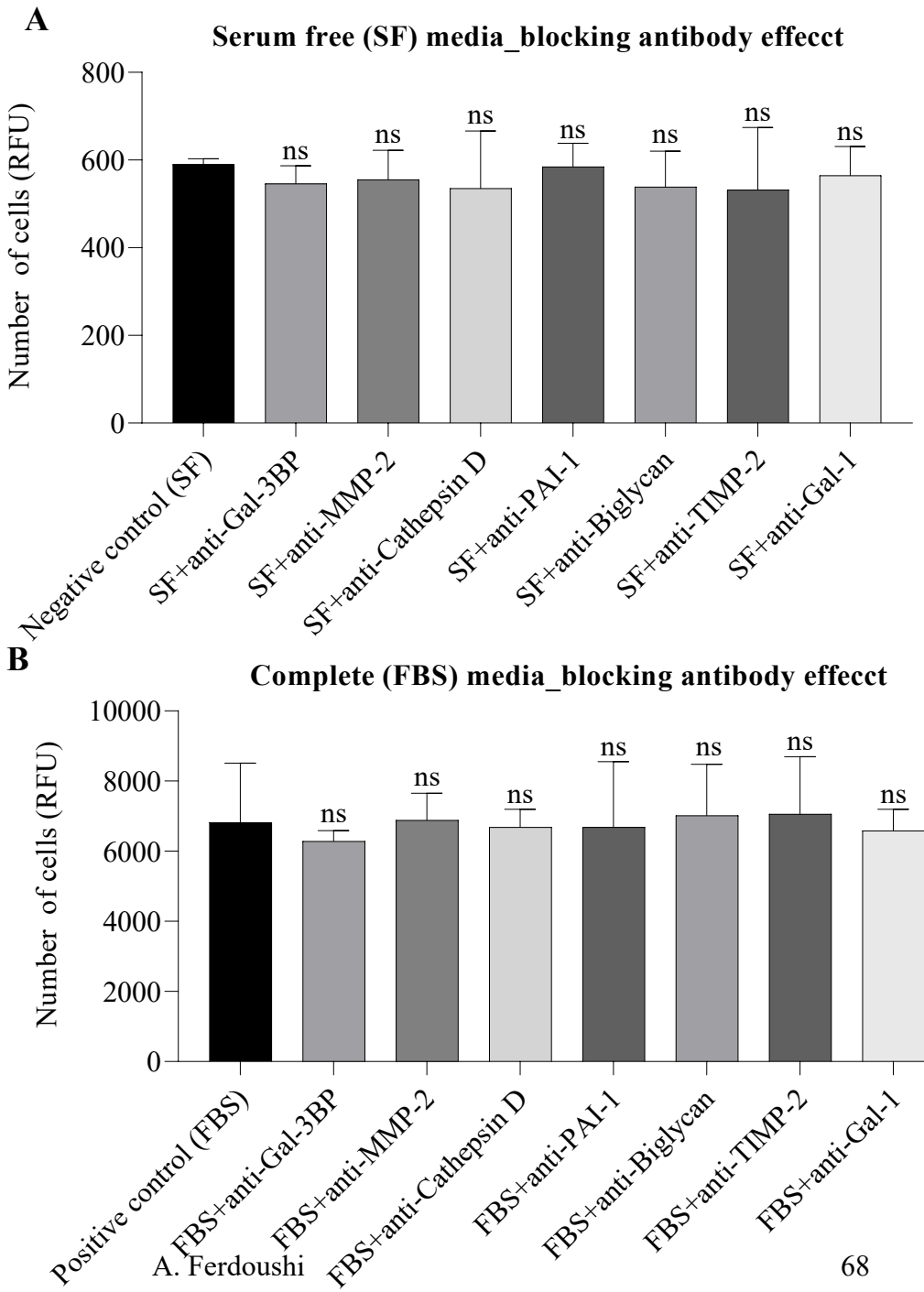

SUPPLEMENTARY FIGURE S6 | Blocking antibodies did not change the invasiveness induced by SF or complete media on PC cells. To find out if the effect of increased invasiveness of PC cells in presence of SC-CM was due to secreted proteins from SCs, or blocking antibodies themselves have any effect in absence of SC-CM, trans-well invasion assays were performed using blocking antibodies against the proteins of interest. No significant decrease in PC cell (MIA PaCa-2) invasiveness was observed in presence of blocking antibodies compared to either negative control (SF media only, **Figure A**) or positive control (serum supplemented media only, denoted FBS, **Figure B**) (p>0.05). Blocking antibodies were used at 6 µg/ml concentration. Statistical significance was confirmed by one-way ANOVA. The error bars represent the SD of the mean. Abbreviations: SF, serum free; FBS, fetal bovine serum; SC-CM, Schwann cell-conditioned media; PC, pancreatic cancer; Gal-3BP, galectin-3 binding protein; MMP-2, matrix metalloproteinase-2; PAI-1, plasminogen activator inhibitor-1; TIMP-2, tissue inhibitor of metalloproteinases-2; Gal-1, galectin-1; *RFU, relative fluorescence* unit; ns, non-significant.

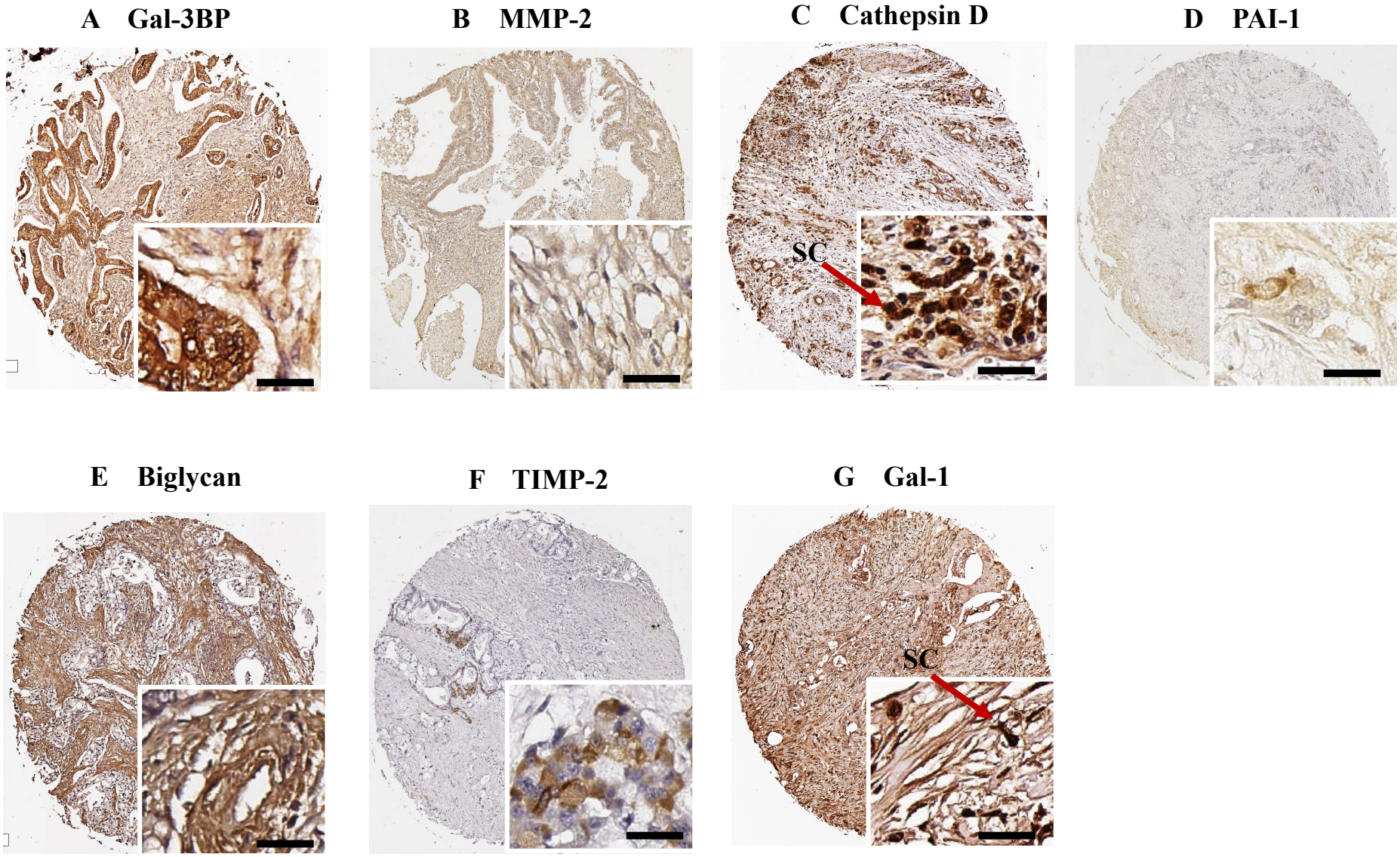

SUPPLEMENTARY FIGURE S7 | Expression of candidate proteins in clinical samples of PC. Immunohistochemical detection of seven candidate proteins was performed on a cohort of pancreatic cancer TMA revealing moderate to high levels of expression of the proteins. Representative images for each proteins are shown. SCs have been indicated by red arrow head. Scale bar: 200 μm. Abbreviations: PC, pancreatic cancer; SC, Schwann cell; TMA, tissue micro array; Gal-3BP, galectin-3 binding protein; MMP-2, matrix metalloproteinase-2; PAI-1, plasminogen activator inhibitor-1; TIMP-2, tissue inhibitor of metalloproteinases-2; Gal-1, galectin-1.

Supplementary material: Western blot full images

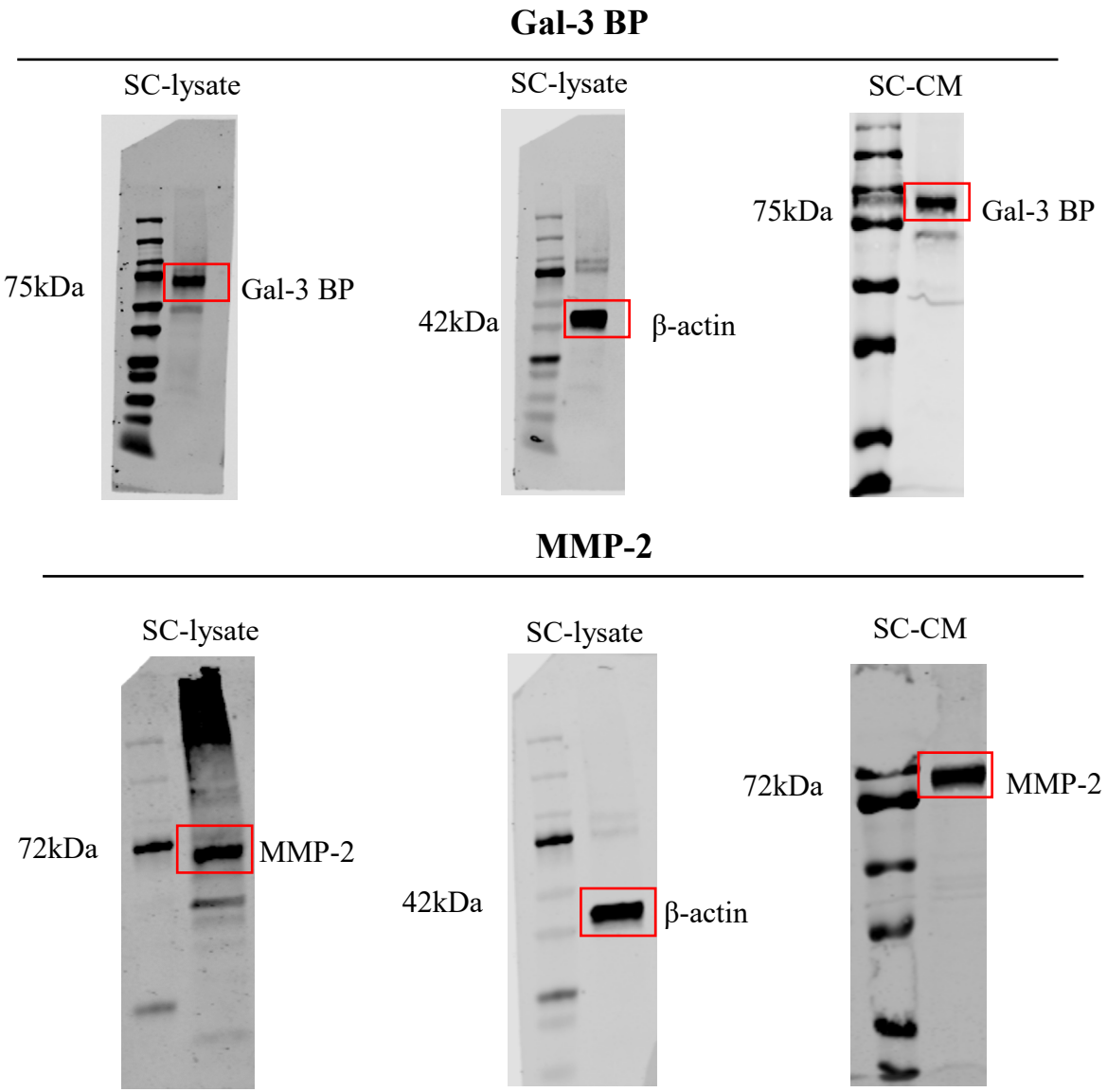

Gal-3BP, galectin-3 binding protein
MMP-2, matrix metalloproteinase-2
SC-CM, Schwann cell-conditioned media

Cathepsin D

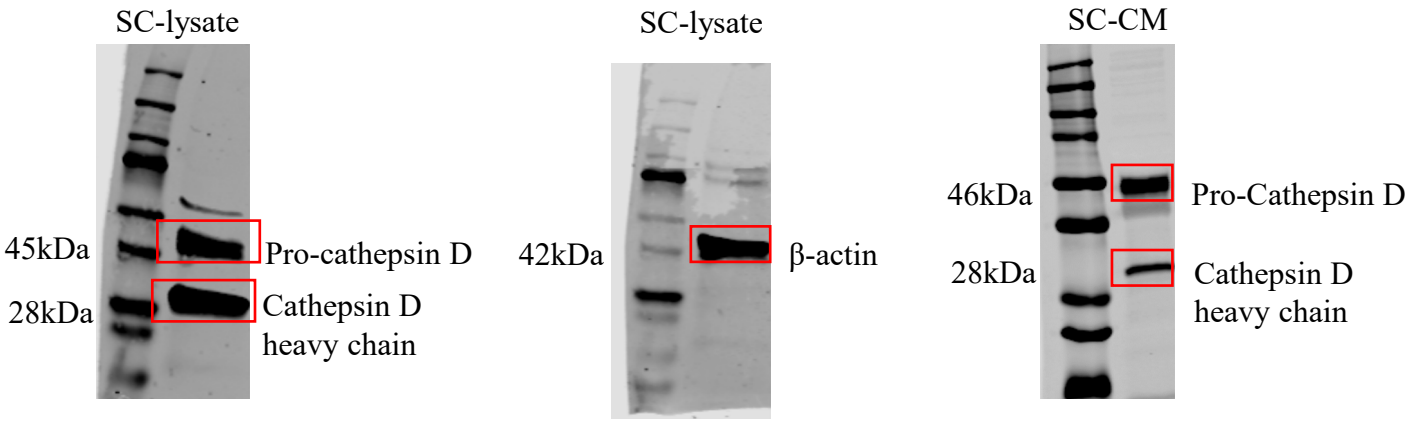

PAI-1

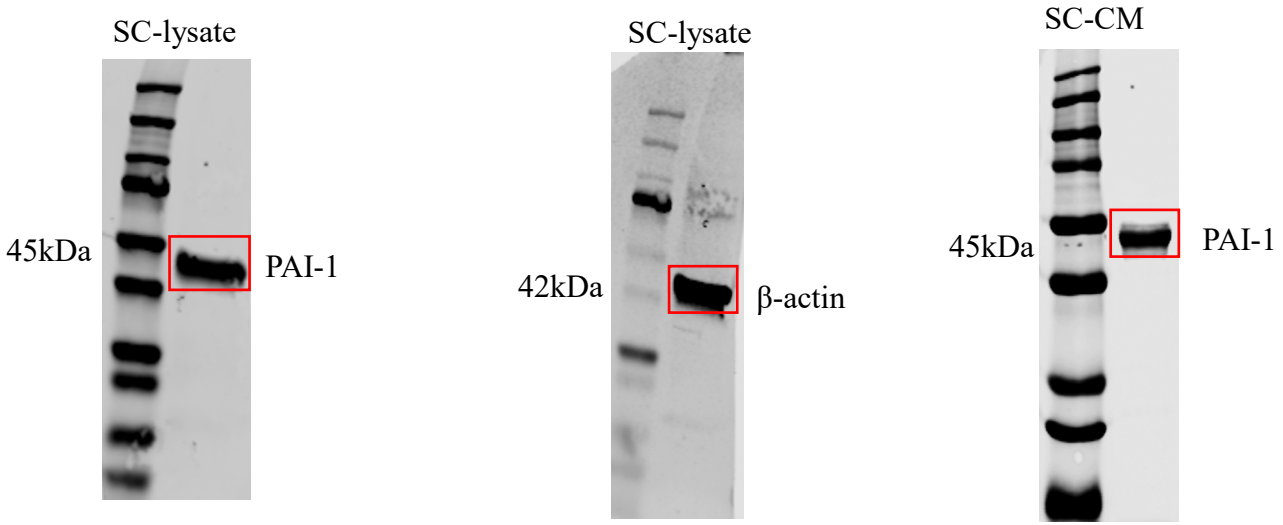

PAI-1, plasminogen activator inhibitor-1
SC-CM, Schwann cell-conditioned media

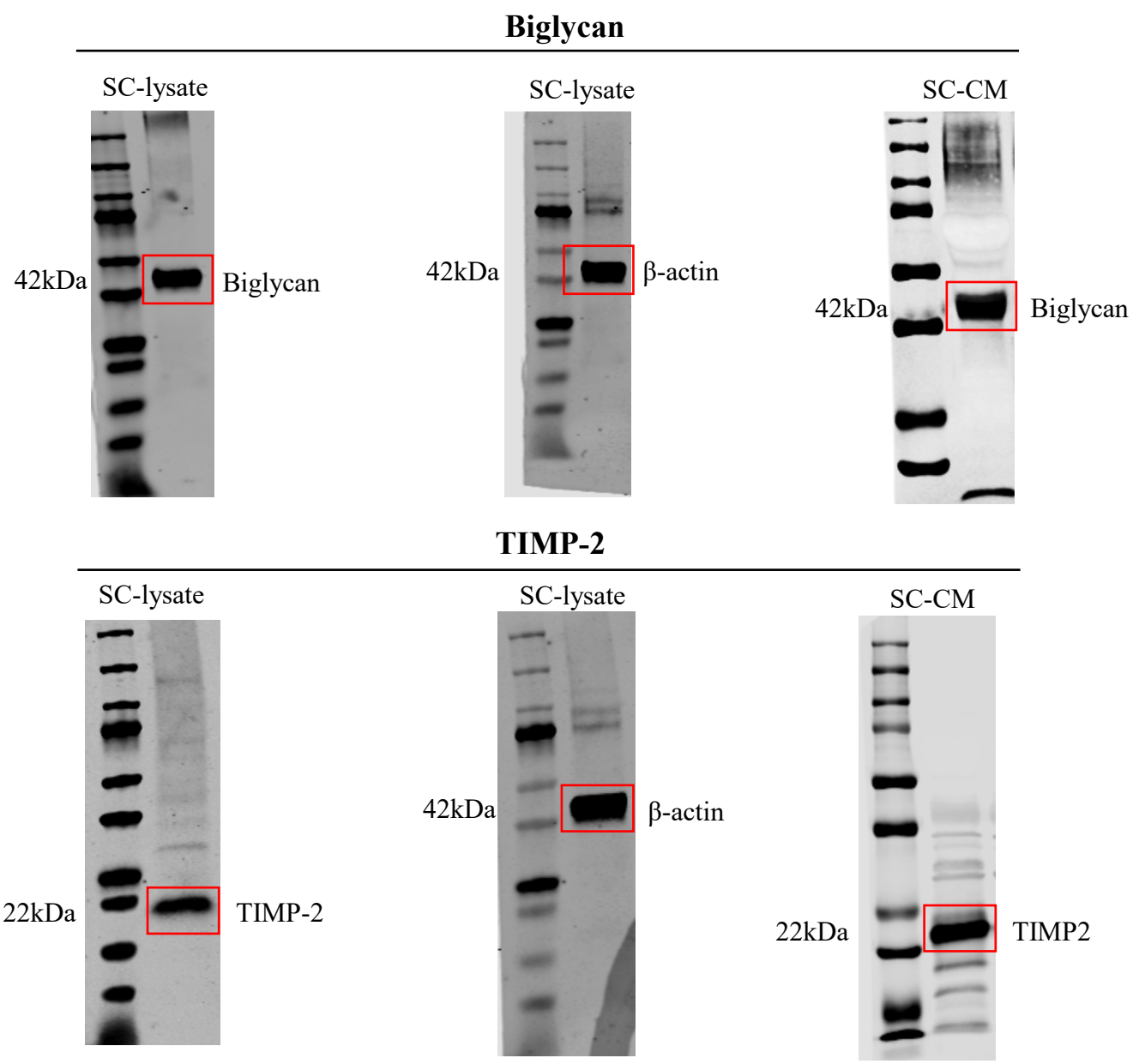

TIMP-2, tissue inhibitor of metalloproteinases-2 SC-CM, Schwann cell-conditioned media

Galectin-1

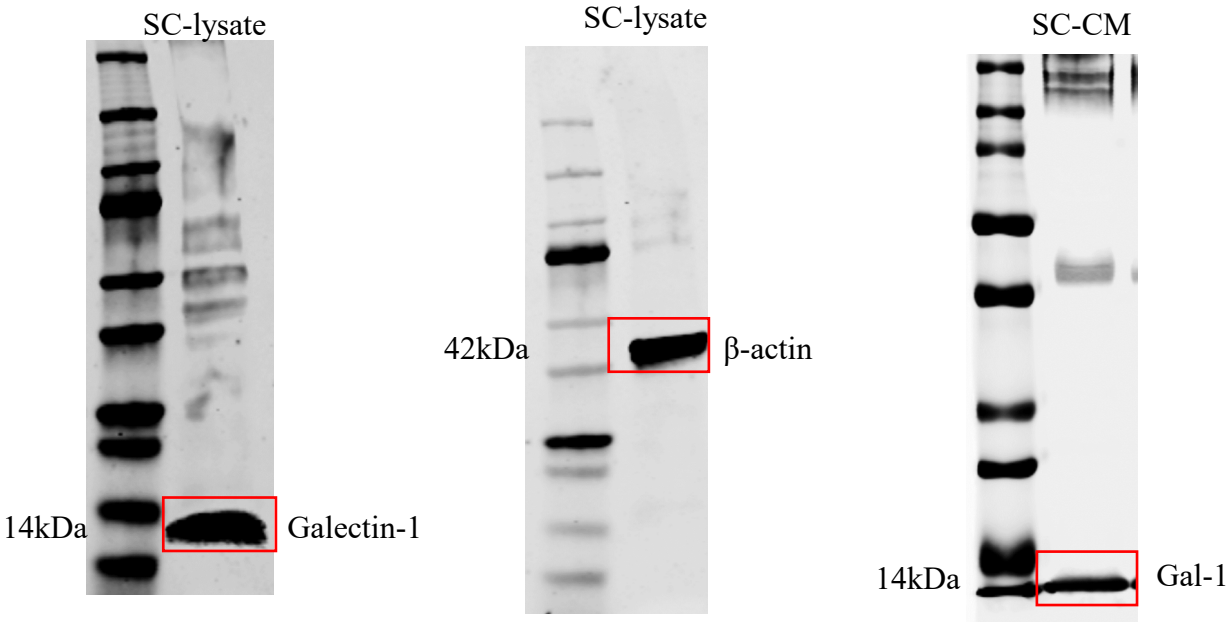

Gal-1, galectin-1
SC-CM, Schwann cell-conditioned media

Western blot full images: Schwann cell marker proteins

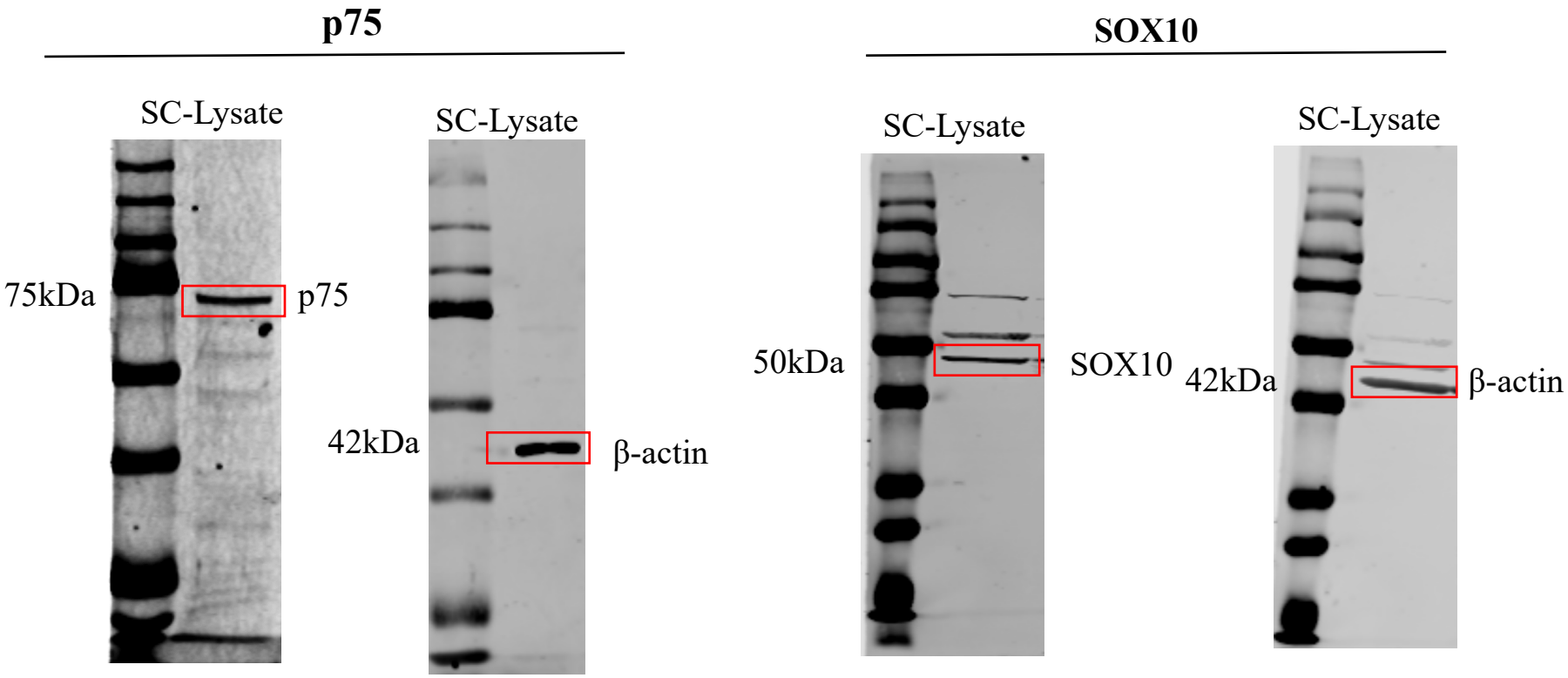

SC-Schwann cell

Chapter 5 | Tumour innervation is associated with poor clinical outcomes in pancreatic cancer

5.1 Preface

Chapter 5 contains an original research article entitled "**Tumour innervation is associated with poor clinical outcomes in pancreatic cancer**" which has been submitted to *Scientific Reports*. The invasion of nerves by cancer cells, called PNI (PNI), has been extensively described in PC and is associated with increased tumour aggressiveness and poor prognosis (Bapat et al., 2011). However, it is unclear if the increased PNI in PC is primarily due to increased invasiveness of PC cells and/or to the increased infiltration of new nerves in the TME. To explore this, in the present study, we have analysed the density and size of nerves in PC. We have identified that both increased nerve density and nerve size are associated with tumour aggressiveness, suggesting that increased nerve infiltration is a primary event leading to higher PNI levels observed in PC.

5.2 Publication

The article "Ferdoushi A, Griffin N, Marsland M, Xu X, Faulkner S, Gao F, Liu H, King SJ, Denham JW, Helden DFv, Jobling P, Jiang CC, Hondermarck H: **Tumour innervation is associated with poor clinical outcome in pancreatic cancer**" submitted to *Scientific Reports* displays from page 76 to 98.

5.3 Supplementary Files

Supplementary file displays on page 99 to 102.

Tumor innervation is associated with poor clinical outcome in pancreatic cancer

Aysha Ferdoushi[1,2,3], Nathan Griffin[1,2], Mark Marsland[1,2], Xiaoyue Xu[4], Sam Faulkner[1,2], Fangfang Gao[1,2], Hui Liu[5], Simon J. King[2], James W Denham[2,6], Dirk F. van Helden[1,2], Phillip Jobling[1,2], Chen Chen Jiang[2,6], Hubert Hondermarck[1,2*]

[1]School of Biomedical Sciences and Pharmacy, Faculty of Health and Medicine, University of Newcastle, Callaghan NSW 2308, Australia.

[2]Hunter Medical Research Institute, University of Newcastle, New Lambton NSW 2305, Australia.

[3]Department of Biotechnology and Genetic Engineering, Mawlana Bhashani Science and Technology University, Tangail 1902, Bangladesh.

[4]School of Population Health, Faculty of Medicine, University of New South Wales, Sydney, NSW 2052, Australia.

[5]Department of Biochemistry and Molecular Biology, School of Laboratory Medicine, Bengbu Medical College, Bengbu 233030, P.R. China.

[6]School of Medicine and Public Health, University of Newcastle, Callaghan NSW 2308, Australia.

*Correspondence: Hubert Hondermarck, School of Biomedical Sciences and Pharmacy, University of Newcastle, Callaghan NSW 2308, Australia. Tel: +61 2 4921 8830. Email: hubert.hondermarck@newcastle.edu.au

Abstract

Pancreatic cancer is a highly aggressive malignancy characterized by poor survival, recurrence after surgery and resistance to therapy. Nerves infiltrate the microenvironment of pancreatic cancers and contribute to tumor progression, however the clinicopathological significance of tumor innervation is unclear. In this study, nerves were quantified by immunohistochemistry in a series of 99 pancreatic cancer cases *versus* 71 normal adjacent pancreatic tissues. The presence of nerves in pancreatic cancer was significantly correlated with worse overall patient survival (HR=2, 95% CI:1.15-3.76, p=0.01). In higher grade tumors (G2+G3), patients positive for nerves had significantly worse survival than those without nerve infiltration (HR=2.0, 95% CI:1.07-3.89, p=0.03). The size of nerves, as measured by cross-sectional area, were significantly higher in pancreatic cancer than in the normal adjacent tissue (p=0.007) and larger nerves were directly associated with worse patient survival (HR=0.39, 95% CI:0.16-0.99, p=0.04). In conclusion, this study suggests that the presence and size of nerves within the pancreatic cancer microenvironment are associated with tumor aggressiveness.

Keywords

Nerve infiltration, nerve size, pancreatic cancer, prognosis.

Introduction

The involvement of nerves in cancer progression is increasingly reported[1]. In animal models of prostate[2] and gastric[3,4] cancer, it has been shown that the infiltration of new nerves in the tumor microenvironment is necessary to cancer growth and metastasis and that denervation strongly inhibits tumor progression. In skin cancer, sensory nerve denervation also blocks tumor initiation[5]. The impact of nerves appears to be due to the release of neurotransmitters by nerve endings in the tumor microenvironment, that stimulate neurotransmitter receptors in cancer and stromal cells, resulting in cancer growth and dissemination[6]. For instance, muscarinic receptors on gastric cancer stem cells activate stem cell expansion[3,4] and in prostate cancer norepinephrine released by adrenergic nerves stimulate an angiogenic switch[7].

In pancreatic cancer (PC), sensory[8] and adrenergic[9] nerves activate tumor progression, whereas cholinergic nerves are inhibitory[10]. However, most data has been acquired from animal models and the impact of innervation in human PC is unclear. The invasion of nerves by cancer cells, termed perineural invasion (PNI), has been extensively described in PC and is generally associated with increased tumor aggressiveness[11]. Despite this, it is unclear if the increased PNI in PC is primarily due to increased invasiveness of PC cells or to the increased infiltration of new nerves in the tumor microenvironment.

In the present study, we have analyzed nerve infiltration in the tumor microenvironment of a cohort of human PC. The data reveal an increased innervation as well as an increase in nerve size, which are both associated with poor clinical outcomes. These findings point to tumor innervation as a risk factor in PC and suggest that increased nerve infiltration is a primary event leading to higher PNI observed in PC.

Materials and Methods

Pancreatic tissue samples. High-density tissue microarrays (TMA) were obtained from US Biomax Inc. (Maryland, USA). The TMA used (catalogue number: HPan-Ade170Sur-01) included a total of 99 PCs and 71 adjacent normal pancreatic tissues (NATs). Pancreatic ductal adenocarcinoma (PDAC) was the major subtypes (99%), minor subtypes included adenosquamous carcinoma (6%), ductal adenocarcinoma/partly mucinous adenocarcinoma (4%), ductal adenocarcinoma/adenosquamous carcinoma (1%) (Supplementary Table S1). The available clinicopathological information was as follows: patient sex and age, histological subtypes, tumor grade, stage, size, lymphatic metastasis status, survival status, surgery date, visit date and survival month. No information on treatment was available. Supplementary Table S1 summarizes the clinicopathological characteristics and distribution of events in the 99 patient population. US Biomax Inc. quality controls are described as follows. Each single tissue spot on every array slide was individually examined by pathologists certified according to WHO published standardizations of diagnosis, classification and pathological grade. Each specimen collected from any clinic was consented to by both hospital and individual. Discrete legal consent form was obtained and the rights to hold research uses for any purpose or further commercialized uses were waived. The study was approved by the Human Research Ethic Committee of the University of Newcastle (HREC reference: H-2012-0063) and all experiments were performed in accordance with relevant guidelines and regulations.

Immunohistochemistry. To investigate the presence of nerves, immunohistochemistry (IHC) against the neuronal maker S-100 was performed as described previously[12]. Following deparaffinization and rehydration of the TMA slides using standard procedures, heat induced epitope retrieval was carried out in a low pH, citrate based antigen unmasking solution

(catalogue number H-3300, Vector Laboratories, California, USA) by a decloaking chamber (Biocare, West Midlands, UK) at 95°C for 30 min and 90°C for 10 sec. IHC was then performed using an ImmPRESS^{TM} HRP IgG (peroxidase) Polymer Detection Kit (catalogue number MP-7405, Vector Laboratories), as per the manufacturer's recommendations. Briefly, after inactivation of endogenous peroxidases with 0.3% H_2O_2, and blocking with 2.5% horse serum, primary antibody (anti-S-100, 1:500 dilution, catalogue number Z0311, Dako, Australia) followed by secondary antibodies were applied to the sections and revealed with DAB Peroxidase (HRP) Substrate Kit (catalogue number SK-4100, Vector Laboratories). Finally, TMA slides were counterstained with hematoxylin (Gill's formulation, Vector Laboratories), dehydrated and cleared in xylene before mounting in Ultramount #4 mounting media (Thermo Fisher Scientific, Victoria, Australia).

Quantitative analysis of neural tissue. Following IHC staining, slides were digitized using the Aperio AT2 scanner (Leica Biosystems, Victoria, Australia)[12]. Identification and quantification of nerves were performed manually and verified by an expert pathologist. The number of nerves that were positive for the nerve markers were also counted for each case. Nerve size (in terms of area) was measured using the Aperio's ImageScope software (v12.4.0.5043, Leica Biosystems).

Statistical analysis. Prism statistical analysis software (version 8.0, GraphPad Software Inc., La Jolla, California, USA) and STATA/SE 14 (StataCorp, USA) were used to conduct all statistical analyses. Univariate and multivariate Cox proportional hazards regression models were performed to examine the associations between nerve infiltration status and survival. Correlation between nerves and other pathological variables were performed using a chi-squared test. To compare differences of means between two groups of replicates an unpaired,

two-tailed t-test was performed unless indicated otherwise. The reported *p*-values were considered statistically significant if they were less than 0.05. Overall survival (OS) analysis was performed by the Kaplan–Meier method. OS was calculated as the time from the date of diagnosis to the date of death. Log-rank test was used to examine the statistical significance on survival distributions by nerve infiltration. Hazard ratio (HR) computed by the Mantel-Haenszel method was used to measure the rapidity of subject death.

Results

Nerve detection in PC and normal pancreatic tissues. Typical morphological features corresponding to nerves were observed by IHC staining for the neuronal marker S-100 (Fig. 1). 27% of PC and 34% of adjacent normal pancreatic tissue were found to be infiltrated by nerves (Table 1). Both thin nerves (Fig. 1D) and larger nerve trunks (Fig. 1, A-C, E, F) were detected in PC. Nerves were typically found invading deep inside the tumor (Fig. 1A, B) or in the periphery of the tumors (Fig. 1E).

Nerve infiltration is associated with worse prognosis in PC. To investigate the potential association between nerve infiltration and clinicopathological outcomes, each clinical case was classified as nerve positive *versus* nerve negative. A complete summary of clinicopathological associations with nerve infiltration is presented in Table 1. No statistically significant associations were found between nerve infiltration and age, sex, tumor grade, tumor stage, tumor size, tumor histological type or lymph node metastasis ($p>0.05$) (Table 1). Importantly, a statistically significant association was detected between the presence of nerves and patient survival ($p=0.006$) with nerve positive tumors being associated with worse patient survival. The presence of nerve infiltration was found significantly associated with shorter overall

survival (OS) (p=0.01, Fig. 2). The results of the univariate and multivariate Cox proportional hazards regression models of examining the association between nerve infiltration and survival are shown in Table 2. In both univariate (95% CI:1.15-3.76, p=0.01) and multivariate (95% CI:1.27-3.50, p=0.004) models, nerve infiltration was found to be significantly associated with poor survival. Nerve positive patients had a 2-fold elevated risk of death compared to patients without nerve infiltration (Table 2).

Patients were further stratified (Fig. 3A-3L) based on clinicopathological parameters and association with nerve infiltration was investigated using Kaplan-Meier survival analysis (Table 3). Male patients positive for nerve infiltration had a 2.7-fold higher risk of death (p=0.01, Table 3), whereas no association were found between nerve infiltration and female patient survival (p=0.47, Fig. 3B). In terms of age, for patients less than 50 years, nerve infiltration was associated with significantly poorer prognosis (p=0.002, Fig. 3C) compared to those without nerve infiltration, equating to an 11-fold elevated risk of death (Table 3). No significant association was found between nerve infiltration and survival of patients aged more than 50 years (p=0.09, Fig. 3D). Male patients with nerve infiltration showed worse survival compared to those without nerve infiltration (8 *versus* 12.5 months, p=0.01). Low grade tumors (G1) and high grade tumors (G2+G3), were stratified based on nerve infiltration status. No significant association was detected for G1 tumors (p=0.13, Fig. 3E), however G2-G3 tumors that were positive for nerves had poorer clinical outcomes (p=0.03, Fig. 3F). In terms of stage, patients with lower stage (0+I) and positive for nerves had poorer clinical outcomes than those negative for nerves (p=0.04, Fig. 3G). A trend was observed between nerve infiltration and shorter OS in patients with higher tumor stage (II+IV), but differences did not reach statistical significance (p=0.09, Fig. 4H). Nerve infiltration was associated with poor clinical outcome in both patients with lower (T1+T2) and higher (T3) tumor size, with marginal statistical significance (p=0.05 and p=0.07, respectively, Fig. 3I, J). In patients without lymph node

metastasis (N0), the nerve infiltrated group showed worse survival compared to those without nerve infiltration (8 *versus* 42 months, p=0.008**,** Fig. 3K) with 3.4-fold elevated risk of death (Table 3). For patients with nodal metastasis (N1), nerve infiltration had no significant association with OS (p=0.59, Fig. 3L) (Table 3).

Together, these results suggest that nerve infiltration is a marker of worse survival among patients of different tumor stages and sizes. In addition, nerve infiltration is a marker of poor survival among patients without lymphatic metastasis and indicates that there is a subpopulation of N0 patients which are at an increased risk of death if the tumor is infiltrated by nerves.

Enlarged nerve cross sectional area is a feature of malignant PC and unfavorable prognosis. To investigate the association between nerve size and pancreatic malignancy, the areas of intrapancreatic tumor nerves, immunolabeled with the neuronal marker S-100, were measured by cross-sectional area (Supplementary Fig. S2). The mean nerve area was significantly higher in PC tissues compared with normal adjacent pancreatic tissue (p=0.007) (Table 4A, Fig. 4A, Supplementary Fig. S3). The mean area of nerves in PC tissues was 14,779 μm^2, which was almost four times greater than that of the normal adjacent tissue (p=0.007) (Table 4A). Sex, tumor size, grade, stage or lymphatic metastasis status were not associated with nerve size in pancreatic tumors (Supplementary Fig. S4).

To investigate the potential association between nerve size and patient survival, the nerves in PC tissue were dichotomized into smaller nerve (area, $\leq$3,800 μm^2) and larger nerve (area, >3,800 μm^2). This cut-off was established based on the median nerve size area (3,800 μm^2). Kaplan–Meier survival analysis demonstrated that patients with bigger nerve size were significantly associated with worse prognosis, where the median survival month for patients

with bigger nerve size was lower than that of smaller nerves (8 *versus* 16 months) (p=0.04, Fig. 4B, Table 4B).

Discussion

PC prognosis is influenced by several clinicopathological factors including tumor size[13,14], grade[15,16], lymph node invasion[17] and depth of invasion[18]. In various malignancies, tumor innervation has been reported to play a pivotal role in driving tumor growth[2,4,9]. The present study demonstrates that the presence and size of nerves in the tumor microenvironment is associated with worse patient survival in PC.

In the present study, IHC staining of the neuronal marker S-100 was performed to detect nerves in the microenvironment of PC. Nerves density and size were measured and analyzed in relation to clinical outcomes. Nerve infiltration was found associated with poor prognosis. Marginal significant differences in nerve infiltration regarding OS of PC has already been reported in a study conducted by Min *et al.*[19]. We have observed that male patients with nerve infiltration had 2.7 times more chance of death compared to those without nerve infiltration. In case of female patients, no significant difference was observed. PC is defined as a disease of elderly populations and rarely occurs before the age of 40[20,21]. Our study demonstrates that patients aged ≤50-years with nerve infiltration had more chance of death compared to without nerve infiltration. This finding suggest that nerve infiltration is a prognostic factor particularly for patients diagnosed with PC at early age. Additionally, higher grade tumors (G2+G3) that were also positive for nerves had significantly worse survival than those without nerves indicating the presence of nerves in the tumor microenvironment. Lymphatic metastasis, which develops in 60-70% patients with PC[22], has been described as one of the most important

prognostic factors[23]. Patients with surgical resection often encounter disease recurrence with a high frequency of lymph node metastases[24]. We found that patients without lymphatic metastasis but infiltrated by nerves had 5 times more chance of death compared to without nerve infiltration with a statistically significant reduction in patient survival. This finding suggests that nerve infiltration is a risk factor for poor survival among patients without lymphatic metastasis. Altogether, our study revealed that nerve infiltration might be a potential prognostic indicator in PC in the case of male patients, patients diagnosed at an early age, higher tumor grade, lower tumor stage and negative lymphatic metastases.

The median nerve area (measured cross-sectionally) was higher in cases of PC tissue compared to normal adjacent tissue. Similar neural alteration was observed by Li *et. al.*, who reported that the median number of nerves and median nerve diameters were greater in PC patients with diabetes mellitus[25]. They concluded that, for patients with hyperglycemia, nerve damage and regeneration are a simultaneous process in the tumor microenvironment of PC where abnormal expression of NGF and p75 play a pivotal role[25]. Increased hypertrophy has previously been suggested in PC[26] and chronic pancreatitis[27,28]. A study in breast cancer revealed that thickness of tumor- related nerve fibers is significantly associated with poor differentiation, lymphatic metastasis, high clinical staging, and a triple negative subtype[29]. In our study, nerve size was correlated with patient survival but not with tumor grade, size, stage or lymphatic metastasis. It has been reported that neurotrophic factors secreted from cancer cells and other stromal cells promote neuronal hypertrophy in cancer and drive cancer progression[29,30] and an increased production of neurotrophic factors may account for the increased nerve size that we report here. Nerve growth factor (NGF) in particular has been shown to be a driver of nerve infiltration in PC[9] and blocking NGF signaling reduces the neural invasion potential of PC cells[31]. Anti-NGF siRNA encapsulated in nanoparticles have been shown to be able to decrease pancreatic tumor

growth in the mouse[32] suggesting that the increase in nerve infiltration and size participate in PC progression.

Together, our findings outline the clinicopathological significance of nerve infiltration in the tumor microenvironment of PC. The association of infiltrating nerves with tumor aggressiveness suggests that increased infiltration of larger size nerves might be the reason for increased PNI commonly found in PC. Further experimental investigations are warranted to confirm this hypothesis and the potential value of using nerve infiltration as a prognostic biomarker in PC.

Abbreviations

HR, hazard ratio; IHC, immunohistochemistry; MNA, mean nerve area; NAT, normal adjacent tissue; OS, overall survival; PC, pancreatic cancer; PDAC, pancreatic ductal adenocarcinoma; PNI, perineural invasion; TMA, tumor microarrays.

Funding

This research was supported by the Maitland Cancer Appeal Committee (NSW Australia), the Hunter Medical Research Institute (HMRI) and the Hunter Cancer Research Alliance (HCRA). This work is also supported by Research Training Program (RTP) Scholarship funded by the Australian Government Department of Education and Training awarded to Aysha Ferdoushi.

Acknowledgment

The authors thank the University of Newcastle, and the funding bodies for supporting this research and Kristen McEwan for providing excellent research assistance.

Author contributions

HH and AF designed the study; AF carried out the experiment and analyzed the data; AF, NG, MM, PJ, HH confirmed the histopathology. AF and XX carried out statistical analysis. AF and HH wrote the manuscript. NG, XX, SF, FG, HL, SJK, JWD, DFvH, PJ and CCJ edited the manuscript. All authors contributed to manuscript revision, read, and approved the submitted version.

Competing interests

The authors have declared no conflict of interest.

Parameters	Nerve negative	Nerve positive	*p*-value
Pathology description	**N (%)**		
Normal (n=71)	47 (66)	24 (34)	0.39
Cancer (n=99)	72 (73)	27 (27)	
Cancer histological subtype			
Ductal adenocarcinoma (n=88)	63 (72)	25 (28)	0.72
Others (n=11)	9 (82)	2 (18)	
Sex			
Male (n=63)	46 (73)	17 (27)	1.00
Female (n=36)	26 (72)	10 (29)	
Age (years)			
≤50 (n=16)	10 (63)	6 (37)	0.38
>50 (n=83)	62 (73)	21 (27)	
Tumor grade			
G1 (n=11)	7 (64)	4 (36)	0.48
G2+G3 (n=88)	65 (74)	23 (40)	
Tumor stage			
0+ I (n=40)	27 (67)	13 (33)	0.36
II+ IV (n=59)	45 (76)	14 (24)	
Tumor size			
T1+T2 (n=78)	58 (74)	20 (26)	0.41
T3 (n=20)	13 (65)	7 (35)	
Lymphatic metastasis status			
Negative (n=50)	35 (70)	15 (30)	0.49
Positive (n=43)	33 (77)	10 (23)	
Survival status (months)			
Survival >10 months (n=49)	42 (86)	7 (14)	**0.006**
Survival ≤10 months (n=50)	30 (60)	20 (40)	

Table 1. Nerve infiltration in pancreatic tumor microenvironment and its correlation with clinicopathological variables. *p*-values were calculated by the chi-squared test. Statistically significant *p*-values were defined as $p<0.05$ (indicated in bold).

	Univariate model		Multivariate model	
	HR (95% CI)	***p*-value**	**HR (95% CI)**	***p*-value**
Nerve Infiltration				
Negative (n=72)	1 (reference)	**0.01**	1 (reference)	**0.004**
Positive (n=27)	2 (1.15-3.76)		2.11 (1.27-3.50)	

Table 2. Univariate and multivariate Cox proportional hazards regression models of the association between nerve infiltration and survival. *P*-values were calculated by the log-rank test. Values in bold indicate significance ($p<0.05$). HR was calculated using univariate Mantel-Haenszel hazard model. HR, hazard ratio; CI, confidence interval.

Parameters	N (%)	Median survival month	HR (95% CI)	*p*-value	N (%)	Median survival month	HR (95% CI)	*p*-value
Sex	**Male**				**Female**			
Nerve +ve	17 (26)	8	1 (reference)	**0.01**	10 (26)	16	1 (reference)	0.47
Nerve -ve	46 (74)	12.5	2.7 (1.26- 6.02)		26 (74)	17	1.4 (0.55-3.50)	
Age (year)	**≤50 year**				**>50 year**			
Nerve +ve	6 (40)	9	1 (reference)	**0.002**	21 (23)	8	1 (reference)	0.09
Nerve -ve	10 (60)	Undefined*	11.6 (2.34- 58)		62 (77)	11	1.7 (0.93- 3.47)	
Grade	**G1**				**G2+G3**			
Nerve +ve	4 (36)	14.5	1 (reference)	0.13	23 (33)	8	1 (reference)	**0.03**
Nerve -ve	7 (64)	Undefined*	3.4 (0.68-17)		65 (67)	12	2.0 (1.07-3.89)	
Stage	**0+ I**				**II +IV**			
Nerve +ve	8 (23)	9	1 (reference)	**0.04**	14 (23)	8	1 (reference)	0.09
Nerve -ve	27 (77)	42	2.7 (1.04-7.17)		45 (77)	11	1.9 (0.88-4.11)	
Tumor size	**T1+T2**				**T3**			
Nerve +ve	20 (25)	8	1 (reference)	0.05	7 (32)	8.5	1 (reference)	0.07
Nerve -ve	58 (75)	12	1.9 (0.98-3.80)		13 (68)	31	3.2 (0.88-11.96)	
Lymph node status	**N0**				**N1**			
Nerve +ve	15 (29)	8	1 (reference)	**0.008**	10 (22)	8	1 (reference)	0.59
Nerve -ve	35 (71)	42	3.4 (1.36-8.31)		33 (78)	10.5	1.2 (0.54-2.86)	

Table 3. Association between nerve infiltration and clinicopathological characteristics. Patients with different clinicopathological parameters were stratified as positive or negative for the presence of nerve infiltration to assess the association of nerve infiltration with clinicopathological parameters in PC. *p*-values were calculated by the log-rank test. Values in bold indicate significance ($p < 0.05$). Star sign (*) denotes if more than 50% of the subjects are alive at the end of the study, then the median survival time is simply not defined/undefined. HR was calculated using univariate Mantel-Haenszel hazard model. HR: hazard ratio.

A	Variables	No. of nerves	MNA (µm^2)	MNA (µm2) ± SEM	*p*-value
	NAT	24	3,957	3,957±866	**0.007**
	Cancerous tissue	27	14,779	14,779±3,405	

B	Nerve size (µm^2)	N (%)	Median survival month	HR (95% CI)	*p*-value
	Bigger nerve (>3,800 µm^2)	17 (59)	8	1 (reference)	**0.04**
	Smaller nerve (≤3,800 µm^2)	10 (41)	16	0.39 (0.15-0.99)	

Table 4. (A) Comparison of nerve related parameters in PC tissue and normal adjacent tissue. Unpaired t-test was performed to compare nerve related parameters in the different groups. Data are represented as mean ± SEM. **(B) Correlation between increased nerve size and patient survival.** *P*-values were calculated by the log-rank test. HR was calculated using univariate Mantel-Haenszel hazard model. Values in bold indicate $p<0.05$. PC, pancreatic cancer; NAT, normal adjacent tissue; MNA, mean nerve area (µm2); SEM, standard error of mean, HR, hazard ratio; CI, confidence interval.

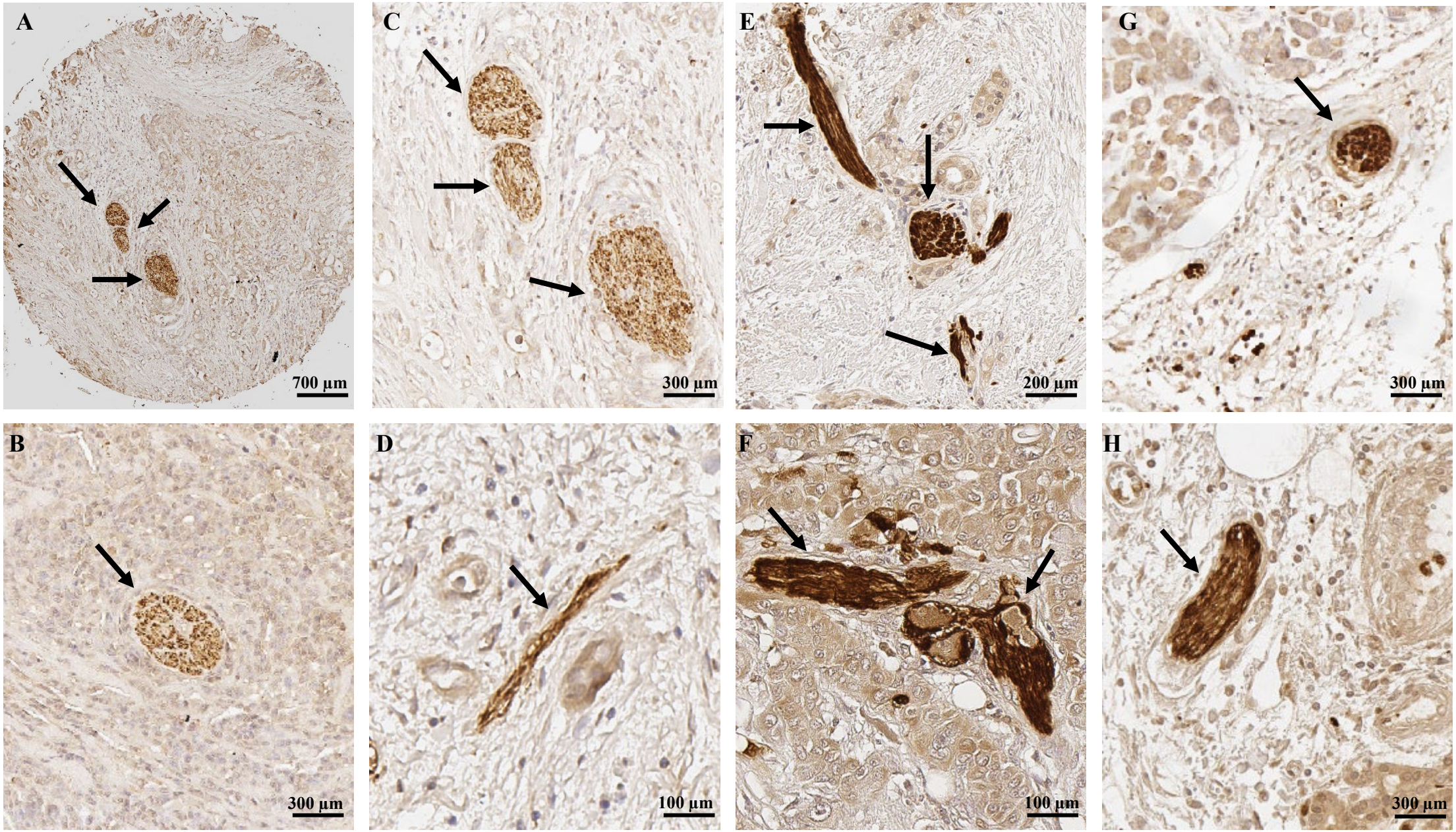

Figure 1

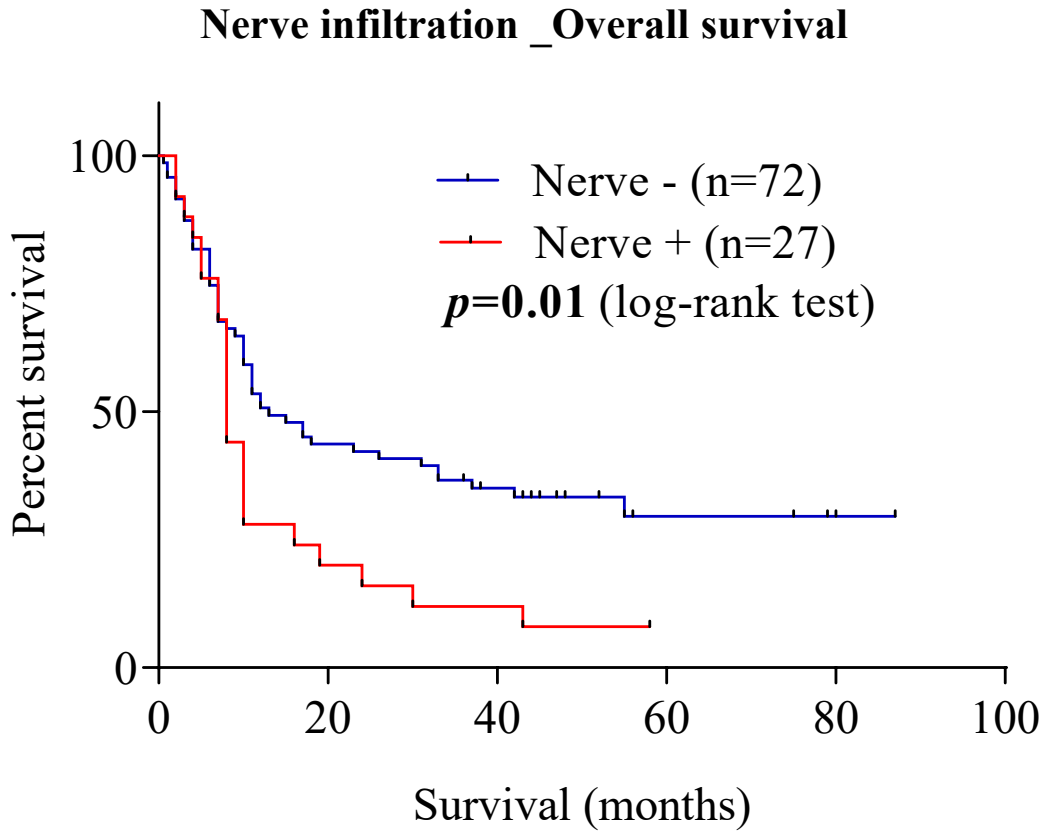
Nerve infiltration _Overall survival
Nerve - (n=72)
Nerve + (n=27)
p=0.01 (log-rank test)
Percent survival
100
50
0
0
20
40
60
80
100
Survival (months)

Figure 2

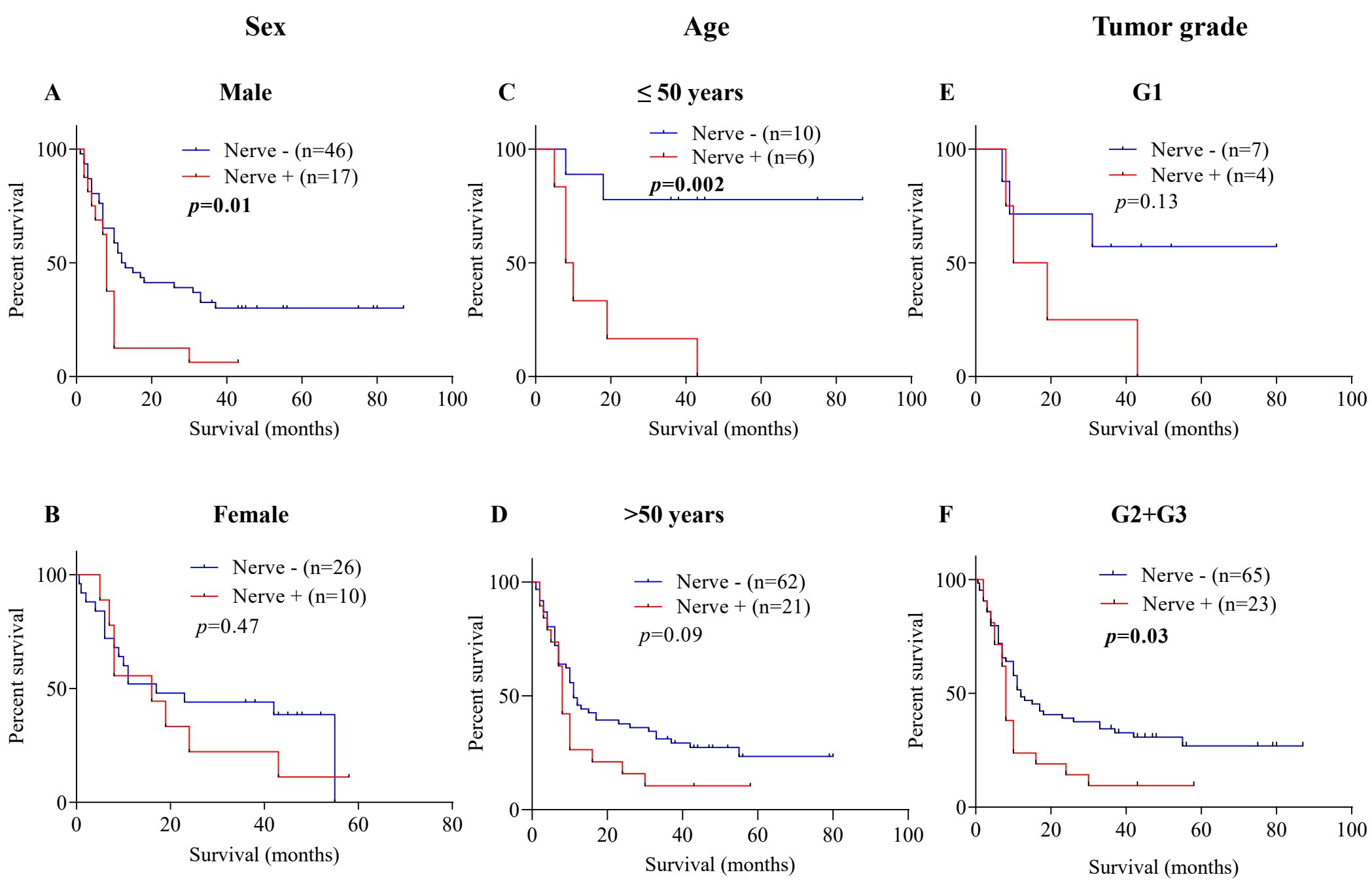
Sex
Age
Tumor grade
A
Male
Nerve - (n=46)
Nerve + (n=17)
p=0.01
Percent survival
Survival (months)
C
≤ 50 years
Nerve - (n=10)
Nerve + (n=6)
p=0.002
E
G1
Nerve - (n=7)
Nerve + (n=4)
p=0.13
B
Female
Nerve - (n=26)
Nerve + (n=10)
p=0.47
D
>50 years
Nerve - (n=62)
Nerve + (n=21)
p=0.09
F
G2+G3
Nerve - (n=65)
Nerve + (n=23)
p=0.03

Figure 3

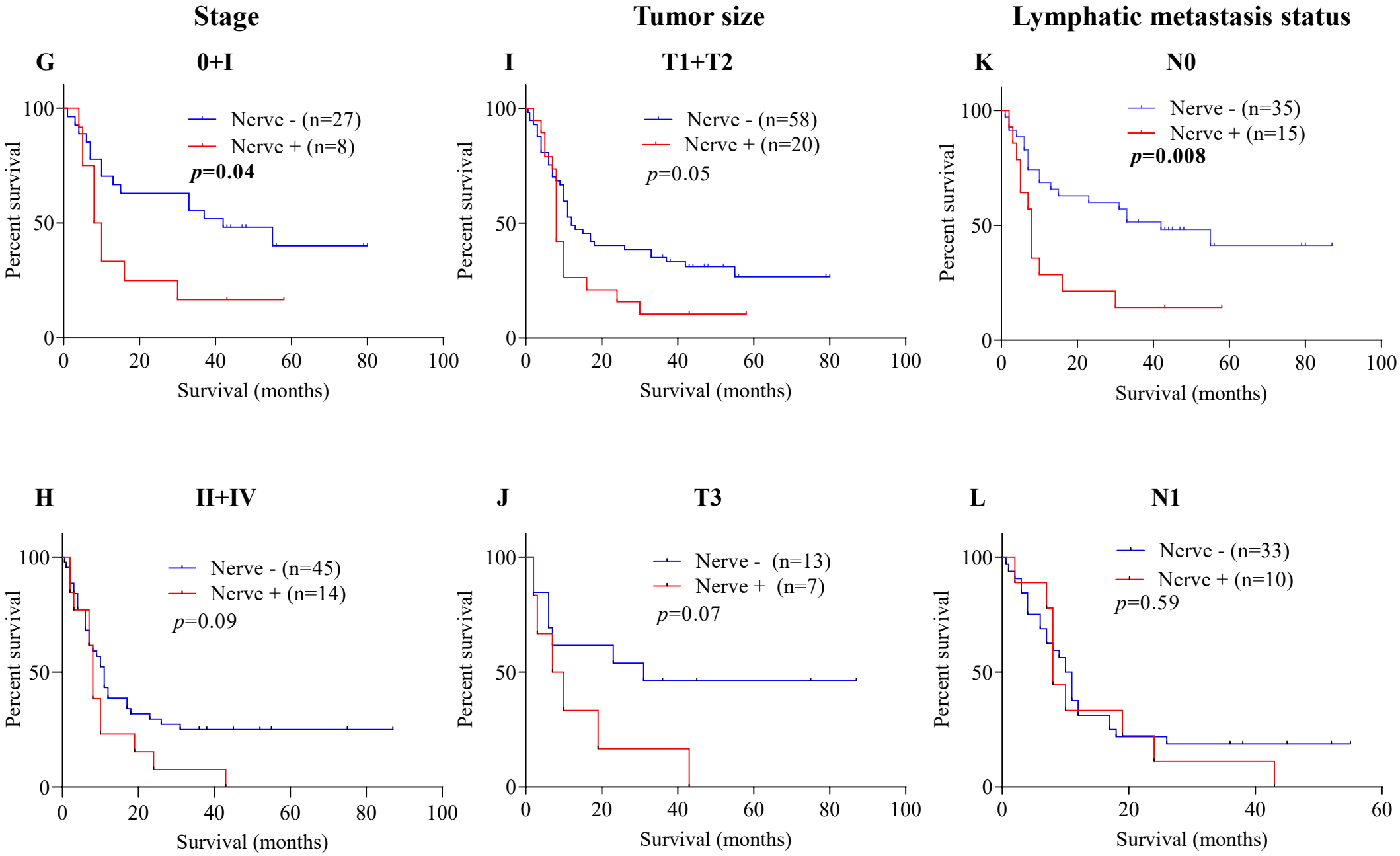

Figure 3 (continued)

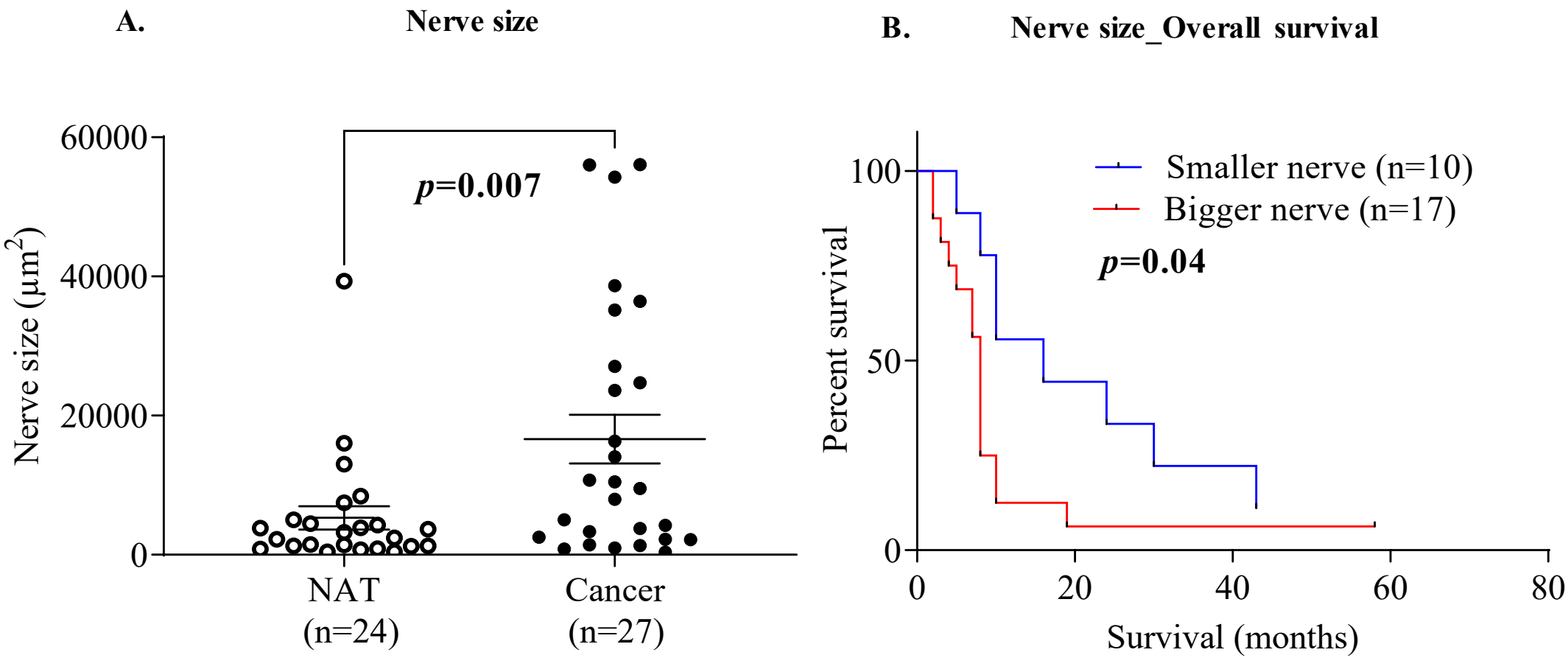
A.
Nerve size
60000
40000
20000
0
Nerve size (µm²)
p=0.007
NAT
(n=24)
Cancer
(n=27)
B.
Nerve size_Overall survival
100
50
0
Percent survival
Smaller nerve (n=10)
Bigger nerve (n=17)
p=0.04
0
20
40
60
80
Survival (months)

Figure legends

Figure 1. Nerves in the tumor microenvironment of PC. Peripheral nerves in human PC and normal adjacent pancreatic tissues were stained using IHC for the neuronal markers S-100; counterstaining was performed with hematoxylin. Representative images of nerve sections from PC tissues (**A,** entire core, **B,** higher magnification of nerves in A, **C-F,** high magnification of nerves in the tumor microenvironment) and normal adjacent pancreatic tissues (**G, H**). Stained nerves are indicated by black arrows. PC, pancreatic cancer.

Figure 2. The presence of nerves in the tumor microenvironment of PC is associated with poor survival. Kaplan-Meier survival curve comparing cases positive *versus* negative for nerve infiltration. Patients with nerve infiltration harbor the worst prognosis i.e. had shorter overall survival compared to without nerve infiltration. The results of comparative analyses are presented in Table 2. PC, pancreatic cancer.

Figure 3. Association between the presence of nerves and overall survival in stratified patient groups. Kaplan-Meier survival curve comparing cases positive *versus* negative for nerve infiltration after patient stratification in function of sex **(A, B)**, age **(C, D),** tumor grade (**E, F**), stage (**G, H**), tumor size (**I, J**) and lymphatic metastasis status (**K, L**). Values in bold indicate significance ($p<0.05$). The results of multiple comparative analyses are presented in the Table 3.

Figure 4. Increased nerve size is associated with pancreatic malignancy and patient survival. Pancreatic tissue sections from PC and normal adjacent tissue (NAT) were analyzed for changes in nerve size (measured by cross-sectional area). The nerve size was bigger in PC

tissue than NAT (**A**). The median value of nerve area was taken as cut-off to define two groups (bigger nerve, nerve area bigger than median value and smaller nerve, nerve area smaller than median value) and used for the Kaplan-Meier analysis and the log-rank test. Bigger nerves in the tumor microenvironment was associated with worse patient survival (**B**). Survival analyses displayed a significantly shorter survival for patients with bigger nerve size than that of smaller nerve size. The results of comparative analyses are presented in Table 4A and 4B. PC, pancreatic cancer.

Supplementary Table S1:

Patient clinicopathological characteristics. Unless indicated otherwise, data show the number of patients in each group, with percentages given in parentheses.

Parameters	Category	N (%)
Pathology description	Normal	71 (42)
	Cancer	99 (58)
Histological subtype	Pancreatic ductal adenocarcinoma (PDAC)	88 (89)
	Adenosquamous carcinoma	6 (6)
	Ductal adenocarcinoma/partly mucinous adenocarcinoma	4 (4)
	Ductal adenocarcinoma/adenosquamous carcinoma	1 (1)
Patients characteristics		
Sex	Male	63 (64)
	Female	36 (36)
Age (years)	≤50	16 (16)
	>50	83 (84)
Tumor characteristics		
Tumor grade	G1	11 (11)
	G2+G3	88 (89)
Tumor stage	0+ I	40 (46)
	II+ IV	59 (54)
Tumor size	T1+T2	78 (80)
	T3	20 (20)
Lymphatic metastasis status	N0	50 (54)
	N1	43 (46)

Supplementary Figure S2:

Examples of nerve measurements. Peripheral nerves were stained using immunohistochemistry for the neuronal maker S-100 and counter stained with haematoxylin. Nerve size was measured by cross-sectional area using Aperio ImageScope software (pen tool-F2), where each nerve section was outlined manually, and the area measurement was automatically obtained. Measurement of same image using different scale bar are shown here: (A) 500µm and (B) 100µm.

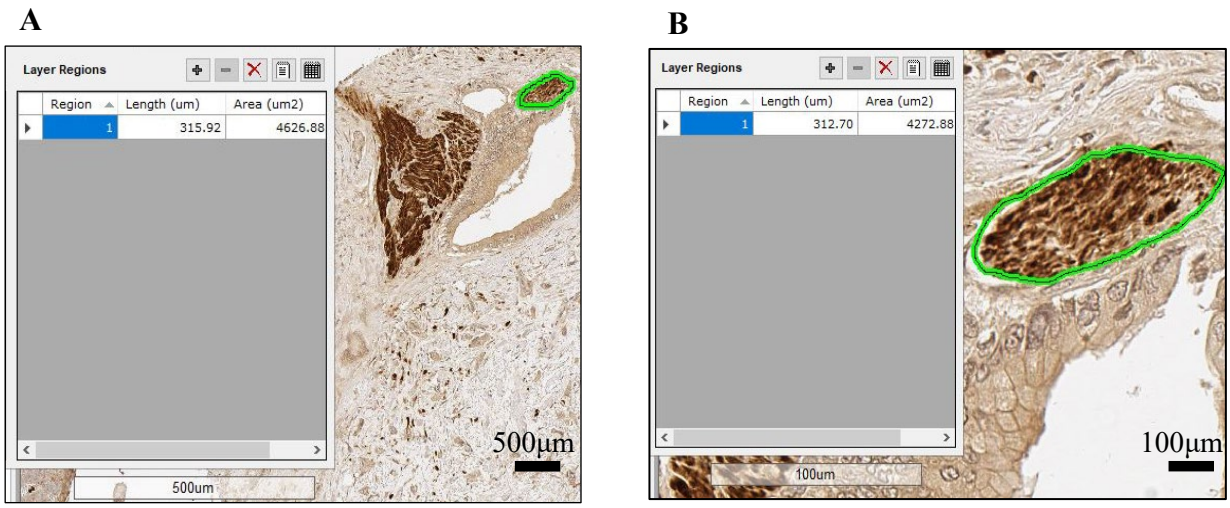

Supplementary Figure S3:

Nerve size is increased in PC tissues. Nerve tissue immunostaining in different groups. S-100 immunostaining in the PC group (A, C) and normal adjacent pancreas (B, D). Increases in the area of nerve tissues were observed in PC compared with normal adjacent pancreatic tissue. Stained nerves are indicated by red arrowheads. Scale bar = 1mm. PC, pancreatic cancer.

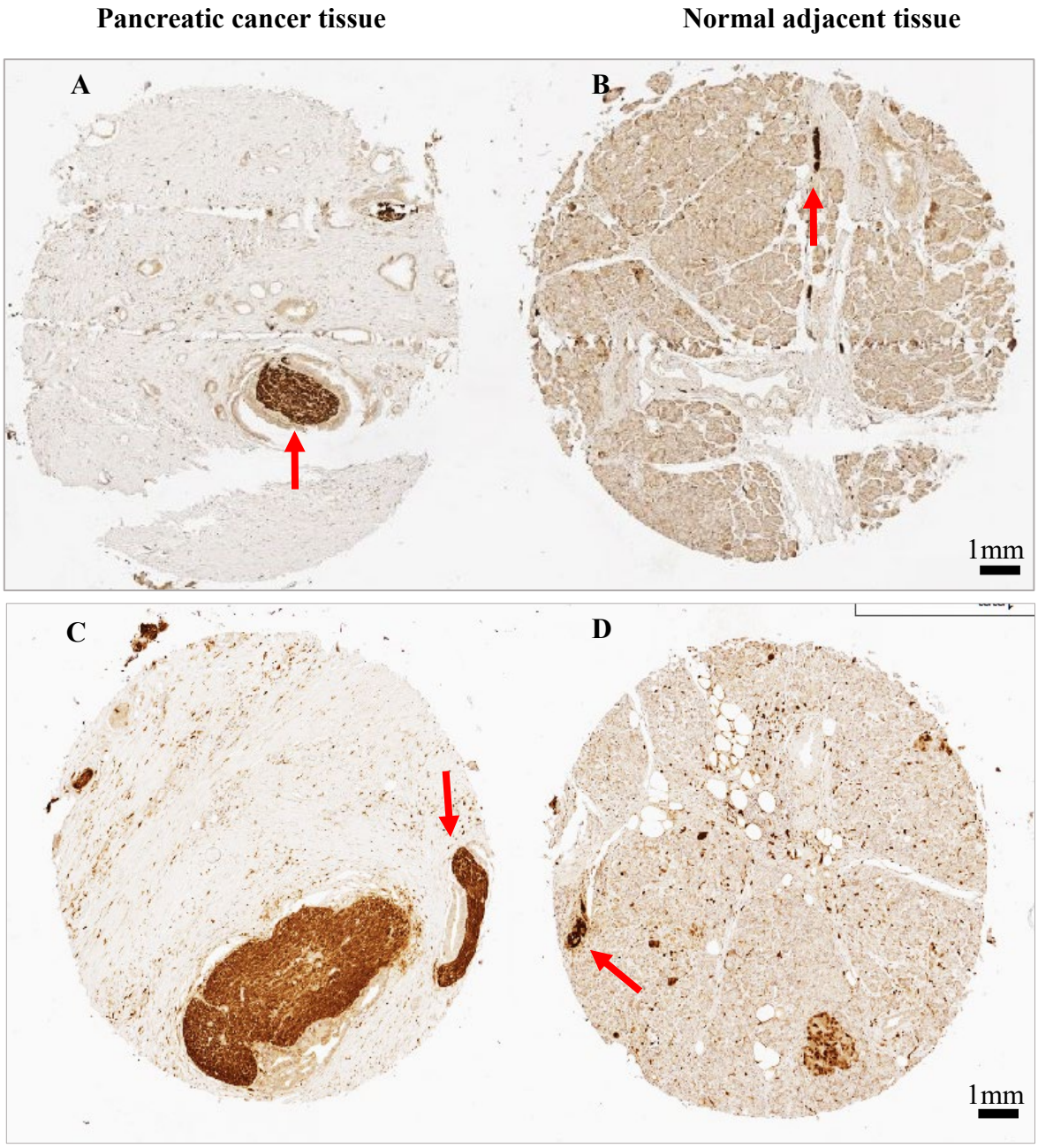

Supplementary Figure S4:

Correlation between nerve size and different clinicopathological characteristics. Nerve size was not associated with sex, stage, grade, tumor size or lymphatic metastasis.

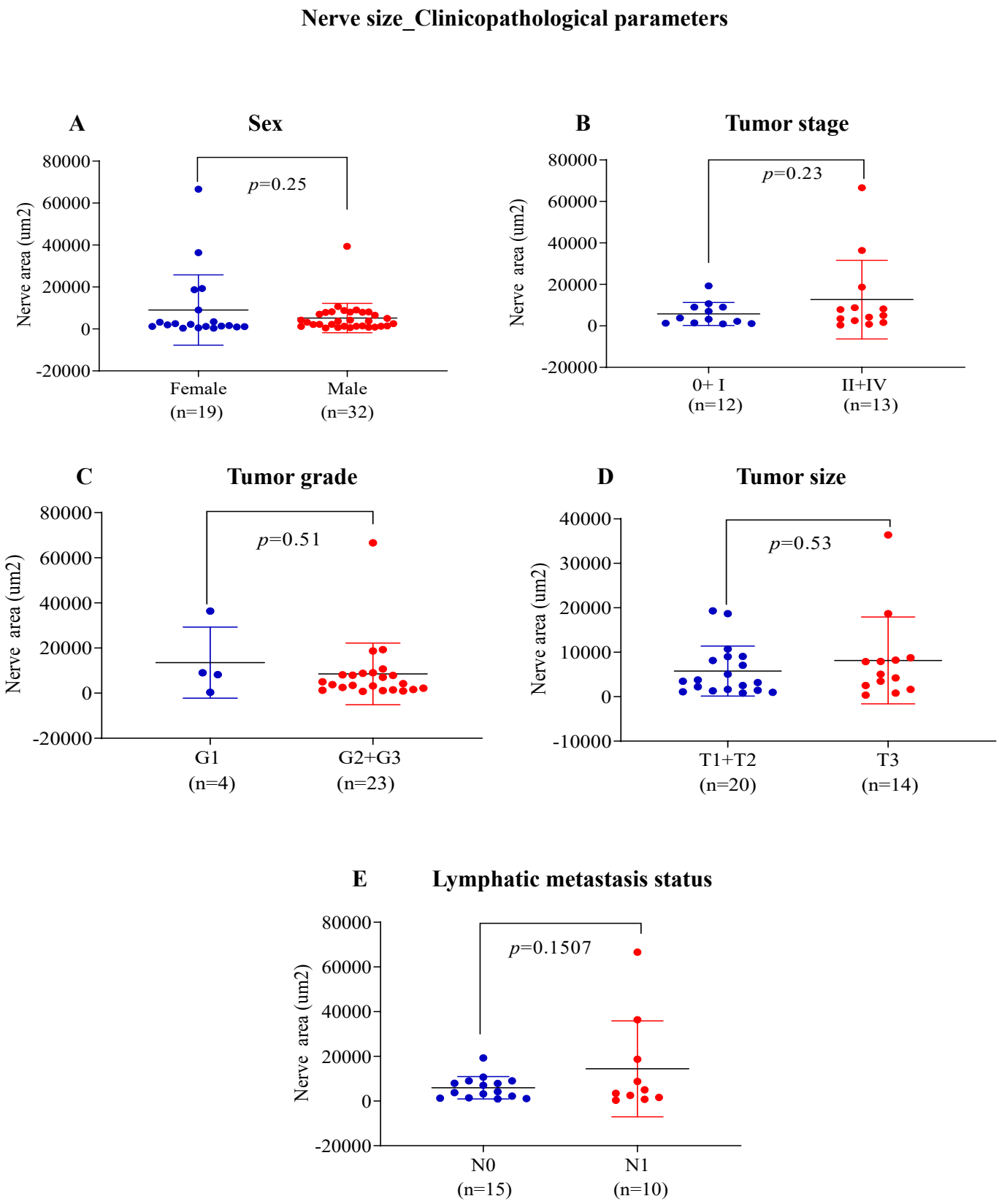

Chapter 6 | General Discussion

Successful treatment of PC is a clinical challenge; hence, the identification of potential therapeutic targets is essential. Targeting stromal components of the TME is now a recognized strategy to inhibit cancer development. As described in the introduction, the infiltration of new nerves in the TME is necessary for primary tumour growth and metastasis and that denervation strongly inhibits tumour progression. Denervation in these experimental models might also have removed associated glial cells from the TME. SC involvement in cancer development (Demir et al., 2014;Deborde et al., 2016;Demir et al., 2016) has added an exciting new dimensionality, as these glial cells are extraordinarily plastic with rich profusion in most organs and a multitude of functions. However, detailed understanding of the molecular and cellular mechanisms involved in the regulation of PC progression by the nerves and supporting SCs is still unclear. It is important to identify the specific functions of each of the cell types. In this regard, targeting nerves and supporting SCs in the TME could be an innovative therapeutic approach to understand the mechanism of disease progression and improve survival outcome. The studies within this thesis provide insights into the role of SCs in PC progression and the clinicopathological significance of nerve infiltration in cancer aggressiveness.

The study presented in Chapter 3 of this thesis describes the protein expression profile of primary human SCs by LC-MS/MS. The present dataset provides a proteome reference for SCs in basal conditions that can be accessed and downloaded by the community investigating pathological situations where SCs are involved. It is noteworthy to highlight that in the SC proteome reported here, several nociception associated channels and proteins were identified, which may contribute to the recently discovered role of SCs in pain sensation (Abdo et al., 2019). For instance, the thermosensitive ion channel TRPV2 (transient receptor potential v2) and the cold receptor TRPM8 (transient receptor potential cation channel subfamily member 8)-associated proteins. Further functional investigations will be performed to determine the molecular mechanisms by which SCs initiate pain and their role in different pain signalling pathways. These proteins may ultimately constitute novel molecular targets for future innovative pain treatments. The role of TRVP2 and TRPM8 channels could be explored in the pain-like responses evoked by acute and chronic ethanol ingestion in mice following the experimental approaches described by Francesco De Logu who has shown that elevated local

concentrations (1%–3%) of ethanol can activate TRPV1 on primary sensory nerves to induce pain and neurogenic inflammation (Trevisani et al., 2002). Aside from pain, cancer progression is another health issue where the involvement of SCs has recently been demonstrated (Shurin et al., 2019). Our SC proteome dataset may provide clues in identifying candidate molecular mediators produced by SCs that may be involved in cancer progression. For instance, the mesencephalic astrocyte-derived neurotrophic factor (MANF) and other growth factors such as myeloid derived growth factor (MY-DGF) and the hepatoma-derived growth factor (HDGF) have been identified with high confidence. Further functional in vitro and in vivo studies will be performed for their potential involvement as SC mediators in cancer progression. In vitro, functional knock-out experiment could be performed using shRNA/siRNA to target the expression of these candidate genes in SCs. For in vivo study, genetically engineered mouse models could be created to knock out the candidate proteins and test the impact on PC cell growth and dissemination.

Cancer cells have been shown to produce neurotrophic growth factors, such as nerve growth factor, to stimulate neuronal outgrowth (Pundavela et al., 2015;Hayakawa et al., 2017) and conversely neuronal cells release neurotransmitters such as noradrenaline to stimulate cancer growth (Hayakawa et al., 2017;Renz et al., 2018a). However, the full extent of molecular mediators involved in the nerve cancer cell cross-talk are yet to be fully defined and in particular the molecular contributors produced by SCs. We have profiled the secretome of human SCs by LC-MS/MS (Chapter 4) and investigated the role of the secreted proteins in different cancer promoting processes such as proliferation and invasion. From 1,470 identified SC-secreted proteins, 7 proteins were validated by Western blot and their involvement in PC cell proliferation and invasion was further demonstrated using blocking antibodies. We have not directly confirmed the blocking of the specific proteins by their antibodies. In the absence of a biological assays associated with a particular protein (which is the case for most tested proteins), it is impossible to test for the blocking activity of the antibody and this is a potential limitation of our study. Further preclinical studies in vivo will need to be performed to determine whether these proteins may become new targets for therapeutic intervention in PC. In doing so, genetically engineered mouse models could be created to knock out the candidate proteins and test the impact on PC cell growth and dissemination.

Our proteomic analysis also identified several other proteins of interest that although were not tested by a functional analysis, may still be important in the stimulation PC cells by SCs (Chapter 4). For instance, this applies to insulin-like growth factor-binding proteins (IGFBP-2, IGFBP-4, IGFBP-5, IGFBP-6, IGFBP-7) and transforming growth factors (TGFβ-1, TGFβ-2, TGFBI). Further studies will be performed to determine the possible involvement of these proteins in cancer PC progression and their potential value as therapeutic targets. Additionally, in our study, the proteome of SCs was analysed only in a rather unstimulated state, i.e. without previous exposure to PC cells. In future studies, it would also be of interest to investigate the proteome of SCs when stimulated by PC cells to further delineate the cross-talk between PC cells and SC in the TME. In doing so, LC-MS/MS would be performed on conditioned media collected after co-culturing SCs with PC cells using a non-contact trans-well Boyden chamber.

The study presented in Chapter 5 describes the association of infiltrated nerves in the TME with PC aggressiveness. The presence of nerves was significantly correlated with worse overall survival (OS). Marginally significant differences in nerve infiltration regarding OS of PC have been reported in a study conducted by Min *et al.* (Yu et al., 2015). In contrast, low intrapancreatic nerve numbers have been shown to correlate with shorter OS of patients with PC in a study conducted by Iwasaki *et al.*(Iwasaki et al., 2019). This is opposite to our observation. A possible explanation for this discrepancy might be the analysis method where the authors analysed both enlarged nerves and fine periacinar nerves, whereas we only analysed the enlarged nerves. For the purpose of analysing, we categorized patients as nerve positive *versus* nerve negative, whereas their categorization was based on low *versus* high nerve number. Additionally, the size of nerves was found to be significantly higher in PC than in the normal adjacent tissue and larger nerves were directly associated with worse patient survival. We believe this pattern is consistent with that expected for a marker of neuronal outgrowth, expressing more activity where the neurites extend. Future IHC could be performed, including two other secondary neural markers named regenerating nerve marker, growth-associated protein 43(GAP-43) or the pan-neural marker protein gene product 9.5 (PGP9.5) to validate the outcome.

Furthermore, studies will need to be conducted in order to clarify the distribution of sympathetic, parasympathetic or sensory nerves and to identify the mechanism(s) by which each of these neuronal subpopulations influence the nature of cancer cells, as the extent and

nature of tumour innervation may have been underestimated. Paraffin embedded TMAs generally do not contain a sufficient amount of tissue, with respect to both area and depth of the core, for the purpose of precisely measuring and dissecting neural infiltration and densities in tumours. Therefore, subsequent studies on this research should utilise thicker sections as well as whole tumour tissue samples to precisely characterise the density and source of tumour innervation. Additionally, immunofluorescent microscopy of fresh or frozen sections should be applied for simultaneously assessing the immunoreactivity of sympathetic, parasympathetic or sensory nerves. Additional studies with large sample size would also help elucidate if nerve infiltration associated cancer aggressiveness could be applied to multiple cancers. Further studies should also be performed to clarify the molecular mechanisms of neural alterations within PC including whether any neurotrophic growth factors are associated with nerve enlargement in cancerous tissue and associated aggressiveness.

Overall, this thesis has contributed to provide novel evidence supporting the potential role and importance of nerves and their supporting SCs in PC progression and clinical outcome. Though we have identified several molecules secreted by SCs involved in PC progression, many questions remain unanswered, which should be addressed in the future. How do the different reported molecules work? Do they act simultaneously or sequentially, and how are they coordinated? Do they behave differently in different cancer types? A comprehensive understanding of the role of nerves and SCs in cancer progression has been outlined in this Thesis and the future may see the identification of novel targets and therapeutic strategies to treat PC more effectively.

Although we have identified several molecules secreted by SCs involved in PC progression, many questions remain unanswered, which should be addressed in the future. How do the different reported molecules work? Do they act simultaneously or sequentially? And how are they coordinated? Do they behave differently in different cancer types? Overall, this thesis has contributed to provide novel evidence supporting the role and importance of nerves and SCs in PC progression and clinical outcome. This opens new perspectives for the development of future therapeutic strategies against PC.

APPENDICES

A.1 Additional publication supplemental to this thesis

The neurotrophic tyrosine kinase receptor TrkA and its ligand NGF are increased in squamous cell carcinomas of the lung.

Preface

This original research article has been published on the journal *Scientific Reports*. In lung cancer, drugs targeting TrkA are in clinical trials (Vaishnavi et al., 2015), but the pathological significance of TrkA and its ligand NGF has remained unclear. In this study, we demonstrated that TrkA and NGF are differentially expressed among the histological subtypes of lung cancers. In particular, we show for the first time that NGF and TrkA are overexpressed more specifically in lung squamous cell carcinomas, suggesting the existence of an autocrine loop of stimulation. Our study indicates that anti-TrkA (NTRK1) therapies, which are currently undergoing clinical trials, may be more efficient in the squamous forms of lung cancer.

Publication

Published article "Gao F, Griffin N, Faulkner S, Rowe CW, Williams L, Roselli S, Thorne RF, **Ferdoushi A**, Jobling P, Walker MM, Hondermarck H: **The neurotrophic tyrosine kinase receptor TrkA and its ligand NGF are increased in squamous cell carcinomas of the lung**. *Scientific Reports*. 2018 May 25;8(1):8135" displays from page 108-118.

Supplementary Files

Supplementary file displays on page 119-120.

SCIENTIFIC REPORTS

OPEN

The neurotrophic tyrosine kinase receptor TrkA and its ligand NGF are increased in squamous cell carcinomas of the lung

Received: 10 January 2018
Accepted: 10 May 2018
Published online: 25 May 2018

Fangfang Gao[1,2], Nathan Griffin[1,2], Sam Faulkner[1,2], Christopher W. Rowe[2,3], Lily Williams[1], Severine Roselli[1,2], Rick F. Thorne[2], Aysha Ferdoushi[1,2], Phillip Jobling[1,2], Marjorie M. Walker[2,3] & Hubert Hondermarck[1,2]

The neurotrophic tyrosine kinase receptor TrkA (NTRK1) and its ligand nerve growth factor (NGF) are emerging promoters of tumor progression. In lung cancer, drugs targeting TrkA are in clinical trials, but the clinicopathological significance of TrkA and NGF, as well as that of the precursor proNGF, the neurotrophin co-receptor p75^{NTR} and the proneurotrophin co-receptor sortilin, remains unclear. In the present study, analysis of these proteins was conducted by immunohistochemistry and digital quantification in a series of 204 lung cancers of different histological subtypes *versus* 121 normal lung tissues. TrkA immunoreactivity was increased in squamous cell carcinoma compared with benign and other malignant lung cancer histological subtypes ($p < 0.0001$). NGF and proNGF were also increased in squamous cell carcinoma, as well as in adenocarcinoma ($p < 0.0001$). In contrast, p75^{NTR} was increased across all lung cancer histological subtypes compared to normal lung ($p < 0.0001$). Sortilin was higher in adenocarcinoma and small cell carcinoma ($p < 0.0001$). Nerves in the tumor microenvironment were negative for TrkA, NGF, proNGF, p75^{NTR} and sortilin. In conclusion, these data suggest a preferential therapeutic value of targeting the NGF-TrkA axis in squamous cell carcinomas of the lung.

Lung cancer is the leading cause of cancer related death worldwide and its incidence is increasing[1]. Lung cancer histological subtypes are divided into two main categories: small cell lung cancers and non-small cell lung cancers (NSCLC). NSCLC represent the majority of lung cancer cases and include squamous cell carcinomas and adenocarcinomas. Despite extensive research, there are few clinically used biomarkers to help determine diagnosis, prognosis and treatment choice in lung cancer[1]. This is particularly problematic for NSCLC where correct identification of histological subtypes is essential to define the appropriate chemotherapeutic regimens. Therefore, the identification of pertinent biomarkers for diagnosis, stratification and therapeutic decision in lung cancer is necessary.

The neurotrophic tyrosine kinase receptor TrkA (NTRK1) and its ligand nerve growth factor (NGF) are essential to the development of the nervous system where they stimulate the outgrowth of sympathetic and sensory neurons[2]. Interestingly, TrkA and NGF are also expressed in several malignancies. In breast cancer, they participate in tumor cell proliferation and spreading *via* the activation of signalling pathways similar to those activated in neurons and including ERK, SRC and AKT[3]. Recent evidence in gastric[4] and pancreatic[5] cancers has shown that the NGF-TrkA signalling pathway is an essential and targetable stimulator of cancer progression. In lung cancer, rearrangements of TrkA have been shown to be oncogenic and are drug-sensitive[6]. TrkA is increasingly regarded as a therapeutic target in lung cancer and clinical trials of drugs against its tyrosine kinase activity are under way[7]. A previous study has shown that the expression of TrkA and NGF is higher in NSCLC[8], but the distribution of TrkA and NGF in the different subtypes of lung cancer remains unclear. In addition, the expression of the other co-receptors for NGF[2], the common neurotrophin receptor p75^{NTR} (also called NGFR or CD271), as well as that of the precursor for NGF

[1]School of Biomedical Sciences & Pharmacy, Faculty of Health and Medicine, University of Newcastle, Callaghan, NSW, 2308, Australia. [2]Hunter Medical Research Institute, University of Newcastle, New Lambton, NSW, 2305, Australia. [3]School of Medicine & Public Health, Faculty of Health and Medicine, University of Newcastle, Callaghan, NSW, 2308, Australia. Correspondence and requests for materials should be addressed to H.H. (email: hubert.hondermarck@newcastle.edu.au)

(proNGF) and its receptor sortilin (a member of the Vacuolar Protein Sorting 10 protein - VPS10P - family of receptors) have not been elucidated. Despite early studies showing that neurotrophic growth factors are expressed in lung cancer[9], the clinicopathological significance warrants clarification.

The present study aimed to clarify the expression and clinicopathological significance of TrkA, NGF, proNGF, $p75^{NTR}$ and sortilin in lung cancer. The expression of these proteins was analysed by immunohistochemistry in a cohort of lung cancers versus normal lung tissues. We report an increased level of TrkA and NGF in squamous cell carcinomas, suggesting that drugs targeting the NGF-TrkA pathway in lung cancer should be used preferentially in this form of the disease.

Results

For all neurotrophins/receptors, representative pictures of immunohistochemical staining are shown in Figs 1–5 and quantification of staining intensities are presented in Table 1. Staining intensities (h-scores) are presented as medians (50^{th} centile value).

TrkA is increased in squamous cell lung carcinoma. Compared with normal lung (Fig. 1A), TrkA labelling was concentrated in cancer epithelial cells (Fig. 1B–F), with an increased staining intensity specifically in squamous cell carcinoma (Fig. 1B–D). Membrane staining was clearly observable. TrkA immunoreactivity was low in normal lung tissue (h-score 18), and lower in adenocarcinoma (h-score 6) ($p < 0.0001$); in squamous cell carcinoma, TrkA intensity (h-score 26) was significantly higher ($p < 0.0001$) (Fig. 1G, Table 1). This increase in h-score was driven by a subpopulation of squamous cell tumours that were strongly positive for TrkA, consistent with a binary receptor expression pattern of TrkA-present (h-score > 50) or TrkA-absent (h-score ≤ 50). When analysed by these parameters (Fig. 1H), 27/96 (28%) of squamous cell carcinomas expressed TrkA, compared to 1/55 (2%) of adenocarcinomas, 0/7 (0%) of small cell cancers and 1/121 normal tissues (<1%) ($p < 0.0001$), with 12/96 (13%) of squamous cell carcinomas showing very strong TrkA expression (h-score >100). Multivariate logistic regression modelling confirmed squamous pathology was significantly associated with increased TrkA h-score, when accounting for age and gender (Odds ratio (OR) 1.03, 1.01–1.04, $p < 0.001$). Given that TrkA was not expressed in most adenocarcinomas and small cell lung cancers, the area under the receiver-operating characteristic (AUROC) for the comparison between normal and cancer samples was only 0.39 (95%CI 0.32 to 0.46) (data not shown). No association was found between TrkA expression and age, grade, tumor size, stage, lymph node status.

NGF and proNGF are increased in squamous cell carcinoma and adenocarcinoma. NGF immunoreactivity was observed at low levels in normal tissues (Fig. 2A), and was increased in cancer vs normal samples (Fig. 2B–F). NGF staining intensity (h-score) was significantly increased from 57 in normal to 95 in cancer samples ($p < 0.0001$) (Fig. 2G). Squamous cell carcinoma (Fig. 2B–D) and adenocarcinoma (Fig. 2E) presented with a NGF h-score of 107 and 84 respectively ($p < 0.0001$) (Fig. 2G, Table 1). Small cell cancers (Fig. 2F) displayed a lower level of NGF staining compared to other cancer subtypes (h-score 54) (Fig. 2G, Table 1) ($p < 0.0001$). Multivariate logistic regression modelling confirmed squamous cell carcinoma and adenocarcinoma were significantly associated with increased NGF h-score compared to benign pathology, when accounting for age and gender (OR 1.09 (1.06–1.12) and 1.08 (1.05–1.11) respectively, $p < 0.001$). The AUROC for the comparison between normal and cancer tissue was 0.88 (95%CI 0.84 to 0.92) (Fig. 2H).

ProNGF was also increased in malignant tissue (Fig. 3B–E) compared to normal lung tissue (Fig. 3A), but the differential in median h-score was less than NGF. Multivariate logistic regression modelling confirmed squamous cell carcinoma and adenocarcinoma were significantly associated with increased proNGF h-score compared to benign pathology, when accounting for age and gender (OR 1.04 (1.02–1.05) and OR 1.04 (1.03–1.06) respectively, $p < 0.001$) (Fig. 3G, Table 1). The AUROC for the comparison between normal and cancer samples was 0.70 (95%CI 0.64 to 0.76) (Fig. 3H).

For both NGF and proNGF, there was no association with age, grade, stage, tumor size, or lymph node invasion (Table 1).

$P75^{NTR}$ is increased in all lung cancer subtypes. Immunostaining for $p75^{NTR}$ was observed in both epithelial and stromal cells of normal (Fig. 4A) and cancer samples (Fig. 4B–F). However, $p75^{NTR}$ staining intensity was higher in cancer, with an h-score of 92 in normal compared to 147 in cancer ($p < 0.0001$) (Fig. 4G, Table 1). The increase in $p75^{NTR}$ staining intensity occurred in all histological subtypes of lung cancer (squamous cell, adenocarcinoma, small cell) but was particularly strong in small cell carcinoma (median h-score of 215) (Fig. 4G, Table 1). Multivariate logistic regression modelling confirmed malignant pathology was significantly associated with increased $p75^{NTR}$ h-score for squamous cell carcinoma (OR 1.04 (1.02–1.05), $p < 0.001$), adenocarcinoma (OR 1.07 (1.05–1.10 $p < 0.001$), when compared to benign pathology, when accounting for age and gender ($p < 0.001$). We were unable to fit a logistic regression model for small cell carcinoma vs benign tissue due to perfect separation of h-scores (Fig. 4G). The AUROC for the comparison of cancer *vs* normal was 0.83 (95%CI 0.79 to 0.88) (Fig. 4H). There was no association between $p75^{NTR}$ staining and tumor size, grade, stage or lymph node status.

Sortilin is increased in adenocarcinoma and small cell lung cancer. Immunostaining for sortilin was weak and found mainly in epithelial cells of both normal (Fig. 5A) and cancer samples (Fig. 5B–F). There was no difference between sortilin staining intensity in benign vs all lung cancer tissues with h-scores of 32 vs 30 respectively ($p = 0.43$). However, there was a higher level of sortilin staining intensity in adenocarcinoma (OR 1.05 (1.03–1.07, $p < 0.001$) and small cell (OR 1.18 (1.06–1.31, $p = 0.002$) when compared to benign pathology in a multivariate logistic regression model. (Fig. 5G, Table 1). The AUROC for comparison of cancer vs normal was 0.46 (95%CI 0.39 to 0.53) (Fig. 5H), confirming that sortilin expression is not significantly modified when comparing all lung cancers to normal tissues. In addition, there were no associations between sortilin expression and age, grade, stage, tumor size or lymph node invasion.

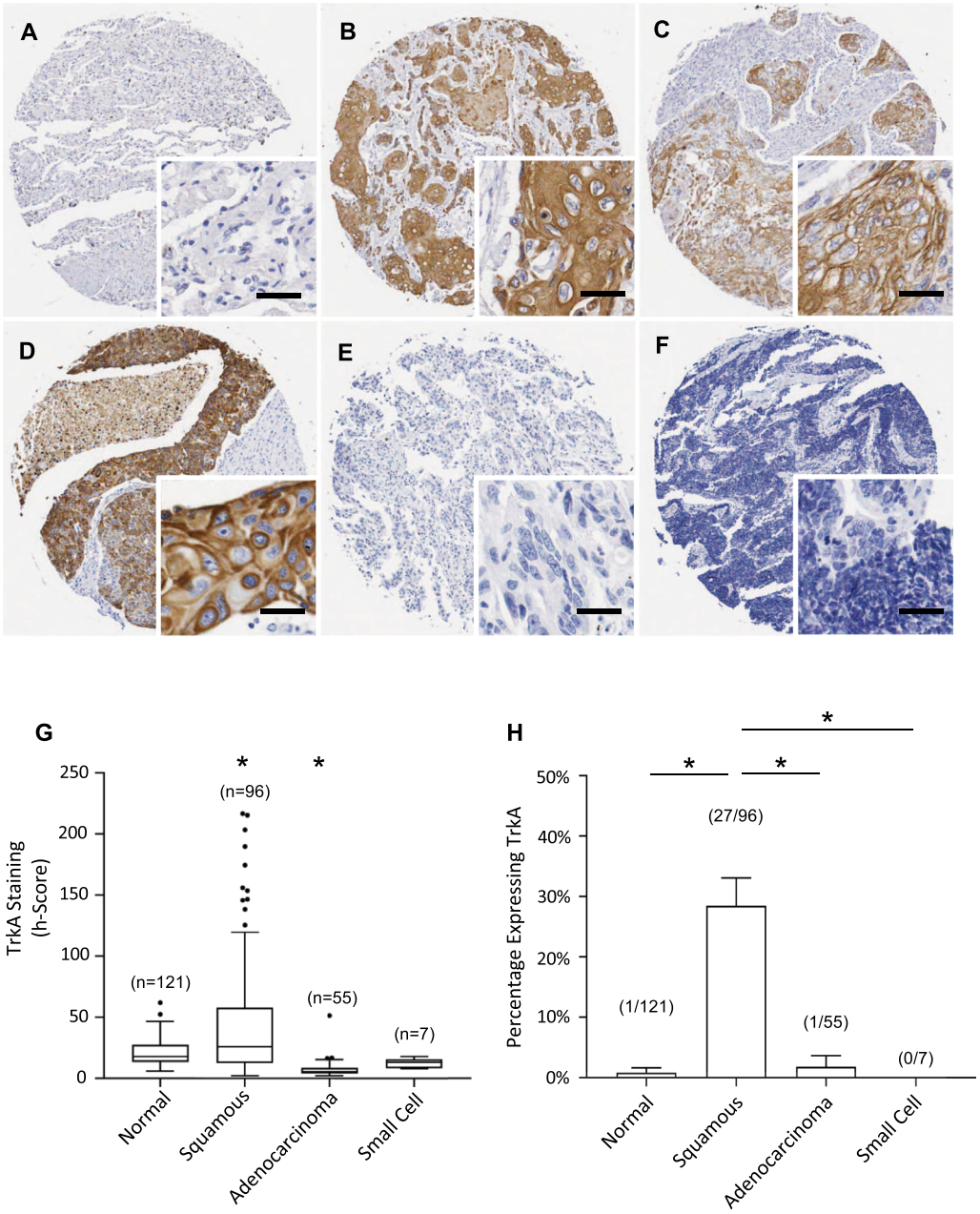

Figure 1. TrkA expression in lung cancers and normal lung tissues. (**A**–**F**) Immunohistochemical detection of TrkA, representative pictures are shown for normal tissue (**A**), squamous cell carcinoma (**B**–**D**), adenocarcinoma (**E**) and small cell cancer (**F**). Scale = 50 μm. (**G**) TrkA staining intensities were significantly higher in squamous cell carcinoma. Corresponding median h-scores are presented in Table 1. The box limits indicate the interquartile range (IQR) with the whiskers extending 1.5 times the IQR from the 25th and 75th percentiles (outliers are represented by dots) ($^{*}p < 0.0001$ in multiple logistic regression model). (**H**) Proportion of tissues expressing TrkA receptor (binary h-score cutoff of 50) in normal lung tissue vs lung cancer subtypes. Squamous cell carcinoma was significantly higher than all other categories ($p < 0.0001$).

Nerves in the tumor microenvironment of lung cancer do not express NGF, proNGF, TrkA, p75^{NTR} and sortilin. The pan-neuronal marker PGP9.5 was used to detect nerves in the tumor microenvironment. Nerve trunks were occasionally detected in lung cancer (Fig. 6A), based on PGP9.5 positivity as well as typical nerve morphology. Serial sections were used and no labelling for NGF (Fig. 6B), proNGF (Fig. 6C), TrkA (Fig. 6D), p75^{NTR} (Fig. 6E) or sortilin (Fig. 6F) was detected. These data show that there is no expression of NGF, proNGF, TrkA, p75^{NTR} and sortilin in nerves which are present in the tumor microenvironment of lung cancer.

Discussion

ProNGF and sortilin have not been described in lung cancers and there has been limited reports on the expression of NGF and its receptors TrkA and p75^{NTR}[8,10,11]. Therefore, with only fragmentary data available, the

clinicopathological significance remained unclear. To address this, we undertook a simultaneous investigation of the protein expression of proNGF, NGF, TrkA, $p75^{NTR}$ and sortilin in the same cohort of lung cancers and normal lung tissues. Our results reveal that TrkA, NGF, proNGF, $p75^{NTR}$ and sortilin are differently expressed across lung cancer histological subtypes, with TrkA and NGF most particularly increased in squamous cell carcinomas.

Prior to investigating protein levels by immunohistochemistry, data mining of gene expression in lung datasets available from The Cancer Genome Atlas (TCGA)[12] using cBioportal[13] was performed. Gene amplification and mRNA upregulation were detected at various frequencies in lung tumors: 6% for NGF, 14% for TrkA, 2% for $p75^{NTR}$ and 4% for sortilin. However, discrepancies between mRNA and protein levels in tumors are now well documented. Global transcriptomic and proteomic analyses estimate that only 30%–60% of changes in protein levels can be explained by corresponding variations in mRNA[14,15] and proteogenomic investigations in colorectal cancer have revealed that mRNA abundance does not reliably predict differences in tumoral protein abundance[16]. This emphasizes the importance of analysing the protein levels directly, in order to define new biomarkers and novel therapeutic targets in oncology.

The participation of TrkA and TrkA fusion proteins in lung cancer progression has been described, with Trk inhibitors undergoing clinical trials[6]. Our data shows a preferential expression of TrkA in squamous cell lung cancer, suggesting that Trk inhibitors should be used more specifically in this histological subtype of lung cancer. A previous investigation has reported an increase in TrkA and NGF in NSCLC and an association with tumor aggressiveness but not histological subtypes[8]. However, in this study staining intensities were visually determined, and no digital quantification assisted by a pathologist (as we have done here) was used, potentially leading to approximation in the quantification of expression levels. In addition, the comparison was done with normal adjacent tissues whereas true normal lung tissues were analysed in our study. Therefore, our study provides a refinement in terms of quantification of TrkA and NGF in lung cancer subtypes, highlighting a significant increase in both TrkA and NGF expression in squamous cell lung cancer. In contrast, as low expression level for TrkA were observed in adenocarcinoma and small cell cancer, it is unlikely that Trk inhibitors will produce any significant clinical impact in these tumors. Interestingly, NGF was also increased in squamous cell lung cancer and to a lesser extent in adenocarcinoma. This concomitant increased expression of both TrkA and its ligand NGF is suggestive of a NGF-mediated autocrine stimulation of squamous cell carcinoma. Similar autocrine stimulation of cancer cell growth via a proNGF/NGF autocrine loop involving TrkA has been described in breast cancer[17,18] and may also apply to lung cancer. Although further functional investigations are warranted to test this hypothesis, our data reveals that TrkA and its ligand NGF are overexpressed in squamous cell lung cancer. This finding may have clinical ramifications, as humanized NGF blocking antibodies have been developed and are in clinical trials for the treatment of pain[19]; they may potentially be repurposed to inhibit the NGF-TrkA signaling axis in lung cancer.

In contrast to NGF, proNGF was only slightly increased in squamous cell lung cancer and adenocarcinoma. ProNGF processing into NGF requires protein convertases, such as furin or metalloproteases, and can occur both intracellularly or after secretion in the extracellular compartment[2]. In the nervous system, proNGF is the predominant protein form of NGF gene expression, with a higher presence of proNGF in comparison to NGF[20]. The regulatory mechanism that controls proNGF processing is poorly described in cancer, but our data suggest that proNGF is largely processed into NGF in squamous cell carcinomas of the lung. The limited differential in proNGF expression between normal and cancerous lung tissue is in line with the data obtained for its receptor sortilin. Sortilin was expressed at the same low levels in normal lung tissue, squamous cell carcinoma and was only higher in adenocarcinoma and small cell cancer. Sortilin has been reported in various cancer cell lines of different origins and its expression is associated to a poor prognosis in breast cancer where it participates in tumor cell migration and invasion[21]. In the squamous cell line A549, sortilin has been shown to participate in the transfer of exosomes in association with TrkB[22], but our data have not highlighted any particular association between sortilin expression and clinicopathological parameters in any histopathological subtypes of lung cancers.

The neurotrophin receptor $p75^{NTR}$ is expressed in a wide range of human tumors and has been shown to be a marker of cancer stem cells of both epithelial and mesenchymal origin[23]. However, the mechanism of $p75^{NTR}$ activity in cancer cells is not fully elucidated and some studies in gastric[24] and prostatic cancer[25,26] have reported a tumor suppressor effect associated with $p75^{NTR}$ suppression. In the present study, $p75^{NTR}$ was expressed in normal lung tissues and overexpressed in all investigated lung cancer histological subtypes. The overexpression of $p75^{NTR}$ was observed in epithelial cells as well as stromal cells. Interestingly $p75^{NTR}$ has recently been shown to be a p53 inactivator[27], and as such $p75^{NTR}$ could actively participate in lung tumor growth, but further functional investigations are needed to explore this hypothesis.

Emerging evidence indicate the stimulatory role of nerves in tumor progression[28]. The nerve-cancer cell crosstalk involves the liberation of neurotransmitters and trophic factors to stimulate cancer cell growth and dissemination, while neurotrophic factors are released by cancer cells to attract nerve outgrowth in the tumor microenvironment[29]. In gastric cancer, NGF has been shown to activate cholinergic nerve-mediated signalling that stimulates the proliferation of stem cells[4]. In prostate cancer, sympathetic and parasympathetic nerves participate in the stimulation of tumor growth and metastasis[30] and proNGF released by prostate cancer cells is a driver of neuronal outgrowth[31]. In lung cancer, autonomic nerve infiltration is associated with pathological risk grading and poor patient prognosis[32], but the drivers of nerve infiltration have not been identified. Our study showing that there is no expression of the receptors TrkA, $p75^{NTR}$ and sortilin in nerves infiltrated in the tumor microenvironment, suggest that NGF/proNGF are not involved in stimulating the growth of nerves in lung cancer.

Overall, this study highlights the overexpression of NGF, proNGF and their receptors TrkA, $p75^{NTR}$ in lung cancer with a differential expression related to histological subtypes. A similar increased expression of these neurotrophins and receptors has already been observed in breast[17,18,33] and thyroid[34,35] cancer, suggesting that the upregulation these proteins is a common molecular feature in these cancers. Pharmacological inhibitors against TrkA[7] and humanized anti-NGF antibodies[19] have been developed and could therefore be used as therapeutic tools in breast, thyroid and lung cancers. The overexpression of TrkA in squamous cell carcinomas of the lung is

Parameter	NGF Intensity			proNGF Intensity			TrkA Intensity			sortilin Intensity			p75NTR Intensity		
	Median h-score	IQR	p-value	Median h-score	IQR	p-value	Median h-score	IQR	p-value	Median h-score	IQR	p-value	Median h-score	IQR	p-value
Normal vs cancer			**<0.0001**			**<0.0001**			**0.002**			0.43			**<0.0001**
Normal (n = 121)	57	46–70		58	47–70		18	13–26		32	26–41		92	81–110	
Cancer (n = 164)	95	76–112		76	58–96		13	6–33		30	20–48		147	116–176	
Histological Type			**0.0001**			**0.0001**			**0.0001**			**0.0001**			**0.0001**
Squamous (n = 98)	107	85–118		73	58–96		26	13–57		25	18–40		132	107–161	
Adenocarcinoma (n = 58)	84	72–98		82	65–98		6	4–9		40	26–66		164	141–184	
Small Cell (n = 8)	54	50–70		52	33–72		13	8–16		56	42–65		215	180–222	
Gender			0.04			0.28			**<0.0001**			**0.002**			**0.0005**
Male (n = 125)	99	80–115		74	58–95		16	7–39		27	19–44		138	112–171	
Female (n = 39)	84	70–108		83	59–109		6	4–13		42	27–58		168	147–189	
Age (yrs)			0.56			0.35			0.31			0.7			0.35
< 50 (n = 40)	94	72–108		72	55–97		16	8–39		30	22–49		154	121–177	
> 50 (n = 124)	96	76–114		76	59–96		11	6–29		31	19–48		141	114–175	
Grade			0.85			0.03			0.24			0.88			0.37
1 (n = 13)	98	84–117		96	89–120		19	10–138		26	18–46		141	82–160	
2 + 3 (n = 135)	97	78–114		74	59–95		14	6–34		29	19–46		142	116–172	
Missing (n = 16)	65	51–89		65	35–83		11	7–15		47	27–58		180	130–215	
T stage			0.88			0.55			0.63			0.71			0.8
T1/T2 (n = 133)	97	75–112		75	58–96		13	6–32		31	20–48		150	115–176	
T3/T4 (n = 31)	95	77–109		76	58–99		13	5–34		27	18–50		142	117–171	
LN Status			0.9			0.78			0.64			0.97			0.48
Negative (n = 70)	96	78–111		76	60–96		13	6–37		31	20–46		149	117–169	
Positive (n = 94)	95	75–112		74	56–96		13	5–31		29	20–49		145	116–178	
Stage			0.38			0.35			0.53			0.93			0.5
I + II (n = 120)	94	75–112		74	58–95		13	6–32		31	20–47		151	116–177	
III + IV (n = 44)	97	79–113		82	58–100		13	5–34		29	20–52		141	114–172	

Table 1. Expression of NGF, proNGF, TrkA, $p75^{NTR}$ and sortilin in lung cancers and association with clinicopathological parameters. Immunohistochemical staining were quantified and h-scores were used to compare protein expression levels. Group-levels medians (IQR, interquartile range) for h-score staining intensities are presented. Family-wise alpha significance level is 0.05/8 = 0.006 using the Wilcoxon Rank-Sum test (pairwise) or Kruskal-Wallis test (multiple comparisons). Statistically significant p-values are shown in bold.

of particular interest, given that TrkA inhibitors have entered clinical trials for the treatment of lung cancer[7]. In the nervous system, neurons responsive to NGF express TrkA and $p75^{NTR}$ and the stimulation of these receptors by NGF induces a cascade of intracellular signalings including SRC, AKT, PI3K, ERK and NFkB. In lung cancer cells, TrkA tyrosine kinase inhibitors induce lung cancer cell growth arrest and apoptosis[36]. Based on the present findings, the biological effect of targeting TrkA and NGF in lung cancer should be revisited in the context of squamous cell carcinomas with more functional *in vitro* and *in vivo* animal models. From a clinical perspective, our data suggest that anti-TrkA therapies may be more effective in squamous cell lung cancer and could eventually be associated with NGF targeting.

Material and Methods

Lung tissue samples. High-density tumor microarrays (TMA) were obtained from US Biomax Inc. (Maryland, USA). The TMAs used (catalogue numbers: LC2086, LC2087 and BC041115) included a total of 204 lung cancers (of adenocarcinoma, squamous cell carcinoma, small cell carcinoma or other minor subtypes) and 121 normal lung tissues. The following clinicopathological information was available: patient age and sex, histological subtype, tumor size, grade, stage and lymph node status. No information on treatment and patient survival was available. US Biomax Inc. quality controls are described as follows. Each single tissue spot on every array slide was individually examined by pathologists certified according to WHO published standardizations of diagnosis, classification and pathological grade. For each specimen collected, informed consent was obtained from both hospital and individual. Discrete legal consent was obtained and the rights to hold research uses for any purpose or further commercialized uses were waived. The study was approved by the Human Research Ethic Committee of the University of Newcastle and all experiments were performed in accordance with relevant guidelines and regulations.

Immunohistochemistry. Immunohistochemistry (IHC) was performed as previously described[34]. After deparaffinization and rehydration of the TMA slides following standard procedures, heat induced epitope retrieval was carried out in a low pH, citrate based antigen unmasking solution (Vector Laboratories, California,

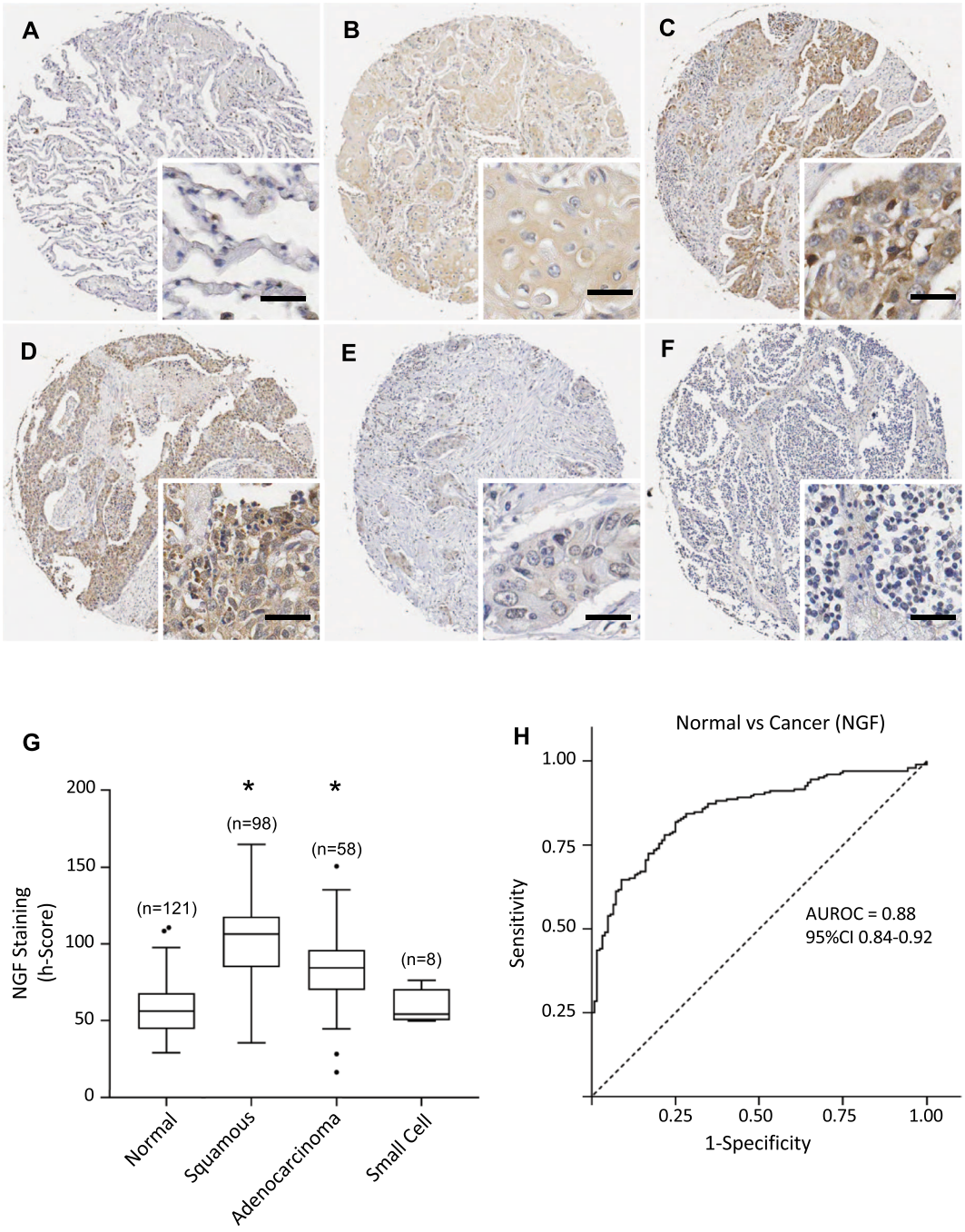

Figure 2. NGF expression in lung cancers and normal lung tissues. (**A**–**F**) Immunohistochemical detection of NGF, representative pictures are shown for normal tissue (**A**), squamous cell carcinoma (**B**–**D**), adenocarcinoma (**E**) and small cell cancer (**F**). Scale = 50 μm. (**G**) NGF staining intensities were significantly higher in squamous cell carcinoma and adenocarcinoma than in normal tissues. Corresponding median h-scores are presented in Table 1. The box limits indicate the interquartile range (IQR) with the whiskers extending 1.5 times the IQR from the 25th and 75th percentiles (outliers are represented by dots) (*$p < 0.0001$ in multiple logistic regression model). (**H**) ROC curve for NGF staining intensity level in lung cancers versus normal tissues. The area under the curve was 0.88 (95%CI 0.84 to 0.92).

USA, catalogue number H-3300) using a decloaking chamber (Biocare, West Midlands, United Kingdom) at 95 °C for 20 min. IHC was then performed using an ImmPRESS^{TM} HRP IgG (Peroxidase) Polymer Detection Kit (Vector Laboratories, California, USA), as per the manufacturer's recommendations. Briefly, after inactivation of endogenous peroxidases with 0.3% H_2O_2, and blocking with 2.5% horse serum, primary followed by secondary antibodies were applied to the sections and revealed with DAB Peroxidase (HRP) Substrate Kit (Vector Laboratories, California, USA, catalogue number SK-4100). The following primary antibodies were used at 1/500 dilution: anti-proNGF (#AB9040, Merck Millipore), anti-NGF (#ab52918, Abcam), anti-TrkA (#2508,

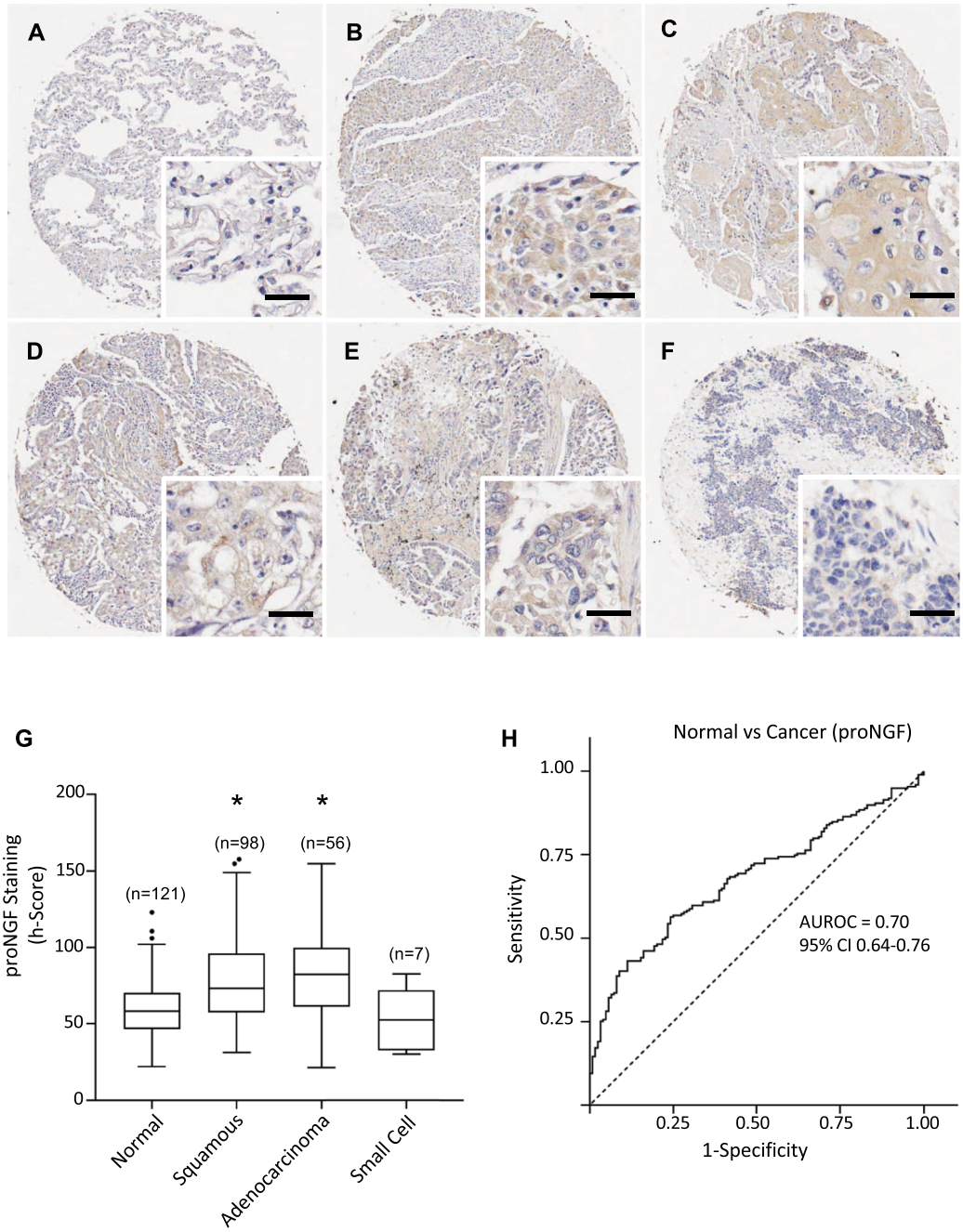

Figure 3. ProNGF expression in lung cancers and normal tissues. (**A**–**F**) Immunohistochemical detection of proNGF, representative pictures are shown for normal tissue (**A**), squamous cell carcinoma (**B**–**D**), adenocarcinoma (**E**) and small cell cancer (**F**). Scale = 50 μm. (**G**) ProNGF staining intensities were significantly higher in squamous cell carcinoma and adenocarcinoma than in normal tissues. Corresponding median h-scores are presented in Table 1. The box limits indicate the interquartile range (IQR) with the whiskers extending 1.5 times the IQR from the 25th and 75th percentiles (outliers are represented by dots) (*$p < 0.0001$ in multiple logistic regression model). (**H**) ROC curve for proNGF staining intensity level in lung cancers versus normal tissues. The area under the curve was 0.70 (95% CI 0.64 to 0.76).

Cell Signaling), anti-p75^{NTR} (#4201, Cell Signaling), anti-sortilin (#ANT-009, Alomone Labs), anti-PGP9.5 (#ab15503, Abcam). Finally, TMA slides were counterstained with hematoxylin (Gill's formulation, Vector Laboratories, California, USA), dehydrated and cleared in xylene before mounting in Ultramount #4 mounting media (Thermo Fisher Scientific, Victoria, Australia). Negative controls, using isotype control antibodies, are shown in Supplementary Fig. 1.

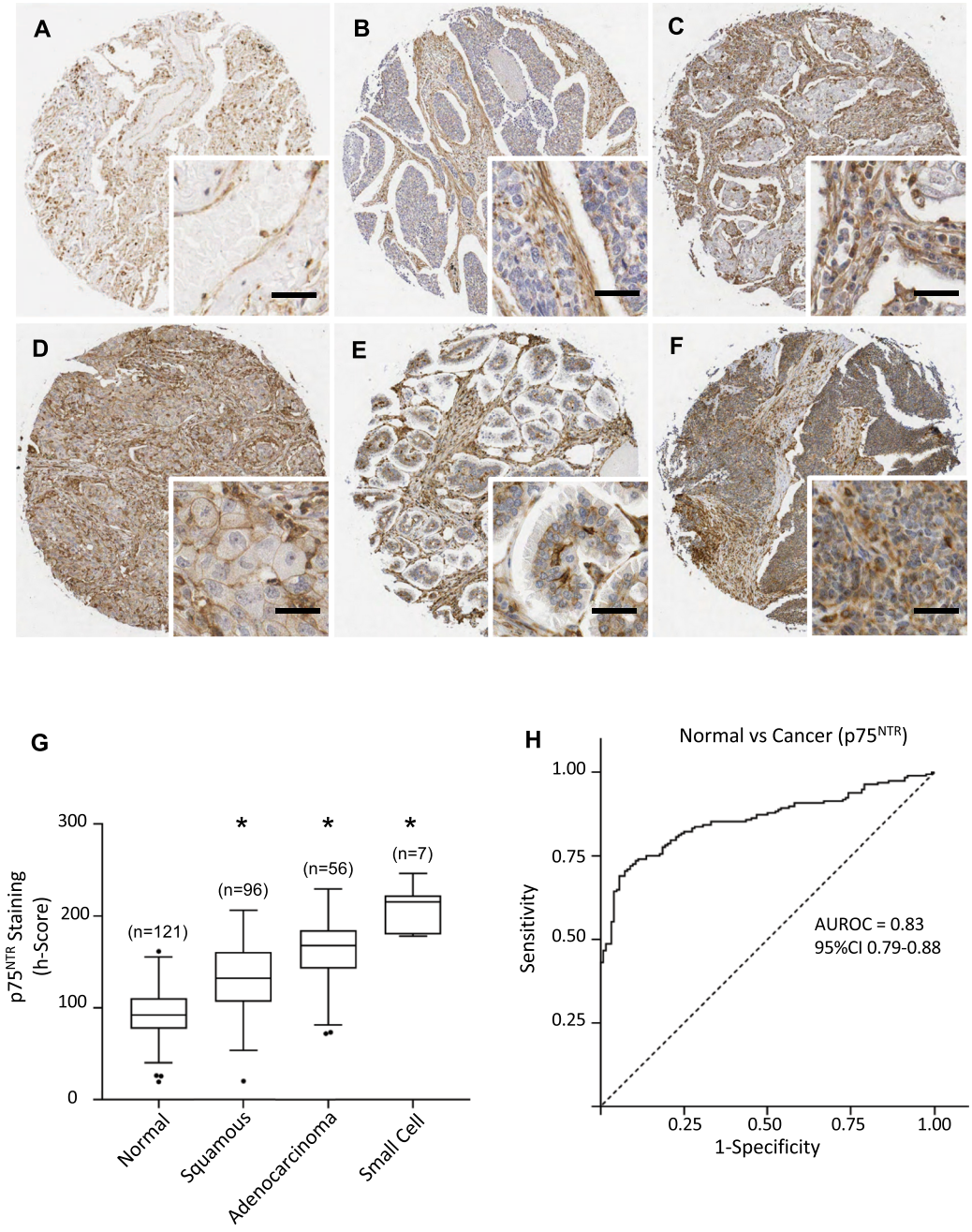

Figure 4. P75^{NTR} expression in lung cancers and normal lung tissues. (**A**–**F**) Immunohistochemical detection of p75^{NTR}, representative pictures are shown for normal tissue (**A**), squamous cell carcinoma (**B**–**D**), adenocarcinoma (**E**) and small cell cancer (**F**). Scale = 50 μm. (**G**) p75^{NTR} staining intensities were significantly higher in squamous cell, adenocarcinoma and small cell cancers. Corresponding median h-scores are presented in Table 1. The box limits indicate the interquartile range (IQR) with the whiskers extending 1.5 times the IQR from the 25th and 75th percentiles (outliers are represented by dots) (*$p < 0.0001$ in multiple logistic regression model). (**H**) ROC curve for p75^{NTR} staining intensity level in lung cancers versus normal tissues. The area under the curve was 0.83 (95% CI 0.79 to 0.88).

Digital quantification of IHC staining intensities. Quantification of staining intensities was performed as previously described[34] using the Aperio AT2 scanner (Leica Biosystems, Victoria, Australia) and the Halo™ image analysis platform (Indica Labs, New Mexico, USA) under the supervision of a pathologist (MMW). Pixel intensity values were used to determine the h-scores for each core (index calculated as the sum of 3x% of pixels with strong staining +2x% of pixels with intermediate staining +1x% pixels with weak staining). Each core of the TMAs was investigated and the data were then submitted to statistical analysis.

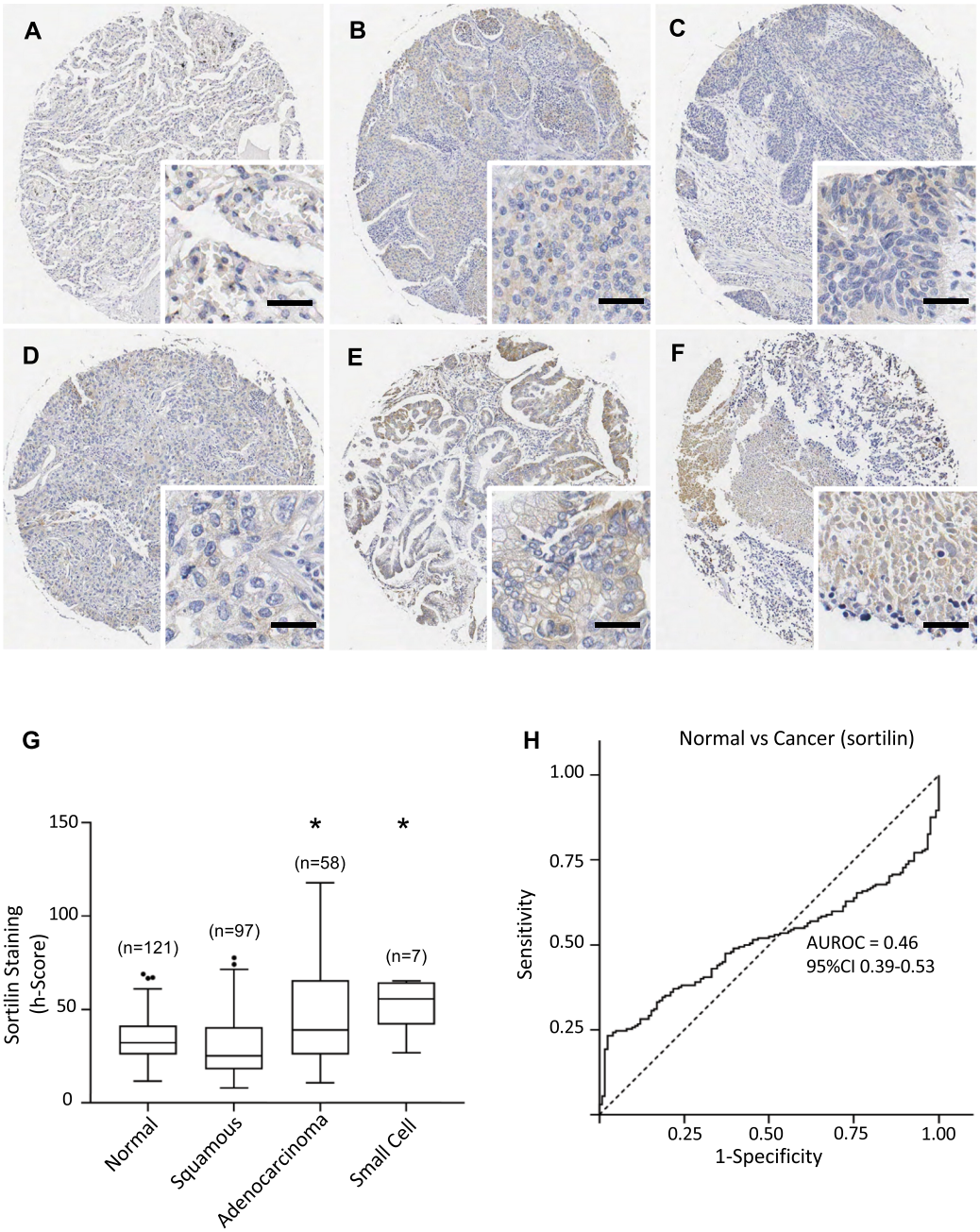

Figure 5. Sortilin expression in lung cancers and normal lung tissues. (**A**–**F**) Immunohistochemical detection of sortilin, representative pictures are shown for normal tissue (**A**), squamous cell carcinoma (**B**–**D**), adenocarcinoma (**E**) and small cell cancer (**F**). Scale = 50 μm. (**G**) Sortilin staining intensities were significantly higher in adenocarcinoma and small cell cancer. Corresponding median h-scores are presented in Table 1. The box limits indicate the interquartile range (IQR) with the whiskers extending 1.5 times the IQR from the 25th and 75th percentiles (outliers are represented by dots) (*$p < 0.0001$ in multiple logistic regression model). (**H**) ROC curve for sortilin staining intensity level in lung cancers versus normal tissues. The area under the curve was 0.46 (95%CI 0.39 to 0.53).

Statistical analysis. H-scores for NGF, proNGF, sortilin, TrkA and p75^{NTR} were analysed as continuous variables. Major lung cancer subtypes (164 cases of adenocarcinoma, squamous cell carcinoma, small cell cancer) were analysed and are presented in Table 1 and Figures, with other minor subtypes excluded from analysis (n = 43). For demographic (age and sex) and disease-specific (histopathology classes of benign, squamous, small cell and adenocarcinoma; tumour size, grade, stage; and nodal status) outcomes of interest, group level medians and interquartile ranges were compared with the Wilcoxon RankSum test, employing a Bonferroni correction for multiple pairwise comparisons (alpha at the family-wise 0.05 level = 0.05/8). All multiple-comparisons used the Kruskal-Wallis test due to unequal variances, with an adjusted multiple-comparison alpha threshold. Analyses were based on complete cases.

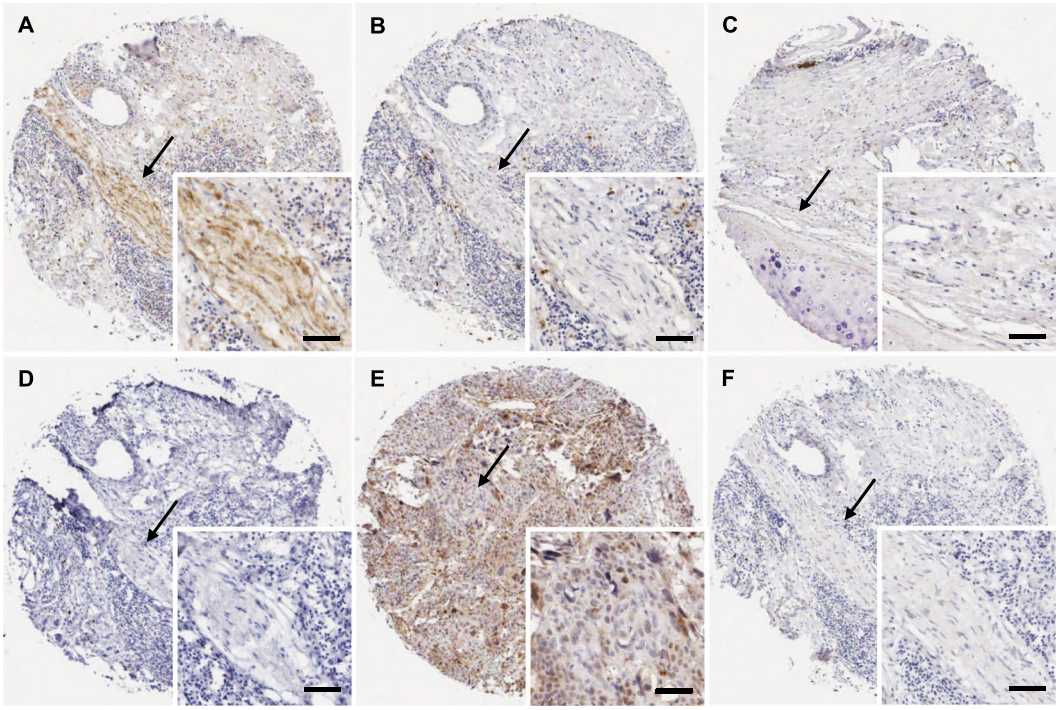

Figure 6. Nerves in the tumor microenvironment of lung cancer do not express NGF, proNGF, TrkA, $p75^{NTR}$ and sortilin. (**A**) Immunohistochemical detection of the pan-neuronal marker PGP9.5 was used to detect nerves in lung cancers. The expression of NGF (**B**), proNGF (**C**), TrkA (**D**), $p75^{NTR}$ (**E**) and sortilin (**F**) was not detected in serial sections. Black arrows indicate a nerve trunk composed of many axons. Scale = 25 μm.

We explored the association between the subtypes of pathology and neurotrophin h-score by fitting multiple logistic regression models to subsets of the data. We considered each of squamous cell carcinoma, adenocarcinoma and small cell cancer separately, dichotomised against the benign tissue group. All models adjusted for age and gender.

The discriminative value of each neurotrophin or receptor H-score as a biomarker of lung malignancy was assessed with receiver-operating characteristic (ROC) curves, where a value of 0.5 indicates no difference, and a value of 1 signifies perfect discrimination. All analyses were performed using Stata (version 14.1, Statacorp, Texas USA). Additional graphics were created using GraphPad Prism 7 (California, USA).

References

1. Herbst, R. S., Heymach, J. V. & Lippman, S. M. Lung cancer. *N Engl J Med* **359**, 1367–1380, https://doi.org/10.1056/NEJMra0802714 (2008).
2. Bradshaw, R. A. *et al.* NGF and ProNGF: Regulation of neuronal and neoplastic responses through receptor signaling. *Adv Biol Regul* **58**, 16–27, https://doi.org/10.1016/j.jbior.2014.11.003 (2015).
3. Hondermarck, H. Neurotrophins and their receptors in breast cancer. *Cytokine Growth Factor Rev* **23**, 357–365, https://doi.org/10.1016/j.cytogfr.2012.06.004 (2012).
4. Hayakawa, Y. *et al.* Nerve Growth Factor Promotes Gastric Tumorigenesis through Aberrant Cholinergic Signaling. *Cancer Cell* **31**, 21–34, https://doi.org/10.1016/j.ccell.2016.11.005 (2017).
5. Lei, Y. *et al.* Gold nanoclusters-assisted delivery of NGF siRNA for effective treatment of pancreatic cancer. *Nat Commun* **8**, 15130, https://doi.org/10.1038/ncomms15130 (2017).
6. Vaishnavi, A. *et al.* Oncogenic and drug-sensitive NTRK1 rearrangements in lung cancer. *Nat Med* **19**, 1469–1472, https://doi.org/10.1038/nm.3352 (2013).
7. Vaishnavi, A., Le, A. T. & Doebele, R. C. TRKing down an old oncogene in a new era of targeted therapy. *Cancer Discov* **5**, 25–34, https://doi.org/10.1158/2159-8290.CD-14-0765 (2015).
8. Wang, X. L., Yao, Y. C. & Yang, M. S. Z. Expression of nerve growth factor and tyrosine kinase A in non-small cell lung cancer. *Int J Clin Exp Patho* **9**, 2153–2158 (2016).
9. Ricci, A. *et al.* Neurotrophins and neurotrophin receptors in human lung cancer. *Am J Respir Cell Mol Biol* **25**, 439–446, https://doi.org/10.1165/ajrcmb.25.4.4470 (2001).
10. Missale, C. *et al.* Nerve growth factor abrogates the tumorigenicity of human small cell lung cancer cell lines. *Proc Natl Acad Sci USA* **95**, 5366–5371 (1998).
11. Dinh, Q. T. *et al.* Substance P expression in TRPV1 and trkA-positive dorsal root ganglion neurons innervating the mouse lung. *Respir Physiol Neurobiol* **144**, 15–24, https://doi.org/10.1016/j.resp.2004.08.001 (2004).
12. Cancer Genome Atlas, N. Comprehensive molecular portraits of human breast tumours. *Nature* **490**, 61–70, https://doi.org/10.1038/nature11412 (2012).
13. Cerami, E. *et al.* The cBio cancer genomics portal: an open platform for exploring multidimensional cancer genomics data. *Cancer Discov* **2**, 401–404, https://doi.org/10.1158/2159-8290.CD-12-0095 (2012).
14. Gygi, S. P., Rochon, Y., Franza, B. R. & Aebersold, R. Correlation between protein and mRNA abundance in yeast. *Mol Cell Biol* **19**, 1720–1730 (1999).

15. Vogel, C. & Marcotte, E. M. Insights into the regulation of protein abundance from proteomic and transcriptomic analyses. *Nat Rev Genet* **13**, 227–232, https://doi.org/10.1038/nrg3185 (2012).
16. Zhang, B. *et al*. Proteogenomic characterization of human colon and rectal cancer. *Nature* **513**, 382–387, https://doi.org/10.1038/nature13438 (2014).
17. Adriaenssens, E. *et al*. Nerve growth factor is a potential therapeutic target in breast cancer. *Cancer Res* **68**, 346–351, https://doi.org/10.1158/0008-5472.CAN-07-1183 (2008).
18. Demont, Y. *et al*. Pro-nerve growth factor induces autocrine stimulation of breast cancer cell invasion through tropomyosin-related kinase A (TrkA) and sortilin protein. *J Biol Chem* **287**, 1923–1931, https://doi.org/10.1074/jbc.M110.211714 (2012).
19. Chang, D. S., Hsu, E., Hottinger, D. G. & Cohen, S. P. Anti-nerve growth factor in pain management: current evidence. *J Pain Res* **9**, 373–383, https://doi.org/10.2147/JPR.S89061 (2016).
20. Fahnestock, M., Michalski, B., Xu, B. & Coughlin, M. D. The precursor pro-nerve growth factor is the predominant form of nerve growth factor in brain and is increased in Alzheimer's disease. *Mol Cell Neurosci* **18**, 210–220, https://doi.org/10.1006/mcne.2001.1016 (2001).
21. Roselli, S. *et al*. Sortilin is associated with breast cancer aggressiveness and contributes to tumor cell adhesion and invasion. *Oncotarget* **6**, 10473–10486, https://doi.org/10.18632/oncotarget.3401 (2015).
22. Wilson, C. M. *et al*. Sortilin mediates the release and transfer of exosomes in concert with two tyrosine kinase receptors. *J Cell Sci* **127**, 3983–3997, https://doi.org/10.1242/jcs.149336 (2014).
23. Chopin, V., Lagadec, C., Toillon, R. A. & Le Bourhis, X. Neurotrophin signaling in cancer stem cells. *Cell Mol Life Sci* **73**, 1859–1870, https://doi.org/10.1007/s00018-016-2156-7 (2016).
24. Jin, H. *et al*. p75 neurotrophin receptor suppresses the proliferation of human gastric cancer cells. *Neoplasia* **9**, 471–478 (2007).
25. Krygier, S. & Djakiew, D. Neurotrophin receptorp75(NTR) suppresses growth and nerve growth factor-mediated metastasis of human prostate cancer cells. *Int J Cancer* **98**, 1–7 (2002).
26. Khwaja, F., Tabassum, A., Allen, J. & Djakiew, D. Thep75(NTR) tumor suppressor induces cell cycle arrest facilitating caspase mediated apoptosis in prostate tumor cells. *Biochem Biophys Res Commun* **341**, 1184–1192, https://doi.org/10.1016/j.bbrc.2006.01.073 (2006).
27. Zhou, X. *et al*. Nerve growth factor receptor negates the tumor suppressor p53 as a feedback regulator. *Elife* **5**, https://doi.org/10.7554/eLife.15099 (2016).
28. Boilly, B., Faulkner, S., Jobling, P. & Hondermarck, H. Nerve Dependence: From Regeneration to Cancer. *Cancer Cell* **31**, 342–354, https://doi.org/10.1016/j.ccell.2017.02.005 (2017).
29. Jobling, P. *et al*. Nerve-Cancer Cell Cross-talk: A Novel Promoter of Tumor Progression. *Cancer Res* **75**, 1777–1781, https://doi.org/10.1158/0008-5472.CAN-14-3180 (2015).
30. Magnon, C. *et al*. Autonomic nerve development contributes to prostate cancer progression. *Science* **341**, 1236361, https://doi.org/10.1126/science.1236361 (2013).
31. Pundavela, J. *et al*. ProNGF correlates with Gleason score and is a potential driver of nerve infiltration in prostate cancer. *Am J Pathol* **184**, 3156–3162, https://doi.org/10.1016/j.ajpath.2014.08.009 (2014).
32. Shao, J. X. *et al*. Autonomic nervous infiltration positively correlates with pathological risk grading and poor prognosis in patients with lung adenocarcinoma. *Thorac Cancer* **7**, 588–598, https://doi.org/10.1111/1759-7714.12374 (2016).
33. Lagadec, C. *et al*. TrkA overexpression enhances growth and metastasis of breast cancer cells. *Oncogene* **28**, 1960–1970, https://doi.org/10.1038/onc.2009.61 (2009).
34. Faulkner, S. *et al*. ProNGF is a potential diagnostic biomarker for thyroid cancer. *Oncotarget* **7**, 28488–28497, https://doi.org/10.18632/oncotarget.8652 (2016).
35. Faulkner, S. *et al*. Neurotrophin Receptors TrkA, p75(NTR), and Sortilin Are Increased and Targetable in Thyroid Cancer. *Am J Pathol* **188**, 229–241, https://doi.org/10.1016/j.ajpath.2017.09.008 (2018).
36. Perez-Pinera, P. *et al*. The Trk tyrosine kinase inhibitor K252a regulates growth of lung adenocarcinomas. *Mol Cell Biochem* **295**, 19–26, https://doi.org/10.1007/s11010-006-9267-7 (2007).

Acknowledgements

The authors acknowledge the assistance of the Hunter Cancer Biobank in the execution of this project and Dr Mark Jones (Clinical Research Design and Statistics Unit, Hunter Medical Research Institute) for statistical advice. This research was supported by the University of Newcastle, the Hunter Cancer Research Alliance (HCRA) and the Maitland Cancer Appeal Committee. This work is also supported by China Scholarship Council support to Fangfang Gao.

Author Contributions

M.M.W., P.J., R.F.T. and H.H. designed the study; F.G., N.G., S.F., L.W., S.R., A.F., C.W.R. carried out and analysed the experiments; H.H. wrote the manuscript. All co-authors have edited the manuscript and approved the final version.

Additional Information

Supplementary information accompanies this paper at https://doi.org/10.1038/s41598-018-26408-2.

Competing Interests: The authors declare no competing interests.

Publisher's note: Springer Nature remains neutral with regard to jurisdictional claims in published maps and institutional affiliations.

The neurotrophic tyrosine kinase receptor TrkA and its ligand NGF are increased in squamous cell carcinomas of the lung.

Fangfang Gao[1,2], Nathan Griffin[1,2], Sam Faulkner[1,2], Christopher W. Rowe[2,3], Lily Williams[1], Severine Roselli[1,2], Rick F. Thorne[2], Aysha Ferdoushi[1,2], Phillip Jobling[1,2], Marjorie M. Walker[2,3], Hubert Hondermarck[1,2,*]

[1]School of Biomedical Sciences & Pharmacy, Faculty of Health and Medicine, University of Newcastle, Callaghan NSW 2308, Australia.
[2]Hunter Medical Research Institute, University of Newcastle, New Lambton NSW 2305, Australia.
[3]School of Public Health & Medicine, Faculty of Health and Medicine, University of Newcastle, Callaghan NSW 2308, Australia.

Corresponding author: Hubert Hondermarck, School of Biomedical Sciences & Pharmacy, Life Sciences Building (LS3-35), University of Newcastle, Callaghan NSW 2308, Australia. Tel: +61 2492 18830. Email: hubert.hondermarck@newcastle.edu.au

Supplementary Figure 1: Negative controls for immunohistochemistry. A. Rabbit isotype control antibody was used in immunohistochemistry for NGF (ab52918, 1:200), TrkA (cs2508, 1:200), $p75^{NTR}$ (cs4201, 1:400) and sortilin (ANT009,1:500). B. Mouse isotype control antibody was used in immunohistochemistry for proNGF (6E10E7, 2.5µg/ml). Scale=25µm

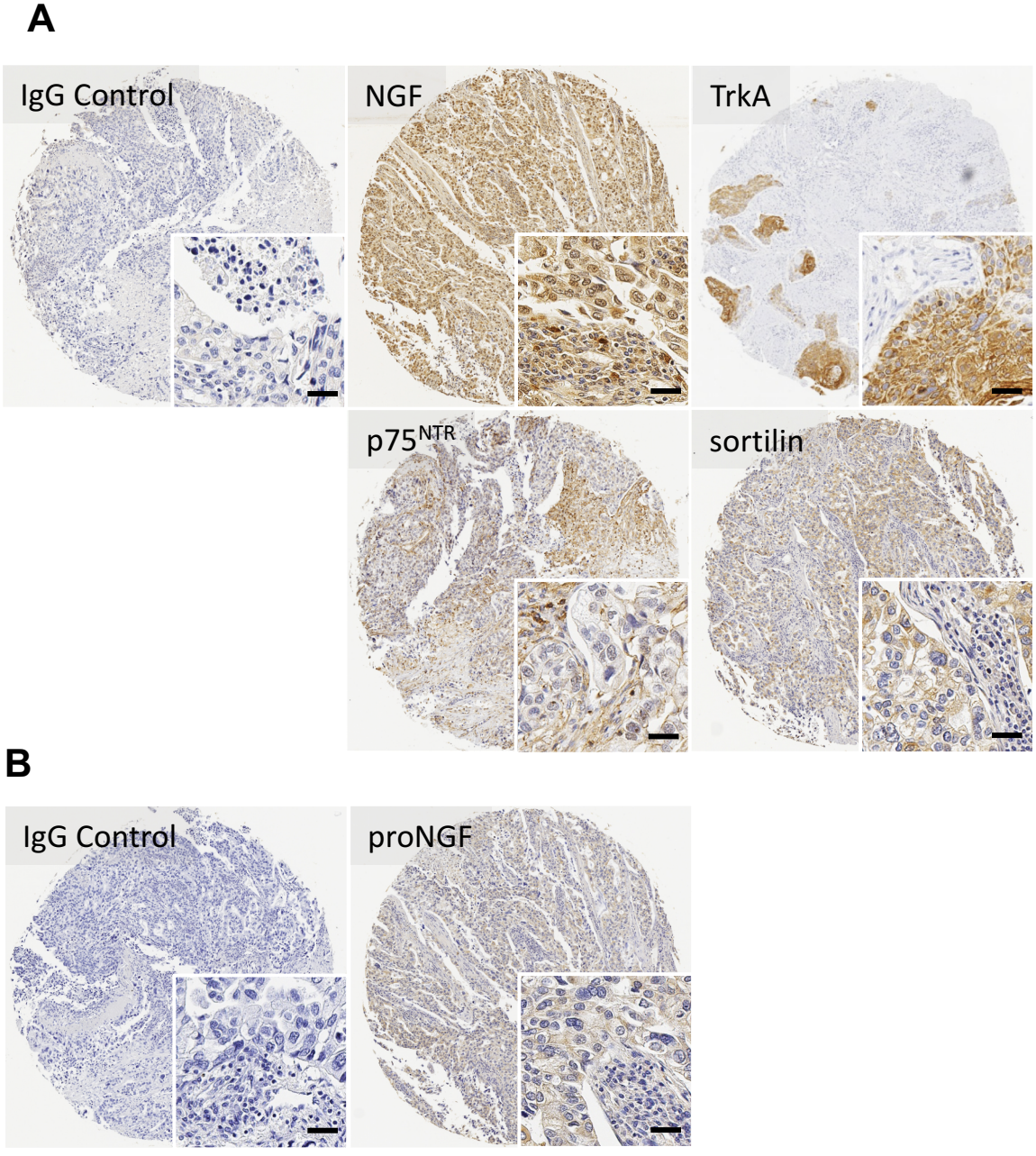

Supplementary Figure 1: Negative controls for immunohistochemistry. A. Rabbit isotype control antibody was used in immunohistochemistry for NGF (ab52918, 1:200), TrkA (cs2508, 1:200), $p75^{NTR}$ (cs4201, 1:400) and sortilin (ANT009,1:500). B. Mouse isotype control antibody was used in immunohistochemistry for proNGF (6E10E7, 2.5µg/ml). Scale=25µm

A.2 Co-authorship declaration

By signing below I confirm that **Aysha Ferdoushi** significantly contributed experimentally and intellectually to the publications entitled "**Proteomic Profile of Human Schwann Cells**", "**Schwann Cell Stimulation of Pancreatic Cancer Cells: A Proteomic Analysis**", "**Tumor innervation is associated with poor clinical outcomes in pancreatic cancer**" and "**The neurotrophic tyrosine kinase receptor TrkA and its ligand NGF are increased in squamous cell carcinomas of the lung**" and endorse its inclusion as part of this thesis.

Signature		Date:	10/09/2020
	Xiang Li		
Signature		Date:	14/09/2020
	Fangfang Gao		
Signature		Date:	10/09/2020
	Nathan Griffin		
Signature		Date:	10/09/2020
	Mark Marsland		
Signature		Date:	10/09/2020
	Hui Liu		
Signature		Date:	10/09/2020
	Xiaoyue Xu		
Signature		Date:	9/09/2020
	M. Fairuz B. Jamaluddin		
Signature		Date:	10/09/2020
	Sam Faulkner		
Signature		Date:	10/09/2020
	Chen Chen Jiang		
Signature		Date:	10/09/2020
	Simon J. King		
Signature		Date:	14/09/2020
	James W Denham		

Signature		Date:	10/09/2020
	Pradeep S. Tanwar		
Signature		Date:	9/09/2020
	Dirk F. van Helden		
Signature		Date:	9/09/2020
	Phillip Jobling		
Signature		Date:	10/09/2020
	Hubert Hondermarck		

Associate Professor Lesley MacDonald-Wicks

(Assistant Dean Research Training)

Faculty of Health and Medicine

Signature: Date:10/09/2020

Bibliography

Abbott, D.E., Tzeng, C.-W.D., Merkow, R.P., Cantor, S.B., Chang, G.J., Katz, M.H., Bentrem, D.J., Bilimoria, K.Y., Crane, C.H., Varadhachary, G.R., Abbruzzese, J.L., Wolff, R.A., Lee, J.E., Evans, D.B., and Fleming, J.B. (2013). The cost-effectiveness of neoadjuvant chemoradiation is superior to a surgery-first approach in the treatment of pancreatic head adenocarcinoma. *Annals of surgical oncology* 20 Suppl 3**,** S500-508.

Abdo, H., Calvo-Enrique, L., Lopez, J.M., Song, J., Zhang, M.D., Usoskin, D., El Manira, A., Adameyko, I., Hjerling-Leffler, J., and Ernfors, P. (2019). Specialized cutaneous Schwann cells initiate pain sensation. *Science* 365**,** 695-699.

Adameyko, I., Lallemend, F., Aquino, J.B., Pereira, J., Topilko, P., Müller, T., Fritz, N., Beljajeva, A., Mochii, M., Liste, I., Usoskin, D., Suter, U., Birchmeier, C., and Ernfors, P. (2009). Schwann Cell Precursors from Nerve Innervation Are a Cellular Origin of Melanocytes in Skin. *Cell* 139**,** 366-379.

Agarwal, B., Correa, A.M., and Ho, L. (2008). Survival in Pancreatic Carcinoma Based on Tumor Size. *Pancreas* 36.

Albo, D., Akay, C.L., Marshall, C.L., Wilks, J.A., Verstovsek, G., Liu, H., Agarwal, N., Berger, D.H., and Ayala, G.E. (2011). Neurogenesis in colorectal cancer is a marker of aggressive tumor behavior and poor outcomes. *Cancer* 117**,** 4834-4845.

Aliaghaei, A., Gardaneh, M., Maghsoudi, N., Salehinejad, P., and Gharib, E. (2016). Dopaminergic Induction of Umbilical Cord Mesenchymal Stem Cells by Conditioned Medium of Choroid Plexus Epithelial Cells Reduces Apomorphine-Induced Rotation in Parkinsonian Rats. *Arch Iran Med* 19**,** 561-570.

Allen, N.J. (2014). Astrocyte regulation of synaptic behavior. *Annu Rev Cell Dev Biol* 30**,** 439-463.

Ambros, I.M., Zellner, A., Roald, B., Amann, G., Ladenstein, R., Printz, D., Gadner, H., and Ambros, P.F. (1996). Role of ploidy, chromosome 1p, and Schwann cells in the maturation of neuroblastoma. *N Engl J Med* 334**,** 1505-1511.

Andersen, N.D., Srinivas, S., Pinero, G., and Monje, P.V. (2016). A rapid and versatile method for the isolation, purification and cryogenic storage of Schwann cells from adult rodent nerves. *Sci Rep* 6**,** 31781.

Anderson, K.D., Guest, J.D., Dietrich, W.D., Bartlett Bunge, M., Curiel, R., Dididze, M., Green, B.A., Khan, A., Pearse, D.D., Saraf-Lavi, E., Widerstrom-Noga, E., Wood, P., and Levi, A.D. (2017). Safety of Autologous Human Schwann Cell Transplantation in Subacute Thoracic Spinal Cord Injury. *J Neurotrauma* 34**,** 2950-2963.

Anderson, N.S., Turner, L., Livingston, S., Chen, R., Nicosia, S.V., and Kruk, P.A. (2009). Bcl-2 expression is altered with ovarian tumor progression: an immunohistochemical evaluation. *Journal of Ovarian Research* 2**,** 16.

Arora, S., Bhardwaj, A., Singh, S., Srivastava, S.K., Mcclellan, S., Nirodi, C.S., Piazza, G.A., Grizzle, W.E., Owen, L.B., and Singh, A.P. (2013). An undesired effect of chemotherapy: gemcitabine promotes pancreatic cancer cell invasiveness through reactive oxygen species-dependent, nuclear factor κB- and hypoxia-inducible factor 1α-mediated up-regulation of CXCR4. *J Biol Chem* 288**,** 21197-21207.

Arslan, A.A., Helzlsouer, K.J., Kooperberg, C., Shu, X.O., Steplowski, E., Bueno-De-Mesquita, H.B., Fuchs, C.S., Gross, M.D., Jacobs, E.J., Lacroix, A.Z., Petersen, G.M., Stolzenberg-Solomon, R.Z., Zheng, W., Albanes, D., Amundadottir, L., Bamlet, W.R., Barricarte, A., Bingham, S.A., Boeing, H., Boutron-Ruault, M.C., Buring, J.E., Chanock, S.J., Clipp, S., Gaziano, J.M., Giovannucci, E.L., Hankinson, S.E., Hartge, P., Hoover, R.N., Hunter, D.J., Hutchinson, A., Jacobs, K.B., Kraft, P., Lynch, S.M., Manjer, J., Manson, J.E., Mctiernan, A., Mcwilliams, R.R., Mendelsohn, J.B., Michaud, D.S., Palli, D., Rohan, T.E., Slimani, N., Thomas, G., Tjonneland, A., Tobias, G.S., Trichopoulos, D., Virtamo, J., Wolpin, B.M., Yu, K., Zeleniuch-Jacquotte, A., and Patel, A.V. (2010). Anthropometric measures, body mass index, and pancreatic cancer: a pooled analysis from the Pancreatic Cancer Cohort Consortium (PanScan). *Arch Intern Med* 170**,** 791-802.

Arthur-Farraj, P.J., Latouche, M., Wilton, D.K., Quintes, S., Chabrol, E., Banerjee, A., Woodhoo, A., Jenkins, B., Rahman, M., Turmaine, M., Wicher, G.K., Mitter, R., Greensmith, L., Behrens, A., Raivich, G., Mirsky, R., and Jessen, K.R. (2012). c-Jun reprograms Schwann cells of injured nerves to generate a repair cell essential for regeneration. *Neuron* 75**,** 633-647.

Asa, S.L. (2011). Pancreatic endocrine tumors. *Mod Pathol* 24 Suppl 2**,** S66-77.

Austin, M., Elliott, L., Nicolaou, N., Grabowska, A., and Hulse, R.P. (2017). Breast cancer induced nociceptor aberrant growth and collateral sensory axonal branching. *Oncotarget* 8**,** 76606-76621.

Ayala, G.E., Dai, H., Powell, M., Li, R., Ding, Y., Wheeler, T.M., Shine, D., Kadmon, D., Thompson, T., Miles, B.J., Ittmann, M.M., and Rowley, D. (2008). Cancer-Related Axonogenesis and Neurogenesis in Prostate Cancer. *Clinical Cancer Research* 14**,** 7593.

Azam, S.H., and Pecot, C.V. (2016). Cancer's got nerve: Schwann cells drive perineural invasion. *J Clin Invest* 126**,** 1242-1244.

Bailey, P., Chang, D.K., Nones, K., Johns, A.L., Patch, A.M., Gingras, M.C., Miller, D.K., Christ, A.N., Bruxner, T.J., Quinn, M.C., Nourse, C., Murtaugh, L.C., Harliwong, I., Idrisoglu, S., Manning, S., Nourbakhsh, E., Wani, S., Fink, L., Holmes, O., Chin, V., Anderson, M.J., Kazakoff, S., Leonard, C., Newell, F., Waddell, N., Wood, S., Xu, Q., Wilson, P.J., Cloonan, N., Kassahn, K.S., Taylor, D., Quek, K., Robertson, A., Pantano, L., Mincarelli, L., Sanchez, L.N., Evers, L., Wu, J., Pinese, M., Cowley, M.J., Jones, M.D., Colvin, E.K., Nagrial, A.M., Humphrey, E.S., Chantrill, L.A., Mawson, A., Humphris, J., Chou, A., Pajic, M., Scarlett, C.J., Pinho, A.V., Giry-Laterriere, M., Rooman, I., Samra, J.S., Kench, J.G., Lovell, J.A., Merrett, N.D., Toon, C.W., Epari, K., Nguyen, N.Q., Barbour, A., Zeps, N., Moran-Jones, K., Jamieson, N.B., Graham, J.S., Duthie, F., Oien, K., Hair, J., Grutzmann, R., Maitra, A., Iacobuzio-Donahue, C.A., Wolfgang, C.L., Morgan, R.A., Lawlor, R.T., Corbo, V., Bassi, C., Rusev, B., Capelli, P., Salvia, R., Tortora, G., Mukhopadhyay, D., Petersen, G.M., Munzy, D.M., Fisher, W.E., Karim, S.A., Eshleman, J.R., Hruban, R.H., Pilarsky, C., Morton, J.P., Sansom, O.J., Scarpa, A., Musgrove, E.A., Bailey, U.M., Hofmann, O., Sutherland, R.L., Wheeler, D.A., Gill, A.J., Gibbs, R.A., Pearson, J.V., Waddell, N., et al. (2016). Genomic analyses identify molecular subtypes of pancreatic cancer. *Nature* 531**,** 47-52.

Bakst, R.L., Xiong, H., Chen, C.H., Deborde, S., Lyubchik, A., Zhou, Y., He, S., Mcnamara, W., Lee, S.Y., Olson, O.C., Leiner, I.M., Marcadis, A.R., Keith, J.W., Al-Ahmadie, H.A., Katabi, N., Gil, Z., Vakiani, E., Joyce, J.A., Pamer, E.,

and Wong, R.J. (2017). Inflammatory Monocytes Promote Perineural Invasion via CCL2-Mediated Recruitment and Cathepsin B Expression. *Cancer Res* 77**,** 6400-6414.
Banerjee, K., Kumar, S., Ross, K.A., Gautam, S., Poelaert, B., Nasser, M.W., Aithal, A., Bhatia, R., Wannemuehler, M.J., Narasimhan, B., Solheim, J.C., Batra, S.K., and Jain, M. (2018). Emerging trends in the immunotherapy of pancreatic cancer. *Cancer letters* 417**,** 35-46.
Bapat, A.A., Hostetter, G., Von Hoff, D.D., and Han, H. (2011). Perineural invasion and associated pain in pancreatic cancer. *Nat Rev Cancer* 11**,** 695-707.
Bapat, A.A., Munoz, R.M., Von Hoff, D.D., and Han, H. (2016). Blocking Nerve Growth Factor Signaling Reduces the Neural Invasion Potential of Pancreatic Cancer Cells. *PLoS One* 11**,** e0165586.
Batabyal, P., Vander Hoorn, S., Christophi, C., and Nikfarjam, M. (2014). Association of diabetes mellitus and pancreatic adenocarcinoma: a meta-analysis of 88 studies. *Ann Surg Oncol* 21**,** 2453-2462.
Bentley, C.A., and Lee, K.F. (2000). p75 is important for axon growth and schwann cell migration during development. *J Neurosci* 20**,** 7706-7715.
Bilimoria, K.Y., Bentrem, D.J., Ko, C.Y., Stewart, A.K., Winchester, D.P., and Talamonti, M.S. (2007). National failure to operate on early stage pancreatic cancer. *Ann Surg* 246**,** 173-180.
Bishop, D.L., Misgeld, T., Walsh, M.K., Gan, W.B., and Lichtman, J.W. (2004). Axon branch removal at developing synapses by axosome shedding. *Neuron* 44**,** 651-661.
Bockman, D.E., Buchler, M., and Beger, H.G. (1994). Interaction of pancreatic ductal carcinoma with nerves leads to nerve damage. *Gastroenterology* 107**,** 219-230.
Boilly, B., Faulkner, S., Jobling, P., and Hondermarck, H. (2017). Nerve Dependence: From Regeneration to Cancer. *Cancer Cell* 31**,** 342-354.
Bose, N., and Masellis, A.M. (2005). Secretory products of breast cancer cells upregulate hyaluronan production in a human osteoblast cell line. *Clin Exp Metastasis* 22**,** 629-642.
Bosetti, C., Lucenteforte, E., Silverman, D.T., Petersen, G., Bracci, P.M., Ji, B.T., Negri, E., Li, D., Risch, H.A., Olson, S.H., Gallinger, S., Miller, A.B., Bueno-De-Mesquita, H.B., Talamini, R., Polesel, J., Ghadirian, P., Baghurst, P.A., Zatonski, W., Fontham, E., Bamlet, W.R., Holly, E.A., Bertuccio, P., Gao, Y.T., Hassan, M., Yu, H., Kurtz, R.C., Cotterchio, M., Su, J., Maisonneuve, P., Duell, E.J., Boffetta, P., and La Vecchia, C. (2012). Cigarette smoking and pancreatic cancer: an analysis from the International Pancreatic Cancer Case-Control Consortium (Panc4). *Ann Oncol* 23**,** 1880-1888.
Bove, G.M. (2008). Epi-perineurial anatomy, innervation, and axonal nociceptive mechanisms. *Journal of bodywork and movement therapies* 12**,** 185-190.
Bramhall, S.R., Schulz, J., Nemunaitis, J., Brown, P.D., Baillet, M., and Buckels, J.A. (2002). A double-blind placebo-controlled, randomised study comparing gemcitabine and marimastat with gemcitabine and placebo as first line therapy in patients with advanced pancreatic cancer. *Br J Cancer* 87**,** 161-167.
Bray, F., Ferlay, J., Soerjomataram, I., Siegel, R.L., Torre, L.A., and Jemal, A. (2018). Global cancer statistics 2018: GLOBOCAN estimates of incidence and mortality worldwide for 36 cancers in 185 countries. *CA Cancer J Clin* 68**,** 394-424.

Brennan, M.F., Kattan, M.W., Klimstra, D., and Conlon, K. (2004). Prognostic nomogram for patients undergoing resection for adenocarcinoma of the pancreas. *Annals of surgery* 240**,** 293-298.

Bressy, C., Lac, S., Nigri, J., Leca, J., Roques, J., Lavaut, M.N., Secq, V., Guillaumond, F., Bui, T.T., Pietrasz, D., Granjeaud, S., Bachet, J.B., Ouaissi, M., Iovanna, J., Vasseur, S., and Tomasini, R. (2018). LIF Drives Neural Remodeling in Pancreatic Cancer and Offers a New Candidate Biomarker. *Cancer Res* 78**,** 909-921.

Bronner, M.E., and Ledouarin, N.M. (2012). Development and evolution of the neural crest: An overview. *Developmental Biology* 366**,** 2-9.

Bründl, J., Schneider, S., Weber, F., Zeman, F., Wieland, W.F., and Ganzer, R. (2014). Computerized quantification and planimetry of prostatic capsular nerves in relation to adjacent prostate cancer foci. *Eur Urol* 65**,** 802-808.

Bunimovich, Y., Keskinov, A., Shurin, G., and Shurin, M. (2016). Schwann cells: a new player in the tumor microenvironment. *Cancer Immunology, Immunotherapy* 66.

Bynigeri, R.R., Jakkampudi, A., Jangala, R., Subramanyam, C., Sasikala, M., Rao, G.V., Reddy, D.N., and Talukdar, R. (2017). Pancreatic stellate cell: Pandora's box for pancreatic disease biology. *World J Gastroenterol* 23**,** 382-405.

Ceyhan, G.O., Bergmann, F., Kadihasanoglu, M., Altintas, B., Demir, I.E., Hinz, U., Muller, M.W., Giese, T., Buchler, M.W., Giese, N.A., and Friess, H. (2009a). Pancreatic neuropathy and neuropathic pain--a comprehensive pathomorphological study of 546 cases. *Gastroenterology* 136**,** 177-186.e171.

Ceyhan, G.O., Demir, I.E., Altintas, B., Rauch, U., Thiel, G., Müller, M.W., Giese, N.A., Friess, H., and Schäfer, K.H. (2008). Neural invasion in pancreatic cancer: a mutual tropism between neurons and cancer cells. *Biochem Biophys Res Commun* 374**,** 442-447.

Ceyhan, G.O., Demir, I.E., Rauch, U., Bergmann, F., Muller, M.W., Buchler, M.W., Friess, H., and Schafer, K.H. (2009b). Pancreatic neuropathy results in "neural remodeling" and altered pancreatic innervation in chronic pancreatitis and pancreatic cancer. *Am J Gastroenterol* 104**,** 2555-2565.

Ceyhan, G.O., Giese, N.A., Erkan, M., Kerscher, A.G., Wente, M.N., Giese, T., Buchler, M.W., and Friess, H. (2006). The neurotrophic factor artemin promotes pancreatic cancer invasion. *Ann Surg* 244**,** 274-281.

Ceyhan, G.O., Schafer, K.H., Kerscher, A.G., Rauch, U., Demir, I.E., Kadihasanoglu, M., Bohm, C., Muller, M.W., Buchler, M.W., Giese, N.A., Erkan, M., and Friess, H. (2010). Nerve growth factor and artemin are paracrine mediators of pancreatic neuropathy in pancreatic adenocarcinoma. *Ann Surg* 251**,** 923-931.

Cha, J.M., Shin, E.K., Sung, J.H., Moon, G.J., Kim, E.H., Cho, Y.H., Dal Park, H., Bae, H., Kim, J., and Bang, O.Y. (2018). Efficient scalable production of therapeutic microvesicles derived from human mesenchymal stem cells. *Scientific reports* 8**,** 1-16.

Chandana, S., and Mahadevan, D. (2009). Translational advances and novel therapies for pancreatic ductal adenocarcinoma: hope or hype? *Expert Rev Mol Med* 11**,** e34.

Chang, J.H., Jiang, Y., and Pillarisetty, V.G. (2016). Role of immune cells in pancreatic cancer from bench to clinical application: An updated review. *Medicine (Baltimore)* 95**,** e5541.

Chang, M.Y., Park, C.H., and Lee, S.H. (2003). Embryonic cortical stem cells secrete diffusible factors to enhance their survival. *Neuroreport* 14**,** 1191-1195.
Chatterjee, D., Katz, M.H., Rashid, A., Wang, H., Iuga, A.C., Varadhachary, G.R., Wolff, R.A., Lee, J.E., Pisters, P.W., Crane, C.H., Gomez, H.F., Abbruzzese, J.L., Fleming, J.B., and Wang, H. (2012). Perineural and intraneural invasion in posttherapy pancreaticoduodenectomy specimens predicts poor prognosis in patients with pancreatic ductal adenocarcinoma. *Am J Surg Pathol* 36**,** 409-417.
Chen, G., Jin, Y., Shi, X., Qiu, Y., Zhang, Y., Cheng, M., Wang, X., Chen, C., Wu, Y., and Jiang, F. (2015). Adipose-derived stem cell-based treatment for acute liver failure. *Stem Cell Research & Therapy* 6**,** 1-11.
Chen, L., Xiang, B., Wang, X., and Xiang, C. (2017). Exosomes derived from human menstrual blood-derived stem cells alleviate fulminant hepatic failure. *Stem Cell Research & Therapy* 8**,** 1-15.
Chow, E., Zeng, L., Salvo, N., Dennis, K., Tsao, M., and Lutz, S. (2012). Update on the systematic review of palliative radiotherapy trials for bone metastases. *Clin Oncol (R Coll Radiol)* 24**,** 112-124.
Colomar, A., and Robitaille, R. (2004). Glial modulation of synaptic transmission at the neuromuscular junction. *Glia* 47**,** 284-289.
Conroy, T., Hammel, P., Hebbar, M., Ben Abdelghani, M., Wei, A.C., Raoul, J.L., Choné, L., Francois, E., Artru, P., Biagi, J.J., Lecomte, T., Assenat, E., Faroux, R., Ychou, M., Volet, J., Sauvanet, A., Breysacher, G., Di Fiore, F., Cripps, C., Kavan, P., Texereau, P., Bouhier-Leporrier, K., Khemissa-Akouz, F., Legoux, J.L., Juzyna, B., Gourgou, S., O'callaghan, C.J., Jouffroy-Zeller, C., Rat, P., Malka, D., Castan, F., and Bachet, J.B. (2018). FOLFIRINOX or Gemcitabine as Adjuvant Therapy for Pancreatic Cancer. *N Engl J Med* 379**,** 2395-2406.
Cooper, A.B., Tzeng, C.W., and Katz, M.H. (2013). Treatment of borderline resectable pancreatic cancer. *Curr Treat Options Oncol* 14**,** 293-310.
Creighton, N., Walton, R., Roder, D., Aranda, S., and Currow, D. (2016). Validation of administrative hospital data for identifying incident pancreatic and periampullary cancer cases: a population-based study using linked cancer registry and administrative hospital data in New South Wales, Australia. *BMJ open* 6**,** e011161-e011161.
Da Cunha, B.R., Domingos, C., Stefanini, A.C.B., Henrique, T., Polachini, G.M., Castelo-Branco, P., and Tajara, E.H. (2019). Cellular Interactions in the Tumor Microenvironment: The Role of Secretome. *Journal of Cancer* 10**,** 4574-4587.
Dauer, P., Nomura, A., Saluja, A., and Banerjee, S. (2017). Microenvironment in determining chemo-resistance in pancreatic cancer: Neighborhood matters. *Pancreatology* 17**,** 7-12.
De Logu, F., Nassini, R., Materazzi, S., Carvalho Gonçalves, M., Nosi, D., Rossi Degl'innocenti, D., Marone, I.M., Ferreira, J., Li Puma, S., Benemei, S., Trevisan, G., Souza Monteiro De Araújo, D., Patacchini, R., Bunnett, N.W., and Geppetti, P. (2017). Schwann cell TRPA1 mediates neuroinflammation that sustains macrophage-dependent neuropathic pain in mice. *Nature Communications* 8**,** 1887.
Deborde, S., Omelchenko, T., Lyubchik, A., Zhou, Y., He, S., Mcnamara, W.F., Chernichenko, N., Lee, S.Y., Barajas, F., Chen, C.H., Bakst, R.L., Vakiani, E.,

He, S., Hall, A., and Wong, R.J. (2016). Schwann cells induce cancer cell dispersion and invasion. *J Clin Invest* 126**,** 1538-1554.
Deborde, S., and Wong, R.J. (2017). How Schwann cells facilitate cancer progression in nerves. *Cellular and molecular life sciences : CMLS* 74**,** 4405-4420.
Demir, I.E., Boldis, A., Pfitzinger, P.L., Teller, S., Brunner, E., Klose, N., Kehl, T., Maak, M., Lesina, M., Laschinger, M., Janssen, K.P., Algul, H., Friess, H., and Ceyhan, G.O. (2014). Investigation of Schwann cells at neoplastic cell sites before the onset of cancer invasion. *J Natl Cancer Inst* 106.
Demir, I.E., Ceyhan, G.O., Rauch, U., Altintas, B., Klotz, M., Muller, M.W., Buchler, M.W., Friess, H., and Schafer, K.H. (2010). The microenvironment in chronic pancreatitis and pancreatic cancer induces neuronal plasticity. *Neurogastroenterol Motil* 22**,** 480-490, e112-483.
Demir, I.E., Friess, H., and Ceyhan, G.O. (2015). Neural plasticity in pancreatitis and pancreatic cancer. *Nat Rev Gastroenterol Hepatol* 12**,** 649-659.
Demir, I.E., Tieftrunk, E., Maak, M., Friess, H., and Ceyhan, G.O. (2011). Pain mechanisms in chronic pancreatitis: of a master and his fire. *Langenbecks Arch Surg* 396**,** 151-160.
Demir, I.E., Tieftrunk, E., Schorn, S., Saricaoglu, O.C., Pfitzinger, P.L., Teller, S., Wang, K., Waldbaur, C., Kurkowski, M.U., Wormann, S.M., Shaw, V.E., Kehl, T., Laschinger, M., Costello, E., Algul, H., Friess, H., and Ceyhan, G.O. (2016). Activated Schwann cells in pancreatic cancer are linked to analgesia via suppression of spinal astroglia and microglia. *Gut* 65**,** 1001-1014.
Donoghue, P.C., Graham, A., and Kelsh, R.N. (2008). The origin and evolution of the neural crest. *Bioessays* 30**,** 530-541.
Dowling, P., and Clynes, M. (2011). Conditioned media from cell lines: a complementary model to clinical specimens for the discovery of disease-specific biomarkers. *Proteomics* 11**,** 794-804.
Drilon, A., Laetsch, T.W., Kummar, S., Dubois, S.G., Lassen, U.N., Demetri, G.D., Nathenson, M., Doebele, R.C., Farago, A.F., Pappo, A.S., Turpin, B., Dowlati, A., Brose, M.S., Mascarenhas, L., Federman, N., Berlin, J., El-Deiry, W.S., Baik, C., Deeken, J., Boni, V., Nagasubramanian, R., Taylor, M., Rudzinski, E.R., Meric-Bernstam, F., Sohal, D.P.S., Ma, P.C., Raez, L.E., Hechtman, J.F., Benayed, R., Ladanyi, M., Tuch, B.B., Ebata, K., Cruickshank, S., Ku, N.C., Cox, M.C., Hawkins, D.S., Hong, D.S., and Hyman, D.M. (2018). Efficacy of Larotrectinib in TRK Fusion–Positive Cancers in Adults and Children. *New England Journal of Medicine* 378**,** 731-739.
Drilon, A., Siena, S., Ou, S.-H.I., Patel, M., Ahn, M.J., Lee, J., Bauer, T.M., Farago, A.F., Wheler, J.J., Liu, S.V., Doebele, R., Giannetta, L., Cerea, G., Marrapese, G., Schirru, M., Amatu, A., Bencardino, K., Palmeri, L., Sartore-Bianchi, A., Vanzulli, A., Cresta, S., Damian, S., Duca, M., Ardini, E., Li, G., Christiansen, J., Kowalski, K., Johnson, A.D., Patel, R., Luo, D., Chow-Maneval, E., Hornby, Z., Multani, P.S., Shaw, A.T., and De Braud, F.G. (2017). Safety and Antitumor Activity of the Multitargeted Pan-TRK, ROS1, and ALK Inhibitor Entrectinib: Combined Results from Two Phase I Trials (ALKA-372-001 and STARTRK-1). *Cancer Discovery* 7**,** 400.
Ducreux, M., Cuhna, A.S., Caramella, C., Hollebecque, A., Burtin, P., Goéré, D., Seufferlein, T., Haustermans, K., Van Laethem, J.L., Conroy, T., and Arnold, D. (2015). Cancer of the pancreas: ESMO Clinical Practice Guidelines for diagnosis, treatment and follow-up. *Ann Oncol* 26 Suppl 5**,** v56-68.

Duell, E.J., Lucenteforte, E., Olson, S.H., Bracci, P.M., Li, D., Risch, H.A., Silverman, D.T., Ji, B.T., Gallinger, S., Holly, E.A., Fontham, E.H., Maisonneuve, P., Bueno-De-Mesquita, H.B., Ghadirian, P., Kurtz, R.C., Ludwig, E., Yu, H., Lowenfels, A.B., Seminara, D., Petersen, G.M., La Vecchia, C., and Boffetta, P. (2012). Pancreatitis and pancreatic cancer risk: a pooled analysis in the International Pancreatic Cancer Case-Control Consortium (PanC4). *Ann Oncol* 23**,** 2964-2970.

Duraikannu, A., Krishnan, A., Chandrasekhar, A., and Zochodne, D.W. (2019). Beyond Trophic Factors: Exploiting the Intrinsic Regenerative Properties of Adult Neurons. *Frontiers in Cellular Neuroscience* 13**,** 128.

Elahi-Gedwillo, K.Y., Carlson, M., Zettervall, J., and Provenzano, P.P. (2019). Antifibrotic Therapy Disrupts Stromal Barriers and Modulates the Immune Landscape in Pancreatic Ductal Adenocarcinoma. *Cancer Res* 79**,** 372-386.

Faijerson, J., Tinsley, R.B., Apricó, K., Thorsell, A., Nodin, C., Nilsson, M., Blomstrand, F., and Eriksson, P.S. (2006). Reactive astrogliosis induces astrocytic differentiation of adult neural stem/progenitor cells in vitro. *J Neurosci Res* 84**,** 1415-1424.

Fangmann, L., Teller, S., Stupakov, P., Friess, H., Ceyhan, G.O., and Demir, I.E. (2018). 3D Cancer Migration Assay with Schwann Cells. *Methods Mol Biol* 1739**,** 317-325.

Faulkner, S., Jobling, P., March, B., Jiang, C.C., and Hondermarck, H. (2019). Tumor Neurobiology and the War of Nerves in Cancer. *Cancer discovery* 9**,** 702-710.

Feig, C., Gopinathan, A., Neesse, A., Chan, D.S., Cook, N., and Tuveson, D.A. (2012). The pancreas cancer microenvironment. *Clin Cancer Res* 18**,** 4266-4276.

Feldmann, G., Beaty, R., Hruban, R.H., and Maitra, A. (2007). Molecular genetics of pancreatic intraepithelial neoplasia. *J Hepatobiliary Pancreat Surg* 14**,** 224-232.

Feng, Z., and Ko, C.P. (2008). The role of glial cells in the formation and maintenance of the neuromuscular junction. *Ann N Y Acad Sci* 1132**,** 19-28.

Ferdoushi, A., Li, X., Griffin, N., Faulkner, S., Jamaluddin, M.F.B., Gao, F., Jiang, C.C., Van Helden, D.F., Tanwar, P.S., Jobling, P., and Hondermarck, H. (2020). Schwann Cell Stimulation of Pancreatic Cancer Cells: A Proteomic Analysis. *Frontiers in Oncology* 10**,** 1601.

Fesinmeyer, M.D., Austin, M.A., Li, C.I., De Roos, A.J., and Bowen, D.J. (2005). Differences in survival by histologic type of pancreatic cancer. *Cancer Epidemiol Biomarkers Prev* 14**,** 1766-1773.

Fouraschen, S.M., Pan, Q., De Ruiter, P.E., Farid, W.R., Kazemier, G., Kwekkeboom, J., Ijzermans, J.N., Metselaar, H.J., Tilanus, H.W., and De Jonge, J. (2012). Secreted factors of human liver-derived mesenchymal stem cells promote liver regeneration early after partial hepatectomy. *Stem cells and development* 21**,** 2410-2419.

Franke, A.J., Rosati, L.M., Pawlik, T.M., Kumar, R., and Herman, J.M. (2015). The role of radiation therapy in pancreatic ductal adenocarcinoma in the neoadjuvant and adjuvant settings. *Semin Oncol* 42**,** 144-162.

Friess, H., Shrikhande, S., Shrikhande, M., Martignoni, M., Kulli, C., Zimmermann, A., Kappeler, A., Ramesh, H., and Buchler, M. (2002). Neural alterations in surgical stage chronic pancreatitis are independent of the underlying aetiology. *Gut* 50**,** 682-686.

Fujii-Nishimura, Y., Yamazaki, K., Masugi, Y., Douguchi, J., Kurebayashi, Y., Kubota, N., Ojima, H., Kitago, M., Shinoda, M., Hashiguchi, A., and Sakamoto, M. (2018). Mesenchymal-epithelial transition of pancreatic cancer cells at perineural invasion sites is induced by Schwann cells. *Pathology international* 68**,** 214-223.

Gajewski, T.F., Schreiber, H., and Fu, Y.X. (2013). Innate and adaptive immune cells in the tumor microenvironment. *Nat Immunol* 14**,** 1014-1022.

Gandhi, S., and Bronner, M. (2018). Insights into neural crest development from studies of avian embryos. *The International journal of developmental biology* 62**,** 183-194.

Gandy, R.C., Barbour, A.P., Samra, J., Nikfarjam, M., Haghighi, K., Kench, J.G., Saxena, P., and Goldstein, D. (2016). Refining the care of patients with pancreatic cancer: the AGITG Pancreatic Cancer Workshop consensus. *Med J Aust* 204**,** 419-422.

Garbay, B., Heape, A.M., Sargueil, F., and Cassagne, C. (2000). Myelin synthesis in the peripheral nervous system. *Prog Neurobiol* 61**,** 267-304.

Gasparini, G., Pellegatta, M., Crippa, S., Lena, M.S., Belfiori, G., Doglioni, C., Taveggia, C., and Falconi, M. (2019). Nerves and Pancreatic Cancer: New Insights into a Dangerous Relationship. *Cancers (Basel)* 11.

Gazdic, M., Arsenijevic, A., Markovic, B.S., Volarevic, A., Dimova, I., Djonov, V., Arsenijevic, N., Stojkovic, M., and Volarevic, V. (2017). Mesenchymal stem cell-dependent modulation of liver diseases. *International Journal of Biological Sciences* 13**,** 1109.

Goel, G., and Sun, W. (2015). Novel approaches in the management of pancreatic ductal adenocarcinoma: potential promises for the future. *J Hematol Oncol* 8**,** 44.

Gonçalves, N.P., Vægter, C.B., Andersen, H., Østergaard, L., Calcutt, N.A., and Jensen, T.S. (2017). Schwann cell interactions with axons and microvessels in diabetic neuropathy. *Nat Rev Neurol* 13**,** 135-147.

Gresset, A., Coulpier, F., Gerschenfeld, G., Jourdon, A., Matesic, G., Richard, L., Vallat, J.-M., Charnay, P., and Topilko, P. (2015). Boundary Caps Give Rise to Neurogenic Stem Cells and Terminal Glia in the Skin. *Stem cell reports* 5**,** 278-290.

Griffin, J.W., and Thompson, W.J. (2008). Biology and pathology of nonmyelinating Schwann cells. *Glia* 56**,** 1518-1531.

Guo, K., Ma, Q., Li, J., Wang, Z., Shan, T., Li, W., Xu, Q., and Xie, K. (2013). Interaction of the sympathetic nerve with pancreatic cancer cells promotes perineural invasion through the activation of STAT3 signaling. *Mol Cancer Ther* 12**,** 264-273.

Haley, E.M., and Kim, Y. (2014). The role of basic fibroblast growth factor in glioblastoma multiforme and glioblastoma stem cells and in their in vitro culture. *Cancer Letters* 346**,** 1-5.

Hamada, S., Masamune, A., Yoshida, N., Takikawa, T., and Shimosegawa, T. (2016). IL-6/STAT3 Plays a Regulatory Role in the Interaction Between Pancreatic Stellate Cells and Cancer Cells. *Dig Dis Sci* 61**,** 1561-1571.

Han, X., Li, Y., Xu, Y., Zhao, X., Zhang, Y., Yang, X., Wang, Y., Zhao, R., Anderson, G.J., Zhao, Y., and Nie, G. (2018). Reversal of pancreatic desmoplasia by re-educating stellate cells with a tumour microenvironment-activated nanosystem. *Nature Communications* 9**,** 3390.

Hayakawa, Y., Sakitani, K., Konishi, M., Asfaha, S., Niikura, R., Tomita, H., Renz, B.W., Tailor, Y., Macchini, M., Middelhoff, M., Jiang, Z., Tanaka, T., Dubeykovskaya, Z.A., Kim, W., Chen, X., Urbanska, A.M., Nagar, K., Westphalen, C.B., Quante, M., Lin, C.S., Gershon, M.D., Hara, A., Zhao, C.M., Chen, D., Worthley, D.L., Koike, K., and Wang, T.C. (2017). Nerve Growth Factor Promotes Gastric Tumorigenesis through Aberrant Cholinergic Signaling. *Cancer Cell* 31**,** 21-34.

Heinemann, V., Reni, M., Ychou, M., Richel, D.J., Macarulla, T., and Ducreux, M. (2014). Tumour-stroma interactions in pancreatic ductal adenocarcinoma: rationale and current evidence for new therapeutic strategies. *Cancer Treat Rev* 40**,** 118-128.

Hingorani, S.R., Harris, W.P., Beck, J.T., Berdov, B.A., Wagner, S.A., Pshevlotsky, E.M., Tjulandin, S.A., Gladkov, O.A., Holcombe, R.F., Korn, R., Raghunand, N., Dychter, S., Jiang, P., Shepard, H.M., and Devoe, C.E. (2016). Phase Ib Study of PEGylated Recombinant Human Hyaluronidase and Gemcitabine in Patients with Advanced Pancreatic Cancer. *Clin Cancer Res* 22**,** 2848-2854.

Hirai, I., Kimura, W., Ozawa, K., Kudo, S., Suto, K., Kuzu, H., and Fuse, A. (2002). Perineural invasion in pancreatic cancer. *Pancreas* 24**,** 15-25.

His, W. (1868). *Untersuchungen über die erste Anlage des Wirbelthierleibes : die erste Entwickelung des Hühnchens im Ei.* Leipzig :: F.C.W. Vogel.

Ho, W.J., Jaffee, E.M., and Zheng, L. (2020). The tumour microenvironment in pancreatic cancer — clinical challenges and opportunities. *Nature Reviews Clinical Oncology* 17**,** 527-540.

Hoelzinger, D.B., Demuth, T., and Berens, M.E. (2007). Autocrine factors that sustain glioma invasion and paracrine biology in the brain microenvironment. *J Natl Cancer Inst* 99**,** 1583-1593.

Hogan, S.A., Levesque, M.P., and Cheng, P.F. (2018). Melanoma Immunotherapy: Next-Generation Biomarkers. *Front Oncol* 8**,** 178.

Huang, D., Su, S., Cui, X., Shen, X., Zeng, Y., Wu, W., Chen, J., Chen, F., He, C., Liu, J., Huang, W., Liu, Q., Su, F., Song, E., and Ouyang, N. (2014). Nerve fibers in breast cancer tissues indicate aggressive tumor progression. *Medicine (Baltimore)* 93**,** e172.

Huang, T., Fan, Q., Wang, Y., Cui, Y., Wang, Z., Yang, L., Sun, X., and Wang, Y. (2020). Schwann Cell-Derived CCL2 Promotes the Perineural Invasion of Cervical Cancer. *Frontiers in Oncology* 10**,** 19.

Iwasaki, T., Hiraoka, N., Ino, Y., Nakajima, K., Kishi, Y., Nara, S., Esaki, M., Shimada, K., and Katai, H. (2019). Reduction of intrapancreatic neural density in cancer tissue predicts poorer outcome in pancreatic ductal carcinoma. *Cancer Sci* 110**,** 1491-1502.

Jacob, D., Okon, I., and E Abstract, K. (2013). *Jacob et al., 2013.*

Jacobetz, M.A., Chan, D.S., Neesse, A., Bapiro, T.E., Cook, N., Frese, K.K., Feig, C., Nakagawa, T., Caldwell, M.E., Zecchini, H.I., Lolkema, M.P., Jiang, P., Kultti, A., Thompson, C.B., Maneval, D.C., Jodrell, D.I., Frost, G.I., Shepard, H.M., Skepper, J.N., and Tuveson, D.A. (2013). Hyaluronan impairs vascular function and drug delivery in a mouse model of pancreatic cancer. *Gut* 62**,** 112-120.

Jahanban-Esfahlan, R., Seidi, K., Monhemi, H., Adli, A.D.F., Minofar, B., Zare, P., Farajzadeh, D., Farajnia, S., Behzadi, R., Abbasi, M.M., Zarghami, N., and Javaheri, T. (2017). RGD delivery of truncated coagulase to tumor

vasculature affords local thrombotic activity to induce infarction of tumors in mice. *Sci Rep* 7**,** 8126.
Jemal, A., Siegel, R., Xu, J., and Ward, E. (2010). Cancer statistics, 2010. *CA Cancer J Clin* 60**,** 277-300.
Jessen, K., Mirsky, R., and Lloyd, A. (2015). Schwann Cells: Development and Role in Nerve Repair. *Cold Spring Harbor perspectives in biology* 7.
Jessen, K.R. (2004). Glial cells. *Int J Biochem Cell Biol* 36**,** 1861-1867.
Jessen, K.R., and Mirsky, R. (2005). The origin and development of glial cells in peripheral nerves. *Nature Reviews Neuroscience* 6**,** 671-682.
Jessen, K.R., and Mirsky, R. (2016). The repair Schwann cell and its function in regenerating nerves. *J Physiol* 594**,** 3521-3531.
Jessen, K.R., and Mirsky, R. (2019). Schwann Cell Precursors; Multipotent Glial Cells in Embryonic Nerves. *Frontiers in molecular neuroscience* 12**,** 69-69.
Jung, K.W., Kim, M.H., Lee, T.Y., Kwon, S., Oh, H.C., Lee, S.S., Seo, D.W., and Lee, S.K. (2007). Clinicopathological aspects of 542 cases of pancreatic cancer: a special emphasis on small pancreatic cancer. *Journal of Korean medical science* 22 Suppl**,** S79-S85.
Kaminski, A., Hahne, J.C., Haddouti El, M., Florin, A., Wellmann, A., and Wernert, N. (2006). Tumour-stroma interactions between metastatic prostate cancer cells and fibroblasts. *Int J Mol Med* 18**,** 941-950.
Kanda, M., Fujii, T., Nagai, S., Kodera, Y., Kanzaki, A., Sahin, T.T., Hayashi, M., Yamada, S., Sugimoto, H., Nomoto, S., Takeda, S., Morita, S., and Nakao, A. (2011). Pattern of lymph node metastasis spread in pancreatic cancer. *Pancreas* 40**,** 951-955.
Kaneko, Y., Ichikawa, M., Kurimoto, Y., Ohta, K., and Yoshimura, N. (2003). Neuronal differentiation of hippocampus-derived neural stem cells cultured in conditioned medium of embryonic rat retina. *Ophthalmic Res* 35**,** 268-275.
Kanwal, B., Biswas, S., Seminara, R.S., and Jeet, C. (2018). Immunotherapy in Advanced Non-small Cell Lung Cancer Patients: Ushering Chemotherapy Through the Checkpoint Inhibitors? *Cureus* 10**,** e3254-e3254.
Kaplan, S., Odaci, E., Unal, B., Sahin, B., and Fornaro, M. (2009). Chapter 2: Development of the peripheral nerve. *Int Rev Neurobiol* 87**,** 9-26.
Karagiannis, G.S., Pavlou, M.P., and Diamandis, E.P. (2010). Cancer secretomics reveal pathophysiological pathways in cancer molecular oncology. *Molecular Oncology* 4**,** 496-510.
Karamitopoulou, E. (2013). Role of Epithelial-Mesenchymal Transition in Pancreatic Ductal Adenocarcinoma: Is Tumor Budding the Missing Link? *Frontiers in Oncology* 3**,** 221.
Katakowski, M., Buller, B., Wang, X., Rogers, T., and Chopp, M. (2010). Functional MicroRNA Is Transferred between Glioma Cells. *Cancer Research* 70**,** 8259.
Khalafalla, F.G., and Khan, M.W. (2017). Inflammation and Epithelial-Mesenchymal Transition in Pancreatic Ductal Adenocarcinoma: Fighting Against Multiple Opponents. *Cancer Growth Metastasis* 10**,** 1179064417709287.
Kiba, T. (2004). Relationships between the autonomic nervous system and the pancreas including regulation of regeneration and apoptosis: recent developments. *Pancreas* 29**,** e51-58.
Kirchgessner, A.L., and Gershon, M.D. (1990). Innervation of the pancreas by neurons in the gut. *J Neurosci* 10**,** 1626-1642.

Kleeff, J., Korc, M., Apte, M., La Vecchia, C., Johnson, C.D., Biankin, A.V., Neale, R.E., Tempero, M., Tuveson, D.A., Hruban, R.H., and Neoptolemos, J.P. (2016). Pancreatic cancer. *Nat Rev Dis Primers* 2**,** 16022.

Klein, A.P. (2013). Identifying people at a high risk of developing pancreatic cancer. *Nat Rev Cancer* 13**,** 66-74.

Kruger, S., Ilmer, M., Kobold, S., Cadilha, B.L., Endres, S., Ormanns, S., Schuebbe, G., Renz, B.W., D'haese, J.G., Schloesser, H., Heinemann, V., Subklewe, M., Boeck, S., Werner, J., and Von Bergwelt-Baildon, M. (2019). Advances in cancer immunotherapy 2019 – latest trends. *Journal of Experimental & Clinical Cancer Research* 38**,** 268.

Kunk, P.R., Bauer, T.W., Slingluff, C.L., and Rahma, O.E. (2016). From bench to bedside a comprehensive review of pancreatic cancer immunotherapy. *Journal for immunotherapy of cancer* 4**,** 14-14.

Lai, E., Puzzoni, M., Ziranu, P., Pretta, A., Impera, V., Mariani, S., Liscia, N., Soro, P., Musio, F., Persano, M., Donisi, C., Tolu, S., Balconi, F., Pireddu, A., Demurtas, L., Pusceddu, V., Camera, S., Sclafani, F., and Scartozzi, M. (2019). New therapeutic targets in pancreatic cancer. *Cancer Treatment Reviews* 81**,** 101926.

Lamounier-Zepter, V., Ehrhart-Bornstein, M., Karczewski, P., Haase, H., Bornstein, S.R., and Morano, I. (2006). Human adipocytes attenuate cardiomyocyte contraction: characterization of an adipocyte-derived negative inotropic activity. *Faseb j* 20**,** 1653-1659.

Landau, E., and Kalnicki, S. (2018). The Evolving Role of Radiation in Pancreatic Cancer. *Surg Clin North Am* 98**,** 113-125.

Lankadasari, M.B., Mukhopadhyay, P., Mohammed, S., and Harikumar, K.B. (2019). TAMing pancreatic cancer: combat with a double edged sword. *Molecular Cancer* 18**,** 48.

Laquente, B., Calsina-Berna, A., Carmona-Bayonas, A., Jiménez-Fonseca, P., Peiró, I., and Carrato, A. (2017). Supportive care in pancreatic ductal adenocarcinoma. *Clin Transl Oncol* 19**,** 1293-1302.

Li, C.C., Eaton, S.A., Young, P.E., Lee, M., Shuttleworth, R., Humphreys, D.T., Grau, G.E., Combes, V., Bebawy, M., Gong, J., Brammah, S., Buckland, M.E., and Suter, C.M. (2013). Glioma microvesicles carry selectively packaged coding and non-coding RNAs which alter gene expression in recipient cells. *RNA Biol* 10**,** 1333-1344.

Li, J., Ma, Q., Liu, H., Guo, K., Li, F., Li, W., Han, L., Wang, F., and Wu, E. (2011). Relationship between neural alteration and perineural invasion in pancreatic cancer patients with hyperglycemia. *PLoS One* 6**,** e17385.

Liebig, C., Ayala, G., Wilks, J.A., Berger, D.H., and Albo, D. (2009). Perineural invasion in cancer: a review of the literature. *Cancer* 115**,** 3379-3391.

Liebl, F., Demir, I.E., Mayer, K., Schuster, T., D'haese, J.G., Becker, K., Langer, R., Bergmann, F., Wang, K., Rosenberg, R., Novotny, A.R., Feith, M., Reim, D., Friess, H., and Ceyhan, G.O. (2014). The impact of neural invasion severity in gastrointestinal malignancies: a clinicopathological study. *Ann Surg* 260**,** 900-907; discussion 907-908.

Lindsey, S., and Langhans, S.A. (2014). Crosstalk of Oncogenic Signaling Pathways during Epithelial-Mesenchymal Transition. *Front Oncol* 4**,** 358.

Liu, B., and Lu, K.Y. (2002). Neural invasion in pancreatic carcinoma. *Hepatobiliary Pancreat Dis Int* 1**,** 469-476.

Liu, J.A., and Cheung, M. (2016). Neural crest stem cells and their potential therapeutic applications. *Dev Biol* 419**,** 199-216.
Liu, Q., Wang, X., and Yi, S. (2018). Pathophysiological Changes of Physical Barriers of Peripheral Nerves After Injury. *Frontiers in neuroscience* 12**,** 597-597.
Logsdon, C.D., and Ji, B. (2013). The role of protein synthesis and digestive enzymes in acinar cell injury. *Nature reviews. Gastroenterology & hepatology* 10**,** 362-370.
Lonardo, E., Frias-Aldeguer, J., Hermann, P.C., and Heeschen, C. (2012). Pancreatic stellate cells form a niche for cancer stem cells and promote their self-renewal and invasiveness. *Cell Cycle* 11**,** 1282-1290.
Lotfinia, M., Kadivar, M., Piryaei, A., Pournasr, B., Sardari, S., Sodeifi, N., Sayahpour, F.-A., and Baharvand, H. (2016). Effect of secreted molecules of human embryonic stem cell-derived mesenchymal stem cells on acute hepatic failure model. *Stem cells and development* 25**,** 1898-1908.
Lucenteforte, E., La Vecchia, C., Silverman, D., Petersen, G.M., Bracci, P.M., Ji, B.T., Bosetti, C., Li, D., Gallinger, S., Miller, A.B., Bueno-De-Mesquita, H.B., Talamini, R., Polesel, J., Ghadirian, P., Baghurst, P.A., Zatonski, W., Fontham, E., Bamlet, W.R., Holly, E.A., Gao, Y.T., Negri, E., Hassan, M., Cotterchio, M., Su, J., Maisonneuve, P., Boffetta, P., and Duell, E.J. (2012). Alcohol consumption and pancreatic cancer: a pooled analysis in the International Pancreatic Cancer Case-Control Consortium (PanC4). *Ann Oncol* 23**,** 374-382.
Madden, E.C., Gorman, A.M., Logue, S.E., and Samali, A. (2020). Tumour Cell Secretome in Chemoresistance and Tumour Recurrence. *Trends in Cancer* 6**,** 489-505.
Magnon, C., Hall, S.J., Lin, J., Xue, X., Gerber, L., Freedland, S.J., and Frenette, P.S. (2013). Autonomic nerve development contributes to prostate cancer progression. *Science* 341**,** 1236361.
Makridakis, M., and Vlahou, A. (2010). Secretome proteomics for discovery of cancer biomarkers. *J Proteomics* 73**,** 2291-2305.
Mathon, N.F., Malcolm, D.S., Harrisingh, M.C., Cheng, L., and Lloyd, A.C. (2001). Lack of replicative senescence in normal rodent glia. *Science* 291**,** 872-875.
Matsuda, Y., Ishiwata, T., Yachida, S., Suzuki, A., Hamashima, Y., Hamayasu, H., Yoshimura, H., Honma, N., Aida, J., Takubo, K., and Arai, T. (2016). Clinicopathological Features of 15 Occult and 178 Clinical Pancreatic Ductal Adenocarcinomas in 8339 Autopsied Elderly Patients. *Pancreas* 45**,** 234-240.
Matsuno, S., Egawa, S., Fukuyama, S., Motoi, F., Sunamura, M., Isaji, S., Imaizumi, T., Okada, S., Kato, H., Suda, K., Nakao, A., Hiraoka, T., Hosotani, R., and Takeda, K. (2004). Pancreatic Cancer Registry in Japan: 20 years of experience. *Pancreas* 28**,** 219-230.
Mehrabadi, S., Sadr, S.S., and Hoseini, M. (2019). Stem Cell Conditioned Medium as a Novel Treatment for Neuroinflamation Diseases. *intjmi* 8**,** 1-12.
Meyer, D., and Birchmeier, C. (1995). Multiple essential functions of neuregulin in development. *Nature* 378**,** 386-390.
Mizisin, A.P. (2014). Mechanisms of diabetic neuropathy: Schwann cells. *Handb Clin Neurol* 126**,** 401-428.
Monje, M., Borniger, J.C., D'silva, N.J., Deneen, B., Dirks, P.B., Fattahi, F., Frenette, P.S., Garzia, L., Gutmann, D.H., Hanahan, D., Hervey-Jumper, S.L., Hondermarck, H., Hurov, J.B., Kepecs, A., Knox, S.M., Lloyd, A.C., Magnon,

C., Saloman, J.L., Segal, R.A., Sloan, E.K., Sun, X., Taylor, M.D., Tracey, K.J., Trotman, L.C., Tuveson, D.A., Wang, T.C., White, R.A., and Winkler, F. (2020). Roadmap for the Emerging Field of Cancer Neuroscience. *Cell* 181**,** 219-222.

Monk, K.R., Feltri, M.L., and Taveggia, C. (2015). New insights on Schwann cell development. *Glia* 63**,** 1376-1393.

Moon, H.J., An, J.Y., Heo, J.S., Choi, S.H., Joh, J.W., and Kim, Y.I. (2006). Predicting survival after surgical resection for pancreatic ductal adenocarcinoma. *Pancreas* 32**,** 37-43.

Moorcraft, S.Y., Khan, K., Peckitt, C., Watkins, D., Rao, S., Cunningham, D., and Chau, I. (2014). FOLFIRINOX for locally advanced or metastatic pancreatic ductal adenocarcinoma: the Royal Marsden experience. *Clin Colorectal Cancer* 13**,** 232-238.

Moore, M.J., Goldstein, D., Hamm, J., Figer, A., Hecht, J.R., Gallinger, S., Au, H.J., Murawa, P., Walde, D., Wolff, R.A., Campos, D., Lim, R., Ding, K., Clark, G., Voskoglou-Nomikos, T., Ptasynski, M., and Parulekar, W. (2007). Erlotinib plus gemcitabine compared with gemcitabine alone in patients with advanced pancreatic cancer: a phase III trial of the National Cancer Institute of Canada Clinical Trials Group. *J Clin Oncol* 25**,** 1960-1966.

Moore, M.J., Hamm, J., Dancey, J., Eisenberg, P.D., Dagenais, M., Fields, A., Hagan, K., Greenberg, B., Colwell, B., Zee, B., Tu, D., Ottaway, J., Humphrey, R., and Seymour, L. (2003). Comparison of gemcitabine versus the matrix metalloproteinase inhibitor BAY 12-9566 in patients with advanced or metastatic adenocarcinoma of the pancreas: a phase III trial of the National Cancer Institute of Canada Clinical Trials Group. *J Clin Oncol* 21**,** 3296-3302.

Morrison, D.K., Murakami, M.S., and Cleghon, V. (2000). "Table S1. Drosophila protein kinases and phosphatases".).

Murakami, T., Hiroshima, Y., Matsuyama, R., Homma, Y., Hoffman, R.M., and Endo, I. (2019). Role of the tumor microenvironment in pancreatic cancer. *Annals of gastroenterological surgery* 3**,** 130-137.

Muralidharan-Chari, V., Clancy, J.W., Sedgwick, A., and D'souza-Schorey, C. (2010). Microvesicles: mediators of extracellular communication during cancer progression. *J Cell Sci* 123**,** 1603-1611.

Mustafa, S., Pan, L., Marzoq, A., Fawaz, M., Sander, L., Rückert, F., Schrenk, A., Hartl, C., Uhler, R., Yildirim, A., Strobel, O., Hackert, T., Giese, N., Büchler, M.W., Hoheisel, J.D., and Alhamdani, M.S.S. (2017). Comparison of the tumor cell secretome and patient sera for an accurate serum-based diagnosis of pancreatic ductal adenocarcinoma. *Oncotarget* 8**,** 11963-11976.

Na'ara, S., Amit, M., and Gil, Z. (2019). L1CAM induces perineural invasion of pancreas cancer cells by upregulation of metalloproteinase expression. *Oncogene* 38**,** 596-608.

Nakamori, S., Ota, D.M., Cleary, K.R., Shirotani, K., and Irimura, T. (1994). MUC1 mucin expression as a marker of progression and metastasis of human colorectal carcinoma. *Gastroenterology* 106**,** 353-361.

Nakhaeifard, M., Haji Ghasem Kashani, M., Goudarzi, I., and Rezaei, A. (2018). Conditioned Medium Protects Dopaminergic Neurons in Parkinsonian Rats. *Cell J* 20**,** 348-354.

Nathan, H., Wolfgang, C.L., Edil, B.H., Choti, M.A., Herman, J.M., Schulick, R.D., Cameron, J.L., and Pawlik, T.M. (2009). Peri-operative mortality and long-

term survival after total pancreatectomy for pancreatic adenocarcinoma: a population-based perspective. *J Surg Oncol* 99**,** 87-92.
Nguyen, D.-H.T., Lee, E., Alimperti, S., Norgard, R.J., Wong, A., Lee, J.J.-K., Eyckmans, J., Stanger, B.Z., and Chen, C.S. (2019). A biomimetic pancreatic cancer on-chip reveals endothelial ablation via ALK7 signaling. *Science Advances* 5**,** eaav6789.
Nothlings, U., Wilkens, L.R., Murphy, S.P., Hankin, J.H., Henderson, B.E., and Kolonel, L.N. (2005). Meat and fat intake as risk factors for pancreatic cancer: the multiethnic cohort study. *J Natl Cancer Inst* 97**,** 1458-1465.
Olson, S.H., Hsu, M., Satagopan, J.M., Maisonneuve, P., Silverman, D.T., Lucenteforte, E., Anderson, K.E., Borgida, A., Bracci, P.M., Bueno-De-Mesquita, H.B., Cotterchio, M., Dai, Q., Duell, E.J., Fontham, E.H., Gallinger, S., Holly, E.A., Ji, B.T., Kurtz, R.C., La Vecchia, C., Lowenfels, A.B., Luckett, B., Ludwig, E., Petersen, G.M., Polesel, J., Seminara, D., Strayer, L., and Talamini, R. (2013). Allergies and risk of pancreatic cancer: a pooled analysis from the Pancreatic Cancer Case-Control Consortium. *Am J Epidemiol* 178**,** 691-700.
Park, H., and Poo, M.M. (2013). Neurotrophin regulation of neural circuit development and function. *Nat Rev Neurosci* 14**,** 7-23.
Pavlou, M.P., and Diamandis, E.P. (2010). The cancer cell secretome: A good source for discovering biomarkers? *Journal of Proteomics* 73**,** 1896-1906.
Peterson, S.C., Eberl, M., Vagnozzi, A.N., Belkadi, A., Veniaminova, N.A., Verhaegen, M.E., Bichakjian, C.K., Ward, N.L., Dlugosz, A.A., and Wong, S.Y. (2015). Basal cell carcinoma preferentially arises from stem cells within hair follicle and mechanosensory niches. *Cell Stem Cell* 16**,** 400-412.
Phinney, D.G., and Pittenger, M.F. (2017). Concise review: MSC‐derived exosomes for cell‐free therapy. *Stem cells* 35**,** 851-858.
Pour, P.M., Bell, R.H., and Batra, S.K. (2003). Neural invasion in the staging of pancreatic cancer. *Pancreas* 26**,** 322-325.
Provenzano, P.P., Cuevas, C., Chang, A.E., Goel, V.K., Von Hoff, D.D., and Hingorani, S.R. (2012). Enzymatic targeting of the stroma ablates physical barriers to treatment of pancreatic ductal adenocarcinoma. *Cancer Cell* 21**,** 418-429.
Pundavela, J., Roselli, S., Faulkner, S., Attia, J., Scott, R.J., Thorne, R.F., Forbes, J.F., Bradshaw, R.A., Walker, M.M., Jobling, P., and Hondermarck, H. (2015). Nerve fibers infiltrate the tumor microenvironment and are associated with nerve growth factor production and lymph node invasion in breast cancer. *Mol Oncol* 9**,** 1626-1635.
Qin, E.Y., Cooper, D.D., Abbott, K.L., Lennon, J., Nagaraja, S., Mackay, A., Jones, C., Vogel, H., Jackson, P.K., and Monje, M. (2017). Neural Precursor-Derived Pleiotrophin Mediates Subventricular Zone Invasion by Glioma. *Cell* 170**,** 845-859.e819.
Rahib, L., Smith, B.D., Aizenberg, R., Rosenzweig, A.B., Fleshman, J.M., and Matrisian, L.M. (2014). Projecting cancer incidence and deaths to 2030: the unexpected burden of thyroid, liver, and pancreas cancers in the United States. *Cancer Res* 74**,** 2913-2921.
Rawla, P., Sunkara, T., and Gaduputi, V. (2019). Epidemiology of Pancreatic Cancer: Global Trends, Etiology and Risk Factors. *World journal of oncology* 10**,** 10-27.

Reni, M., Cereda, S., Milella, M., Novarino, A., Passardi, A., Mambrini, A., Di Lucca, G., Aprile, G., Belli, C., Danova, M., Bergamo, F., Franceschi, E., Fugazza, C., Ceraulo, D., and Villa, E. (2013). Maintenance sunitinib or observation in metastatic pancreatic adenocarcinoma: A phase II randomised trial. *European Journal of Cancer* 49**,** 3609-3615.

Renz, B.W., Takahashi, R., Tanaka, T., Macchini, M., Hayakawa, Y., Dantes, Z., Maurer, H.C., Chen, X., Jiang, Z., Westphalen, C.B., Ilmer, M., Valenti, G., Mohanta, S.K., Habenicht, A.J.R., Middelhoff, M., Chu, T., Nagar, K., Tailor, Y., Casadei, R., Di Marco, M., Kleespies, A., Friedman, R.A., Remotti, H., Reichert, M., Worthley, D.L., Neumann, J., Werner, J., Iuga, A.C., Olive, K.P., and Wang, T.C. (2018a). beta2 Adrenergic-Neurotrophin Feedforward Loop Promotes Pancreatic Cancer. *Cancer Cell* 33**,** 75-90.e77.

Renz, B.W., Tanaka, T., Sunagawa, M., Takahashi, R., Jiang, Z., Macchini, M., Dantes, Z., Valenti, G., White, R.A., Middelhoff, M.A., Ilmer, M., Oberstein, P.E., Angele, M.K., Deng, H., Hayakawa, Y., Westphalen, C.B., Werner, J., Remotti, H., Reichert, M., Tailor, Y.H., Nagar, K., Friedman, R.A., Iuga, A.C., Olive, K.P., and Wang, T.C. (2018b). Cholinergic Signaling via Muscarinic Receptors Directly and Indirectly Suppresses Pancreatic Tumorigenesis and Cancer Stemness. *Cancer Discov* 8**,** 1458-1473.

Riethmacher, D., Sonnenberg-Riethmacher, E., Brinkmann, V., Yamaai, T., Lewin, G.R., and Birchmeier, C. (1997). Severe neuropathies in mice with targeted mutations in the ErbB3 receptor. *Nature* 389**,** 725-730.

Roberts, S.A., and Lloyd, A.C. (2012). Aspects of cell growth control illustrated by the Schwann cell. *Current Opinion in Cell Biology* 24**,** 852-857.

Roberts, S.L., Dun, X.P., Doddrell, R.D.S., Mindos, T., Drake, L.K., Onaitis, M.W., Florio, F., Quattrini, A., Lloyd, A.C., D'antonio, M., and Parkinson, D.B. (2017). Sox2 expression in Schwann cells inhibits myelination in vivo and induces influx of macrophages to the nerve. *Development* 144**,** 3114-3125.

Rochefort, M.M., Ankeny, J.S., Kadera, B.E., Donald, G.W., Isacoff, W., Wainberg, Z.A., Hines, O.J., Donahue, T.R., Reber, H.A., and Tomlinson, J.S. (2013). Impact of Tumor Grade on Pancreatic Cancer Prognosis: Validation of a Novel TNMG Staging System. *Annals of Surgical Oncology* 20**,** 4322-4329.

Röder, P.V., Wu, B., Liu, Y., and Han, W. (2016). Pancreatic regulation of glucose homeostasis. *Experimental & molecular medicine* 48**,** e219-e219.

Roger, E., Martel, S., Bertrand-Chapel, A., Depollier, A., Chuvin, N., Pommier, R.M., Yacoub, K., Caligaris, C., Cardot-Ruffino, V., Chauvet, V., Aires, S., Mohkan, K., Mabrut, J.-Y., Adham, M., Fenouil, T., Hervieu, V., Broutier, L., Castets, M., Neuzillet, C., Cassier, P.A., Tomasini, R., Sentis, S., and Bartholin, L. (2019). Schwann cells support oncogenic potential of pancreatic cancer cells through TGFβ signaling. *Cell death & disease* 10**,** 886-886.

Rutledge, A., Jobling, P., Walker, M.M., Denham, J.W., and Hondermarck, H. (2017). Spinal Cord Injuries and Nerve Dependence in Prostate Cancer. *Trends Cancer* 3**,** 812-815.

Sakamoto, Y., Kitajima, Y., Edakuni, G., Sasatomi, E., Mori, M., Kitahara, K., and Miyazaki, K. (2001). Expression of Trk tyrosine kinase receptor is a biologic marker for cell proliferation and perineural invasion of human pancreatic ductal adenocarcinoma. *Oncol Rep* 8**,** 477-484.

Saloman, J.L., Albers, K.M., Li, D., Hartman, D.J., Crawford, H.C., Muha, E.A., Rhim, A.D., and Davis, B.M. (2016a). Ablation of sensory neurons in a genetic

model of pancreatic ductal adenocarcinoma slows initiation and progression of cancer. *Proc Natl Acad Sci U S A* 113**,** 3078-3083.
Saloman, J.L., Albers, K.M., Rhim, A.D., and Davis, B.M. (2016b). Can Stopping Nerves, Stop Cancer? *Trends Neurosci* 39**,** 880-889.
Saloman, J.L., Singhi, A.D., Hartman, D.J., Normolle, D.P., Albers, K.M., and Davis, B.M. (2018). Systemic Depletion of Nerve Growth Factor Inhibits Disease Progression in a Genetically Engineered Model of Pancreatic Ductal Adenocarcinoma. *Pancreas* 47**,** 856-863.
Salonen, V., Aho, H., Roytta, M., and Peltonen, J. (1988). Quantitation of Schwann cells and endoneurial fibroblast-like cells after experimental nerve trauma. *Acta Neuropathol* 75**,** 331-336.
Salvo, E., Saraithong, P., Curtin, J.G., Janal, M.N., and Ye, Y. (2019). Reciprocal interactions between cancer and Schwann cells contribute to oral cancer progression and pain. *Heliyon* 5**,** e01223.
Sato, K., Sasaki, K., Akiyama, Y., and Yamaguchi, K. (2001). Mass spectrometric high-throughput analysis of serum-free conditioned medium from cancer cell lines. *Cancer Letters* 170**,** 153-159.
Schaaij-Visser, T.B., De Wit, M., Lam, S.W., and Jiménez, C.R. (2013). The cancer secretome, current status and opportunities in the lung, breast and colorectal cancer context. *Biochim Biophys Acta* 1834**,** 2242-2258.
Schafer, D.P., and Stevens, B. (2015). Microglia Function in Central Nervous System Development and Plasticity. *Cold Spring Harb Perspect Biol* 7**,** a020545.
Schnelldorfer, T., Ware, A.L., Sarr, M.G., Smyrk, T.C., Zhang, L., Qin, R., Gullerud, R.E., Donohue, J.H., Nagorney, D.M., and Farnell, M.B. (2008). Long-term survival after pancreatoduodenectomy for pancreatic adenocarcinoma: is cure possible? *Ann Surg* 247**,** 456-462.
Schuh, C.M.a.P., Sandoval-Castellanos, A.M., De Gregorio, C., Contreras-Kallens, P., and Haycock, J.W. (2020). "The Role of Schwann Cells in Peripheral Nerve Function, Injury, and Repair," in *Cell Engineering and Regeneration,* eds. J.M. Gimble, D. Marolt Presen, R. Oreffo, H. Redl & S. Wolbank. (Cham: Springer International Publishing), 1-22.
Shah, N.M., Marchionni, M.A., Isaacs, I., Stroobant, P., and Anderson, D.J. (1994). Glial growth factor restricts mammalian neural crest stem cells to a glial fate. *Cell* 77**,** 349-360.
Shan, C., Wei, J., Hou, R., Wu, B., Yang, Z., Wang, L., Lei, D., and Yang, X. (2016). Schwann cells promote EMT and the Schwann-like differentiation of salivary adenoid cystic carcinoma cells via the BDNF/TrkB axis. *Oncol Rep* 35**,** 427-435.
Sharma, C., Eltawil, K.M., Renfrew, P.D., Walsh, M.J., and Molinari, M. (2011). Advances in diagnosis, treatment and palliation of pancreatic carcinoma: 1990-2010. *World journal of gastroenterology* 17**,** 867-897.
Shore, S., Vimalachandran, D., Raraty, M.G., and Ghaneh, P. (2004). Cancer in the elderly: pancreatic cancer. *Surg Oncol* 13**,** 201-210.
Shurin, G.V., Kruglov, O., Ding, F., Lin, Y., Hao, X., Keskinov, A.A., You, Z., Lokshin, A.E., Laframboise, W.A., Falo, L.D., Shurin, M.R., and Bunimovich, Y.L. (2019). Melanoma-induced reprogramming of Schwann cell signaling aids tumor growth. *Cancer Research***,** canres.3872.2018.
Siegel, R.L., Miller, K.D., and Jemal, A. (2016). Cancer statistics, 2016. *CA Cancer J Clin* 66**,** 7-30.

Sinha, S., Fu, Y.Y., Grimont, A., Ketcham, M., Lafaro, K., Saglimbeni, J.A., Askan, G., Bailey, J.M., Melchor, J.P., Zhong, Y., Joo, M.G., Grbovic-Huezo, O., Yang, I.H., Basturk, O., Baker, L., Park, Y., Kurtz, R.C., Tuveson, D., Leach, S.D., and Pasricha, P.J. (2017). PanIN Neuroendocrine Cells Promote Tumorigenesis via Neuronal Cross-talk. *Cancer Res* 77**,** 1868-1879.

Skog, J., Würdinger, T., Van Rijn, S., Meijer, D.H., Gainche, L., Sena-Esteves, M., Curry, W.T., Jr., Carter, B.S., Krichevsky, A.M., and Breakefield, X.O. (2008). Glioblastoma microvesicles transport RNA and proteins that promote tumour growth and provide diagnostic biomarkers. *Nature cell biology* 10**,** 1470-1476.

Speer, A.G., Thursfield, V.J., Torn-Broers, Y., and Jefford, M. (2012). Pancreatic cancer: surgical management and outcomes after 6 years of follow-up. *Med J Aust* 196**,** 511-515.

Sroka, I.C., Chopra, H., Das, L., Gard, J.M., Nagle, R.B., and Cress, A.E. (2016). Schwann Cells Increase Prostate and Pancreatic Tumor Cell Invasion Using Laminin Binding A6 Integrin. *J Cell Biochem* 117**,** 491-499.

Stastna, M., and Van Eyk, J.E. (2012). Secreted proteins as a fundamental source for biomarker discovery. *Proteomics* 12**,** 722-735.

Stierli, S., Imperatore, V., and Lloyd, A.C. (2019). Schwann cell plasticity-roles in tissue homeostasis, regeneration, and disease. *Glia*.

Stierli, S., Napoli, I., White, I.J., Cattin, A.-L., Monteza Cabrejos, A., Garcia Calavia, N., Malong, L., Ribeiro, S., Nihouarn, J., Williams, R., Young, K.M., Richardson, W.D., and Lloyd, A.C. (2018). The regulation of the homeostasis and regeneration of peripheral nerve is distinct from the CNS and independent of a stem cell population. *Development* 145**,** dev170316.

Stolinski, C. (1995). Structure and composition of the outer connective tissue sheaths of peripheral nerve. *J Anat* 186 (Pt 1)**,** 123-130.

Stoll, G., Jander, S., and Myers, R.R. (2002). Degeneration and regeneration of the peripheral nervous system: from Augustus Waller's observations to neuroinflammation. *J Peripher Nerv Syst* 7**,** 13-27.

Stout, M.C., Narayan, S., Pillet, E.S., Salvino, J.M., and Campbell, P.M. (2018). Inhibition of CX3CR1 reduces cell motility and viability in pancreatic adenocarcinoma epithelial cells. *Biochem Biophys Res Commun* 495**,** 2264-2269.

Su, D., Guo, X., Huang, L., Ye, H., Li, Z., Lin, L., Chen, R., and Zhou, Q. (2020). Tumor-neuroglia interaction promotes pancreatic cancer metastasis. *Theranostics* 10**,** 5029-5047.

Sunderland, S. (1965). The connective tissues of peripheral nerves. *Brain* 88**,** 841-854.

Takahashi, Y., Sipp, D., and Enomoto, H. (2013). Tissue interactions in neural crest cell development and disease. *Science* 341**,** 860-863.

Talathi, S.S., Zimmerman, R., and Young, M. (2020). "Anatomy, Abdomen and Pelvis, Pancreas," in *StatPearls*. (Treasure Island (FL): StatPearls Publishing Copyright © 2020, StatPearls Publishing LLC.).

Taniuchi, M., Clark, H.B., Schweitzer, J.B., and Johnson, E.M., Jr. (1988). Expression of nerve growth factor receptors by Schwann cells of axotomized peripheral nerves: ultrastructural location, suppression by axonal contact, and binding properties. *J Neurosci* 8**,** 664-681.

Taupin, P., Ray, J., Fischer, W.H., Suhr, S.T., Hakansson, K., Grubb, A., and Gage, F.H. (2000). FGF-2-Responsive Neural Stem Cell Proliferation Requires CCg, a Novel Autocrine/Paracrine Cofactor. *Neuron* 28**,** 385-397.

Taveggia, C., Zanazzi, G., Petrylak, A., Yano, H., Rosenbluth, J., Einheber, S., Xu, X., Esper, R.M., Loeb, J.A., Shrager, P., Chao, M.V., Falls, D.L., Role, L., and Salzer, J.L. (2005). Neuregulin-1 type III determines the ensheathment fate of axons. *Neuron* 47**,** 681-694.

Théry, C., Zitvogel, L., and Amigorena, S. (2002). Exosomes: composition, biogenesis and function. *Nature Reviews Immunology* 2**,** 569-579.

Toole, B.P., and Slomiany, M.G. (2008). Hyaluronan: a constitutive regulator of chemoresistance and malignancy in cancer cells. *Seminars in cancer biology* 18**,** 244-250.

Trevisani, M., Smart, D., Gunthorpe, M.J., Tognetto, M., Barbieri, M., Campi, B., Amadesi, S., Gray, J., Jerman, J.C., Brough, S.J., Owen, D., Smith, G.D., Randall, A.D., Harrison, S., Bianchi, A., Davis, J.B., and Geppetti, P. (2002). Ethanol elicits and potentiates nociceptor responses via the vanilloid receptor-1. *Nat Neurosci* 5**,** 546-551.

Tzekova, N., Heinen, A., and Küry, P. (2014). Molecules involved in the crosstalk between immune- and peripheral nerve Schwann cells. *J Clin Immunol* 34 Suppl 1**,** S86-104.

Ubogu, E.E. (2013). The Molecular and Biophysical Characterization of the Human Blood-Nerve Barrier: Current Concepts. *Journal of Vascular Research* 50**,** 289-303.

Vaishnavi, A., Le, A.T., and Doebele, R.C. (2015). TRKing down an old oncogene in a new era of targeted therapy. *Cancer Discov* 5**,** 25-34.

Venkat, R., Edil, B.H., Schulick, R.D., Lidor, A.O., Makary, M.A., and Wolfgang, C.L. (2012). Laparoscopic distal pancreatectomy is associated with significantly less overall morbidity compared to the open technique: a systematic review and meta-analysis. *Ann Surg* 255**,** 1048-1059.

Verkhratsky, A., Ho, M.S., Zorec, R., and Parpura, V. (2019). The Concept of Neuroglia. *Advances in experimental medicine and biology* 1175**,** 1-13.

Von Hoff, D.D., Ervin, T., Arena, F.P., Chiorean, E.G., Infante, J., Moore, M., Seay, T., Tjulandin, S.A., Ma, W.W., Saleh, M.N., Harris, M., Reni, M., Dowden, S., Laheru, D., Bahary, N., Ramanathan, R.K., Tabernero, J., Hidalgo, M., Goldstein, D., Van Cutsem, E., Wei, X., Iglesias, J., and Renschler, M.F. (2013). Increased survival in pancreatic cancer with nab-paclitaxel plus gemcitabine. *N Engl J Med* 369**,** 1691-1703.

Walker, E.J., and Ko, A.H. (2014). Beyond first-line chemotherapy for advanced pancreatic cancer: an expanding array of therapeutic options? *World journal of gastroenterology* 20**,** 2224-2236.

Wang, M., and Kaufman, R.J. (2016). Protein misfolding in the endoplasmic reticulum as a conduit to human disease. *Nature* 529**,** 326-335.

Wang, S., Lee, J.-S., Hyun, J., Kim, J., Kim, S.U., Cha, H.-J., and Jung, Y. (2015). Tumor necrosis factor-inducible gene 6 promotes liver regeneration in mice with acute liver injury. *Stem cell research & therapy* 6**,** 20.

Warshaw, A.L., and Fernandez-Del Castillo, C. (1992). Pancreatic carcinoma. *N Engl J Med* 326**,** 455-465.

Wasif, N., Ko, C.Y., Farrell, J., Wainberg, Z., Hines, O.J., Reber, H., and Tomlinson, J.S. (2010). Impact of tumor grade on prognosis in pancreatic cancer: should we include grade in AJCC staging? *Ann Surg Oncol* 17**,** 2312-2320.

Weiss, T., Taschner‐Mandl, S., Bileck, A., Slany, A., Kromp, F., Rifatbegovic, F., Frech, C., Windhager, R., Kitzinger, H., Tzou, C.H., Ambros, P.F., Gerner, C., and Ambros, I.M. (2016). Proteomics and transcriptomics of peripheral nerve

tissue and cells unravel new aspects of the human Schwann cell repair phenotype. *Glia* 64**,** 2133-2153.
Wekerle, H., Schwab, M., Linington, C., and Meyermann, R. (1986). Antigen presentation in the peripheral nervous system: Schwann cells present endogenous myelin autoantigens to lymphocytes. *Eur J Immunol* 16**,** 1551-1557.
Weng, Y., Sui, Z., Shan, Y., Jiang, H., Zhou, Y., Zhu, X., Liang, Z., Zhang, L., and Zhang, Y. (2016). In-Depth Proteomic Quantification of Cell Secretome in Serum-Containing Conditioned Medium. *Anal Chem* 88**,** 4971-4978.
Whatcott, C.J., Diep, C.H., Jiang, P., Watanabe, A., Lobello, J., Sima, C., Hostetter, G., Shepard, H.M., Von Hoff, D.D., and Han, H. (2015). Desmoplasia in Primary Tumors and Metastatic Lesions of Pancreatic Cancer. *Clin Cancer Res* 21**,** 3561-3568.
Winograd, R., Byrne, K.T., Evans, R.A., Odorizzi, P.M., Meyer, A.R., Bajor, D.L., Clendenin, C., Stanger, B.Z., Furth, E.E., Wherry, E.J., and Vonderheide, R.H. (2015). Induction of T-cell Immunity Overcomes Complete Resistance to PD-1 and CTLA-4 Blockade and Improves Survival in Pancreatic Carcinoma. *Cancer Immunol Res* 3**,** 399-411.
Wisnoski, N.C., Townsend, C.M., Jr., Nealon, W.H., Freeman, J.L., and Riall, T.S. (2008). 672 patients with acinar cell carcinoma of the pancreas: a population-based comparison to pancreatic adenocarcinoma. *Surgery* 144**,** 141-148.
Wolfgang, C.L., Herman, J.M., Laheru, D.A., Klein, A.P., Erdek, M.A., Fishman, E.K., and Hruban, R.H. (2013). Recent progress in pancreatic cancer. *CA: a cancer journal for clinicians* 63**,** 318-348.
Wong, S.C., Chan, C.M., Ma, B.B., Lam, M.Y., Choi, G.C., Au, T.C., Chan, A.S., and Chan, A.T. (2009). Advanced proteomic technologies for cancer biomarker discovery. *Expert Rev Proteomics* 6**,** 123-134.
Woodhoo, A., and Sommer, L. (2008). Development of the Schwann cell lineage: from the neural crest to the myelinated nerve. *Glia* 56**,** 1481-1490.
Wu, Y.S., Chung, I., Wong, W.F., Masamune, A., Sim, M.S., and Looi, C.Y. (2017). Paracrine IL-6 signaling mediates the effects of pancreatic stellate cells on epithelial-mesenchymal transition via Stat3/Nrf2 pathway in pancreatic cancer cells. *Biochim Biophys Acta Gen Subj* 1861**,** 296-306.
Xagorari, A., Siotou, E., Yiangou, M., Tsolaki, E., Bougiouklis, D., Sakkas, L., Fassas, A., and Anagnostopoulos, A. (2013). Protective effect of mesenchymal stem cell-conditioned medium on hepatic cell apoptosis after acute liver injury. *International journal of clinical and experimental pathology* 6**,** 831.
Xue, H., Lu, B., and Lai, M. (2008). The cancer secretome: a reservoir of biomarkers. *Journal of Translational Medicine* 6**,** 52.
Yamada, S., Nakao, A., Fujii, T., Sugimoto, H., Kanazumi, N., Nomoto, S., Kodera, Y., and Takeda, S. (2009). Pancreatic cancer with paraaortic lymph node metastasis: a contraindication for radical surgery? *Pancreas* 38**,** e13-17.
Ydens, E., Lornet, G., Smits, V., Goethals, S., Timmerman, V., and Janssens, S. (2013). The neuroinflammatory role of Schwann cells in disease. *Neurobiol Dis* 55**,** 95-103.
Yeung, Y.T., Mcdonald, K.L., Grewal, T., and Munoz, L. (2013). Interleukins in glioblastoma pathophysiology: implications for therapy. *Br J Pharmacol* 168**,** 591-606.

Yu, M., Zhou, Q., Zhou, Y., Fu, Z., Tan, L., Ye, X., Zeng, B., Gao, W., Zhou, J., Liu, Y., Li, Z., Lin, Y., Lin, Q., and Chen, R. (2015). Metabolic phenotypes in pancreatic cancer. *PloS one* 10**,** e0115153-e0115153.

Zagoura, D.S., Roubelakis, M.G., Bitsika, V., Trohatou, O., Pappa, K.I., Kapelouzou, A., Antsaklis, A., and Anagnou, N.P. (2012). Therapeutic potential of a distinct population of human amniotic fluid mesenchymal stem cells and their secreted molecules in mice with acute hepatic failure. *Gut* 61**,** 894-906.

Zahalka, A.H., Arnal-Estape, A., Maryanovich, M., Nakahara, F., Cruz, C.D., Finley, L.W.S., and Frenette, P.S. (2017). Adrenergic nerves activate an angio-metabolic switch in prostate cancer. *Science* 358**,** 321-326.

Zhang, Q., Zeng, L., Chen, Y., Lian, G., Qian, C., Chen, S., Li, J., and Huang, K. (2016). Pancreatic Cancer Epidemiology, Detection, and Management. *Gastroenterol Res Pract* 2016**,** 8962321.

Zhang, S.H., Shurin, G.V., Khosravi, H., Kazi, R., Kruglov, O., Shurin, M.R., and Bunimovich, Y.L. (2020). Immunomodulation by Schwann cells in disease. *Cancer Immunology, Immunotherapy* 69**,** 245-253.

Zhao, C.M., Hayakawa, Y., Kodama, Y., Muthupalani, S., Westphalen, C.B., Andersen, G.T., Flatberg, A., Johannessen, H., Friedman, R.A., Renz, B.W., Sandvik, A.K., Beisvag, V., Tomita, H., Hara, A., Quante, M., Li, Z., Gershon, M.D., Kaneko, K., Fox, J.G., Wang, T.C., and Chen, D. (2014). Denervation suppresses gastric tumorigenesis. *Sci Transl Med* 6**,** 250ra115.

Zhou, J., Enewold, L., Stojadinovic, A., Clifton, G.T., Potter, J.F., Peoples, G.E., and Zhu, K. (2010). Incidence rates of exocrine and endocrine pancreatic cancers in the United States. *Cancer Causes Control* 21**,** 853-861.

Zhou, Y., Shurin, G.V., Zhong, H., Bunimovich, Y.L., Han, B., and Shurin, M.R. (2018). Schwann Cells Augment Cell Spreading and Metastasis of Lung Cancer. *Cancer Research* 78**,** 5927.

Zullo, J., Matsumoto, K., Xavier, S., Ratliff, B., and Goligorsky, M.S. (2015). The cell secretome, a mediator of cell-to-cell communication. *Prostaglandins Other Lipid Mediat* 120**,** 17-20.